AN INVESTIGATION OF THE TUBE EXPANDING PROCESS WITH PARTICULAR REFERENCE TO HIGH PRESSURE BOILERS.

THESIS

presented by

JOHN MALCOLM ALEXANDER B.Sc.(Eng), A.C.G.I., A.M.I.Mech.E.

for the

DEGREE of Ph. D.

in the Faculty of Engineering

of the

UNIVERSITY OF LONDON,

and for the

DIPLOMA

of the

IMPERIAL COLLEGE OF SCIENCE AND TECHNOLOGY.

1953.

ACKNOWLEDGEMENTS.

This research was carried out in the Mechanical Engineering Department of the City and Guilds College, under the direction of Professor Hugh Ford D.Sc.(Eng), Ph.D, Wh.Sc., M.I.Mech.E., between 1 October 1950 and 31 October 1952.

I wish to thank Professor Hugh Ford for his constant interest and guidance during the course of the work, aand the staff of the Mechanical Engineering Department for their assistance. I should also like to thank Dr. W.B.Carlson of Messrs. Babcock and Wilcox for his practical advice.

The work was carried out under a contract with the British Shipbuilding Research Association, to whom acknowledgement is made for permission to publish the contents of this thesis.

AN INVESTIGATION OF THE TUBE EXPANDING PROCESS WITH PARTICULAR REFERENCE TO HIGH PRESSURE BOILERS.

ABSTRACT.

Previous investigators have concentrated on determining the strength of the joint and the effect of alteration of expanding conditions on this resultant joint strength. A theory for the process, assuming uniform pressure expanding, was proposed by A. Nadai (1943) in which it was stated that the zone of plastic deformation could not extend to a radius greater than 1.75 times the radius of the inside of the tube. This figure was apparently corroborated by experimental evidence given by the flaking-off of mill-scale.

A more fundamental investigation has been made in this research in that the variation of quantities during the expanding process itself and the residual stress and strain distribution left in the joint have been measured for the first time. The zone of plastic deformation is shown to extend to a greater distance than predicted by Nadai. A theory for uniform pressure expanding is developed based on the incremental strain equations of Prandtl-Reuss including work-hardening, which gives a realistic basis for the comparison of the residual stresses and strains induced in the expanding process. A theoretical estimate of the effect of 'secondary' yielding on release of the expanding pressure is also made.

The residual seat pressure that can be generated by roller tube expanders is much lower than would be expected from the theory, and this undesirable effect is attributed mainly to axial movement between the tube and plate. It is shown experimentally that residual seat pressures of the order indicated in the theory can be attained by expanding the tubes into the boiler by means of axial compression, and a design of 'riveting' machine for this purpose is suggested. A modified design of propulsive expander for giving a controlled increase of tube inside diameter is also proposed.

CONTENTS.

	Page No.
ACKNOWLEDGEMENTS.	(ii)
ABSTRACT.	(iii)
SYMBOLS.	1
SURVEY OF EXISTING INFORMATION.	6
INTRODUCTION.	11
THE SPECIMENS.	15
THE TUBE EXPANDERS.	17
THE APPARATUS.	
1. Expander Drive Units.	18
2. Main Bed of Apparatus.	21
MEASURING AND RECORDING INSTRUMENTS.	
1. Measurement of Extrusion and Torque.	22
2. Strain Gauge Circuits.	
(a) Torque measurement.	23
(b) Dynamic strain measurement.	25
(c) Static strain measurement.	30
3. Indication of Other Quantities.	32
4. Cinematograph Technique.	33
STRAIN GAUGE TECHNIQUE AND CALIBRATION.	
1. Introduction.	35
2. Standard Procedure.	36
3. Behaviour of British Thermostat Gauges.	38
4. Zero Drift.	45
5. Calibration of Strain Gauges	48
6. Strain Analysis from Resistance Strain Gauge Readings.	50
7. Estimation of the Errors Involved in Using the Static Strain Recorder.	62
8. Measurement of Insulation Resistance.	67
9. Error Introduced by Low Insulation Resistance.	69
EXPERIMENTAL PROCEDURE.	71
DESCRIPTION OF A TYPICAL EXPERIMENT. (SPECIMEN NO. 2. 2 in. O.D. TUBE).	73
INDIVIDUAL EXPERIMENTS.	
Trial Experiment No. 1 (Specimen No.1, 2 in. O.D.Tube).	76

CONTENTS. (CONTINUED).

	Page No.
Experiment No. 3 (Specimen No. 3, 1 in. O.D. Tube).	77
Experiment No. 4 (Specimen No. 4, 4 in. O.D. Tube).	78
Experiment No. 4a (Specimen No. 4, 4 in. O.D. Tube).	79
Experiment No. 5 (Specimen No. 5, 4 in. O.D. Tube).	80
Experiment No. 6 (Specimen No. 6, 4 in. O.D. Tube).	84
PUSH-OUT TESTS.	86
HARDNESS AND THICKNESS MEASUREMENTS ON SPECIMEN 4.	89
TENSILE TESTS (1½ IN. BOILER PLATE).	91
TENSILE AND TORSION TESTS (2½ IN. BOILER PLATE).	93
HARDNESS-YIELD STRESS CORRELATION (2½ IN. BOILER PLATE).	94
THE THEORY OF THE PROCESS OF EXPANDING A HOLE FROM ZERO RADIUS IN A THIN INFINITE PLATE.	
1. Summary.	96
2. Survey of Previous Theories.	96
3. Introduction.	98
4. Solution in the Plastic Region.	102
5. Solution in the Elastic Region.	110
6. Numerical Solution.	114
7. Conclusions.	115
DISCUSSION OF THE EXPERIMENTAL RESULTS.	
1. Geometrical Similarity.	117
2. Criteria of the Degree of Expanding.	119
3. Parallel Expanding.	120
4. Extent of Plastic Zone.	122
COMPARISON OF THE EXPERIMENTAL RESULTS WITH THEORETICAL PREDICTIONS.	
1. Residual Strain Distribution and Seat Pressure.	123
2. Work-hardening and Thickening.	127
3. Conclusions.	129
MODIFIED DESIGN OF PROPULSIVE EXPANDER.	132
ALTERNATIVE METHODS OF OBTAINING TUBE-SEAT JOINT.	135
TUBE RIVETING EXPERIMENTS. (SPECIMENS 7 AND 8).	140
A POSSIBLE DESIGN OF TUBE RIVETING MACHINE.	142
GENERAL CONCLUSIONS.	143

CONTENTS. (CONTINUED).

	Page No.
SUGGESTIONS FOR FUTURE INVESTIGATION.	147
APPENDIX 1.	149
APPENDIX 2.	153
APPENDIX 3.	158
BIBLIOGRAPHY.	165
TABLES 1 TO 75.	
TABLES A1 AND A2.	
FIGURES 1 TO 116.	
FIGURES A1 AND A2.	

SYMBOLS.

(In alphabetical order).

α Cone angle swept out by the rollers if their axes lie in the same plane as the mandrel axis, i.e. when $\alpha_s = 0$.

α_i Angle between generating surfaces of plate in which $h_i = nr_i$.

α_M Angle of taper of mandrel.

α_R Angle of taper of roller.

α_s Angle of skew of rollers with respect to the mandrel axis.

β $= V(b^2 - a''^2)/a''(b^2 - r_0''^2)$

δ Central deflection of calibrating beam.

ϵ Hydrostatic strain $= (\epsilon_r + \epsilon_\theta + \epsilon_z)/3$

$\bar{\epsilon}$ Logarithmic strain in tensile test.

$\epsilon_r\ \epsilon_\theta\ \epsilon_z$ Logarithmic radial, circumferential, and axial direct strains.

θ Angle defining the current direction of the vector component representing the stress state in the plane of deviatoric states of stress, σ_r σ_θ and σ_z being erected as vectors in a rectangular cartesian coordinate system. (Also used for general angular measure as indicated in the text).

λ $= T/S$

μ Coefficient of friction.

ν	Poisson's Ratio.
σ	Hydrostatic stress $= (\sigma_r + \sigma_\theta + \sigma_z)/3$
$\bar{\sigma}$	Current true yield stress in uniaxial tensile test.
σ_o	Initial true yield stress in uniaxial tensile test.
$\sigma_r\ \sigma_\theta\ \sigma_z$	Radial, circumferential, and axial direct stresses.
ϕ	$= r/c$ (Also used for general angular measure as indicated in the text).

σ'_r	etc.	Deviatoric stresses.
ϵ'_r	etc.	Deviatoric strains.
$d\sigma_r$	etc.	Stress increments.
$d\epsilon_r$	etc.	Strain increments.
$d\bar{\epsilon}^p$		Equivalent plastic strain increment $= +\sqrt{\frac{2}{3}}\left\{d\epsilon_{ij}^p\, d\epsilon_{ij}^p\right\}^{\frac{1}{2}}$ (in the conventional tensor notation).

a	Current radius of hole in pla te.
a''	Final radius of the hole in the plate.
a, b, c	Used for arbitrary constants, and for resistance in ohms, as indicated in the text.
A	Current area between gauge points in tensile test.
A, B	Used for arbitrary distances between centre-lines of strain-gauge grids.
A_o	Initial area between gauge points in tensile test.
b	Outside radius of plate disc.
b_g	Width of strain gauge grid.
c	Current radius to plastic-elastic interface.
D	Galvanometer deflection (mm.).
e	Unit (Engineer's) strain.

E	Young's Modulus.
E_B	D.C. voltage applied to strain gauge circuit (volts).
F	Push-out load.
G	Shear Modulus.
h	Current thickness of plate at radius r.
h_i	Initial thickness of plate at radius r_i.
h_g	Distance between centre-line of calibrating beam and centre-line of the wire grid of the strain gauge.
H	Work-hardening function. For the tensile test $\bar{\sigma} = H\int d\bar{\epsilon}^p = H\left\{\int_{l_o}^{l}\left(\frac{dl}{l}-\frac{d\bar{\sigma}}{E}\right)\right\} = H\left(\log\frac{l}{l_o}-\frac{\bar{\sigma}}{E}\right)$.
H'	Slope of curve of $\bar{\sigma}$ vs. $\left(\log\frac{l}{l_o}-\frac{\bar{\sigma}}{E}\right)$.
I	Current (amperes), with appropriate suffix as indicated in the text.
I_G	Current through strain gauge (amperes).
I_M	Current through microammeter (amperes).
I_R	Current through ratio arms of Wheatstone's bridge (amperes).
k	Fractional resistance change of strained resistance strain gauge. (Also used to denote arbitrary constant, with appropriate suffix).
l	Current length between gauge points in tensile test.
l_e	Exposed length of rollers.
l_g	Length of strain gauge grid.
l_o	Initial length between gauge points in tensile test.

L	Current load applied in tensile test.
m	$= 2\tan\frac{\alpha_i}{2}$. (Arbitrary constant).
M	Microammeter reading (micro-amperes).
n	Number of strain gauge circuits on static strain recorder.
p	Expanding pressure ($= -\sigma_r$ at the appropriate radius).
$\bar{p}$	Mean seat pressure between tube and plate $= \frac{p_F + p_B}{2}$
p_B	Seat pressure (back of plate).
p_F	Seat pressure (front of plate).
q	Hydrostatic tension.
r	Current radius to any element.
r''	Final radius to any element.
r_1	Initial outside radius of tube.
r_i	Initial radius to any element.
r_o	Initial inside radius of tube.
r_o'	Radius of inside of tube at instant of closing initial clearance between tube and plate.
r_o''	Final radius of inside of tube.
R	Resistance of one ratio arm of Wheatstone's bridge (ohms). Also used generally for resistance (ohms), with appropriate suffix as indicated in the text.
R_E	Resistance of total zeroing circuit (ohms).
R_G	Resistance of strain gauge (ohms).
R_M	Resistance of microammeter (ohms).

R_s	Resistance of shunt across potential divider of zeroing circuit (ohms).
R_v	Resistance of potential divider of zeroing circuit (ohms).
S	True longitudinal sensitivity factor of strain gauge.
S'	Apparent longitudinal sensitivity factor of strain ga uge from calibration.
S''	Apparent longitudinal sensitivity factor of strain gauge used in calculations.
T	True transverse sensitivity factor of strain gauge. (Also used to denote torque) .
t	Thickness of ca librating beam.
u	Radial outward displacement of any element (with appropriate suffix as outlined in the text).
u_o	Radial displacement of inside of tube, $= r''_o - r'_o$.
v	Velocity, defined as $v = \frac{du}{dc}$, i.e. using the parameter c (radius to plastic- elastic interface), as the time-scale.
x	Axia l displacement of front elements of the pla te. (Also used for distance of centre-line of strain-gauge from an arbitrary datum).

Note:- Numbers in brackets in the tex t refer to the Bibliography.

SURVEY OF EXISTING INFORMATION.

For many years the practice of expanding boiler tubes into their tube plates has been adopted as being the most convenient method of making the joint. The process closely resembles the 'autofrettage' of gun barrels in which a state of residual stress of the desired type is generated by the application and subsequent release of internal pressure. In practice, the tube is loosely inserted in a hole in the boiler tube plate and expanded until the clearance between the tube and plate has been closed, by which time the material of the tube is, in general, deforming plastically. Further expansion of the tube causes the material of the seat plate also to deform plastically around the edge of the hole. Release of the expanding pressure allows a small inward elastic recovery of the tube and plate, and due to the nature of the original expanded stress distribution in the system a residual compressive stress is left between the tube and plate, generally referred to as the 'seat pressure'.

The standard tools for expanding boiler tube joints are the roller expander, and , for small tubes, the ball drift expander. The roller expander consists of three or more rollers supported in a cage through the centre of which a tapered mandrel is passed. Axial movement of the mandrel causes the rollers to move radially outward, whilst rotation of the mandrel causes the rollers to rotate against the inside of the tube. The rollers are generally given a small 'angle of lead' to the mandrel axis,

so that they roll forward and move radially outward at the same time. This mechanism, then, expands the tube into the tube plate. In the propulsive type of expander, the expanding pressure is released and the expander removed by reversing the direction of mandrel rotation, whilst in the retractive type of expander the rollers are inserted to a given distance into the tube and roll out of the open end of the tube. In both types the rollers are tapered in the opposite direction to the mandrel taper with a view to rolling a parallel hole. The retractive expander has been introduced in order to expand long seat widths, since the width of seat which can be rolled by the propulsive expander is limited by roller length.

Ball drift expanders, although restricted to small bore tubes, may also be used to expand long seat widths. A ball is forced into the bore of the tube by a series of blows from an air hammer, thus resulting in a series of short expanded joints. By using a split ball the retractive principle can be utilized.

An excellent survey of the relevant information concerning the expanding process was made by A.M. Baxter in 1947 (1). This survey showed that much work had been done by way of establishing the more important factors affecting the tightness and strength of boiler tube joints expanded by roller type tube expanders. Notable in the field of experimental research were Grimison and Lee (2) and Shannon and his co-authors (3), whilst the theoretical aspect of the problem was considered by A. Nadai (4) and Goodier and Schoessow (5).

A study of the extensive literature referred to in Baxter's survey leads to the conclusion that a great deal of 'ad hoc' experimental research has been carried out into the problem of tube expanding, often leading to inconclusive or confusing results. There are a large number of variables in the expanding process, and it appears that attempts to study the effects of variation of one of them on its own have not always yielded conclusive information. The main variables are as follows:-

(a). Number of rollers in expanding tool.

There is much controversy regarding the relative advantages of 3, 4, 5, or 6 -roller expanders, the available evidence being inconclusive.

(b). Width of tube seat.

Some writers have stated a maximum useful length of tube seat, whilst others state that the holding strength is proportional to this length.

(c). Condition of surfaces. Grooves.

Itis not at all clear from the experimental evidence whether it is better to have smooth or rough contact surfaces between tube and plate. The presence of grooves machined in the tube seat has in general been shown to be beneficial, although some investigators have quoted results show ing superior behaviour of ungrooved seats.

(d). Joint design.

Shannon and his colleagues found that by expanding short ferrules into the already expanded tubes the seat pressure

was considerably increased, but gave little information on which to base joint design.

(e). Optimum degree of expanding.

It has been shown by many investigators that the holding strength of a rolled joint reaches a maximum for a certain degree of expanding and then decreases if rolling is continued beyond this point. The need for a reliable criterion on which to base the degree of expanding is therefore apparent. Practical methods which have been used with some success are:-

(i). The gauging of the outside diameter of the tube immediately next to the tube plate on the gas side of water-tube boilers.

(ii). The gauging of the inside diameter of the tube.

(iii). The measurement of the energy input and hence the work done.

(iv). The measurement of mandrel travel.

(v). The measurement of the elongation or extrusion of the tube.

(vi). The flaking or 'popping' of mill-scale from the tube seat is used as a rough indication of the extent of plastic deformation.

All these methods are arbitrary in that the effect of the variable chosen as criterion on the resultant joint strength must be determined beforehand experimentally.

(f). Tube and plate material.

From the point of view of joint strength it has been shown on theoretical grounds by Goodier and Schoessow that a hard plate and soft tube combination is more desirable than the reverse, and this is in qualitative agreement with experimental tests for holding power.

Other important variables are introduced as a consequence of the more practical requirements of tube expanding, for example, the presence of adjacent joints, the effect of varying the dimensions of the joints and of the expanders, the speed of expanding, and the initial clearance between tube and seat. Finally, the effect on the joint strength of temperatures and pressures of the order of those generated in the boiler has not been systematically investigated. Some estimate has been made by Shannon and his colleagues, but little experimental work has been carried out, apart from the strength tests under hydraulic pressure of Grimison and Lee.

INTRODUCTION.

Bearing in mind the work of previous investigators already mentioned, it was decided that a more fundamental approach to the problem was necessary. From the theoretical standpoint, the problem is difficult because of the impossibility of determining analytically the stress and strain distribution developed by the rollers as they move round the tube. It might be possible to estimate the effect of one roller being pressed into the edge of a hole in a plate, assuming the plastic-rigid material envisaged by Hencky and Geiringer under plane strain conditions. The boundary condition at the interface between roller and hole is difficult to prescribe, however, and the configuration would change under continued indentation. In addition to this, release of the load would impose an elastic stress distribution on that engendered during the indentation, possibly followed by further yielding and stress change. In practice the roller is rotating round the inside of the hole, so that the process is not the symmetrical one of pure indentation, and the boundary condition becomes even more complicated.

Nadai's theory, in which a uniform pressure expanding is assumed, although giving a valuable estimate of the stress distribution around the joint, is inadequate for comparison with experimental results, due to the incorrect equations on which it is based. As is now well known, these equations do not properly represent the physical behaviour of a metal, and lead to incorrect values of the strain induced. Thus any

estimate of work-hardening based on these equations is also incorrect, since work-hardening is dependent on both the stress and strain history of the expanding.

It was therefore decided to develop a more comprehensive theory for expanding a hole in a plate based on the incremental strain equations of Prandtl-Reuss, including work-hardening, as set out very clearly in Dr.R.Hill's book.(6). An experimental stress-strain curve obtained for the material used in the expanding experiments could be incorporated in the theory, and would allow comparison between the experimental measurements and the theoretical predictions. In this way an idea could be obtained of the difference between the practical process of expanding a tube in a plate by means of roller expanders, and the theoretical predictions for expanding a hole in a plate by uniform pressure. The experiments carried out in this research were designed bearing this type of comparison in mind, and the tube and plate materials were chosen to be similar, allowing an approximation to the theoretical analysis which assumes a continuous tube-plate medium.

The experiments were also intended to examine the tube expanding process itself in relation to as many variables as possible, to discover which were the principle variables and to study how they follow the actual build-up of strains during the expanding. It was also desired to show that there would be no 'size effect', i.e. for geometrically similar systems, the distribution of stress and strain in and around any joint would be the same provided that each joint received

the same degree of expanding. This must clearly be true for the theoretical homogeneous isotropic material, but it appeared advisable to verify it for commercial work-hardening materials. Once this similarity principle had been established the field of investigation could then be restricted, apart from occasional checks, to the most convenient joint size, varying each of the variables so as to determine their separate effect.

Accordingly an apparatus was made which would allow a joint to be expanded under completely controlled conditions. The joint was standardised as a length of tube which could be expanded into a flat circular disc. The mandrel torque, the dynamic strains generated in the discs, the back and total extrusion, and the residual strain distribution were all measured accurately. Standard propulsive and retractive type three roller expanders were used. Plumber's resin was melted on to the surfaces of the discs in an attempt to indicate the extent of plastic deformation.

For the largest size of disc-tube combination the dimensions were chosen to represent a typical joint in a high-pressure boiler shell. Two other geometrically similar systems were also tested, having linear dimensions of one half and one quarter this size.

Having expanded these joints, the tubes were pushed out and the elastic recovery of the plates measured in order to estimate the mean seat pressure. Tensile and torsion tests were carried out on the plate material and a correlation

obtained between the current yield stress and the hardness number. In this way comparison could be made between the measured work-hardening from hardness measurements made across the faces of a specimen and that predicted theoretically. The thickness of the specimen after expanding was also measured for comparison with the theory.

To conclude the research other methods of expanding a joint were briefly considered and the effect of 'riveting' tubes into seat plates investigated. This was done by bulging short lengths of tube under axial compression until they were expanded into their seat plates. A tentative design for a machine capable of performing this operation was developed, and a design of propulsive expander which would give a controlled increase in inside diameter of the tube has also been proposed.

No attempts were made in this research to determine the detailed effects of variation of particular variables. The aim was to examine the process in as general a manner as possible, making use of the recently developed mathematical theory of plasticity, and thereby indicate the most advantageous directions for further investigation. The experiments were restricted to one joint configuration, although the size was varied, and an attempt made to obtain repeatable experimental techniques. Roller type expanders without belling rolls were used, no experiments being carried out with ball drift expanders.

THE SPECIMENS.

The tube and plate system, shown in Figure 1, consists of a 9 inch length of tube and a circular disc for the tube plate. The dimensions of Specimens 3, 1 and 2, 4 and 6 are in the ratio of 1:2:4 respectively, with the exception of the tube length, which was the same for all the specimens. A slight departure from strict geometrical similarity was present owing to the allowable tolerances on tube diameters. It was thought preferable to have these variations rather than machine the tubes. The general proportions were chosen as being typical of high pressure boiler tube joints.

The tubes, supplied by Messrs. Stewart and Lloyds,* were of cold drawn mild steel manufactured to the usual specification and limits (B.S.S. 494, 512). The boiler plate was supplied by Messrs. Yarrow & Co. Ltd.,* and a representative sample of the 1½in. plate had the following analysis:-/

0.23% C, 0.11% Si, 0.012% S, 0.046% P

0.56% Mn, 0.16% Ni, 0.11% Cr.

The discs were flame-cut from the plate and machined all over so that the faces were parallel to ± 0.005 in., the hole being bored to the appropriate clearance size over that of the fully prepared tube. The effect of flame-cutting was found to be:-

Depth of hardened zone - about 0.01 in.

Depth of heat affected zone - about 0.1 in.

---

* Thanks are due to these firms for their assistance.

/ Kindly supplied by the Metallurgy Department, Imperial College.

The tubes were cut to length and the mill-scale was removed from the outside by scraping and by using emery cloth. A small 'land' was machined on each end of the tube as far as the mean diameter to accommodate the legs of the device for measuring the total extrusion (see Fig. 1).

THE TUBE EXPANDERS.

Those used in the experiments to show geometrical similarity were of the standard propulsive type, having three rollers supported at 120° apart in a cage which inclined the rollers at a slight angle to the axis of the tapered mandrel, this angle of inclination being approximately equal for all of the three sets of propulsive type tube expanders used. The rollers were tapered in the opposite direction to the mandrel so as to give so-called 'parallel' expanding, whilst the angle of inclination between the roller axis and the mandrel axis gave the expanders a self-feeding action into the tube. A cage on the roller cage prevented entry of the rollers beyond a certain limit. The propulsive expanders (supplied by Messrs Easterbrook and Allcard), are shown in Fig. 2, the dimensions being given in Fig. 3. The propulsive expanders were used without any form of lubricant in the experiments.

Experiment No 5 was carried out using retractive expanders supplied by Messrs. Babcock and Willcox Ltd., and were of the design shown diagrammatically in Fig. 4. A photograph of these expanders showing the pronounced mandrel taper as compared with the propulsive type is shown in Fig. 5. Their precise action is described later (Experiment 5).

THE APPARATUS.

1. Expander Drive Units.

Very little information could be found about the torque required to expand joints of the size used in these investigations, and, owing to delay in the delivery of the expanders, trial expansions could not be made. A maximum torque of about 120 lb.ft. was estimated for the intermediate size joint.

In view of the finite response time of the microammeters used in the measurements a mandrel speed of about 20 r.p.m. was used and although this is lower than normal practice, it is not considered that any discrepancy will arise from this cause. Another reason for using a low speed was the question of the temperature rise in the joint due to the expanding process. An excessive temperature rise would have an adverse effect on the strain gauges positioned near the joint. The speed used leads to one revolution of the mandrel every 3 seconds, and one revolution of the cage every 14 seconds, approximately. Accordingly, any lag in response would be negligible for such slowly varying strains.

A ½ H.P., 950 r.p.m., 400 V D.C. shunt motor and 54.6:1 reduction gear were available in the College so that a torque of approximately 118 lb.ft. could be obtained. A variable resistance was inserted in series with the shunt field of the motor to increase the speed to approximately 1100 r.p.m. Provision for reversing the direction of

rotation of the motor was made to allow observations to be made during removal of the expanders.

The reduction gear output shaft was parallel with the input shaft so that the two could be mounted in line on an angle frame as shown in Fig. 6. This drive unit mounted on its angle section frame was then suspended by means of two suitable brackets on bearings, thus allowing the complete drive unit to rotate. By providing a torque arm and spring balance the driving torque could be measured on the 'swinging field' principle, giving a mechanical check on the torque as measured by a resistance strain gauge torsionmeter on the drive shaft. Suitable stops were provided to limit the rotation of the drive unit which was completely statically balanced, as was also the spring balance, and the torque arm from which it was suspended.

The reduction gear output shaft, which was ¾ in. diameter, passed through the inside of the front bearing bracket, and extended for a distance of about 10 ins. in front of this bearing. The strain gauge torsionmeter was mounted on this extended shaft, together with the necessary slip rings, and the device for driving the expander mandrel, as shown in Fig. 7. The bearings of the drive unit were bolted to cast iron A pedestals fixed to a trolley mounted on mild steel wheels. The wheels could run inside a pair of channels forming the main bed of the apparatus as shown in Figs. 6 and 8. Anti-friction bearings were used for the trolley so that the whole drive unit could move freely,

following the progress of the expanding process.

To ensure that only a pure torque would be transmitted, and to take up any misalignment, a modified form of Oldham's Coupling was used as shown in Figs. 7, 9, and 10. This device was equally effective when reversed for withdrawing the mandrel.

The expander drive unit just described was used for expanding the smallest and intermediate-sized specimens. A more powerful drive unit was used for expanding the largest sized specimens. As the results will show, the readings from the strain gauge torsionmeter agreed well with the mechanically measured torque variation, and observations of the 'mechanical' torque were therefore not made on the largest power unit.

Assuming that the destribution of stress and strain is the same for all the specimens, in terms of some dimensionless parameter such as $\frac{r}{r_o}$ say, then, in expanding the joint, the total work done per unit volume at any value of $\frac{r}{r_o}$ would be the same for each specimen. Hence, neglecting friction of the rollers etc., the total energy to be supplied for the same degree of expanding for any specimen would be proportional to its volume. This energy is $\int T\,d\theta$, where T is the torque after any angle θ turned through by the mandrel. If the total angle is the same for all sets, then the torque would also be proportional to the volume. The maximum torque in the Trial Experiment on the medium sized set was about 150 lb. ft. and a drive unit giving a torque of 1500 lb.ft. was therefore designed for the largest set.

This assembly, comprising a 400 V, 1000 r.p.m., 5 H.P., D.C. shunt motor, 54:1 worm reduction gear, and 5:4 V-belt drive is shown in Fig. 10. This assembly was designed to be interchangeable with the smaller drive unit, utilizing the same trolley, and had a 2 in. diameter shaft on which the same type of torsionmeter was mounted.

2. Main Bed of Apparatus.

This consisted of the two channel runners already mentioned which were bolted to two heavy cross braced cast-iron A pedestals. To support the specimens steel straps were fabricated to embrace both the disc and the tube as shown in Fig. 7. The straps holding the disc were bolted to upright members (Fig. 6), whilst those holding the tube were bolted to short lengths of channel which could bear on a cross-piece in order to prevent rotation of the tube, although allowing axial extrusion to take place.

MEASURING AND RECORDING INSTRUMENTS.

1. Measurement of Extrusion and Torque.

The 'back extrusion'* of the tube from the disc was recorded by a dial gauge secured to the strap round the tube, the plunger of the dial gauge bearing on the rear face of the disc.

The 'total extrusion'† was measured by a pair of calipers fabricated from rigid channel section as shown in Figs. 6 and 7. A taut spring held the tips of the caliper legs against the lands on the tube ends, and the total extrusion at the mean diameter of the tube was determined from the readings of a dial gauge situated at a point about midway along the caliper legs. This caliper was calibrated in position against known displacement of either front or back leg, the mean calibration thus being obtained (Fig. 11).

The total and back extrusion and the spring balance

---

* Back Extrusion. This is the amount by which a section of the tube remote from the back of the tube plate moves away from it during the expanding operation.

† Total Extrusion. This is the sum of the back extrusion and the front extrusion, the front extrusion being the amount by which the front end of the tube moves away from the front of the tube plate, usually being measured at the inside diameter of the tube.

for mechanical torque measurement were recorded during the experiments by visual observation of the instruments at known time intervals.

2. Strain Gauge Circuits.

(a) Torque measurement.

The circuit used for the measurement of torque was as shown diagrammatically at the bottom of Fig. 12. It can be shown by application of either Kirchhoff's Laws or Thevenin's Theorem that if each gauge undergoes a very small and equal fractional resistance change k, - gauges A and C undergoing like changes, gauges B and D undergoing equal and opposite changes to A and C, then:-

$$I_M = \frac{2I_G}{1 + \frac{R_M}{R_G}} k \qquad \text{.....(1)}$$

(see Bibliography, Reference 7).

Since the smaller shaft was only $\frac{3}{4}$ in. diameter, it was not considered practical to use a gauge of much greater gauge length than $\frac{1}{8}$ in. As can be seen from equation (1) above, to obtain the greatest possible values of I_M, the highest possible value of R_G is required. The British Thermostat $\frac{1}{8}$ in x 4 mm., R_G = 400 ohms, gauge was chosen as the most suitable for this application.

When used in conjunction with a centre zero microammeter 50-0-50 microamps, 2½ in. scale, R_M = 172.9 ohms, E_B = 10V, I_G = 12.5 mA, the calibration shown in Fig. 13 was

obtained. In order to record the smaller torques involved in expanding the smallest specimen, the voltage E_B was increased to 30V, the calibration being then as shown in Fig. 14.

To zero the microammeter when the shaft was unstrained, a variable resistance was provided between the lower arms of the bridge (Fig. 12). It consisted of a variable component R_V and a fixed shunt component R_S, and necessitated the use of five slip rings. The slip ring assembly is shown in Fig. 7, contact being effected by means of a set of tensioned flexible wire strands passed round grooved brass slip rings to give an arc of contact of 180°. This method had been found to give a very good electrical contact for a slowly rotating shaft (7).

The strain gauges were so arranged on the shaft as to be almost insensitive to bending, direct, or temperature strains (8).

The torque-indicating microammeter was situated at the bottom right-hand side of the instrument panel, shown in Fig. 15.

For the Trial Experiment a different torque indicating microammeter, scaled 0 to 100 microamps, R_M = 270 ohms, was used, with a change-over switch. The calibration for this instrument is shown in Fig. 16. The centre-zero instrument was found to be more convenient.

The calibration curves of the torsionmeters on the large drive unit are shown in Fig. 17 (Experiment 4),

Fig. 18 (Experiment 4a), and Fig. 19 (Experiments 5 and 6).

(b) Dynamic strain measurement.

The circuits used for indicating the varying strains of the plate during the expanding process were as indicated diagrammatically at the top of Fig. 12. Neglecting the zeroing circuit, it can be shown that if the active gauge undergoes a fractional resistance change k, then:-

$$I_M = \frac{I_G}{1 + \frac{R+2R_M}{R_G}} \cdot k \qquad \text{.....(2)}$$

For a given gauge current I_G, $\frac{R+2R_M}{R_G}$ must be small for I_M to be large, so that R and R_M must be made as small, whilst R_G must be as large as possible. To make the circuits adaptable, and in view of the necessity of being able to photograph these instruments, a centre-zero 50-0-50 microamps 2½ ins. spade pointer instrument for vertical panel mounting was employed. The use of centre-zero instruments enables any of the circuits to be used for indicating either tensile or compressive strains.

Since these gauges were to be applied to a circular field of strain which, near the hole, would have a high rate of change with radius, it was again necessary to have a short gauge length, the width of the gauge also being required to be small. A method of allowing for the variation of strain under the grid of a strain gauge is detailed later in this thesis. It would also not be very convenient to

change the size of gauge applied to each specimen, although this would have been desirable from the principle of geometrical similarity. After consideration of all the various types of strain gauge commercially available, it was again decided to use the $\frac{1}{8}$ in. X 4 mm., 400 ohm British Thermostat gauges, although it was realised that a correction factor might have to be applied to allow for the circular strain field, especially in the case of the smallest joint.

The choice of a value for the resistances R was largely determined by practical considerations such as the available supply voltage, bearing in mind the large current which would be taken from the supply if these resistances were very low, since $I_R = \frac{E_B}{2R}$. It was considered that the minimum number of these circuits necessary to indicate the variation of strain was eight, enabling the measurement of radial and circumferential strains at two different stations along a given radius on the front and on the back of the plate. (Since 90° 'rosette' strain gauges of this type were not available it would be necessary to displace some of the gauges through 120° on the plate, there being three rollers in the expanders. A justification for this is given by the arguments put forward in Appendix 1).

Another consideration was that the heating effect of the current I_R must be kept to an absolute minimum so that any stray draughts in the laboratory would not cause a variation in the resistance of either of the ratio arms R of the Wheatstone's bridge circuit. A differential resistance

change of this type might well cause more deflection on the microammeter than straining of the active strain gauge. After experimenting with the ½ in., 400 ohm strain gauges it was decided that they could withstand a current of 50 mA for short periods of time without their sensitivity being affected, provided that they were shielded from stray draughts. In a test on these lines it was found that the sensitivity of the gauges was unaffected after having carried a current of 50 mA for 66 hours.

The probable maximum strain to be recorded by these gauges would be about 0.1%, and a suitable resistance for the ratio arms R was accordingly calculated to be 50 ohms. For 23 Gauge Bureka wire wound in an open spiral a current of about 2A gives a temperature rise of 100°C. Assuming that the heating effect is proportional to $I_R^2 R$, a current of 0.4A would give a temperature rise of 4°C. Both of the resistances R in any circuit would therefore undergo this temperature rise initially, and the worst condition to cause deflection on the microammeter would be if a current of air at a different temperature were to circulate around one of these resistances and not round its companion resistance. Since this condition would be unlikely, the maximum difference in temperature between any two of these resistances could safely be assumed to be always less than 1°C. Since the temperature coefficient of resistance of commercial Bureka wire varies between $\pm \frac{40}{10^6}$ per °C, this would mean a fractional resistance change of $\frac{40}{10^6}$ under the worst condition.

This represents about 2% of the deflection corresponding to 0.1% strain, an error within the acceptable limits of accuracy in strain gauge measurement.

The 23G bare Eureka wire was oxidised by passing a heavy current through it and was wound on wood formers. Each of the resistances was then matched by means of a sensitive galvanometer against a sub-standard resistance of 50 ohms and arranged in a bank as shown in Fig. 15. Between each pair of these resistances a further length of 23G wire was connected to form the resistance R_s, and a potential divider R_v (100 ohms, 3 watts), mounted on the instrument panel underneath the appropriate microammeter, was connected across the open length of Eureka wire as shown in Fig. 12. Inevitably, differences in the initial resistance of the active and dummy gauges exist, and the combination of a coarse adjustment - by moving the points a and b along the open length of wire, and the fine adjustment - by means of the potential divider R_v, allowed as fine an adjustment as desired (by moving the points a and b closer together). The resistances R_v would take a maximum current of 173 mA, but the current they were carrying in this circuit was only about 0.17 mA, so that the heating effect of this current would be negligible as affecting the bridge balance, especially if the points a and b were chosen suitably. This could be achieved by arranging that balance was obtained with the slider of the potential divider R_v approximately in the centre of its movement.

After the Trial Experiment certain changes were made:-

(i) The circuit calibrations were brought into line with each other so that readings could be plotted directly in terms of microamperes from all the instruments. This was effected by calibrating each of the eight circuits with the same strain gauge and inserting a small amount of resistance in series with the particular microammeter. In this way all the calibrations were reduced to that of the least sensitive circuit.

(ii) Since the largest strain recorded in the Trial Experiment exceeded 0.1%, it was decided to reduce the applied voltage E_B from 40V to 30V, thus reducing I_G to 37.5 mA.

The eight circuits were then calibrated using eight different strain gauges, the calibration curves obtained being shown in Figs. 20 to 27. These calibration curves were obtained for typical gauges strained in the standard four-point loading apparatus shown in Fig. 28. The average of these eight curves was taken as being a mean calibration to allow for random differences in resistance and sensitivity between individual strain gauges. In connection with the mean calibration, two corrections are necessary:- (i) to allow for the distance between the surface of the calibrating beam and the centre-line of the gauge grid, and (ii) to allow for the different transverse strain which would exist in an actual test. These corrections, described in more detail later, have been made in arriving at the calibration constants given in Fig. 27.

The complete electrical circuit diagram is shown in

Fig. 12, and the back of the instrument panel in Fig. 29. Each microammeter could be shunted with a shunt resistance of 0.1 ohms so as to limit the current for test purposes and zeroing, and there was also a cut-out switch in the microammeter circuit. The main bed of the apparatus and the trolley drive unit were earthed to the neutral line of the three-wire 400V D.C. supply, both from safety considerations and also to give more electrical stability to the various sensitive measuring instruments used.

Some of these refinements were not installed in the Trial Experiment, the voltage was 40V and the strain gauges were cemented to the specimen with High Solids Durofix (a nitro-cellulose cement) instead of the resin cement used for the later experiments. This necessitated the use of different calibration factors for each circuit.

(c) Static strain measurement.

Indication of the residual strains on the faces of the disc after removal of the expanders was given by strain gauges connected to a Savage and Parsons 50 Way Static Strain Recorder, shown in the forefront of Fig. 30. It consists essentially of a sensitive galvanometer and a pair of non-inductive sub-standard 100 ohms resistances which can be switched on to any one of a maximum of 50 circuits, as shown diagrammatically in Fig. 31, in which two only of the circuits are shown. Each circuit can be zeroed by means of manganin helical potentiometer spex resistors of approximate resistance

2 ohms. The slider on the balancing slide wire is attached to a scale on the front of the instrument, this scale being calibrated in terms of fractional resistance change (per cent), up to a maximum of 1%. Either the null or the deflection method may be used, but the null method is preferable since any errors due to contact resistance in the galvanometer circuit are then eliminated. The instrument is designed to give the minimum errors from such causes as internal contact resistances and thermo-electric e.m.f's. The D.C. supply for the bridge circuits may be obtained either from a battery or from the 230V A.C. mains through a power pack inside the instrument. The latter method was adopted for these experiments. Precise details of the construction and operation of these static strain recorders are given in a brochure issued by Savage and Parsons with each instrument. To economise on the amount of wire used, one short lead from each of the gauges was connected to one of two common terminal boxes, and then through a common 'bus-bar' lead to the instrument, precautions being taken to eliminate bus-bar errors, the effects of which are detailed later.

It was necessary to use a short gauge length strain gauge, and a nominal length of ½ in. was decided upon. First attempts to use the British Thermostat ¼in. X 4 mm. gauges with a nitro-cellulose adhesive were unsatisfactory, but, as they were considerably cheaper than the Tinsley gauge (6 mm. X 1.5 mm. which gave, however, excellent results), further tests were made and it was found that the British Thermostat

gauges were very reliable when baked on the specimen with a phenol formaldehyde resin cement. The actual positions of the strain gauges on the various specimens are shown in Figs. 32 to 36.

The tests on these gauges and the technique used for cementing strain gauges is described in detail later, from which investigation the required calibration figures have been obtained for use in this research.

3. Indication of Other Quantities.

Make-and-break trips on the drive shaft and the cage of the expander cage were connected to voltmeters on the photographic recording panel (Fig. 15). The circuits were actuated by a battery so that each revolution of the mandrel and each half revolution of the cage were recorded by the camera. The cage relay circuit also rang a bell so that the three observers could note the readings from the dial gauges and spring balance. In the Trial Experiment, only one trip per cage revolution was used giving fourteen second intervals between readings. A stop clock mounted on the recording panel gave a true time base.

Plumber's resin melted onto both faces of the plate was intended to give an estimate of the extent of plastic yielding, the technique being that described by Blair (9).

4. Cinematograph Technique.

A 35 mm. Ensign box type cinematograph camera, with an F 3. 5 Zeiss lens and diaphragm was used, mounted on a suitable stand and driven by a variable speed electric motor (see Fig. 15). It was estimated that it would require eight frames per second to be sure of following the movement of the microammeter pointers adequately. With this particular camera shutter, the corresponding exposure time is approximately 1/16 second. In the Trial Experiment Ilford H.P.3 film was used but the grain size was rather coarse and the graduations on the microammeters could not be easily read. Another disadvantage was that the camera could only deal with 30 metre lengths of film which meant that, taking eight frames per second, the film would last for only 2½ minutes, whereas about 3½ minutes were required for a full test. A complete record of the Trial Experiment was in fact not obtained.

The Trial Experiment showed immediately that a camera speed of eight frames per second was too high. A speed of four frames per second was finally used giving an exposure time of 1/8 second. Ilford Pan. F film, which is much 'slower' and has a smaller grain size and higher contrast than Ilford H.P.3 was employed. Two Osram No. 1 photoflood bulbs at a distance of three feet from the panel were used as illumination, the aperture of the camera being set at F.8. Excellent results were obtained under these conditions, and with the camera speed halved, a 30 metre length of film now lasted for 4½ minutes,

adequate for a complete phase of an experiment. The film was left in its negative form, and read either under a microscope or by projection through an enlarger onto a screen.

STRAIN GAUGE TECHNIQUE AND CALIBRATION.

1. Introduction.

Electrical resistance strain gauges were used extensively in this research. Although the use and characteristics of these gauges are now well known, there are still many problems which are encountered where existing information is inadequate, particularly for the newly developed short gauge length gauges.

Several difficulties had to be surmounted in the present investigation, and, in addition, methods of analysis of the measured strains were developed. While the topics discussed in this section are not necessarily inter-related, it is nevertheless felt that the solutions which were found to the various problems should be recorded, as they may well be of interest and use to other investigators.

2. Standard Procedure.

Although resistance strain gauges are now very widely used, each investigator who has applied them personally in large numbers develops his own technique, since the care taken in attaching and connecting up the gauges is the main factor in ensuring consistent and reliable results.

The technique, which has been standardised in the Mechanical Engineering Department of the College, was originally developed for Tinsley strain gauges. It is as follows:-

(i) Preparation of the surface of the specimen by roughening with grade 0 emery cloth to provide a key for the cement, followed by thorough cleaning and degreasing with acetone.

(ii) Preparation of the gauge by quickly wiping the surface to be stuck with acetone.

(iii) Even application of the nitro-cellulose cement to the surface. The cement used was 'High Solids Durofix', i.e. ordinary Durofix with other constituents added to reduce 'creep' of the gauge under strain.

(iv) Application of the gauge to the surface. To ensure perfect adhesion it is necessary to squeeze out all surplus cement from under the gauge, maintaining a slight pressure for about ten minutes. This is best achieved with flat surfaces by the application of a 1 lb. weight to the gauge, but a rotating movement of the finger is often preferable particularly on curved surfaces.

(v) Allowing the gauge to dry in air for from 4 to 5 days. This is very important.

(vi) Drying out the gauge under an infra-red lamp for about 6 hours.

(vii) Immediate application of M Jell 171 to a thickness of about $\frac{1}{8}$ in. M Jell is a protective wax coating which moisture proofs the gauge, thus preventing electrolosis of the gauge grid, 'leakage to earth', and straining of the gauge due to swelling of the matrix which might occur in very damp atmospheres.

(viii) Measurement of the leakage to earth (i.e. the insulation resistance between the gauge grid and the metal surface). An insulation resistance of about 150 megohms is usually possible with nitro-cellulose cement, and when this value has been reached it is safe to assume that all the moisture and acetone have been dried out. The insulation resistance can be measured with the Savage and Parsons unit by a slight modification of the circuit, and this is described in detail later.

(ix) Measurement of the resistance of the gauge grid. This should be within the makers' tolerances.

(x) Short lengths of wire are soldered to the strain gauge leads and secured to the specimen, either by taping if the specimen is of suitable size and form, or by tying the leads with a fine cord and securing the cord to the specimen with Chatterton's compound. It is necessary to prevent the full weight of the leads being transmitted to the gauge.

A high insulation resistance is necessary since a low resistance to earth introduces errors in the measurement of the fractional resistance change resulting from the application of strain. This is also demonstrated later.

In the main investigation, British Thermostat gauges were chosen as being cheaper and more readily obtainable than Tinsley gauges. The British Thermostat gauges are normally supplied with ordinary Duxofix on their surfaces, so that it

is only necessary to dip them in acetone to soften the cement and then apply them in the normal way. (Unlike Tinsley gauges which are bonded with a nitro-cellulose cement, British Thermostat gauges are bonded with a resin and are therefore not soluble in acetone). Since High Solids Durofix is superior to ordinary Durofix, the gauges were ordered specially from British Thermostat, to be untreated, so that the cementing procedure described above could be carried out.

3. Behaviour of British Thermostat Gauges.

Difficulty was experienced when the above technique was used with British Thermostat gauges, especially those of the shorter $\frac{1}{4}$ in. gauge length, although it was entirely satisfactory with Tinsley gauges of short gauge length. The $\frac{1}{8}$ in. Tinsley (and more recently the $\frac{1}{8}$ in. gauge length Tinsley) gauges have been frequently used with consistently accurate results, and it was not anticipated that any difficulty would arise with the $\frac{1}{4}$ in. British Thermostat gauges.

However, in the Trial Experiment, the $\frac{1}{4}$ in. 200 ohm British Thermostat gauges gave inconsistent results when measuring the residual strains in the plate. The gauges had been purchased as a large batch in order to ensure close limits for the sensitivity factors of all the gauges, and since delay in the delivery of the Tinsley gauges would have meant a serious delay in the experimental work, it was decided to investigate the cause of the erratic behaviour of the gauges. Accordingly,

extensive tests were made to determine the characteristics of the ¼ in. British Thermostat gauges.

The tests were all carried out by cementing the gauges to steel beams and calibrating them in the normal way, in the standard four-point loading apparatus shown in Fig. 28. The fractional resistance change of the gauges was measured by the Savage and Parsons Static Strain Recorder. Calibration was generally carried out by straining the gauge either in tension or compression from zero to about 0.1% strain, readings being taken for both increasing and decreasing strain. Particular attention was paid to the initial calibration, since in an application where permanent deformation of the test surface (such as in this tube expanding work) occurs, there would be no opportunity to 'settle in' the gauge by repeated applications of load before actually carrying out a test. Tests were also made to determine the 'creep' of the cement under the steady application of 0.1% strain.

Typical initial calibration curves for both the ¼ in. 200 ohms and ¼ in. 400 ohms British Thermostat gauges, supplied untreated and cemented using the technique outlined above with High Solids Durofix are shown in Figs. 37 and 38. Typical creep-time curves for these gauges are shown in Fig. 39.

These results show that the gauge sensitivities vary greatly from gauge to gauge, probably indicating faulty cementing, whilst there is a pronounced difference between ascending and descending values, culminating in a large residual

zero error. It was found that the difference between ascending and descending values could be partly eliminated by successive straining of the gauge for about six or seven cycles, but the sensitivities remained sensibly the same.

Further tests were carried out on ½ in. 200 ohms British Thermostat gauges, with cemented back as normally supplied by the makers. Typical calibration curves and 'creep' curves for these tests are shown in Figs. 40 and 41. These results indicate little improvement on the previous tests, the sensitivities are perhaps more nearly equal, but the higher rate of creep of the ordinary Durofix is clearly shown. The above results have since been broadly confirmed by the Research Department of the Royal Aircraft Establishment, Farnborough, who carried out similar tests on these ½ in. 200 ohms British Thermostat gauges at our request. They confirm that the sensitivities vary by about ± 6% over any batch of gauges tested, and that the average figure obtained for the sensitivity is much lower than that quoted by the makers (1.99). Gauges applied by the makers on our calibrating bars showed no better results.

Many more tests were made, the cementing technique being varied in several ways, e.g. increased drying times and omission of Bi Jell, but the results were generally as outlined above. The best results obtained were by using the untreated gauges with High Solids Durofix, the gauges being thoroughly soaked in acetone before application to the steel with its

layer of Durofix, and the drying out time being increased to about 14 days in air, 8 hours infra-red. Typical results are shown in Fig. 42 from which it can be seen that the sensitivities are not exceptionally different from one another, and the 'looping' of the graphs is small.

From these tests it was decided that short length resin-bonded gauges of this type are not suitable for cementing to steel with nitro-cellulose cement, complete drying out of all the cement under the gauge grid being much more critical than with the longer gauge length gauges. It is, of course, difficult for the acetone solvent in the Durofix to evaporate away as it is restricted to evaporating from the sides of the gauge grid, passage upwards through the resin being practically impossible. The bond of the gauge matrix is also not homogeneous because the Durofix permeates up into the gauge paper backing for some indeterminate distance. Above the backing there is the paper to which the gauge grid itself is bonded (also to some indeterminate extent) by the resin baked on during manufacture of the gauge. It is thought that soaking the gauge in acetone immediately prior to sticking, softens the paper backing of the gauge and allows the Durofix to permeate more easily up into closer proximity to the gauge grid.

As a result of all these experiences, it was decided to try baking the gauges on to the steel with a resin cement. The cement used was 'Rockite' J 153, a resin of the pure phenol-formaldehyde type supplied by British Resin Products, Ltd. It

was found necessary to interpose a piece of 0.0015 in. thick tissue paper between the gauge and the steel to ensure efficient adhesion, and the final technique adopted was as follows:-*

(i) Thorough cleaning and degreasing surface with carbon tetrachloride, followed by acetone.

(ii) Application of layer of resin cement to surface (with a small paint brush).

(iii) Application of layer of tissue paper.

(iv) Application of layer of resin cement.

(v) Application of gauge.

(vi) Application of layer of greaseproof paper over gauge.

(vii) Application of felt pad.

(viii) Application of slight pressure in the form of a flat weight.

(ix) Baking complete assembly in an oven at 120°C. for about 16 hours.

(x) Soldering short lengths of wire, and application of coating of Mi-Jell over gauge as before.

---

* This method is generally as outlined by the Vibrations Research Department of De Havillands (Propellers), to whom acknowledgement is made for their information.

Very good results were obtained using this technique, as shown in Figs. 47 to 48. Tests were made on gauges, having varied the baking temperature between 80°C. and 120°C., as shown. It was found that the gauge sensitivities were sensibly the same from one gauge to another, and all much higher than those obtained with the nitro-cellulose cement. Since this resin cement seems to permeate right through the gauge and transform it from a paper gauge into a gauge made from plastic, the higher gauge sensitivities obtained may be due to the greater activity of the top layer of wires of the two layer strain gauge grid.* A marked effect of baking temperature on the creep characteristic was noted, as shown. The creep when baked at 80°C. appears to be even greater than that of ordinary Durofix used with these gauges, whilst baking at 120°C. appears to eliminate creep altogether. The insulation resistance of gauges baked on in this way was found to be very high, of the order of 3000 megohms.

Finally, gauges cemented on to calibrating beams using this new technique were strained up to 0.2% strain and taken through a large number of cycles of strain, their characteristics still remaining unchanged. It was also checked that re-baking the gauges for a further period of time without pressure would not affect them, as shown in Fig. 49. This was necessary since

---

* The Tinsley gauge is wound as a flat grid, the British Thermostat is wound on a circular former and flattened.

it was convenient to bake the gauges on one side of a specimen first, then turning the specimen over to bake the gauges on the other side.

On the basis of these results it was decided to bake all the gauges on to the smallest and intermediate sized specimens. Owing to the size of the largest specimens, 8 x 1.5 mm. 50 ohm and 17 x 2.5 mm. 100 ohm Tinsley strain gauges were used to determine the static residual strains, and $\frac{1}{8}$ in. x 4 mm. 400 ohm British Thermostat gauges soaked in acetone immediately prior to sticking, for measuring the dynamic strains, all cemented onto the plate with High Solids Durofix. Initial calibration curves for the Tinsley gauges are shown in Fig. 50.

Since the temperature necessary to apply plumber's resin is 120°C. (See Bibliography, Ref. 9) plumber's resin as applied immediately after removing the specimens from the oven in the case of the smallest and intermediate sized specimens. For the largest specimen it was necessary to apply the plumber's resin before cementing the gauges onto the steel, as had been done for the first specimen used in the Trial Experiment.

In all cases the compensating gauges were cemented to suitable sized discs of the boiler plate at the same time and with the same technique as the active gauges. They were held in close proximity to the specimen in order to minimise 'zero drift'*.

---

* See next section for definition.

4. Zero Drift.

Definition. Zero Drift is a term used to denote the apparent fractional resistance changes which may be observed over fairly long periods after having initially zeroed a circuit. It is due to random causes such as temperature, humidity, and other atmospheric changes, and possible changes in the electrical characteristics of the circuits.

It was found that the main factor causing zero drift was fractional resistance change due to differential temperature changes between active and dummy gauges, and not thermo-electric e.m.f's. This was ascertained by heating the specimen with its active gauges, and observing the consequent zero drift. The bridge voltage was then quickly reversed in polarity and the zero drift again noted. Since reversal of the bridge voltage does not alter the sense of the bridge unbalance due to fractional resistance change, but does alter the sense of bridge unbalance due to thermo-electric e.m.f's, the amount of unbalance due to thermo-electric e.m.f's could be found. The magnitude of unbalance due to this effect was never greater than the equivalent of 0.00025 per cent fractional resistance change, the applied voltage being 2V only (gauge current 5 mA).

Now the zero drift from all causes was, in the worst case (Trial Experiment), 0.029 per cent fractional resistance change, so that increasing the bridge voltage to reduce the errors due to thermo-electric e.m.f's as suggested in an article by Urwin and Swainger (10) was not justified in this instance.

It was found, in fact, that increasing the bridge voltage did not reduce zero drift to any appreciable extent, but it was decided to increase the bridge voltage from 3V to 6V for the later experiments using the British Thermostat gauges since this considerably reduced the time necessary to take readings from the static strain recorder. The gauge current was then 15 mA. A voltage of 3V was used for the experiment on the largest specimen giving a gauge current of 15 mA through the 17 X 2.5 mm. 100 ohms Tinsley gauges, and a current of 30 mA through the 8 X 1.5 mm. 50 ohms gauges.

It is thought that the British Thermostat gauges are more susceptible to zero drift than are the Tinsley gauges, due possibly to the different type of wire used, although no extensive tests have been carried out to prove this. The differential coefficient of linear expansion between the gauge wire and the metal on which the gauge is cemented also plays a part in producing zero drift, and it may well be that the one manufacturer's gauge is more suitable for a given metal than the other's.

In addition to the usual precautions against zero drift, an extra precaution was taken, in that another small disc of boiler plate having gauges cemented to it was clamped to the outside edge of the specimen, the gauges being wired into the active side of the Savage and Parsons instrument. These gauges were unstrained during an experiment, and the mean value of their zero drift was used as an indication of the probable mean zero drift of all the gauges on the specimen. This could be shown to

be true by simply taking readings of zero drift from time to time prior to an experiment, and comparing the zero drift of the gauges on the specimen with that of the 'reference' gauges. Such a set of results is shown in Table 1, from which it can be seen that these reference gauges do, in fact, give a fair indication of the mean zero drift of the gauges on the specimen.

The ideal method for reducing zero drift is to cement the compensating gauges to small strips of the material under test and secure each strip to the specimen beside its active gauge. This method, suggested by Dr. Carlson of Messrs. Babcock and Willcox and mentioned in the brochure of Savage and Parsons could not be used owing to space limitations.

As shown in Appendix 2, the strain at the edge of the plate is very small and is in fact zero at an angle of approximately 28 degrees to the radial direction. Also, it is thought that there is virtually no zero drift between active and compensating gauges cemented to the same piece of material. It is therefore suggested that in future experiments the zero drift may be reduced still further by cementing the compensating gauges around the edge of the disc so that their longitudinal axes lie at an angle of approximately 28 degrees to the radial direction.

5. Calibration of Strain Gauges.

Throughout this work the four-point loading apparatus already mentioned has been used for calibrating the gauges. For accurate results, allowance must be made for the finite thickness of the gauge, the effective strain being measured not at the extreme fibre of the calibrating beam, but at a small distance beyond it. Allowance can be made for this in determiningthe gauge factor, as follows:-

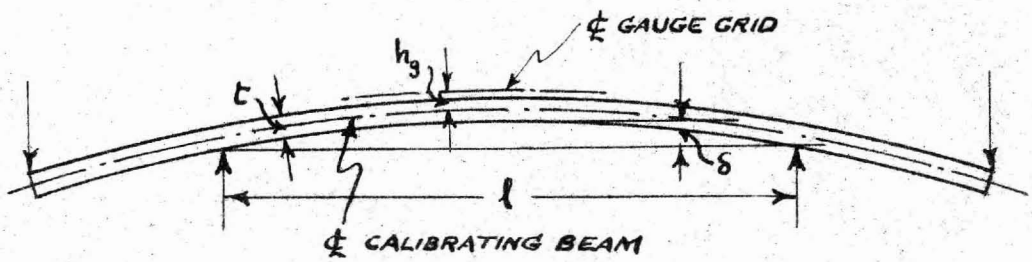

Referring to the diagram above, if e = the strain along the surface of the beam, then

$$e = \frac{\delta t}{\delta^2 + \frac{l^2}{4}}$$, and, neglecting δ^2 in comparison with $\frac{l^2}{4}$.

$$e = \frac{4t}{l^2}\delta$$

Thus, if the dimensions of the beam are such that t = 0.25 in., l = 10 ins.,

$e = \frac{\delta}{100}$, i.e. δ measured in inches would give the per cent strain at the surface of the beam.

Now, if it is assumed that the strain in any longitudinal fibre of the strain gauge is proportional to its distance from the neutral surface of the beam, then

$$\frac{e_g}{e} = \frac{2h_g}{t}$$

$$\therefore e_g = \frac{2h_g}{t} \times \frac{4t}{l^2}\delta = \frac{8h_g\delta}{l^2}$$

$$\therefore e_g = 0.08h_g\delta \text{ , if } l = 10 \text{ ins.}$$

Thus $\frac{e_g}{\delta} = 8h_g$, where e_g is the per cent strain at the gauge grid.

In the case of gauges baked on with resin cement.

$h_g = \frac{t}{2}$ + thickness of cement (+ thickness of tissue paper + thickness of cement)

+ distance of centre-line of gauge grid to surface of gauge

Thickness of cement taken as 0.001 in. for both Durofix and Resin cement.

Thickness of tissue paper as 0.0015 in.

Surface to centre-line of gauge as 0.007 in. for British Themostat gauges.

0.003 in. for Tinsley gauges.

Now $S' = \frac{k_g}{e_g}$ where k_g is % fractional resistance change,

e_g is % strain along the gauge grid.

$$\therefore S' = \frac{k_g}{\delta} / \frac{e_g}{\delta} = \frac{k_g}{\delta} / 8h_g$$

$\frac{k_g}{\delta}$ may be determined by plotting k_g against δ and finding the slope of the graph or the mean slope if more than one gauge is calibrated.

6. Strain Analysis from Resistance Strain Gauge Readings.

The readings given by resistance strain gauges must be interpreted in relation to the nature of the strain field existing in the particular application under consideration. In the present investigation, certain corrections have to be applied to the readings and the main items are discussed in the following sections:-

(i) Effect of transverse sensitivity of gauge to strain.

Consider strain gauge to be on a field of strain e_1 and e_2 as shown below:-

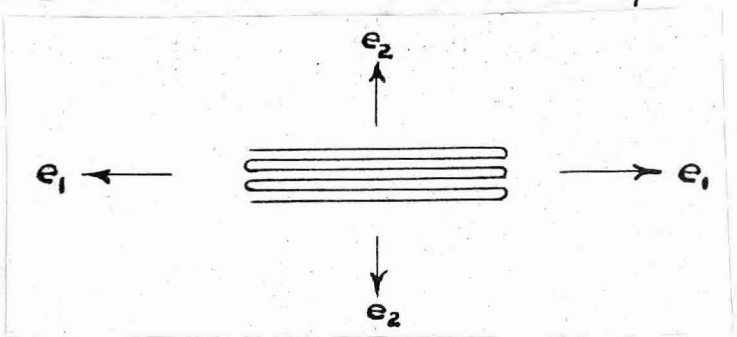

Then, if k_1 is the fractional resistance change due to e_1 only

k_2 is the fractional resistance change due to e_2 only

$k_1 = Se_1$, and

$k_2 = Te_2$.

Hence, the total fractional resistance change recorded is

$$k = k_1 + k_2 = Se_1 + Te_2 = Se_1 + \lambda Se_2 = S(e_1 + \lambda e_2).$$

In the experiments under consideration, very approximately

$e_2 = -e_1$ (condition for pure shear)

$k = S(e_1 - \lambda e_1) = Se_1(1 - \lambda)$, or

$$e_1 = \frac{k}{S(1-\lambda)} = \frac{k}{S''} \qquad \ldots\ldots\ldots(1)$$

By cementing gauges to a surface which is subjected to

a field of strain such that e_2 is zero, the cross-sensitivity may be determined fairly accurately. A curved sheet of steel subjected to bending produces such a field of strain, since there is no anticlastic bending provided that the width of the sheet is large compared with its thickness. In a separate investigation carried out in the College the value of λ has been experimentally determined for several different types of gauges. The values relevant to this research are approximately as follows:-

Make	Resistance in ohms	Gauge length	Gauge Width	λ per cent
Tinsley	100	17 mm.	2.5 mm.	+ 2
Tinsley	50	8 mm.	1.5 mm.	+ 2
British Thermostat	400	½ in.	4 mm.	- 1
British Thermostat	200	½ in.	4 mm.	- 2

By using the normal form of calibrating beam subjected to four-point loading, a spurious value for S is found, namely S', due to the small transverse strain induced by the anticlastic bending of the beam. This transverse strain may be taken approximately as

$e_2 = -\nu e_1$, provided that the beam is not very wide in relation to its thickness.

Hence, in the calibration of the gauges,

$k = S(e_1 + \lambda e_2) = Se_1(1 - \lambda\nu)$.

$$\therefore \quad e_1 = \frac{k}{S'} = \frac{k}{S(1-\lambda\nu)} \qquad \ldots\ldots(2)$$

From (1),

$$S'' = S(1-\lambda)$$

From (2)

$$S' = S(1-\lambda\nu)$$

$$S'' = \frac{1-\lambda}{1-\lambda\nu} S' \qquad \ldots\ldots(3)$$

Equation (3) gives the value of the apparent sensitivity to be used in these experiments in terms of the apparent sensitivity measured on the normal calibrating beam, the necessa ry allowance for transverse sensitivity of the gauges having thereby been made.

The factor $\frac{1-\lambda}{1-\lambda\nu} \triangleq 1 + \lambda\nu - \lambda$, neglecting terms of second order and higher

$$S'' = \left[1 - \lambda(1-\nu)\right] S'$$

Assuming $\nu = 0.3$ for the material of the calibrating beam

$$\underline{S'' = (1 - 0.7\lambda)\, S'}$$

(ii) <u>Correction to be made to allow for variation of the strain field under the strain gauge grid.</u>

It is assumed that there are three strain gauges positioned with the centre-lines through their grids at distances x_1, x_2, and x_3 from some arbitrary reference point as shown on the diagra m overleaf. l_g is the length of the gauge grid (or width, depending on the direction of the strain e in reference to the direction x). To fix ideas, it is assumed that e is the strain in the direction x, that l_g is the <u>length</u> of the gauge grid, and e

does not vary in the direction at right angles to x, i.e. across the width of the gauge.

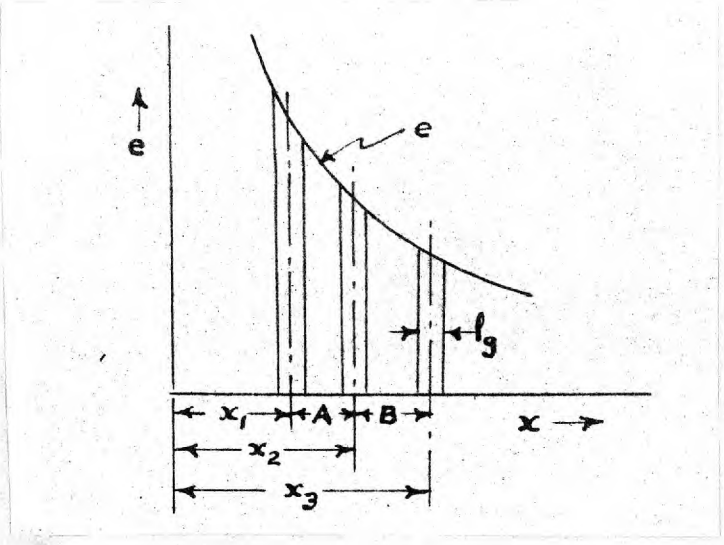

It may be assumed that, in between $x_1 - \frac{l_g}{2}$ and $x_3 + \frac{l_g}{2}$,

$$e = ax^2 + bx + c$$

Thus $e_1 = ax_1^2 + bx_1 + c$

$e_2 = ax_2^2 + bx_2 + c$

$e_3 = ax_3^2 + bx_3 + c$

Where e_1 , e_2 , e_3 are the actual strains at the centre of each gauge grid.

The strains recorded by the strain gauges are, however, assumed to be the mean value of the strains under their grid lengths, thus each strain gauge records a strain such as

$$e_2' = \frac{1}{l_g}\int_{x_2-\frac{l_g}{2}}^{x_2+\frac{l_g}{2}} e\,dx = \frac{1}{l_g}\int_{x_2-\frac{l_g}{2}}^{x_2+\frac{l_g}{2}} (ax^2 + bx + c)\,dx$$

$$\therefore \quad e_2' = a\left(x_2^2 + \frac{l_g^2}{12}\right) + bx_2 + c = e_2 + \frac{al_g^2}{12} \qquad \text{.....(1)}$$

Now the correction to be made to e_2' to give e_2 is $e_2 - e_2'$, since $e_2' + (e_2 - e_2') = e_2$, thus the correction is

$$e_2 - e_2' = e_2 - e_2 - \frac{al_g^2}{12} = -\frac{al_g^2}{12}$$

It is now necessary to determine a in terms of the observed strains e'_1, e'_2, e'_3 and the distances A and B between the gauges (as shown on the diagram).

Now
$$e'_1 = \left(x_1^2 + \frac{l_g^2}{12}\right)a + x_1 b + c$$
$$e'_2 = \left(x_2^2 + \frac{l_g^2}{12}\right)a + x_2 b + c$$
$$e'_3 = \left(x_3^2 + \frac{l_g^2}{12}\right)a + x_3 b + c$$

$$\therefore \quad a = \frac{\begin{vmatrix} e'_1 & x_1 & 1 \\ e'_2 & x_2 & 1 \\ e'_3 & x_3 & 1 \end{vmatrix}}{\begin{vmatrix} x_1 + l_g^2/12 & x_1 & 1 \\ x_2 + l_g^2/12 & x_2 & 1 \\ x_3 + l_g^2/12 & x_3 & 1 \end{vmatrix}}$$

But $x_1 = x_2 - A$, and $x_3 = x_2 + B$

$$\therefore \quad a = \frac{Be'_1 - (A + B)e'_2 + Ae'_3}{AB(A + B)} \qquad \text{.....(2)}$$

Hence the correction term $\epsilon_2 - e'_2 = -\frac{a l_g^2}{12}$

$$= \left[(A + B)e'_2 - Ae'_3 - Be'_1\right] \frac{l_g^2}{12AB(A + B)}$$

If A = B, then the correction term $\epsilon_2 - e'_2$

$$= \frac{2e'_2 - e'_3 - e'_1}{24}\left(\frac{l_g}{A}\right)^2 \qquad \text{.....(3)}$$

An alternative method of plotting strain gauge results to give some indication of the length of the gauge grid in relation to the distribution of the strain under the gauge, is to plot the results in the form of a histogram as shown overleaf.

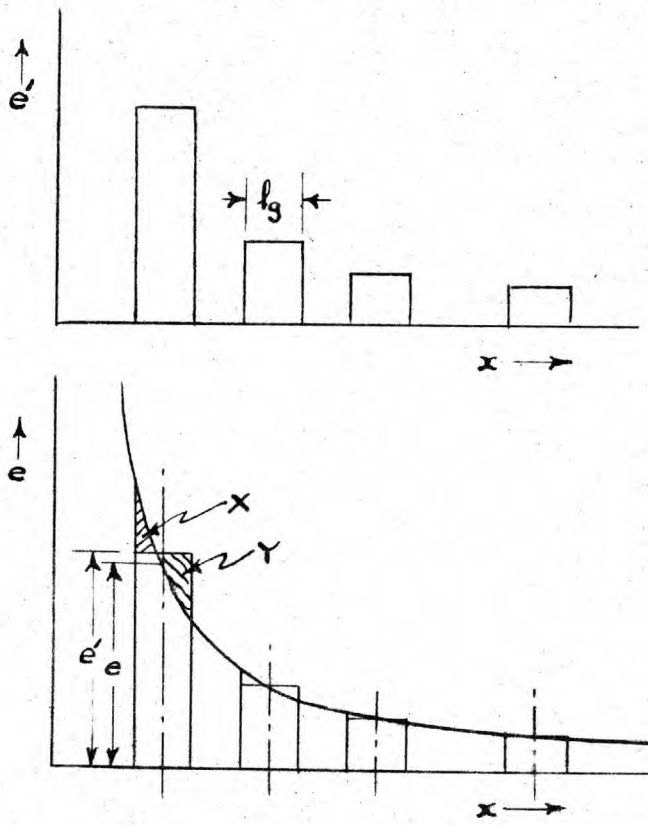

A curve may then be drawn through the results in such a way that area X ≏ area Y for each gauge.

This method of plotting has been adopted for some of the experimental residual strain distributions obtained. In order to estimate the errors introduced by the rapid strain gradient across the grid during the measurement of the dynamic strains, the following analysis has been made, in which correction factors are derived from consideration of the measured residual strain distribution.

From Experiment 2, between $\frac{r}{r_o} = 1.75$ and 3.42

$e'_1 \triangleq -1000$
$e'_2 = -75.9$
$e'_3 = -20.5$

} For convenience, these figures, which are per cent fractional resistance change X 10^3, have been taken.

Also $l_g = \frac{1}{4}$ in., $A = \frac{5}{8}$ in., $\therefore \left(\frac{l_g}{A}\right)^2 = \frac{4}{25}$

Thus the correction to $e'_2 = e_2 - e'_2 = \frac{2e'_2 - e'_1 - e'_3}{24}\left(\frac{l_g}{A}\right)^2$

$$= \frac{-151.8 + 1021}{24} \cdot \frac{4}{25} = +5.79$$

Thus $e_2 = -75.9 + 5.79 = -70.1$

Similarly, from the same experiment, between $\frac{r}{r_o} = 2.58$ and 4.25

$e'_1 = -75.9$
$e'_2 = -20.5$
$e'_3 = -12.7$

$$\left(\frac{l_g}{A}\right)^2 = \frac{4}{25}$$

$$e_2 - e'_2 = \frac{-41 + 88.6}{24} \cdot \frac{4}{25} = 0.318$$

Thus $e_2 = -20.18$

Summarizing, between $\frac{r}{r_o} = 1.75$ and 3.42,

$e_1 \triangleq -1000$
$e_2 = -70.1$
$e_3 = -20.18$

Now, from equation (1), $e'_2 = e_2 + \frac{A l_g^2}{12}$, where

$$a = \frac{\begin{vmatrix} e_1 & x_1 & 1 \\ e_2 & x_2 & 1 \\ e_3 & x_3 & 1 \end{vmatrix}}{\begin{vmatrix} x_1^2 & x_1 & 1 \\ x_2^2 & x_2 & 1 \\ x_3^2 & x_3 & 1 \end{vmatrix}} = \frac{Be_1 - (A + B)e_2 + Ae_3}{AB(A + B)}$$

$$a = \frac{e_1 - 2e_2 + e_3}{2A^2} \quad , \text{ if } A = B$$

$$\frac{al_g^2}{12} = \frac{e_1 - 2e_2 + e_3}{24} \cdot \left(\frac{l_g}{A}\right)^2$$

For this case, therefore, if $\frac{l_g}{A} = \frac{\frac{1}{2}}{\frac{5}{8}} = \frac{4}{5}$, $\left(\frac{l_g}{A}\right)^2 = \frac{16}{25}$.

This value of $\frac{l_g}{A}$ also applies to the $\frac{1}{2}$ in. gauge length gauges used on the smallest specimen at $\frac{r}{r_o} = 2.58$

$$\frac{al_g^2}{12} = \frac{-1000 + 140.2 - 20.2}{24} \cdot \frac{16}{25} = -23.5$$

Thus $e'_2 = -70.1 - 23.5 = -93.6$

Hence, at this point on the smallest specimen, the strain measured by the $\frac{1}{2}$ in. gauge length gauges should be reduced by approximately

$$\frac{23.5}{93.6} \times 100 = 25\%$$

The position is worse for the dynamic gauges which are double this length, since $\left(\frac{l_g}{A}\right)^2$ is then increased four times and $\frac{al_g^2}{12}$ becomes -94.

Thus $e'_2 = -70.1 - 94 = -164.1$, and a correction of $\frac{94}{164.1} \times 100 = 57.3\%$ reduction in the observed strains would have to be made to arrive at the true strain at the mid-point of the gauge. Consequently, in Experiment 3 on the smallest sized specimen, the instruments recording the dynamic radial strains at $\frac{r}{r_o} = 1.875$ exceeded full-scale deflection.

Summarising, the corrections necessary to the dynamic radial strains recorded at $\frac{r}{r_o} = 2.5$ are approximately as follows:-

Smallest Specimen. No 3. - Reduce observed readings by 57%

Intermediate - Fixed Specimens. Nos. 1 and 2 - Reduce observed readings by 25%.

Largest Specimens. Nos. 4 and 6 - Reduce observed readings by 8%.

The correction is negligible for all other gauges recording dynamic strains.

From this analysis it can be seen that only from the largest specimens will some idea be obtained of the actual radial strains at this point, although for all the specimens these gauges will indicate the relative magnitude of the strains as between the front and back of the plate.

(iii) Estimation of the error introduced by the use of rectangular strain gauges on circular strain fields.

Consider a strain gauge having a grid size l_g X b_g recording the radial strain on an axially symmetrical circular field of strain such that $e_r \triangleq - e_\theta$.

Radial strain.

If e_r is the radial strain at any radius r (principal strain)

e_θ is the circumferential strain at the radius r (principal strain)

e is the strain at angle θ to principal plane

ϕ is the angle subtended by the grid at radius r

(see diagram overleaf for indication of these symbols)

Then $\frac{\partial e_r}{\partial \theta} = \frac{\partial e_\theta}{\partial \theta} = 0$

Consider elements of the wire grid at radius r angle θ to the centre-line through the grid, as shown:-

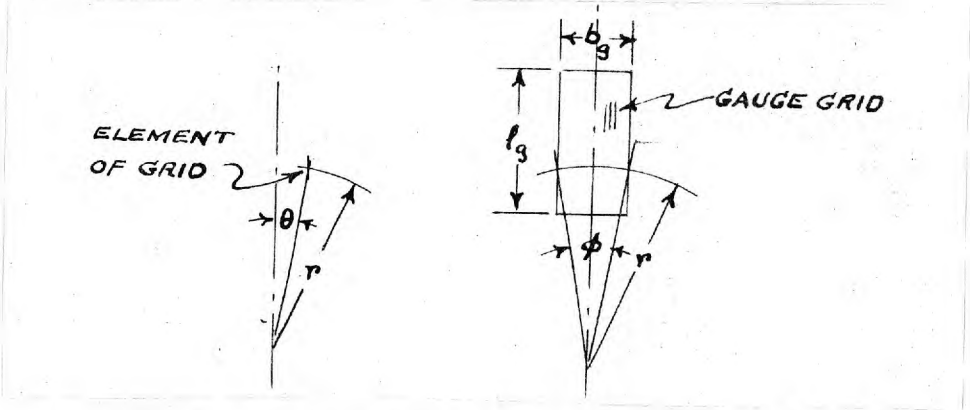

Then strain along the element of wire = $e = \frac{e_\theta + e_r}{2} - \frac{e_\theta - e_r}{2}\cos 2\theta$

For an infinite plate, $e_r = -e_\theta$

$$e = e_r \cos 2\theta$$

Hence, around an arc of radius r , the mean strain measured by such elements of the wire grid

$$\bar{e} = \frac{\int_{-\phi/2}^{\phi/2} e\,d\theta}{\phi} = \frac{\int_{-\phi/2}^{\phi/2} e_r \cos 2\theta\,d\theta}{\phi} = e_r \frac{\sin\phi}{\phi}$$

An ideal strain gauge grid for measuring radial strains would have the shape shown, $r_2 - r_1$ being the minimum possible size, and this ideal strain gauge would record the mean of the radial strains under its grid, viz:-

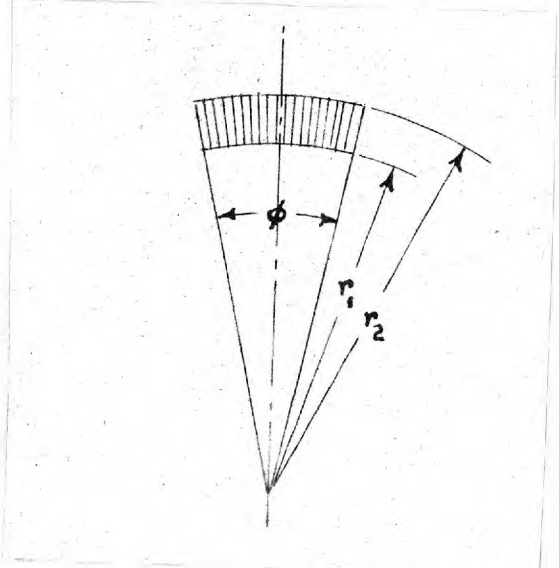

$$\frac{\int_{r_1}^{r_2} e_r\,dr}{r_2 - r_1}$$

Assuming, for simplicity, that the actual strain gauge has the shape shown below:-

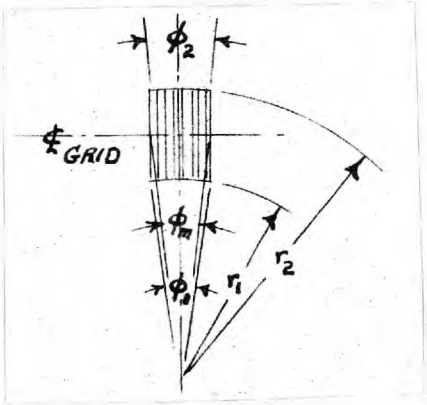

the strain recorded would be $\dfrac{\int_{r_1}^{r_2} e_r \frac{\sin\phi}{\phi}\, dr}{r_2 - r_1}$

where $\frac{\sin\phi}{\phi}$ is a function of r, varying from $\frac{\sin\phi_1}{\phi_1}$ at radius r_1 to $\frac{\sin\phi_2}{\phi_2}$ at radius r_2.

As a first approximation $\frac{\sin\phi}{\phi}$ can be assumed to be a constant for the complete grid and equal to

$\frac{\sin\phi_m}{\phi_m}$, where ϕ_m is the angle subtended at the centre of the grid, at which point $r = \frac{r_1 + r_2}{2} = r_m$.

Then, strain recorded $= \frac{\sin\phi_m}{\phi_m} \dfrac{\int_{r_1}^{r_2} e_r\, dr}{r_2 - r_1}$

The largest error is introduced in this research in the case of the $\frac{1}{8}$ in. X 4 mm. radial gauge situated close to the 1 in. diameter hole in Specimen No. 3.

Then $r_m = \frac{l_g}{2} + \frac{5}{16}$ in. = 0.813 in., b_g = 4 mm. = 0.1575 in.

$$\tan\frac{\phi_m}{2} = \frac{b_g}{2r_m} = \frac{0.1575}{1.626} = 0.09685$$

$$\therefore \quad \frac{\phi_m}{2} = 5^\circ - 32' = 0.09657 \text{ Radians}$$

$\phi_m = 11^\circ - 4' = 0.19314$ Radians

$\sin\phi_m = 0.19195 \quad \therefore \quad \frac{\sin\phi_m}{\phi_m} = 0.993$

Thus the mean strain $\frac{\int_{r_1}^{r_2} e_r\,dr}{r_2 - r_1}$ would be 'underestimated' by the strain gauge by approximately 0.7 per cent.

Circumferential strain.

Consider a strain gauge measuring circumferential strain as shown below:-

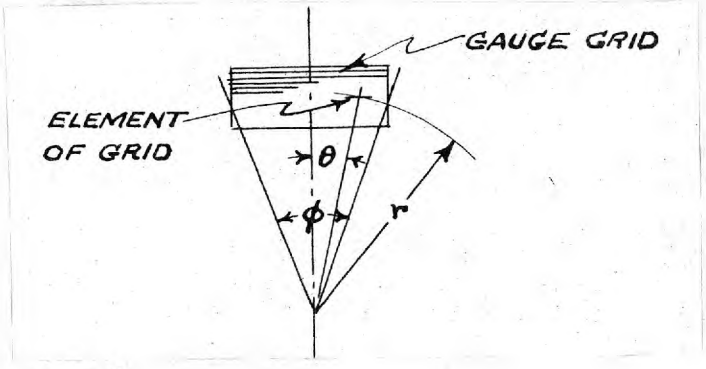

As before, $e = e_\theta \cos 2\theta$

$$\bar{e} = e_\theta \frac{\sin\phi}{\phi}$$

In an 'ideal' strain gauge as shown opposite, in which $r_2 - r_1$ was the minimum possible size, the mean strain recorded would be

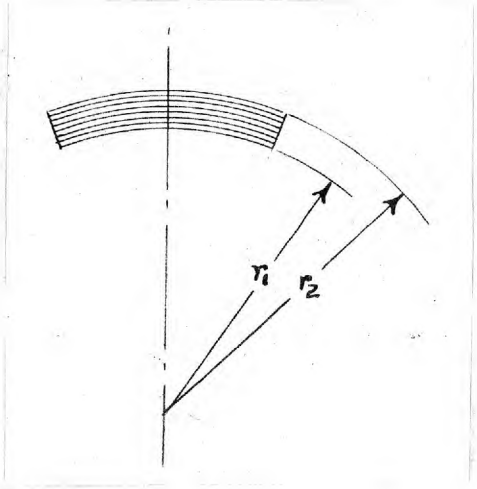

$$\frac{\int_{r_1}^{r_2} e_\theta\,dr}{r_2 - r_1}$$

Actual strain recorded = $\frac{\int_{r_1}^{r_2} e_\theta \frac{\sin\phi}{\phi}\,dr}{r_2 - r_1} \simeq \frac{\sin\phi_m}{\phi_m} \frac{\int_{r_1}^{r_2} e_\theta\,dr}{r_2 - r_1}$

as before.

The largest error is introduced in this research in the case of the ¼ in. gauge length grid situated close to the 1 in. diameter hole of Specimen No. 3.

Then $r_m = 0.813$ in., $l_g = 0.25$ in.

$$\tan \frac{\phi_m}{2} = \frac{l_g}{2r_m} = \frac{0.25}{2(0.813)} = 0.1537$$

$$\therefore \frac{\phi_m}{2} = 8^\circ - 44', \quad \phi_m = 17^\circ - 28' = 0.3049 \text{ Radians},$$

$$\sin \phi_m = 0.3002 \quad \therefore \frac{\sin \phi_m}{\phi_m} = \frac{0.3002}{0.3049} = 0.985.$$

Thus the mean strain $\frac{\int_{r_1}^{r_2} e_\theta \, dr}{r_2 - r_1}$ would be 'underestimated' by the strain gauge by approximately 1.5 per cent.

These errors are negligible.

7. Estimation of the Errors Involved in Using the Static Strain Recorder.

The Savage and Parsons 50 Way Static Strain Recorder was used for all static strain gauge measurements made in the research. It is a very accurate and satisfactory instrument, but certain precautions must be taken for the best results. A simplified circuit diagram of the unit is shown overleaf, on which the symbols used to represent the various resistances and currents in the circuit are indicated.

Considering circuit number 1, when the apex resistor is balanced initially, (the gauges being unstrained), if there are n pairs of active and dummy gauges all having approximately the

same resistance, the current through the bus bar leads $I_{L_1} = I_{L_2} = nI_1$. Hence the condition for balance of circuit number 1 is:-

$$\frac{nI_1 R_{L_1} + I_1 (R_{A_1} + a)}{IR} = \frac{nI_1 R_{L_2} + I_1 (R_{D_1} + b)}{IR}$$

Hence $(R_{A_1} + a) - (R_{D_1} + b) = n(R_{L_2} - R_{L_1})$ .....(1)

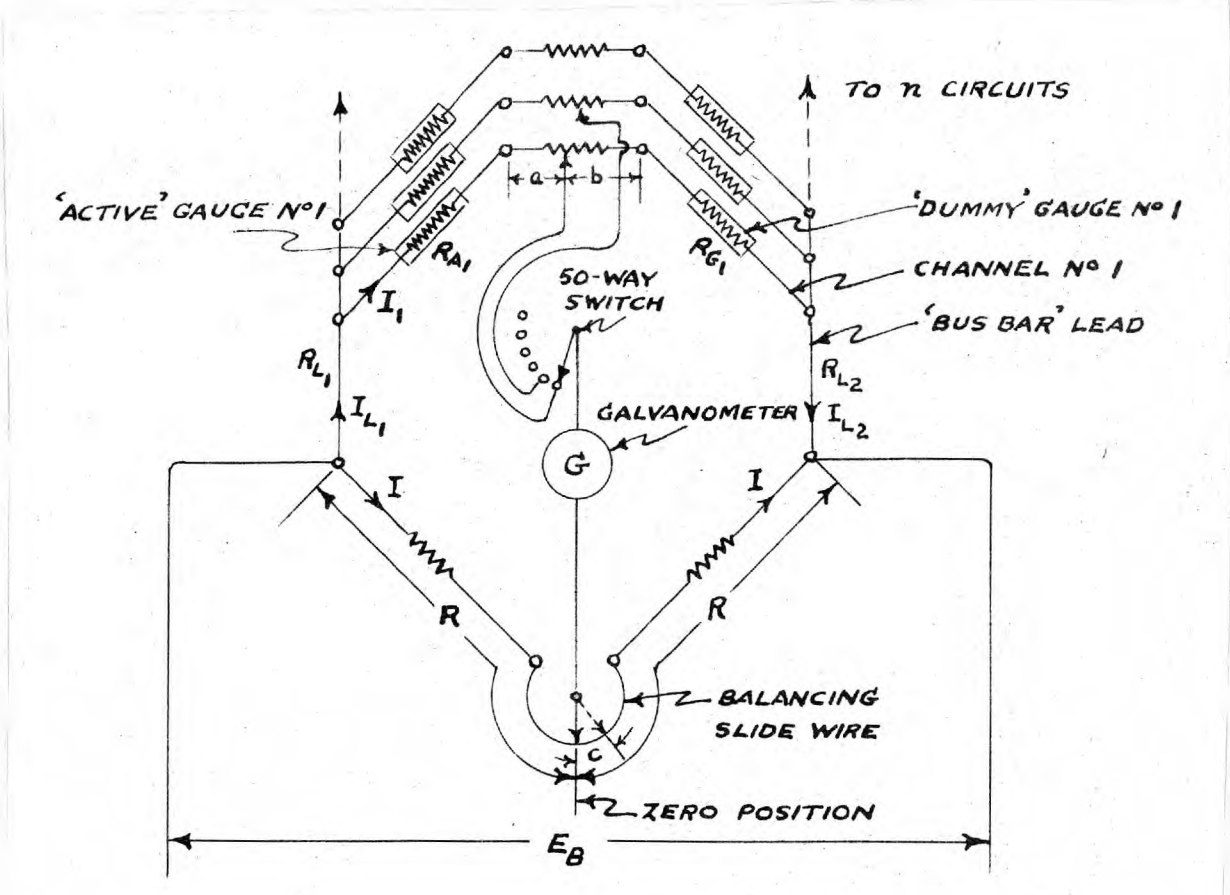

Simplified Circuit Diagram of Savage and Parsons Unit.

For there to be no current flowing through the galvanometer equation (1) must hold. Since n is not always constant, as gauges may be removed or put into circuit, $R_{L_2} - R_{L_1}$ must be zero, unless it is possible to re-zero all the circuits on removal or addition of gauges.

Error introduced on straining active gauge R_{A_1}.

If the resistance of R_{A_1} increases due to straining, to $R_{A_1}(1 + k)$, balance is again obtained by moving the slider so that the left-hand ratio arm (on the diagram) has resistance $R + c$, the right-hand ratio arm resistance $R - c$, so that:-

$$\frac{nI_1 R_{L_1} + I_1\left[(1 + k)R_{A_1} + a\right]}{I(R + c)} = \frac{nI_1 R_{L_2} + I_1(R_{D_1} + b)}{I(R - c)}$$

Hence $$\frac{nR_{L_1} + R_{A_1} + a + kR_{A_1}}{R + c} = \frac{nR_{L_2} + R_{D_1} + b}{R - c}$$

$$= \frac{nR_{L_1} + R_{A_1} + a}{R - c} \qquad \text{(from equation (1))}$$

$$\therefore\ kR_{A_1} = \frac{R + c}{R - c}(nR_{L_1} + R_{A_1} + a) - (nR_{L_1} + R_{A_1} + a)$$

$$\therefore\ k = \left(1 + \frac{nR_{L_1} + a}{R_{A_1}}\right)\cdot\frac{2c}{R - c} \quad . \quad \text{Let } k' = \frac{c}{R}$$

Then $$k = 2k'\left(1 + \frac{nR_{L_1} + a}{R_{A_1}}\right)\frac{1}{1 - k'} \qquad \ldots\ldots(2)$$

Equation (2) gives the actual relation between k and k'. The instrument is calibrated in terms of $2k'$ so that if, for example, $2k' = 0.002$, the dial records 0.002 or 0.2% fractional resistance change.

As a specific example of the errors that may be introduced assume a gauge to be calibrated by itself on the equipment up to a value of 0.1% strain and $2k'$ to be indicated as 0.2%.

Then, if n = 1, $R_{L1} = 0.2\Omega$, $R_{A1} = 100\Omega$, a = 1Ω, 2k' = 0.002, (taking typical figures)

$$k = 0.002\left(1 + \frac{0.2 + 1}{100}\right)(1 + 0.001 + \ldots.)$$

$$= 0.002 \times 1.012 \times 1.001 = 0.002026$$

Error due to a and R_{L1}. Error due to non-linearity of slide wire.

Thus, although the actual gauge factor $S = \frac{k}{e}$ of the gauge $= \frac{0.002026}{0.001} = 2.026$, it would be indicated by the equipment as having an apparent value of $\frac{2k'}{e} = \frac{0.002}{0.001} = 2.000$

If a gauge were calibrated with all the fifty channels in circuit, and 2k' again = 0.2%, then n = 50 in equation (2), and

$$k = 0.002 \times 1.11 \times 1.001$$

Error due to a and nR_{L1}. Error due to non-linearity of slide wire.

$$= 0.002222$$

Thus, although the actual gauge factor of the gauge would be 2.222 in this case, the gauge factor indicated would still be 2.000.

Alternatively, since $2k' = \frac{k}{1.111}$ under these conditions, if the gauge having a true gauge factor $\frac{k}{e} = 2.026$ were now calibrated with all fifty channels in circuit, the indicated gauge factor would now be $\frac{2.026}{1.111} = 1.823$ instead of 2.000, as before, that is to say with an error of -9%.

Conclusions regarding the use of the static strain recorder.

(i) On this equipment, the gauge factor determined from the indicated value will always be lower than the true sensitivity. (Due to the apex resistors, the resistance of the bus bar leads, and to non-linearity of the balancing slide wire).

(ii) The greater the number of gauges connected to the equipment through the bus bars when calibration is being carried out, the lower the apparent sensitivity. (Can be as much as 9% below the apparent sensitivity indicated for the calibration of a single gauge on its own).

(iii) Linearity of strain response is affected only by the inherent inaccuracy of the balancing slide wire circuit, which is negligible for strains below about 0.2% ($\frac{1}{1-k'} \simeq 1 + 0.002 + ..$) and would give approximately the same percentage error as the per cent strain on the specimen tested.

(iv) Calibration of sample gauges must be carried out with the same total number of gauges in circuit as are required in an actual experiment, and the figure obtained for the gauge factor quoted as the apparent sensitivity and used in all subsequent calculations for that experiment in determining strains.

(v) To reduce the error between the apparent sensitivity with a large number of gauges and that with only one gauge, the bus bar leads must have as low a resistance as possible, preferably less than 0.01 ohm, thus reducing the term nR_{L_1} when n is large.

(vi) So that the initial balancing of a channel shall be unaffected by the removal or addition of other gauges to the equipment, the resistances of the bus bar leads must be exactly equal. The worst condition is when n is changed from 1 to 50, or from 50 to 1.

8. Measurement of Insulation Resistance.

The insulation resistance of each active or dummy gauge may be measured by a simple modification of the external circuit on the Savage and Parsons unit as shown below:-

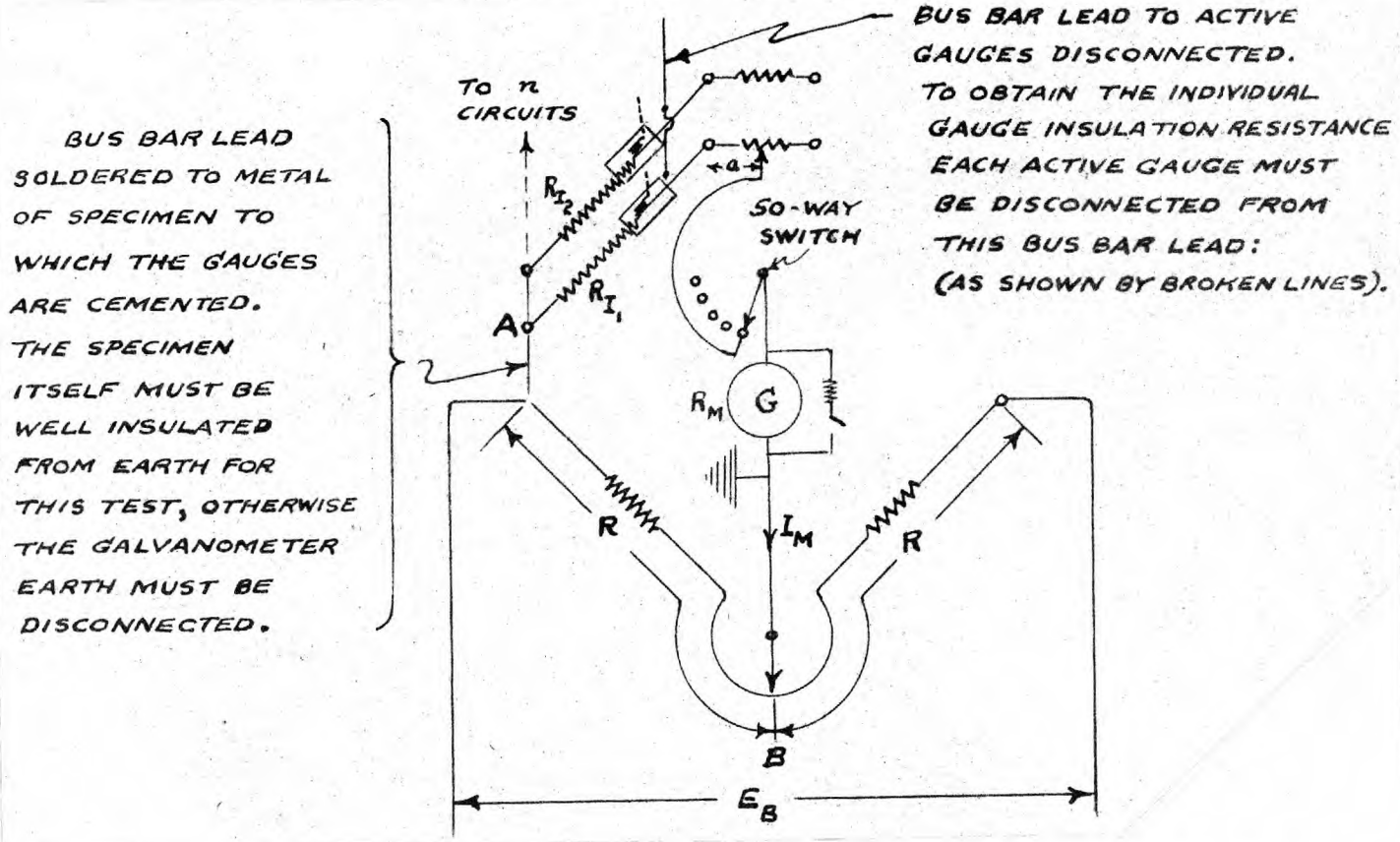

All the dummy gauges are disconnected by removal of the bus bar lead if the insulation resistance of the active gauges is required. The bus bar lead to the active gauges is

disconnected and replaced by a lead soldered to the metal surface of the specimen. To obtain the individual gauge insulation resistance, each gauge is disconnected from this bus bar lead, as shown.

If the galvanometer is now switched on to circuit number 1 the total resistance to passage of current through the galvanometer is $R_{I_1} + a + R_M$. (Where R_{I_1} is the insulation resistance of the active gauge in circuit number 1, a and R_M as shown on the diagram).

Since R_{I_1} is very large ($> 1M\Omega$, say), then $a + R_M$ is negligible in comparison. ($a \doteq 1\Omega$, $R_M \doteq 60\Omega$). Also, the resistance of R_{I_1} and R in parallel is approximately equal to R, since $\frac{1}{R_{I_1}}$ is negligible in comparison with $\frac{1}{R}$. Accordingly, the voltage across the points AB may be taken as $\frac{E_B}{2}$ and the current through the galvanometer is approximately

$$I_M = \frac{E_B}{2R_{I_1}} \qquad \therefore \quad R_{I_1} = \frac{E_B}{2I_M}.$$

Since the deflection of the galvanometer is 113 mm. per μA (unshunted), the actual deflection $D = I_M \times 10^6 \times 113$ mm.

$$\therefore \quad I_M = \frac{D}{113 \times 10^6}$$

$$\therefore \quad R_{I_1} = \frac{E_B}{2D} \times 113 \times 10^6 \text{ ohms, if } E_B \text{ is in volts, D in mm.}$$

$$\therefore \quad R_{I_1} = 56.5 \frac{E_B}{D} \ M\Omega .$$

e.g., if $E_B = 10V$, $D = 5$ mm., $R_{I_1} \doteq 113\ M\Omega$.

To safeguard the galvanometer, which can be shunted so as to give $\frac{1}{10}$, $\frac{1}{100}$, or $\frac{1}{1000}$ of the deflection, and completely shunted, it is advisable to test first at a low voltage in the completely shunted position. If there were a short-circuit in the circuit under measurement, there would then be a small deflection of the galvanometer spot due to the fact that the short length of wire shunting the galvanometer in its completely shunted position would have some small resistance.

It is important to note that the specimen must be adequately insulated from earth for this test, since if it is not, the resistance R will be effectively short-circuited and there will be no voltage applied across the circuit under test. If it is not possible to insulate the specimen from earth, it would then be necessary to disconnect the earth connection of the galvanometer inside the Savage and Parsons equipment.

9. Error Introduced by Low Insulation Resistance.

Let R_G = Resistance of strain gauge wire.

R_I = Insulation resistance of parallel leakage to earth.

k = Fractional resistance change of active gauge due to strain = $\frac{\delta R_G}{R_G}$.

R_C = Combined resistance of gauge and insulation resistance in parallel = $\frac{R_G R_I}{R_G + R_I}$.

k" = Fractional resistance change of combined circuit = $\frac{\delta R_C}{R_C}$

On straining the gauge its resistance changes to $R_G + \delta R_G$

$$\therefore \quad R_c + \delta R_c = \frac{R_I (R_G + \delta R_G)}{R_I + R_G + \delta R_G}$$

$$\therefore \quad 1 + \frac{\delta R_c}{R_c} = \frac{(R_I + R_G)(R_G + \delta R_G)}{R_G (R_I + R_G + \delta R_G)}$$

$$\therefore \quad 1 + k'' = (1 + k) \frac{\frac{R_I}{R_G} + 1}{\frac{R_I}{R_G} + 1 + k}$$

$$\text{Hence } k'' = \frac{R_I k}{R_I + R_G (1 + k)}$$

$$\text{and} \quad \frac{k''}{k} = \frac{R_I}{R_I + R_G (1 + k)}$$

For 0.1% error, $\frac{k''}{k} = 0.999$, hence $R_I = 999\ (1 + k)\ R_G$.

Thus, if $R_G = 400$ ohms, $k = 0.001$, $R_I = 999 \times 1.001 \times 400$

$= 1.001 \times 399{,}600$ say 400,000 ohms.

$$\therefore \quad \underline{R_I \neq 0.4 \text{ M}\Omega}.$$

EXPERIMENTAL PROCEDURE.

Having prepared the tube and plate specimen and secured it to the bed of the apparatus, an experiment was carried out as follows:-

1. Initial zeroing of all strain gauge circuits and rezeroing after about 1½ hours for the static strain gauges, and ½ hour for the dynamic gauges, these times being roughly those necessary for the zero drift to become negligible.
2. Testing of the circuits indicating cage and mandrel rotation.
3. Positioning of the tube in the plate so that it protruded for a distance of about ½ in. (Fig. 1), light rolling in of the tube up to 'nip' on the plate,* and adjustment of the dial gauges recording extrusion.
4. Inserting expander cage and mandrel with the rollers entered tightly in the tube, and engaging the drive unit.
5. Loading camera and switching on floodlights, having previously adjusted focus, diaphragm, and camera speed.
6. Starting stop-clock.
7. Starting camera.
8. Starting expander mandrel rotation.
9. Stopping mandrel rotation, having allowed expanding to continue until the cage of the expander cage met the tube end or until the chosen indicator for the degree of expanding had reached an appropriate value.

---

* Referred to as 'tack rolling'.

10. Stopping camera.

11. Reversing motor rotation and driving device. (Not necessary for the retractive expanders).

12. Starting camera.

13. Starting mandrel rotation in opposite direction to remove the expanders.

14. Stopping mandrel rotation when the torque had dropped to zero.

15. Stopping camera.

This procedure was repeated until the chosen indicator for the degree of expanding had reached an appropriate value. For the Trial Experiment this indicator was the flaking off of the plumber's resin round the hole, but for other experiments the total and back extrusion were used as well.

The residual strains on the disc were recorded immediately after the experiment.

DESCRIPTION OF A TYPICAL EXPERIMENT.

(SPECIMEN NO. 2. 2 in. O.D. TUBE).

Expanding was carried on until the cape of the expander cage reached the tube, this point being indicated in the experimental results by a sharp rise in the mandrel driving torque, as seen in Fig. 51. The plumber's resin had not indicated the required amount of yielding at this stage, and, after withdrawing the expanders, the joint was re-expanded with a view to obtaining the full extent of the plastic zone on both the front and the back of the disc. This condition was never reached, however, as can be seen from Fig. 52. (At least, according to Nadai's theory of the maximum extent of yielding which gives a value of $\frac{r}{r_o} = 1.751$ (Bibliography 4)). Complete records of the variation of strain on the plate and of the mandrel torque are shown in Fig. 51, the graphs being plotted to a time base. The torque readings obtained from the spring balance are also plotted and show good agreement.

Comments on the salient features of the curves obtained are made on the graphs themselves. It can be seen that the strains build up first on the front of the plate, but at the latter end of the expanding those on the back of the plate build up and exceed those on the front. This feature was common to both passes of the cage. It may also be observed that when the strains on the back of the plate exceed those on the front, the strains on the front decrease slightly, indicating a bending effect. (A 'dishing' of the plate). The build-up of the mean strain

between the front and back of the plate appears to be reflected in the torque curve, which shows a similar pattern, neglecting the rise of torque due to the cape meeting the tube end and the fall to zero due to the reversibility of the driving unit.

The variation of strain and torque during removal of the expanders also shows characteristic features. The minimum radial strains for each curve during this phase remain sensibly constant, the peaks gradually reducing as the rollers move out of the tube until they have no further effect. Both the maximum and the minimum peaks of the circumferential strains decrease, however, during this period. The torque decreases in steps to zero, when the rollers have been removed completely, each step approximately coinciding with 120° of cage rotation. There is a rise of torque before the decrease between each step, which points to the existence of a ' bump' of material on the inside of the tube which is gradually 'ironed' out by the rollers. Evidence of this is also given by the continued extrusion of the tube during removal of the expanders as shown in Fig. 53 (other tests Figs. 58, 61, 66). It is probable that there exists a wave of material which progresses round the tube in front of each roller during the expanding process which leaves a mound on the inside of the tube when the expander stops. In this experiment the strains on the back of the plate had in all cases become greater than those on the front, indicating that parallel expanding had not been achieved. The main fact shown by the strain variation during removal of the expanders is that the distribution of residual strain in the

plate is approximately axially symmetrical, as it would be, of course, if the expanding had been effected by a hydrostatic pressure. (See Appendix 1).

The graphs of extrusion versus cage revolution shown in Fig. 53 indicate that the back extrusion is similar but smaller than the total extrusion, and that the front extrusion is greater than the back extrusion at all stages. This is in general agreement with the finding that the strains on the back of the plate were greater than those on the front: at the back of the plate the constraint offered by the elastic body of the tube behind the joint causes the displaced material to move radially outwards rather more than at the front where the tube is free to extrude axially to a greater extent. (Note: the 'total extrusion' here is that measured at the mean diameter and not at the inside diameter of the tube as is usually the case. The final ratio $\frac{\text{Back extrusion}}{\text{Total extrusion}}$ was 0.427, but it would have been much less if referred to the total extrusion at the inside diameter.

The residual strain distribution is shown in Fig. 54, together with the final readings indicated by the microammeters. These results showed good agreement after a correction had been made to allow for the slight zero drift of the dynamic gauges. There was little scatter in the points, which agreed with the theoretical form of curve in the elastic region of the plate (See Appendix 2).

The results from which the graphs were plotted for this experiment are shown in Tables 2, 3, and 4.

INDIVIDUAL EXPERIMENTS.

Trial Experiment No.1 (Specimen No.1, 2 in. O.D. Tube).

This experiment was carried out to test the general technique and, as described previously, certain modifications were made for the subsequent experiments. A complete record was not obtained due to the film lasting for insufficient time. The initial phase of expanding the tube until it nipped the plate took rather a long time and was difficult to control, and it is suggested that a separate investigation be made later. During this phase the tube was a loose fit in the disc and was held in position by hand. The only information given during this part of the experiment was the torque, which was in any case very small, and all subsequent experiments were started from the 'nip'.

Part of the first pass of the cage from 'nip' until the cage touched the tube is shown in Fig. 55. The end of this first pass of the cage was not recorded, but the subsequent removal of the expander is shown. Part of the re-expanding of the tube is given in Fig. 56, but the end of this expansion and the following removal of the expanders were not recorded, because of shortage of film. The extent of yielding is shown in Fig. 57, and the total and back extrusion versus cage revolution in Fig. 58.

The residual strains are shown in Fig. 59, a correction for zero drift having been made. These readings were not as satisfactory as in other tests because British Thermostat gauges had been fixed with nitro-cellulose cement, and, as described

previously, it was found necessary to bake these gauges on, a technique which was very successfully used in Experiments 2, 3, and 5.

The results from which the graphs were plotted for this experiment are shown in Tables 5, 6, and 7.

Experiment No. 3 (Specimen No. 3, 1 in. O.D. Tube).

The expanding process was carried on until the total and back extrusion had attained values of approximately half those of Specimen No. 2, as required for geometrical similarity. Owing to the relatively longer rollers of the smallest expander it was found possible to achieve this extrusion in only one pass of the cage, and the expanders were then removed. A complete record of the variation of strain in the plate and torque on the mandrel during this experiment is shown in Fig. 60. Graphs of total and back extrusion versus cage revolution are shown in Fig. 61, the extent of yielding (from plumber's resin) in Fig. 62, and the residual strains in Fig. 63.

There is a marked difference in the appearances of the graphs showing the variation of quantities during the expanding process from either of the preceeding experiments, owing to the larger size of the strain gauges in relation to the specimen. Both of the instruments recording the maximum radial strains exceeded full scale deflection due to the relatively higher value of the mean strain along their length.

In this experiment also the residual strains were larger on the back than on the front of the plate, the difference being

greater than in either of the previous experiments.

The results from which the graphs were plotted for this experiment are shown in Tables 8, 9, and 10.

Experiment No. 4 (Specimen No. 4, 4 in. O.D. Tube).

This specimen was too large to go into the oven for baking the gauges, and therefore Tinsley gauges were used, fixed with "High Solids" Durofix nitro-cellulose cement. Having expanded the tube up to nip, it was intended to carry on expanding until the total end back extrusion had attained values of approximately double those for Experiment No. 2. Several attempts were made to do this, as shown by the strains and torque record in Figs. 64 and 65, but the experiments had to be abandoned temporarily owing to the failure of the worm reduction gear of the drive unit. The total and back extrusion v. cage revolution are shown in Fig. 66, the extent of yielding in Fig. 67, and the residual strain distribution in Fig. 68.

The first expanding of this specimen was much more extended than in the previous experiments, the strains developed in the plate being quite small. In the second pass, however, the increase in torque and strain was very rapid, so that after only about 3 revolutions of the cage the torque had attained a value of 580 lb.ft., the circumferential strain at $\frac{r}{r_o} = 2.5$ reaching a peak value of about 0.066% strain, although strains on the back of the plate were still negligible. The expanders were reversed and restarted for a third time, producing an expansion which was similar to the second in its form. The expanders were again

reversed and left pending the construction of a stronger worm reduction gear for the drive unit.

The results from which the graphs were plotted for this experiment are shown in Tables 11, 12, and 13.

Experiment No. 4a (Specimen No. 4, 4 in. O.D. Tube).

The worm reduction gear of the large drive unit was replaced by another of larger dimensions, and the expanding continued. Prior to re-expanding the joint all the strain-measuring circuits were adjusted to record the final readings obtained in Experiment 4, since a fair period of time had elapsed during the modification of the drive unit, and the various strain gauge readings had drifted, although not unduly. The experiment was concluded successfully, expanding being continued until the total extrusion was approximately double that for Specimen 2. The back extrusion (see Fig. 66) was relatively much less for this experiment and was therefore not used as a criterion for the degree of expanding. The variation of strain and torque is shown in Fig. 69, the extent of yielding in Fig. 67, and the residual strains in Fig. 70.

The fourth and fifth passes of the cage into Specimen 4 showed similar patterns to the second and third (Experiment 4), the maximum torque attained being about 1600 lb.ft. During the last expanding the strains appeared to attain a maximum on the front of the plate but were still increasing on the back of the plate when the cage of the cage met the tube end. In Experiments 4 and 4a there was no marked increase of torque when the cage met

the tube, and no decrease of torque on stopping the rotation, since the drive was irreversible. The characteristic stepped torque variation during removal of the expanders was again apparent.

The residual strains on Specimen 4 indicated that there had been much more expanding on the front than on the back of the disc. The reason for this is easily seen from Fig. 66 and 67. The front extrusion had been so great that the cage came in contact with the 'land' on the tube before the rollers had fully penetrated the joint, and in subsequent passes this trouble was aggravated.

The results from which the graphs were plotted for this experiment are shown in Tables 14, 15, and 16.

Experiment No.5. (Specimen No 5, 4 in. O.D. Tube).

This experiment was carried out using retractive expanders supplied by Messrs. Babcock and Millcox Ltd., of the design shown diagrammatically in Fig. 4. A photograph of these expanders showing the pronounced mandrel taper as compared with the propulsive type is shown in Fig. 5.

The action of these expanders is briefly as follows:- in the initial expanding phase the nut A (Fig.4) is held stationary by a spanner while the mandrel is rotated clockwise. Since there is a left hand thread on the mandrel extension B, the mandrel is thereby caused to move forward axially relative to the expander body and cage C, thus causing the rollers D to move outwards against the reverse taper E of the mandrel, until they meet the

inside of the tube. Further rotation of the mandrel brings load onto the thrust race F, the rollers being forced to rotate round the inside of the tube and expand it. A comprehensive table supplied by the makers gives the correct number of mandrel turns required to close the initial clearance between tube and plate. Having closed the initial clearance, the nut A is then released, and due to the pronounced taper on the mandrel the radial pressure on the rollers is sufficient to provide an axial force tending to force the nut A against the thrust race F. Since the tangential frictional force between the nut A and the mandrel screw thread B is much higher than that in the thrust race, the nut rotates with the mandrel and the rollers are constrained to rotate describing the same external diameter, since relative movement between mandrel and cage in an axial direction is thereby prevented. The rollers are inclined axially with the mandrel axis so that they roll forward and out of the tube, rolling a parallel hole.

Having closed the initial clearance, the expander is again inserted to a fixed distance, the rollers brought into contact with the inside of the tube and a prescribed number of expanding turns given to the mandrel (depending on the tube thickness), the nut again being held stationary during this phase. The nut is then released and parallel rolling follows until the whole width of the tube seat has been expanded by the prescribed amount.

Details of Specimen 5 are given in Figs. 1 and 36, photographs being shown in Figs. 71 and 72. It was not now considered necessary to measure the radial strain distribution,

since this can be obtained from the circumferential strain distribution in an axially symmetrical system of this nature, as shown later. Accordingly, only circumferential strain gauges were cemented, British Thermostat gauges, baked on, being used. In order to measure the residual circumferential strains more accurately, in the plastic zone of the plate, the distances between a large number of centre punch marks situated at the opposite ends of various diameters were measured, as accurately as possible, by means of a travelling microscope before and after the experiment. By this means, the radial displacement and hence the circumferential strain could be determined at any one of these diameters. These marks were made by a punch having a pyramid point for ease of centreing the microscope graticule, and are shown in Fig. 72 (almost exactly in the centre of the photograph).

It was found that if these expanders were not well-lubricated, on release of the nut they would not roll parallel but continued to expand on the self-feeding principle. This was because the thrust from the nut was transferred to the retaining ring instead of to the thrust race, so that the friction between the nut and the retaining ring exceeded that between the nut and the screw thread, causing the nut to rotate with the cage. Thus relative movement between the nut and the mandrel was possible, allowing further uncontrolled expanding.

This trouble was overcome by lubricating the rollers and inside of the tube (as recommended by the makers) and expanding was carried out with a view to obtaining the relative tube extrusion

achieved in the first four experiments. To do this it was necessary to give two passes of the expanders. The variation of strain and torque during the first of these is shown in Fig. 73; the second pass being very similar has been omitted. The rise of torque during the expanding phase is apparent, the variation being due to the difficulty of manually preventing the nut from rotating. The strains on the back of the plate rise first, followed by the strains on the front of the plate as the expanders roll out of the tube. The extrusion is shown in Fig. 74 and the residual strain distribution in Fig. 75. The residual strain distribution has been plotted against the parameter $\left(\frac{r_o''}{r''}\right)^2$ for reasons explained later.

On inspection of the tube after this experiment it was found that the inside was very badly torn, as shown in Fig. 71. It is thought that this phenomenon is a characteristic of parallel rolling in which there is of necessity a considerable amount of slipping and rubbing causing severe shearing stresses at the inside surface of the tube. It is also thought that annealed tubes may not suffer so seriously from this defect.

From the graph showing the extrusion of the tube from the plate (Fig. 74) it can be seen that the final ratio $\frac{\text{Back extrusion}}{\text{Total extrusion}} \simeq 0.4$. For the earlier experiments with the propulsive expanders this ratio was approximately 0.43. One of the main advantages put forward for the retractive type expanders is that most of the extrusion is restricted to be towards the front of the tube. For the particular size and shape of specimen tested this claim was therefore not substantiated.

Plumber's resin was applied to the plate and tube of this specimen and flaked off to the extent shown very clearly by the light patches in Fig. 72. The separate disc of boiler plate clamped to the main specimen shown in Fig. 72 carried auxiliary strain gauges which were used to give an indication of 'zero drift' during the experiment.

The results from which the graphs were plotted for this experiment are shown in Tables 17, 18, and 19.

Experiment No. 6. (Specimen No. 6, 4 in. O.D. Tube).

The cage of the cage on the largest set of expanders was machined off, so that the rollers could penetrate further into the tube, and traverse the complete width of the tube seat. Specimen No. 6 was accordingly prepared, the dimensions being identical with those of Specimen No. 4, the positions of the dynamic strain gauges being also as for that specimen, and punch marks being made on the faces of the specimen. Expanding was carried out in the normal way. On reversal of the mandrel rotation, however, it was found that the rollers would not release themselves but continued to rotate in the same path. It was eventually necessary to free the mandrel by using a drift, so that this experiment had to be abandoned. The initial expanding phase was complete, and the records of strain and torque variation are shown in Fig. 76.

Since the only difference between the expander used in this experiment and the original expander was the absence of a cage, it is concluded that a cage is necessary in order to allow the rollers to partially free themselves at the end of the expanding

phase before reversal of mandrel rotation.

It can be seen from Fig. 76 that even in the initial expanding the strains on the back of the plate eventually exceed those on the front, thus verifying the correspondence between the strain history of the largest specimen and those of the smaller specimens.

PUSH-OUT TESTS.

The strength of a joint is largely dependent on the seat pressure, and the load required to push or pull a tube out of its seat plate is largely influenced by the surface finish of the component parts of the joint. In view of this it was decided that the only really worth while indication of the strength of the joint would be that obtained by calculating the seat pressure after measuring the elastic recovery of both faces of the seat plate on removal of the tube. From this point of view it is of little importance whether the tube is pushed out or pulled out. As the former method was easier it was adopted, a plug being fabricated so as to fit into the tube end which had previously been machined flush with the face of the plate. The push-out loads were measured and, having determined the mean seat pressure a value of the (static) coefficient of friction could then be calculated by use of a theory put forward by Goodier and Schoessow (5).

In order to determine whether the characteristic lack of parallelism of the tube-seat interface observed in all the specimens would affect joint strength in any way, the tube of Specimen No. 2 was pushed out from the back against the taper. The tube of Specimen No. 1 which had been expanded a similar amount to Specimen No. 2 was pushed out from the front.

As shown in Appendix 2, the strains induced in a thin circular finite plate having a central hole expanded by internal pressure p within the elastic limit are:-

$$e_\theta = k_1 + k_2\left(\frac{a''}{r''}\right)^2 \qquad \text{Where } k_1 = \frac{p(1-\nu)}{E\left[\left(\frac{b}{a''}\right)^2 - 1\right]}$$

and $$e_r = k_1 - k_2\left(\frac{a''}{r''}\right)^2 \qquad k_2 = \frac{p(1+\nu)}{E\left[1 - \left(\frac{b}{a''}\right)^2\right]}$$

Hence $$p = \frac{E\left[1 - \left(\frac{a''}{b}\right)^2\right]}{1+\nu} k_2$$

In these tests, therefore, if the tube is pushed out of the plate, the elastic recovery of the plate will be such as to relieve the strains given by the above equations, which were associated with the tube seat pressure.

These relieved strains were measured by means of the strain gauges already present on the specimens and the results plotted against $\left(\frac{a''}{r''}\right)^2$, so that the slope of the resulting straight line would give the value of k_2. It should be remembered that near the edge of the hole the radius of curvature of the circumferential fibres is small so that the strain gauges there would tend to record lower values of the strain, as already shown.

The equation derived by Goodier and Schoessow for the case of a push-out test is:-

$$F = \bar{p} \cdot \frac{2\pi a''}{\beta}\left(e^{\beta\mu h} - 1\right) \qquad \text{Where } \beta = \frac{\nu\left(b^2 - a''^2\right)}{a''\left(b^2 - r_o''^2\right)}$$

$$\text{Hence } \mu = \frac{1}{\beta h}\log_e\left(\frac{F\beta}{2\pi a''\bar{p}} + 1\right)$$

Certain of the symbols used by Goodier and Schoessow have been altered to conform with the nomenclature used in this research- for clearness a cross-section of a typical test joint is shown

below together with the relevant dimensions:-

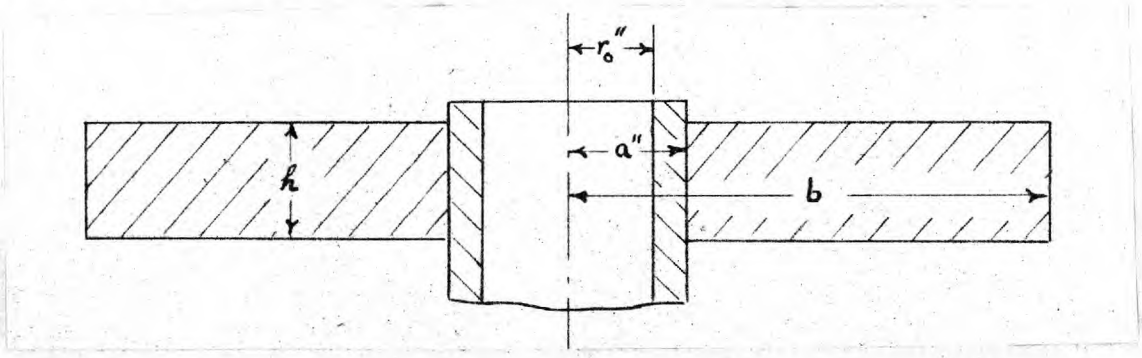

The actual dimensions of the specimens were obtained from measurements taken.

The values determined experimentally for Young's Modulus and Poisson's Ratio were:- E = 13460 Tons per sq. in.

ν = 0.3

(See Tension and Torsion Tests).

The results obtained for the various specimens are shown in Figs. 77 to 80 and summarized in Table 20. The push-out load recorded is the observed maximum load required to initiate movement between tube and plate. Push-out tests were not carried out on Specimens 4 and 6 since they could not be accomodated in the Denison testing machine. It will be noticed that the coefficient of friction calculated for Specimen No. 5 was much higher than for the other specimens. This was due to the very rough surface finish of the hole machined in this particular specimen.

HARDNESS AND THICKNESS MEASUREMENTS ON SPECIMEN NO. 4.

In order to make further comparisons with theoretical predictions it was decided to cut out a section of the plate of Specimen No. 4 and measure the hardness variation across the front and back faces. Having done this, it would then be possible to determine the yield stress variation by using the yield stress-hardness correlation obtained for the boiler plate material as described later. By this means comparison could be made between the measured work-hardening and that predicted theoretically. This method was considered preferable to cutting out, machining, and testing miniature specimens, since there would be yield stress variation both across the diameter and along the length of such specimens (due to the unequal expanding through the thickness of the plate).

It was also found possible to estimate the thickening of the plate by grinding flats along a diameter of the plate and measuring the step so formed between the base of the flat ground groove and the surface of the plate. This measurement was made using a dial gauge, having 0.0001 inch graduations, securely fixed to a post and rotating the attachment slightly so that the dial gauge plunger traversed the step. Assuming that there had been no thickening of the plate in the elastic region, it would then be possible to extrapolate the curve representing the original profile of the plate and therefore determine the thickened zone.

The measured variation of hardness across the back and front faces of the plate is shown in Fig. 81, whilst the estimated

thickening of the plate is shown in Fig. 82. In addition to the above measurements the hardness along the seat of the plate was measured and is shown in Fig. 83. There is a great deal of scatter in these results, possibly due to the original machining of the hole. The hardness along the outside of the tube in contact with the seat was also measured, the results being shown in Fig. 84.

TENSILE TESTS (1½ IN. BOILER PLATE).

All the tensile tests to be described were carried out on round specimens machined from strips which had been flame cut from the boiler plate used. No tests were carried out to determine any anisotropy which may have been present in the hot-rolled plate, and no tensile tests were carried out on the cold drawn mild steel tubes used. A 50 Ton Denison Testing Machine was used for all the tests.

In order to determine accurately the mean value of Young's Modulus for the material, separate tensile tests were carried out using a Martens and a Ewing extensometer on different specimens. The specimen diameter was approximately 0.7 in., the gauge length of the Martens extensometer being 5.896 ins., and that of the Ewing 8 ins.

The graphs obtained from the Martens extensometer are shown Figs. 85 and 86 giving a value of Young's Modulus of E = 13460 Tons per sq. in. (30.15×10^6 lbs. per sq. in.). Bending of the specimen, introduced by the grips of the testing machine, for the particular plane in which the Martens extensometer was positioned, produced strains of ± 1.75% of the mean strain.

The graph obtained from the Ewing extensometer is shown in Fig. 87, giving a value for E of 13460 Tons per sq. in. Such good agreement was not expected, and may have been due to a favourable combination of errors.

In order to determine the stress-strain curve accurately up to the occurrence of 'necking', an extensometer was designed which would be capable of measuring large strains over a known gauge

length. It is common practice to measure the large extensions which occur in a tensile test after the initial yield point by the careful use of a pair of dividers and a graduated scale, the distance between centre punch marks being measured after small increments of load. Since an accurate stress-strain curve was required for use in the theory, this method was not suitable. A sketch of the extensometer used is shown in Fig. 88, from which it can be seen that the gauge points are located by two spring loaded plungers capable of moving in as the specimen contracts. One disadvantage of the extensometer is that it will not compensate for any bending of the specimen which may occur, but it was not considered that there would be much bending in the plastic phase of the test.

A stress-strain curve obtained in this way is shown in Fig. 89, and a stress-strain curve for the same material after annealing is shown in Fig. 90. The lower ultimate strength and more pronounced yield point is clearly apparent for the annealed specimen. The stress-strain curve obtained for the unannealed 1½ in. thick boiler plate material (Fig. 89) was used in the theory.

TENSILE AND TORSION TESTS (2½ IN. BOILER PLATE).

A specimen of 1 inch diameter suitable for testing in tension in the 50 Ton Denison testing machine, and in torsion in the available torsion testing machine, was prepared. The torsion tests were carried out first, since the keyways in the ends of the specimen would subsequently be distorted in the grips of the tension testing machine. A mirror type torsion meter was used together with the scales and telescopes of the Martens apparatus.

The specimen was twisted in both senses, the graph shown (Fig. 91) being that for a right hand twist. A value for the Shear Modulus of G = 4980 Tons per sq. in. was obtained. The specimen was then tested in tension, the graph obtained being shown in Fig. 12. The elastic limit was low, approximately 12.4 Tons per sq. in., and was inadvertently exceeded during this test. The value of Young's Modulus obtained was E = 13000 Tons per sq. in. The value of Poisson's Ratio calculated from these results was therefore $\nu = \frac{E}{2G} - 1 = 0.306$. Since the value of Poisson's Ratio obtained by this method is very sensitive to small errors in determining E or G, a value of $\nu = 0.3$ was assumed for all calculations made in this research.

HARDNESS-YIELD STRESS CORRELATION (2½ IN. BOILER PLATE).

In order to correlate the hardness of this steel with the current yield stress, a specimen of 0.998 in. diameter was prepared, and two diametrically opposed flats ground along the length of the specimen. These flats were 0.2126 in. wide, thus giving a net cross-sectional area of 0.7784 sq. in. A tensile test was carried out up to the initiation of necking, the strains being measured by means of the extensometer already described.

The procedure adopted was to strain the specimen a small amount, recording the load and extension in the normal way, then to release the load, and transfer the specimen complete with extensometer on to the table of a Vickers hardness testing machine. The hardness of the specimen was then measured by indenting the ground flat surface with the pyramid indenter, taking the mean of from 3 to 5 readings along the length of the flat. The true stress was determined in the usual way (see theory) and the results obtained are shown plotted to a base of unit strain in Fig. 93. The actual correlation between yield stress and V.P.N.(Vickers Pyramid Numeral) is shown in Fig. 94, together with the correlation suggested for mild steel by Tabor in his book (12). It is suggested by Tabor that the effect of the indenter is to induce local work hardening giving a rise in the yield stress corresponding with about 8% strain. It should therefore be possible to obtain the Vickers Pyramid Numeral corresponding to a given yield stress directly from a known stress-strain curve by taking the yield stress at a point of 8% higher strain and multiplying this yield stress in kg/sq.mm. by the factor 2.9 for mild steel, and 3.0 for

copper. As can be seen by comparing the two curves of Fig. 94 the hardness values obtained by Tabor's method are lower than those which were obtained experimentally in this research. One possible reason for this is that the steel tested was not a true mild steel.

The correlation obtained experimentally was used in the comparison of the work hardening measured across the faces of Specimen No. 4 with the work hardening predicted theoretically.

THE THEORY OF THE PROCESS OF EXPANDING A HOLE FROM ZERO RADIUS IN A THIN INFINITE PLATE.

1. Summary.

To allow the experimental results of this research to be compared with theoretical predictions, it was first necessary to develop a theory which would adequately allow for work hardening and deformation. In common with all the previous theories, this theory is based on the assumption of a uniform hydrostatic pressure expanding, whilst the experimental work has been carried out using roller type boiler-tube expanders. It is, therefore, to be expected that most of the differences between the experimental results and the theoretical predictions will be due to this difference between uniform pressure and roller expanding. Comparison between the theory and the experimental observations made in this research will follow later.

An estimate of the effect of 'secondary' yielding due to the residual stresses attaining the yield criterion on release of the expanding pressure is also made, on the assumption that the yield stress remains constant and that there is no thickening of the plate. This is an extension of Nadai's theory and is given in Appendix 3.

2. Survey of Previous Theories.

The previous relevant theories for this process are inadequate for the following reasons:-

(1) Nadai's theory (4).

Nadai's equations postulate a one-to-one relationship between total stress and total strain in the plastic region. The

result of using these equations is to lead to an infinite axial strain at the edge of the hole. This means an infinite thickening of the plate at the edge of the hole, which is not physically possible. Also, the equilibrium equation used does not allow for thickening of the plate, and the plastic region is supposedly only able to extend to a value of $\frac{c}{a} = 1.751$, where c is the radius to the plastic-elastic interface, and a is the radius of the hole. This extent of yielding corresponds to a certain fixed increase in diameter of the hole - it is not made clear what happens when the diameter of the hole is increased still further than this. Secondary yielding on release of the expanding pressure due to the residual stresses attaining the yield criterion is not mentioned. Work-hardening, although mentioned, is not adequately incorporated into the solution due to the erroneous total stress-total strain relations used.

(ii) Taylor's theory (11), as extended by Hill (6, p. 307).

This theory postulates a plastic-rigid material, so that the strains and deformations in the elastic region of the plate are zero. Since most of the experimental measurements in this research were of necessity made in the elastic region and the region of small plastic strains, this theory is inadequate for comparison purposes. In addition, the von Mises 'flow rule' is used in conjunction with the Tresca criterion which is not strictly compatible with the assumption that Lode's parameters are equal. It is assumed that the process of expanding a hole from zero radius in a thin infinite plate of initially constant thickness produces a deformation which remains geometrically similar. This is not

so, as is discussed in the text following, although it is not thought that any serious errors are introduced by this assumption, for moderate degrees of expanding. Work-hardening is not contemplated, and the state of residual stress and strain after release of the expanding pressure is not considered.

3. Introduction.

If the problem is to be tractable mathematically, it is necessary to assume that the configurations of stress and strain remain geometrically similar during the expanding, and that the thickness of the plate may be taken as being small enough to average the stresses through the plate.* A plate in which the thickness is initially proportional to the radius satisfies all these conditions, provided that the angle α_i in the diagram below is small. (The problem is then one of plane stress in which $\sigma_z = 0$).

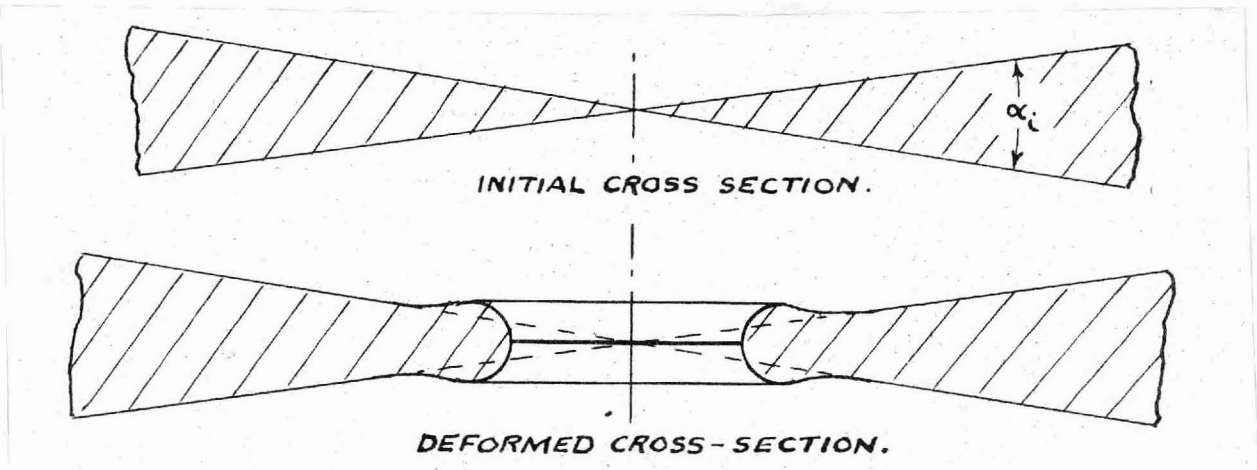

In fact, since the shear stresses must be zero all round the boundary of the plate, the principal planes in such a plate would form some such system as is illustrated overleaf, including

---

* As stated by R. Hill: Mathematical Theory of Plasticity, p. 311

in their network the boundaries of the plate.

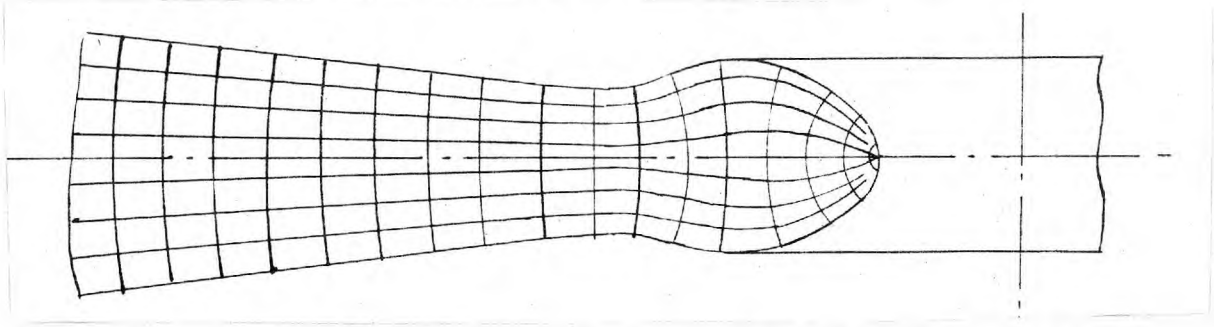

Thus any solution which assumes that the cylindrical coordinate axes are <u>themselves</u> the principal planes must be an approximation, although not far from the true condition along the central ligament of the plate. With the restriction that the angle α_i is small, however, this departure from coincidence between principal planes and cylindrical coordinate axes becomes negligible.

A solution of greater interest, especially in connection with this research, would be that to the expanding of a cylindrical cavity in a thin infinite plate of initially uniform thickness. This system would not remain geometrically similar, however, as illustrated below at two stages of the expanding.

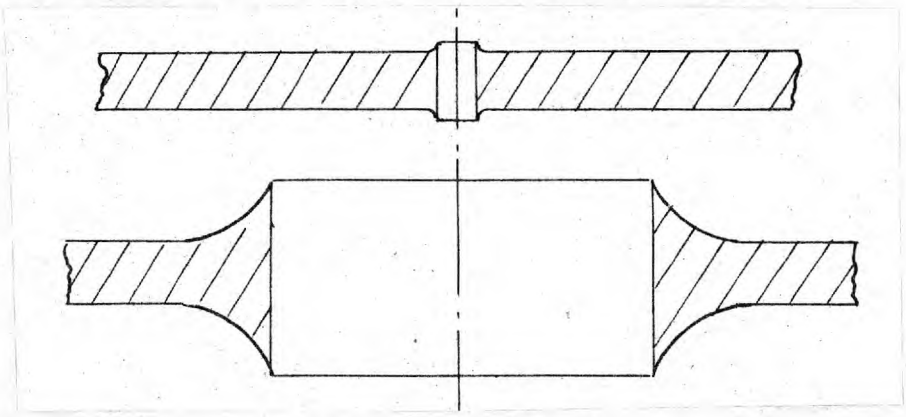

Alternatively, if the assumption of geometrical similarity is made, a solution to the problem will be obtained in which the

thickness h is expressed as a function of the single parameter $\frac{r}{c}$, where r is the radius to any element, and c is the radius to the plastic-elastic interface. Such a solution might be as illustrated below:-

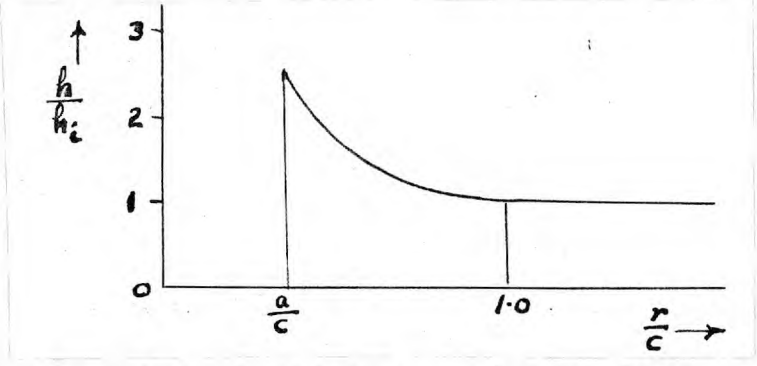

h_i is the original thickness of the plate, and a the radius of the hole, $\frac{a}{c}$ being a constant, by the principle of geometrical similarity. Thus a plate may be considered at two stages in its deformation - (a) when c = 1 inch, and (b) when c = 10 inches, say. According to the solution obtained, then, the actual appearance of the cross-section of the plate at these two stages would be as illustrated below:-

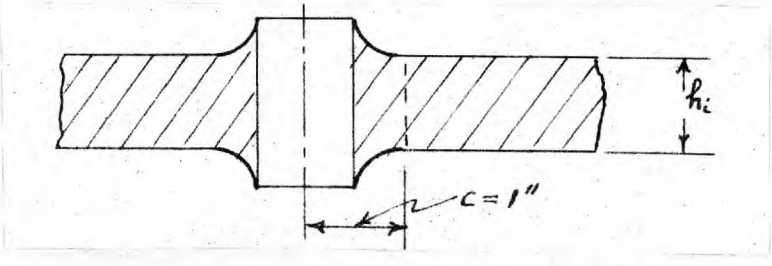

Case (a)

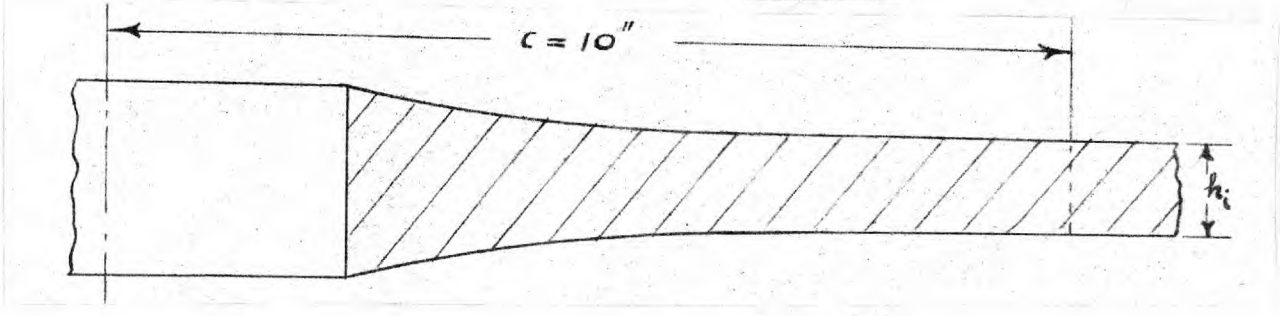

Case (b)

It can be seen that these two systems are not geometrically similar, so that the solution obtained does not satisfy the initial assumption of geometrical similarity.

The assumption of geometrical similarity will be made, nevertheless, in both of the above cases, i.e. for a plate of initial thickness h_i proportional to initial radius r_i, and for a plate of initially constant thickness h_i, and the two solutions compared. A plastic-elastic material having the known stress-strain curve of the boiler plate used in the experiments will be considered, and work-hardening will be included in the analysis. All previous solutions to the problem of expanding a hole in a plate of constant thickness have tacitly assumed geometrical similarity.

Practical experience would suggest that continued expansion of a hole in a plate of constant thickness would lead to material progressively building up around the edge of the hole, with consequent loss of geometrical similarity. This was in fact the case in Taylor's experiment (11), in which a hole was expanded in a lead sheet by a well lubricated mandrel of shallow taper. This objection does not apply to a plate having initial thickness proportional to radius, since once the shape of the deformed cross-section has developed, geometrical similarity is maintained and the problem is solved for all physical sizes of the expanding hole.

The solution for a hole expanded from a finite radius is obtained from that for expanding a hole from zero radius simply by discarding that part of the solution round the edge of the

hole which is not required. This is a consequence of the fact that the outer annular fibres of the plate receive radial pressure only transmitted from the inner fibres, and the inner fibres may be equally well replaced by an externally applied pressure.

4. Solution in the Plastic Region.

With the assumption of geometrical similarity, all variables become functions of the single parameter $\phi = \frac{r}{c}$.

Considering an annular section of the plate it may be shown that the stress equilibrium equation is

$$\frac{\partial}{\partial r}(h\sigma_r) = \frac{h}{r}(\sigma_\theta - \sigma_r) \qquad \text{.....(1)}$$

Now $$\frac{\partial}{\partial r} \equiv \frac{\partial \phi}{\partial r} \cdot \frac{d}{d\phi} = \frac{1}{c}\frac{d}{d\phi}$$

Hence (1) becomes $$\frac{d}{d\phi}(h\sigma_r) = \frac{h}{\phi}(\sigma_\theta - \sigma_r) \qquad \text{.....(2)}$$

The Reuss equations, in cylindrical coordinates, become

$$d\epsilon'_r = \frac{3\sigma'_r d\bar{\sigma}}{2\bar{\sigma}H'} + \frac{d\sigma'_r}{2G} \qquad \text{.....(3)}$$

$$d\epsilon'_\theta = \frac{3\sigma'_\theta d\bar{\sigma}}{2\bar{\sigma}H'} + \frac{d\sigma'_\theta}{2G} \qquad \text{.....(4)}$$

$$d\epsilon'_z = \frac{3\sigma'_z d\bar{\sigma}}{2\bar{\sigma}H'} + \frac{d\sigma'_z}{2G} \qquad \text{.....(5)}$$

$$d\epsilon = \frac{1-2\nu}{E} d\sigma \qquad \text{.....(6)}$$

(Compressibility Relation)

Where $$d\epsilon = \frac{d\epsilon_r + d\epsilon_\theta + d\epsilon_z}{3}, \quad d\sigma = \frac{d\sigma_r + d\sigma_\theta + d\sigma_z}{3},$$

$$\sigma'_r = \sigma_r - \sigma, \quad \sigma'_\theta = \sigma_\theta - \sigma, \quad \sigma'_z = \sigma_z - \sigma,$$

$$d\epsilon'_r = d\epsilon_r - d\epsilon, \quad d\epsilon'_\theta = d\epsilon_\theta - d\epsilon, \quad d\epsilon'_z = d\epsilon_z - d\epsilon.$$

It is convenient to define the stresses in terms of the angular displacement θ of the resultant vector representing the sum of the deviatoric stress vectors in the $\sigma_r\ \sigma_\theta\ \sigma_z$ space (σ_r, σ_θ, and σ_z being erected in rectangular cartesian coordinates).

It can be shown that this vector lies in the plane $\sigma_r + \sigma_\theta + \sigma_z = 0$. This is the plane generally referred to as 'the plane of deviatoric states of stress'. The projections of the vectors $\sigma'_r\ \sigma'_\theta\ \sigma'_z$ on to this plane are of length $\sqrt{\frac{2}{3}}\sigma'_r$, $\sqrt{\frac{2}{3}}\sigma'_\theta$, and $\sqrt{\frac{2}{3}}\sigma'_z$, and when added together are assumed to lie on the current yield circle of radius $\sqrt{\frac{2}{3}}\bar{\sigma}$. The circle is, of course, the trace of the von Mises yield criterion represented by a cylindrical surface, where it cuts the plane of deviatoric states of stress. In order to simplify the analysis the factor $\sqrt{\frac{2}{3}}$ may be omitted, so that the actual values of the deviatoric stresses may be plotted, their vectorial sum being a vector of length $\bar{\sigma}$.

Considering, therefore, the plane of deviatoric states of stress, the following two-dimensional system of coordinates may be used:-

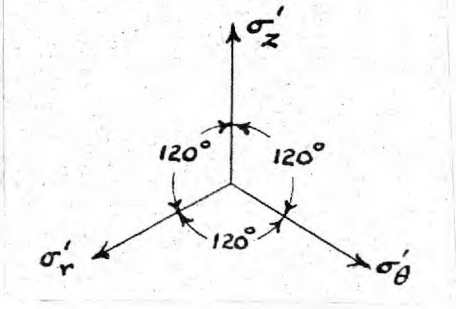

Summation of the vectors representing the projections of the deviatoric stresses on this plane may then be carried out, it being remembered that $\sigma'_r + \sigma'_\theta + \sigma'_z = 0$.

Thus, the state of stress at a point might be as represented by the vectors shown below. (To completely specify the state of stress the length of the vector representing the hydrostatic component must also be given):-

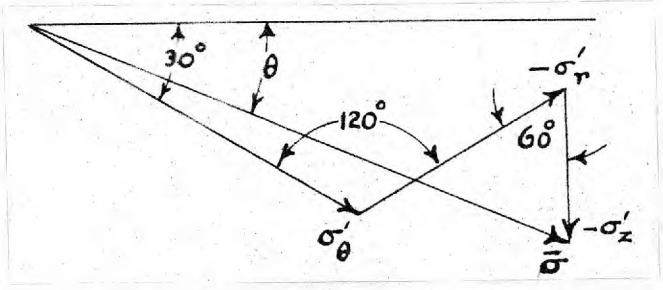

It can be shown from consideration of the above diagram that

$$\sigma'_r = -\frac{2}{3}\bar{\sigma}\cos\left(\theta+\frac{\pi}{6}\right) \quad \ldots(7) \qquad \sigma_r = \frac{2}{\sqrt{3}}\bar{\sigma}\sin\left(\theta-\frac{\pi}{6}\right) \quad \ldots\ldots(10)$$

$$\sigma'_\theta = \frac{2}{3}\bar{\sigma}\cos\left(\theta-\frac{\pi}{6}\right) \quad \ldots(8) \qquad \sigma_\theta = \frac{2}{\sqrt{3}}\bar{\sigma}\sin\left(\theta+\frac{\pi}{6}\right) \quad \ldots\ldots(11)$$

$$\sigma'_z = -\frac{2}{3}\bar{\sigma}\sin\theta \quad \ldots(9) \qquad \sigma_z = 0 = \sigma'_z + \sigma \quad \ldots\ldots(12)$$

Hence $$\sigma = -\sigma'_z = \frac{2}{3}\bar{\sigma}\sin\theta \quad \ldots\ldots(13)$$

In terms of this angle θ, the equilibrium equation becomes:-

$$\frac{d}{d\phi}\left\{h\bar{\sigma}\sin\left(\theta-\frac{\pi}{6}\right)\right\} = \frac{h}{\phi}\bar{\sigma}\cos\theta \quad \ldots\ldots(14)$$

whence

$$\frac{d\epsilon_z}{d\phi} = \frac{1}{h}\frac{dh}{d\phi} = \frac{2}{(\sqrt{3}\tan\phi-1)\phi} - \frac{d\theta}{d\phi}\cot\left(\theta-\frac{\pi}{6}\right) - \frac{1}{\bar{\sigma}}\frac{d\bar{\sigma}}{d\phi} \quad \ldots\ldots(15)$$

The compressibility relation becomes:-

$$\frac{d\epsilon}{d\phi} = \frac{2(1-2\nu)}{3E}\left(\bar{\sigma}\frac{d\theta}{d\phi}\cos\theta + \frac{d\bar{\sigma}}{d\phi}\sin\theta\right) \quad \ldots\ldots(16)$$

In the case of an axially symmetrical system undergoing large strains, $d\epsilon_r$ and $d\epsilon_\theta$ are inter-related since $d\epsilon_r = \frac{\partial}{\partial r}(du)$, and $d\epsilon_\theta = \frac{du}{r}$.

In order to express this strain compatibility for large strains it is a simplification to introduce the concept of the velocity v of an element, using the parmeter c as the time scale.†

Then $v = \frac{\partial u}{\partial c}$

$$d\epsilon_r = \frac{\partial v}{\partial r} dc = \frac{1}{c} \frac{dv}{d\phi} dc$$

$$d\epsilon_\theta = \frac{v}{r} dc = \frac{1}{c} \frac{v}{\phi} dc$$

Thus

$$\frac{d\epsilon_r}{dc} = \frac{1}{c} \frac{dv}{d\phi}$$

$$\frac{d\epsilon_\theta}{dc} = \frac{1}{c} \frac{v}{\phi}$$

It can be shown that $\frac{d}{dc} \equiv \frac{v - \phi}{c} \frac{d}{d\phi}$

$$\therefore \quad \frac{d\epsilon_r}{d\phi} = \frac{1}{v - \phi} \frac{dv}{d\phi}$$

$$\frac{d\epsilon_\theta}{d\phi} = \frac{1}{v - \phi} \frac{v}{\phi}$$

Thus both $d\epsilon_r$ and $d\epsilon_\theta$ may be expressed in terms of v and ϕ.

From these relations:-

$$\frac{d\epsilon}{d\phi} = \frac{1}{3}\left(\frac{d\epsilon_r}{d\phi} + \frac{d\epsilon_\theta}{d\phi} + \frac{d\epsilon_z}{d\phi}\right) = \frac{1}{3}\left\{\frac{\frac{dv}{d\phi} + \frac{v}{\phi}}{v - \phi} + \frac{d\epsilon_z}{d\phi}\right\} \qquad \text{.....(17)}$$

$$\frac{d\epsilon'_r}{d\phi} = \frac{d\epsilon_r}{d\phi} - \frac{d\epsilon}{d\phi} = \frac{1}{3}\left\{\frac{2\frac{dv}{d\phi} - \frac{v}{\phi}}{v - \phi} - \frac{d\epsilon_z}{d\phi}\right\} \qquad \text{.....(18)}$$

---

† This is the system used in R. Hill's treatment of the problem.

$$\frac{d\epsilon'_\theta}{d\phi} = \frac{d\epsilon_\theta}{d\phi} - \frac{d\epsilon}{d\phi} = \frac{1}{3}\left\{\frac{\frac{2v}{\phi} - \frac{dv}{d\phi}}{v-\phi} - \frac{d\epsilon_z}{d\phi}\right\} \qquad \ldots\ldots(19)$$

$$\frac{d\epsilon'_z}{d\phi} = \frac{d\epsilon_z}{d\phi} - \frac{d\epsilon}{d\phi} = \frac{1}{3}\left\{2\frac{d\epsilon_z}{d\phi} - \frac{\frac{dv}{d\phi} + \frac{v}{\phi}}{v-\phi}\right\} \qquad \ldots\ldots(20)$$

Equating (17) and (16)

$$\frac{1}{v-\phi}\left(\frac{dv}{d\phi} + \frac{v}{\phi}\right) + \frac{d\epsilon_z}{d\phi} = \frac{2(1-2\nu)}{E}\left(\bar{\sigma}\frac{d\theta}{d\phi}\cos\theta + \frac{d\bar{\sigma}}{d\phi}\sin\theta\right) \qquad \ldots\ldots(21)$$

Eliminating $\frac{3d\bar{\sigma}}{2\bar{\sigma}H'}$ between the equations (4) and (5)

$$\frac{\sigma'_z}{\sigma'_\theta}\left(2G\frac{d\epsilon'_\theta}{d\phi} - \frac{d\sigma'_\theta}{d\phi}\right) = 2G\frac{d\epsilon'_z}{d\phi} - \frac{d\sigma'_z}{d\phi} \qquad \ldots\ldots(22)$$

Substitution for σ'_z and σ'_θ in terms of θ and $\bar{\sigma}$, and for $\frac{d\epsilon'_\theta}{d\phi}$ and $\frac{d\epsilon'_z}{d\phi}$ from (19) and (20) leads to

$$\frac{d\epsilon_z}{d\phi} + \frac{v}{\phi(v-\phi)}\frac{\sqrt{3}\tan\theta - 1}{2} - \frac{\frac{dv}{d\phi}}{v-\phi}\cdot\frac{\sqrt{3}\tan\theta + 1}{2} + \frac{\bar{\sigma}}{2G\cos\theta}\frac{d\theta}{d\phi} = 0 \qquad \ldots\ldots(23)$$

Also, substitution for σ'_θ in terms of θ and $\bar{\sigma}$ and for $\frac{d\epsilon'_\theta}{d\phi}$ from (19) in equation (4) leads to

$$\frac{\frac{2v}{\phi} - \frac{dv}{d\phi}}{3v-\phi} - \frac{d\epsilon_z}{d\phi} = \left(\frac{3}{H'} + \frac{1}{G}\right)\frac{d\bar{\sigma}}{d\phi}\cos\left(\theta - \frac{\pi}{6}\right) - \frac{\bar{\sigma}}{G}\frac{d\theta}{d\phi}\sin\left(\theta - \frac{\pi}{6}\right) \qquad \ldots\ldots(24)$$

Equations (15), (21), (23), and (24) form the basis of a solution to the problem. The four dependent variables are ϵ_z, θ, $\bar{\sigma}$, and v, the independent variable being ϕ. An analytical solution appears to be out of the question, but since ϵ_z, θ, $\bar{\sigma}$, and v are known on the plastic-elastic boundary ($\phi = 1$), a step-by-step method of integration may be employed, substituting finite increments $\Delta\epsilon_z$, $\Delta\theta$, $\Delta\bar{\sigma}$, Δv, and $\Delta\phi$ in the above equations, and solving each step by a trial and error process, using the mean values of the functions over the step considered. Increments of

$\Delta\phi = -0.02$ were considered small enough to give a reasonably accurate solution, although near the edge of the hole the solution must be approximate only, since some of the derivatives become infinite.

Rewriting these equations in the incremental form found most convenient for solution:-

$$\Delta\epsilon_z - \cot(30^\circ-\theta) + \frac{1}{\bar{\sigma}}\Delta\bar{\sigma} = \frac{2}{\sqrt{3}\tan\theta - 1}\ \frac{\Delta\phi}{\phi} \qquad \text{.....I}$$

$$\Delta\epsilon_z - \frac{2(1-2\nu)}{E}\bar{\sigma}(\cos\theta)\Delta\theta - \frac{2(1-2\nu)}{E}(\sin\theta)\Delta\bar{\sigma} - \frac{\Delta r}{\phi - r} = \frac{r}{\phi - r}\frac{\Delta\phi}{\phi} \qquad \text{.....II}$$

$$\Delta\epsilon_z + \frac{\bar{\sigma}}{2G\cos\theta}\Delta\theta + \frac{\sqrt{3}\tan\theta + 1}{2(\phi - r)}\Delta r = \frac{r}{\phi - r}\cdot\frac{\Delta\phi}{\phi}\cdot\frac{\sqrt{3}\tan\theta - 1}{2} \qquad \text{.....III}$$

$$\Delta\epsilon_z + \frac{\bar{\sigma}}{G}\left\{\sin(30^\circ-\theta)\right\}\Delta\theta + \left(\frac{3}{H'} + \frac{1}{G}\right)\left\{\cos(30^\circ-\theta)\right\}\Delta\bar{\sigma} - \frac{\Delta r}{\phi - r} = \frac{2r}{r-\phi}\frac{\Delta\phi}{\phi} \qquad \text{.....IV}$$

Subtracting II from IV,

$$\Delta\theta\left[\frac{\bar{\sigma}}{G}\sin(30^\circ-\theta) + \frac{2(1-2\nu)}{E}\bar{\sigma}\cos\theta\right] + \Delta\bar{\sigma}\left[\left(\frac{3}{H'} + \frac{1}{G}\right)\cos(30^\circ-\theta) + \frac{2(1-2\nu)\sin\theta}{E}\right] = \frac{3r}{r-\phi}\frac{\Delta\phi}{\phi} \qquad \text{.....V}$$

The procedure for solution is as follows:-

For any increment $\Delta\phi$ - Δr, $\Delta\theta$, and $\Delta\bar{\sigma}$ are guessed from the previous solution. Half these increments are then added to the known values of the functions at the last known point in the solution, giving the mean values of the functions over that increment. These mean values are then substituted in the above equations, and the increments calculated as follows:-

a. Eliminate $\Delta\epsilon_z$ from III - II.

b. Eliminate $\Delta\epsilon_z$ from III - I.

c. Eliminate Δr from a and b.

d. Eliminate $\Delta\theta$ from c and V. Hence determine $\Delta\bar{\sigma}$.

e. Determine $\Delta\theta$ from c.

f. Determine Δv from a.

g. Determine $\Delta\epsilon_\zeta$ from II.

If these calculated increments are very different from those assumed the process must be repeated until the difference becomes insignificant.

Since the deformation is geometrically similar, the ratio $\frac{a}{c}$ must remain constant. At the edge of the hole $v = \frac{da}{dc} = \frac{a}{c} = \phi$, and the solution is completed when the velocity v becomes equal to ϕ.

To determine the strains and displacements from the velocity,

$$\Delta\epsilon_\theta = \frac{v}{r-\phi}\,\frac{\Delta\phi}{\phi} \qquad \text{for each increment of } \Delta\phi.$$

Hence $\epsilon_\theta = \sum_{\phi}^{\phi=1} \Delta\epsilon_\theta$

Now $d\epsilon_\theta = \frac{du}{r} = \frac{dr}{r}$

$\therefore \epsilon_\theta = \int_{r_i}^{r} \frac{dr}{r} = \log \frac{r}{r_i}$ where r_i was the original radius to any element before deformation.

Now $r_i = r - u$

$$\therefore \epsilon_\theta = \log \frac{r}{r-u} = \log \frac{1}{1-\frac{u}{r}}$$

$$\therefore 1 - \frac{u}{r} = \exp(-\epsilon_\theta) \quad \text{or} \quad \frac{u}{r} = 1 - \exp(-\epsilon_\theta)$$

and $$\frac{u}{c} = \phi\left\{1 - \exp(-\epsilon_\theta)\right\} \qquad \ldots\ldots(25)$$

At the edge of the hole, $u = a$, $\phi = \frac{a}{c}$

$$\therefore \quad \frac{a}{c} = \frac{a}{c}\left\{1 - \exp\,(-\epsilon_\theta)\right\} \qquad \text{and} \quad \epsilon_\theta \to \infty$$

Similarly, $d\epsilon_z = \frac{dh}{h}$

$\therefore \quad \epsilon_z = \log \frac{h}{h_i}$, where h_i was the original thickness at radius r_i.

Thus $\frac{h}{h_i} = \exp \epsilon_z$ .....(26)

For the plate in which $h_i = mr_i$

$$\frac{h}{h_i} = \frac{h}{mr_i} = \frac{h}{m(r - u)} = \exp \epsilon_z$$

But $\epsilon_\theta = \log \frac{r}{r - u} \quad \therefore \quad \frac{r}{r - u} = \exp \epsilon_\theta$

$$\therefore \quad \frac{h}{mr} = \exp\,(\epsilon_z - \epsilon_\theta), \text{ and}$$

$$\frac{h}{mc} = \phi \exp\,(\epsilon_z - \epsilon_\theta) \qquad .....(27)$$

It can be seen from equation (27), therefore, that the deformed shape of the plate of initial thickness $h_i = mr_i$ has a thickness h which is determined by some function of $\frac{r}{c}$ and is also proportional to the radius of the plastic-elastic interface c. This is a necessary condition for geometrical similarity.

5. Solution in the Plastic Region.

(i) Plate in which h_i is proportional to r_i.

It is assumed that $h_i = mr_i$ where m is an arbitrary constant. ($\frac{h_i}{2r_i} = \tan\frac{\alpha_i}{2}$ $\therefore$ $m = 2\tan\frac{\alpha_i}{2}$). Since, in the elastic region, h_i and r_i will not be very different from h and r, the equations may be considered in terms of h and r.

The equilibrium equation is, as before,

$$\frac{\partial}{\partial r}(h\sigma_r) = \frac{h}{r}(\sigma_\theta - \sigma_r)$$

$$\therefore \quad m\frac{\partial}{\partial r}(r\sigma_r) = m(\sigma_\theta - \sigma_r)$$

Hence $$r\frac{\partial\sigma_r}{\partial r} = \sigma_\theta - 2\sigma_r \qquad \text{.....(28)}$$

Also $$\frac{u}{r} = \epsilon_\theta = \frac{1}{E}(\sigma_\theta - \nu\sigma_r) \qquad \text{.....(29)}$$

$$\frac{\partial u}{\partial r} = \epsilon_r = \frac{1}{E}(\sigma_r - \nu\sigma_\theta) \qquad \text{.....(30)}$$

Differentiating (29),

$$\frac{\partial u}{\partial r} = \frac{r}{E}\left(\frac{\partial\sigma_\theta}{\partial r} - \nu\frac{\partial\sigma_r}{\partial r}\right) + \frac{1}{E}(\sigma_\theta - \nu\sigma_r)$$

Equating to (30) and using equation (28),

$$r^2\frac{d^2\sigma_r}{dr^2} + 4r\frac{d\sigma_r}{dr} + (1+\nu)\sigma_r = 0 \qquad \text{.....(31)}$$

The solution to this second order differential equation is

$$\sigma_r = \frac{A}{r^{k_1}} + \frac{B}{r^{k_2}} \qquad \text{.....(32)}$$

Where $k_1 = \frac{3}{2} + \sqrt{\frac{5}{4} - \nu}$

$k_2 = \frac{3}{2} - \sqrt{\frac{5}{4} - \nu}$

A and B are arbitrary constants.

In order to determine these constants, it is assumed that the plate is finite, the radius to the outer edge being $r = x$, the pressure there being $\sigma_r = 0$. The radius to the plastic-elastic interface is $r = c$, the transmitted pressure there being $\sigma_r = -p_c$

Thus, when $r = c \quad \sigma_r = -p_c$

$r = x \quad \sigma_r = 0$

Substituting in equation (32),

$$0 = \frac{A}{x^{k_1}} + \frac{B}{x^{k_2}}$$

$$-p_c = \frac{A}{c^{k_1}} + \frac{B}{c^{k_2}}$$

Hence $B = \dfrac{p_c}{\dfrac{x^{k_1-k_2}}{c^{k_1}} - \dfrac{1}{c^{k_2}}}$

Similarly $A = -Bx^{k_1-k_2} = -\dfrac{p_c}{\dfrac{1}{c^{k_1}} - \dfrac{1}{c^{k_1}x^{k_1-k_2}}}$

Since the plate is, in fact, infinite, let $x \to \infty$

Then $B \to 0$ and $A \to -p_c c^{k_1}$

$$\therefore \sigma_r = -p_c\left(\frac{c}{r}\right)^{k_1} \qquad \text{.....(33)}$$

Similarly $\sigma_\theta = r\dfrac{\partial \sigma_r}{\partial r} + 2\sigma_r$ from (28)

$$\therefore \sigma_\theta = p_c\left(\frac{c}{r}\right)^{k_1}(k_1 - 2) \qquad \text{.....(34)}$$

On the plastic-elastic boundary $r = c$ the stresses must just satisfy the yield criterion of von Mises, viz

$$\sigma_r^2 - \sigma_r\sigma_\theta + \sigma_\theta^2 = \sigma_o^2 \qquad \text{.....(35)}$$

Substituting the values for σ_r and σ_θ from (33) and (34) leads to

$$p_c^2(k_1^2 - 3k_1 + 3) = \sigma_0^2 .$$

Substituting $k_1 = \frac{3}{2} + \sqrt{\frac{5}{4} - \nu}$, $p_c = \frac{\sigma_0}{\sqrt{2-\nu}}$ .....(36)

(The positive radical is taken in (36) since the radial pressure must be positive).

Hence it can be shown that:-

$$\sigma_r = -\frac{\sigma_0}{\sqrt{2-\nu}} \cdot \frac{1}{\phi^{3/2+\sqrt{5/4-\nu}}} \qquad .....(37)$$

$$\sigma_\theta = \frac{(\sqrt{5/4-\nu} - \frac{1}{2})}{\sqrt{2-\nu}} \cdot \sigma_0 \cdot \frac{1}{\phi^{3/2+\sqrt{5/4-\nu}}} \qquad .....(38)$$

$$\sigma_z = 0 \qquad .....(39)$$

$$\epsilon_r = \frac{-1+\frac{1}{2}\nu - \nu\sqrt{5/4-\nu}}{\sqrt{2-\nu}} \cdot \frac{\sigma_0}{E} \cdot \frac{1}{\phi^{3/2+\sqrt{5/4-\nu}}} \qquad .....(40)$$

$$\epsilon_\theta = \frac{\nu - \frac{1}{2} + \sqrt{5/4-\nu}}{\sqrt{2-\nu}} \cdot \frac{\sigma_0}{E} \cdot \frac{1}{\phi^{3/2+\sqrt{5/4-\nu}}} \qquad .....(41)$$

$$\epsilon_z = \frac{\frac{3}{2}\nu - \nu\sqrt{5/4-\nu}}{\sqrt{2-\nu}} \cdot \frac{\sigma_0}{E} \cdot \frac{1}{\phi^{3/2+\sqrt{5/4-\nu}}} \qquad .....(42)$$

The velocity in the elastic region may be determined as follows:-

$$d\epsilon_\theta = \frac{1}{E}(d\sigma_\theta - \nu d\sigma_r) = \frac{du}{r} = \frac{v dc}{r}$$

$$\therefore v = \frac{r}{E}\frac{d}{dc}(\sigma_\theta - \nu\sigma_r) = \frac{\phi(\nu-\phi)}{E}\frac{d}{d\phi}(\sigma_\theta - \nu\sigma_r)$$

Hence $v = \frac{(1+\nu)(\frac{1}{2}+\sqrt{5/4-\nu})}{\sqrt{2-\nu}} \cdot \frac{\sigma_0}{E} \cdot \frac{1}{\phi^{1/2+\sqrt{5/4-\nu}}}$ .....(43)

On the plastic-elastic boundary ($\phi = 1$),

$$\sigma_r = -\frac{\sigma_0}{\sqrt{2-\nu}}$$

$$\theta - \frac{\pi}{6} = \sin^{-1}\frac{\sqrt{3}\sigma_r}{2\sigma_0} = \sin^{-1}\left(-\frac{\sqrt{3}}{2\sqrt{2-\nu}}\right)$$

$$\therefore \theta = \frac{\pi}{6} + \sin^{-1}\left(-\frac{1}{2}\sqrt{\frac{3}{2-\nu}}\right) \qquad \ldots\ldots(44)$$

$$v = \frac{(1+\nu)\left(\frac{1}{2}+\sqrt{5/4-\nu}\right)}{\sqrt{2-\nu}}\,\frac{\sigma_0}{E} \qquad \ldots\ldots(45)$$

$$\epsilon_z = \frac{\frac{3}{2}\nu - \nu\sqrt{5/4-\nu}}{\sqrt{2-\nu}} \cdot \frac{\sigma_0}{E} \qquad \ldots\ldots(46)$$

(ii) Flat Plate. h; constant.

From the well known Lamé equations it can be shown that the solution is:-

$$\sigma_r = -\frac{\sigma_0}{\sqrt{3}\phi^2} \qquad \ldots\ldots(47)$$

$$\sigma_\theta = +\frac{\sigma_0}{\sqrt{3}\phi^2} \qquad \ldots\ldots(48)$$

$$\sigma_z = 0 \qquad \ldots\ldots(49)$$

$$\epsilon_r = -\frac{\sigma_0(1+\nu)}{\sqrt{3}E} \cdot \frac{1}{\phi^2} \qquad \ldots\ldots(50)$$

$$\epsilon_\theta = +\frac{\sigma_0(1+\nu)}{\sqrt{3}E} \cdot \frac{1}{\phi^2} \qquad \ldots\ldots(51)$$

$$\epsilon_z = 0 \qquad \ldots\ldots(52)$$

The velocity in the elastic region is

$$v = \frac{\phi(v-\phi)}{E}\,\frac{d}{d\phi}(\sigma_\theta - \nu\sigma_r)$$

$$\therefore v = \frac{\frac{2\sigma_0}{\sqrt{3}E}\cdot\frac{(1+\nu)}{\phi}}{1+\frac{2\sigma_0}{\sqrt{3}E}\cdot\frac{(1+\nu)}{\phi^2}} \simeq \frac{2\sigma_0}{\sqrt{3}E}\cdot\frac{(1+\nu)}{\phi} \qquad \ldots\ldots(53)$$

When $\phi = 1, \sigma_r = -\frac{\sigma_0}{\sqrt{3}}$

Hence $\theta - \frac{\pi}{6} = \sin^{-1}\frac{\sqrt{3}\sigma_r}{2\sigma_0} = \sin^{-1}\left(-\frac{1}{2}\right) = -\frac{\pi}{6}$

$$\therefore \theta = 0, \quad v = \frac{2\sigma_0(1+\nu)}{\sqrt{3}E}, \quad \epsilon_z = 0 \qquad \ldots\ldots(54),\ (55),\ (56).$$

6. Numerical Solution.

The material considered in this analysis was the 0.2% mild steel boiler plate. Samples of this steel were tested as described previously, and the following values for the elastic constants determined experimentally:-

E = 13460 Tons per sq. in.

$\nu = 0.3$

In order to derive the curve $\bar{\sigma} = H\left(\int d\bar{e}^{P}\right)$ from the experimental curve already obtained (Fig. 89), the following procedure was adopted:-

Now $\bar{\sigma} = \frac{L}{A} = \frac{Ll}{A_o l_o}$ (assuming that the volume of the specimen between the gauge points remains constant)*

and $e = \frac{l - l_o}{l_o} = \frac{l}{l_o} - 1 \quad \therefore \frac{l}{l_o} = 1 + e$.

Also $\bar{\epsilon} = \int d\epsilon = \int_{l_o}^{l} \frac{dl}{l} = \log \frac{l}{l_o} = \log(1 + e)$

$\therefore \bar{\sigma} = \frac{L}{A_o}(1 + e)$.

The curve of $\bar{\sigma}$ versus $\log \frac{l}{l_o} - \frac{\bar{\sigma}}{E}$ obtained is shown in Fig.95.

A curve of H' versus $\bar{\sigma}$ may be derived from this for use in the theory already outlined and is shown in Fig. 96.

The solution for the plate in which $h_i = mr_i$ is shown in tabular form in Table 21, and the distribution of stress and strain in Figs. 97 and 98.

The solution for the plate of constant thickness is shown in tabular form in Table 22, and the distribution of stress and strain in Figs. 99 and 100.

---

* By application of the Reuss equations it may be shown that $\bar{\sigma} = \frac{L}{A_o}(1+e)\exp\left\{-(1-2\nu)\frac{\bar{\sigma}}{E}\right\}$. The correction is negligible.

7. Conclusions.

The two solutions are, as would be expected, very similar - the one referring to the plate of originally constant thickness must be regarded as approximate only. The solution for the plate of original thickness proportional to original radius should give a fairly accurate estimate of the actual distribution of stress and strain which would be induced in practice. It would be instructive to devise experiments to expand plates of this type and material by uniform pressure as acheck on the deformation pattern.

In order to determine the residual stress distribution throughout the plate on release of the expanding pressure, an approximation would be to assume that the plate had its original contur, and that a hypothetical elastic distribution of stress and strain induced by the expanding pressure was subtracted from that due to the original expanding. This has been done for the case of expanding a hole until the plastic zone has extended to a radius such that $\frac{a}{c} = 0.26$ in both cases. It can be seen from Fig. 97, for the case $h_i = mr_i$, that the residual stresses would probably not exceed the yield criterion, but that for the case h_i = constant they would, (Fig. 99). In order to estimate whether the residual stresses would exceed the yield criterion, the Tresca criterion may be used as an approximation. For 'Secondary' yielding to occur, then, the maximum algebraic difference of the principal residual stresses must exceed the value of $\bar{\sigma}$ at the radius considered, it being remembered that the third principal residual stress is $\sigma_z = 0$.

By comparing Figs. 98 and 100 it appears also that the assumption that the plate maintains its original contour for the purpose of determining the released elastic stress and strain distribution is much better for the plate having $h_i = m r_i$. In fact, down to a value of $\frac{a}{c}$ about 0.17, the deformed contour is very little different from the original for this particular steel.

It is relevant to consider the general effect of secondary yielding on release of the expanding pressure, due to the residual stresses attaining the yield criterion. This has been done by extending Nadai's theory, since it is possible to do this without reference to the strain distribution, provided that the yield stress is assumed constant (no work-hardening), and that there is negligible thickening of the plate over the range considered.* An analytical solution is then possible in terms of the stresses only, and is given in Appendix 3 for the case $\frac{c}{a} = 1.751$. As shown in Fig. A2 there is a reduction in the magnitude of the residual radial stresses at every point throughout the plate, and although no reference is made to the strains in the theory, it is apparent that there must also be a reduction in the residual circumferential strain distribution.

---

* It has been shown that there is in fact negligible thickening in the region considered, by use of the theory outlined for a plastic-elastic material having a constant yield stress. (This region corresponds with the rigid annulus of plastic material envisaged in Hill's theory).

DISCUSSION OF THE EXPERIMENTAL RESULTS.

1. Geometrical Similarity.

Specimens 1, 2, 3, 4, and 6 were geometrically similar in their dimensions and, as has been outlined, an attempt was made to expand them to the same relative degree. Certain deviations from strict similarity existed in these tests, however. Some of these have already been indicated, such as the variations in the expanding tools as regards the relative lengths of the rollers and their angles of inclination, and the use of one size of strain gauge grid for all specimens. The first of these was unavoidable with the available expanders, but some estimate can be made of the effect of a finite area of strain gauge grid where the strain gradient is changing rapidly. Except for the radial gauges immediately adjacent to the tube seat the effect is small and unimportant in comparison with the general experimental accuracy, but the radial strain gradient near the tube seat was far greater than had been expected and little comparison can be made between these particular gauges in the three tests. An estimate of the discrepancy was made in the section dealing with strain gauge technique and calibration. In comparing the results, therefore, the most representative readings are the circumferential dynamic strains at $\frac{r}{r_o} = 2.5$.

It was possible to determine the shapes of the final joints without actually sectioning and these configurations are shown in Figs. 52, 57, 62, and 67. It is clear that the different relative roller length was the main cause of the deviations from similarity,

a factor which could not be foreseen. Indeed, no investigation of this factor appears to have been made, previous workers having assumed parallel expanding, whereas, even with so-called parallel expanders, the nature of the deformation is critically dependent on the roller length.

This has introduced a pronounced difference in strains as between the front and back of the discs, and also between one test and another. The supposed theoretical maximum extent of the plastic zone, as indicated by plumber's resin, was achieved on the backs of Specimens 1, 2, and 3, and on the front of No. 4. Accordingly, restricting the comparison to the circumferential dynamic gauges at $\frac{r}{r_o} = 2.5$ on these faces, it will be seen that the strain records bear a distinct resemblance to one another.

The main evidence that geometrical similarity holds in these experiments is demonstrated most conclusively by comparing the residual (static) strain distributions on the four faces already mentioned. For such a comparison it is only necessary to consider ϵ_θ, the circumferential strain, since the equation of strain compatibility for an axially symmetrical system relates ϵ_r the radial strain, and ϵ_θ, viz. $\epsilon_r = \epsilon_\theta + r\frac{\partial \epsilon_\theta}{\partial r}$, (small strains). The values of ϵ_θ at various ratios of $\frac{r}{r_o}$ for all the experiments concerned are plotted in Fig. 101. Within the inevitable differences in the tests it is seen that the agreement is satisfactory the points lying about a smooth curve.

The above relationship between the strains allows a check to be made of the accuracy of the strain measurement, since a curve

of ϵ_r can be derived from ϵ_θ. Fig. 102 shows the derived curve compared with the actual radial strain readings. Bearing in mind the small strains which had to be measured, the agreement is satisfactory.

In Table 23 the principal characteristics of the three main experiments (2, 3, and 4a) are tabulated. Owing to the breakdown of the drive unit during Experiment 4a and Experiment 6 the results of these tests cannot be properly compared with the others as, in consequence, the expanding process followed a completely different course. It will be seen from the columns for Specimens 3 and 2, however, that there is clear evidence that geometric similarity holds. The only serious exception is in the total work done; the ratio should be 1:8, the departure from this being thought due to either the relatively greater amount of friction in the smaller expander or to some difference in the degree of expanding.

2. Criteria of the Degree of Expanding.

Whatever the seat pressure may be in an expanded joint, the strains generated in the plate must be a measure of the degree of expanding. Referring to the Figures showing the torque variation during the actual expanding process, it would therefore appear that the torque is a good indicator of the expansion since it follows closely the build-up of the mean strain in the plate. Previous investigations do not appear to have made a continuous measurement of the torque.

The torque is in fact a better indicator than the extrusion since the latter does not follow the strains, especially towards the end of the expanding when the extrusion increases rapidly while the strains fall off slightly. This is not to say that the extrusion could not be used as a practical criterion once a trial expansion had been made to determine the extrusion corresponding to the optimum degree of expanding.

3. Parallel Expanding.

The expanding tools used in this research are the standard type designed to give so-called parallel expanding. The records of the process, the residual strains and the extent of plastic yielding all show that parallel expansion of the joints was not obtained. Fig. 62 shows diagrammatically the position of the rollers at successive stages during expanding. It can be seen that as the rollers penetrate the tube they have to move an increasing volume of material because, in addition to their radial movement, they encounter at their forward ends a part of the tube which is still at the original diameter. All this material must be plastically deformed and moved radially outwards. Owing to the constraint offered by the tube beyond the joint, higher strains are built up on the back of the plate than on the front where this heavy deformation does not occur and where the extrusion can take place freely.

It was interesting to discover that even using retractive expanders there was more expanding on the back than on the front

of the plate (Fig. 75). Retractive expanders roll a parallel hole in the opposite direction to that of propulsive expanders, so that it was expected that the plate would be expanded equally on both sides. The fact that it was not indicates that this lack of parallelism is a characteristic of the lack of symmetry of the joint, in that extrusion is unrestricted at the front of the tube, but restricted at the back of the tube by the elastic mass of the tube behind the plate.

The fact that the tube plates were, in general, expanded more on the back than on the front leads to the conclusion that, after expanding, the interface between tube and plate was slightly tapered in an axial direction. An attempt has been made to show this taper on the diagrams illustrating the deformed cross-sections of the joints (Figs. 52, 57, 62, and 67), the actual displacement of the interface having been estimated by extrapolating the curves of ϵ_θ versus $\frac{r}{r_o}$ for each joint. From the results of the push-out tests it can be seen that no increase in push-out load was observed for Specimen 2, in which the tube was pushed out against the taper. In fact, both the mean seat pressure and the push-out load were less for this specimen than for Specimen 1. The ratio $\frac{F}{P}$ was 1.69 for Specimen 1 and 1.55 for Specimen 2, so that the relative push-out load was, in fact, less. That this lack of parallelism has little effect on the push-out load was subsequently observed during the push-out tests on riveted tube joints, which also often exhibited a pronounced lack of parallelism.

4. Extent of Plastic Zone.

The extent of the flaking of the plumber's resin is indicated on Figs. 52, 57, 62, and 67. This indicates that the maximum extent of yielding was to a radius of $\frac{r}{r_o} = 1.75$, which happens to agree exactly with that derived from Nadai's theory. An alternative approach is from consideration of the residual circumferential strain readings. It can be shown that $\epsilon_\theta = k_1 + k_2\left(\frac{r_o}{r}\right)^2$ in the elastic region (Appendix 2), and therefore, a straight line should be obtained when ϵ_θ is plotted against $\left(\frac{r_o}{r}\right)^2$. The point where the smooth curve drawn through the values of ϵ_θ for the tests departs from linearity should indicate the ratio $\frac{r}{r_o}$ at which the plastic-elastic interface exists. Fig. 103, which is a mean curve of ϵ_θ versus $\left(\frac{r_o}{r}\right)^2$ for Experiments 1, 2, 3, and 4a, shows that this departure from linearity occurs at $\frac{r}{r_o} = 2.83$, a value much higher than that found from plumber's resin. The fact that this extended zone is not indicated by the flaking of plumber's resin is probably explained in that the strains are so small.

Two further checks on the actual extent of the plastic zone are provided by the hardness and thickness measurements made across the faces of Specimen 4 (Figs. 81 and 82). It can be seen that there was less work hardening on the back of the plate due to the fact that the rollers had not penetrated for the full seat width in this experiment. On the assumption that thickening and work hardening can only occur in the plastic region of the plate, these results clearly substantiate that the plastic zone had penetrated to a value of at least $\frac{r}{r_o} = 2.6$ on the front of the plate.

COMPARISON OF THE EXPERIMENTAL RESULTS WITH THEORETICAL PREDICTIONS.

1. Residual Strain Distribution and Seat Pressure.

The theory applying to the flat plate will be used as a basis for comparison, on the assumption that for fairly small deformations the system remains geometrically similar. The criterion of degree of expansion will be taken as the enlargement* of the inside diameter of the tube from that at tack rolling.

The definition of circumferential strain for the large displacements involved will be, as for the theory, $\epsilon_\theta = \log \frac{r}{r-u} = \log(1 + e_\theta)$ where $e_\theta = \frac{u}{r-u}$. The tube and plate are assumed to form one continuous medium so that the inside diameter of the tube at tack rolling corresponds with the initial diameter of the hole in the theory. Hence, at the inside of the tube the residual circumferential strain will be $\epsilon_\theta = \log \frac{r_o''}{r_o'} = \log (1 + \frac{u_o}{r_o'})$. The value of the residual circumferential strain at the inside of the tube has been calculated for the various specimens from measurements taken and is shown in Table 24.

A curve of ϵ_θ versus $\frac{r}{c}$ derived from the theory for expanding a hole in a flat plate has been plotted from the results given in Table 22 and is shown in Fig 104.

---

* 'Tack rolling' refers to the enlargement of the tube necessary to close the initial clearance between tube and plate. The inside diameter of the tube at the instant of closing the initial clearance may be calculated on the assumption that the volume of the tube remains constant. Then $r_1^2 - r_o^2 = a^2 - r_o'^2$, where r_o' is the inside radius of the tube at the instant of closing the clearance, r_o the original inside radius.

Considering Specimens 1, 2, and 3, a mean curve was drawn through the results giving the residual strain distribution and was shown in Fig. 104 as a graph of ϵ_θ versus $\left(\frac{r_o''}{r''}\right)^2$. Accordingly, a mean value of the residual circumferential strain at the inside of the tube for these three specimens has been taken, and was calculated from Table 24 as 0.05485. The experimental curve has been extended to a value of $\left(\frac{r_o''}{r''}\right)^2 = 1$ (the inside of the tube) and is shown replotted in Fig. 105. The mean value of $\left(\frac{r_o''}{a''}\right)^2$ for these three specimens was, from Table 24, 0.611, so that the extent of the tube and plate may be shown on the diagram as indicated.

In order to derive the theoretical curve of residual circumferential strain versus $\left(\frac{r_o''}{r''}\right)^2$ it is necessary to include the strains associated with the assumed elastic recovery of the system on release of the expanding pressure. This must be done by a trial and error process. The hypothetical elastic circumferential strain distibution in an infinite plate associated with the expanding pressure p is $\epsilon_\theta = \frac{1+\nu}{E}\left(\frac{r_o}{r}\right)^2 p$. At the inside of the tube this strain is $\frac{0.966}{10^4}\,p$, using the values of ν and E determined experimentally.

From the theoretical curve of ϵ_θ versus $\frac{r}{c}$ a circumferential strain of 0.05862 corresponds with a value of $\frac{r}{c} \doteq 0.247$ and therefore an expanding pressure of $p \doteq 39$ Tons per sq. in. Thus the released elastic circumferential strain at the edge of the hole would be $\epsilon_\theta = \frac{0.966 \times 39}{10^4} = 0.00377$. Since 0.05862 - 0.00377 = 0.05485, this is the theoretical value of $\frac{r_o''}{c}$ required, and it is possible to determine the theoretical residual circumferential

strain distribution as shown in Table 25 and plotted in Fig. 105. It can be seen that the actual residual circumferential strains throughout the plate are considerably less than the theoretical strains associated with the measured increase in inside diameter of the tube above that at tack rolling.

In order to determine the theoretical residual seat pressure the procedure broadly outlined in the theory must be followed. Thus, at the outside of the tube $\frac{r}{c} = \frac{a''}{c} = \frac{a''}{r_o''} \times \frac{r_o''}{c} = \frac{1}{\sqrt{0.611}} \times 0.247 = 0.316$. The radial stress at this value of $\frac{r}{c}$ generated by expanding up to a value of $\frac{r_o''}{c} = 0.247$ is approximately 32.6 Tons per sq. in., from the theory (for this particular steel). Assuming an elastic release of stress on release of the expanding pressure, the released radial stress distribution is $\sigma_r = -p\left(\frac{r_o''}{r''}\right)^2$. At the radius $r'' = a''$ this is $\sigma_r = -p\left(\frac{r_o''}{a''}\right)^2 = 39 \times 0.611 = -23.85$ Tons per sq. in. Hence the residual radial stress at this radius, i.e. the theoretical seat pressure, is approximately 32.6 - 23.9 = 8.7 Tons per sq. in. From Table 20, the mean seat pressure measured from the push-out tests on these three specimens was 3.32 Tons per sq. in. only.

Regarding Specimen 5, the residual strain distribution across the plate was measured more accurately in the plastic region, as already described, and the experimental curve for this specimen is plotted together with the theoretical curve in Fig. 106. Following the same procedure as before, from the theoretical curve of ϵ_θ versus $\frac{r}{c}$, a circumferential strain of 0.05364 corresponds with a value of $\frac{r}{c} \simeq 0.253$, and therefore an expanding pressure

$p \simeq 38.4$ Tons per sq. in. Thus the released strain at the edge of the hole would be $\epsilon_\theta = \frac{0.966 \times 38.4}{10^4} = 0.00371$. Since 0.05364 - 0.00371 = 0.04993, the measured strain at the inside of the tube, this is the theoretical value of $\frac{r_0^2}{c}$ required. The theoretical residual seat pressure is that corresponding with the value $\frac{r}{c} = \frac{a^2}{c} = \frac{1}{0.616} \times 0.253 = 0.323$, namely 32.1 - 23.7 = 8.4 Tons per sq. in. The actual measured seat pressure was, for this specimen, 2.76 Tons per sq. in. only.

It should be noted that both in the case of determining the theoretical strain distribution and the theoretical residual seat pressure, no allowance has been made for any 'secondary' yielding which may occur. As already shown, this effect would be small for the case of the theoretical uniform pressure expanding and insignificant in relation to the large discrepancies which exist between the experimental and theoretical results.

It is concluded from these comparisons that the seat pressure obtained between tube and plate by roller expanding is considerably less then the theoretical residual radial stress which occurs at a corresponding radius round a hole expanded by uniform pressure in an infinite plate, an approximate relation being Actual Seat Pressure $\simeq$ 0.35 x Theoretical Seat Pressure * This low seat pressure is accompanied by a distribution of residual

---

* On reference to the published literature on the subject, the maximum seat pressure obtainable by roller expanding appears to be of the order of 4 Tons per sq. in., although Shannon and his colleagues (5) state that seat pressures of about 7 Tons per sq. in. were attained by expanding short ferrules into the already expanded tubes.

circumferential strain which is lower than the theoretical, and it would appear that these effects are not unconnected.

Attention is directed to the fact that comparison has been made between the measured results and the theoretical distribution of stress and strain round a hole expanded in a plate by uniform pressure. In view of the very large difference between the experimental and theoretical results, it would seem justifiable to actually expand a hole in a plate and measure the residual stress and strain distribution, both by uniform pressure and by roller expanders. Reference to this is made in greater detail in the section "Suggestions for Future Investigation", at the end of this thesis.

2. Work-hardening and Thickening.

The hardness and thickness variation was measured across the faces of Specimen 4 as described previously. In order to compare the extent of yielding with theoretical predictions the results for the front of the plate only will be considered (Figs. 81 and 82). By using the hardness-yield stress correlation determined experimentally for this material, the variation of yield stress across the front face of the plate of Specimen 4 is as shown in Fig. 107. The value of r_o'' for this specimen was 1.63 ins., r_o' = 1.5125 ins., so that the inside of the tube had undergone a plastic strain of $\epsilon_\theta = \log(1 + \frac{u_o}{r_o'}) = \log(1 + \frac{0.1175}{1.5125})$ = 0.075. Added to this would be an elastic strain of approximately 0.004, so that the required theoretical value of $\frac{r''}{c}$

corresponding with a strain of 0.079 would be, from Fig. 104, $\frac{r_o''}{c} = 0.228$.

The theoretical yield stress distribution throughout the plate was determined for this value of $\frac{r_o}{c}$ and scaled down by the factor $\frac{3}{4}$ since the ordinates of the stress-strain curve for the 2½ ins. plate were approximately $\frac{3}{4}$ of the corresponding ordinates for the 1½ ins. plate over this range of strain (the stress-strain curve used in the theory was that for the 1½ ins. plate). The theoretical curve is also shown in Fig. 107, and shows, for this type of comparison, good agreement with the experimental curve.

In comparing the experimental and theoretical thickening, the front only of Specimen 4 has been considered, the experimental values of the ratio $\frac{h}{h_i}$ having been determined by considering the displacement x of the front of the plate. The experimental value of $\frac{h}{h_i}$ would then be the ratio of x plus half the original thickness of the plate to half the original thickness of the plate, i.e.

$$\frac{h}{h_i} = \frac{\frac{h_i}{2} + x}{\frac{h_i}{2}} = 1 + \frac{2x}{h_i}$$

The total front extrusion occuring at the mean radius of the tube was 0.259 in. Since the original distance of the 'step' in the front of the tube from the centre of the plate was approximately $\frac{h_i}{2} + \frac{1}{16}$ in. = 1.13 + 0.0625 = 1.193 ins., the experimental value of $\frac{h}{h}$ for this radius ($\frac{r''}{r_o''} = 1.125$), could be taken as $1 + \frac{0.259}{1.193} = 1.217$.

The experimental curve of $\frac{h}{h_i}$ versus $\frac{r''}{r_o''}$ obtained in this way is shown together with the theoretical curve associated with

a value of $\frac{r_d''}{c} = 0.228$ in Fig. 108 . It was quite clear from the appearance of all the joints expanded that relative movement had taken place between the tube and plate, and this effect is illustrated in Fig. 108 in the discontinuity of the experimental curve of $\frac{h}{h_i}$ versus $\frac{r''}{r_o''}$.

Regarding the hardness measurements made on the tube (Fig. 84), the hardness was found to be generally higher than that of the plate. The distribution of hardness along the tube indicates very well the degree of working which it had received, and its magnitude justifies the assumption that the tube and plate can be regarded as being made of the same material.

3. Conclusions.

It is now possible to arrive at some conclusions from the comparison of the experimental and theoretical results. The most important fact is that the seat pressures obtained by roller expanding a tube in a plate are only about 75% of the residual radial stress existing at a corresponding radius round a hole expanded by uniform pressure.* Coupled with this is the fair correspondence between the experimental and theoretical work-hardening across the plate, but the very large difference between the observed and theoretical displacements.

Considering the axial displacements the movement between

---

* Throughout this argument it is assumed that the theory developed for expanding a hole in a thin infinite plate by uniform pressure is approximately true for the actual uniform pressure process. It will be suggested later that this theory be checked experimentally.

the tube and seat requires consideration. This relative movement was observed in all the experiments, the movement of the tube being both to the front and to the back of the plate, thus justifying the term 'extrusion' in reference to this movement. It is clear therefore that there must be large frictional shear forces brought into play between the tube and plate, and furthermore that if the tube and plate were continuous these forces would exist as shear stresses along a corresponding annulus. Thus it can again be realised that the theory, in which the assumption was made that axial cylindrical fibres of the plate are principal planes, is only approximate, since shear stresses could not exist along such planes.

It can only be concluded that because of this relative movement between tube and plate, the axial strain of the tube is higher, whilst the axial strain of the plate is lower than the theoretical, as shown in Figs. 105 and 106. Therefore it seems reasonable to suppose that if the axial strain of the tube could be restricted during the expanding process, more circumferential strain could be generated in the plate together with more axial strain in the plate and possibly a higher value of the seat pressure. The liberal addition of grooves in the seat might possibly bring this restriction about and not only produce greater structural strength but also higher seat pressures.

The fact that the actual degree of work-hardening in the plate is of the same order as, if not higher than, the theoretical (Fig. 107) is much more difficult to explain. It has already been

shown that both the residual axial and circumferential strains in the plate are less than the theoretical, so that, on the face of it, the plate has undergone less plastic straining than that required to produce this degree of work-hardening. The writer is of the opinion that the clue to this apparent anomaly lies in the severe distortion of the plate as exemplified by the graphs showing the complete history of straining in the plate during the expanding process itself. It is clear from these graphs that as the rollers pass under any station in the plate the strain increases rapidly being doubtless accompanied by plastic yielding and work-hardening. When any roller has passed under that station the strains decrease rapidly, generally to their original value, and it is difficult to say whether or not yielding has again occurred during this decrease of strain. Bearing in mind the fact that the degree of work hardening eventually attained is so much higher than that apparently associated with the residual strains in the plate, it may well be that plastic yielding does occur during this phase. That 'secondary' yielding of this type can occur has already been mentioned in connection with the theory for uniform pressure expanding, and it will probably be more pronounced for roller expanding.

In view of the very large differences between the experimental and theoretical residual strains, there seems little to be gained by trying to make any comparison between the build-up of strains measured during the roller expanding process and that predicted by an analogous uniform pressure expanding of a hole in a plate.

MODIFIED DESIGN OF PROPULSIVE EXPANDER.

One of the main disadvantages of the propulsive type of expander of conventional design is the lack of control which it is possible to exercise over its operation. It has been clearly shown by many writers, notably Grimison and Lee (2), that there is an optimum degree of expanding, and that either increase in diameter of the inside of the tube over that at tack rolling, or extrusion, may be used as the criterion for the correct dgree of rolling. There are doubtless other suitable criteria for determining the degree of expanding, for instance it has been shown in this research that the torque variation closely follows the build-up of the mean strains in the plate.

Retractive expanders of the design already described allow a much closer control of the degree of expanding, since the number of mandrel rotations during the expanding phase determines the increase in inside diameter of the tube. Other advantages of retractive expanders are that no severe step is formed on the inside of the tube, and any length of tube seat can be rolled. The main disadvantages of the retractive type of expander appear to be the large torque required to restrain the nut from rotation during the expanding phase, since the self-feeding principle is not utilised, and the weakening of the mandrel necessitated by its large reverse taper. Also the large taper of the mandrel causes an excessive amount of rubbing on the inside of the tube .

In using the standard type of propulsive expanders, having a cape on the cage which comes against the tube end when the

rollers have entered the tube to their maximum extent, the degree of expanding is dependent on the initial axial clearance between this cage and the tube end. Small variations in this clearance lead to large variations in the degree of expanding, and its amount is difficult to control since it is largely dependent on the initial 'biting' of the rollers into the tube by the operator.

It therefore seems worthwhile to develop an improved design of propulsive expander which would allow a controlled increase of inside diameter followed by a parallel rolling phase so that any length of seat could be expanded. Accordingly the largest expander was modified as shown in Fig. 109. Control of the increase of inside diameter of the tube is achieved by positioning the nut A at a prescribed distance X from the thrust race B, having previously caused the rollers to bite into the tube. It is well known that mandrel travel gives a fairly accurate measure of the increase in tube inside diameter, and the self-feeding principle would allow a continuous expanding of the tube to be effected. Having completed the initial expanding phase the nut bears against the thrust race and, owing to the high friction between the nut and the mandrel thread, rotates with the mandrel thus preventing further relative axial movement between mandrel and cage. Continued rotation of the mandrel results in parallel rolling until the cage C comes against the tube end. Removal of the expanders is effected by reversal of rotation of the mandrel.

The initial clearance between tube and plate could be closed by suitable adjustment of the distance X, so that further expanding could be made from the 'tack-rolled' condition. Disadvantages of this expander would be that care would have to be taken by the operator that the rollers did not completely enter the tube before the distance X had been closed. If this happened the front end of the tube would have to be expanded again, the position of the nut being left as before. Also a step would be formed on the inside of the tube in common with the usual designs of propulsive expander, but this could be minimised by using 'torpedo' nosed rollers, having a generous radius on their leading flanks.

This expander has not yet been fully tested in a combined tube-plate joint, but has operated fairly successfully in long lengths of tube. The existing rollers have too sharp radii on their leading flanks, however, which causes the formation of a severe step, and it is suggested that these rollers be modified before testing the expanders in a combined tube-plate joint.

If necessary a simpler design of this modified tube expander could be developed, having the threaded mandrel extension integral with the tapered section.

ALTERNATIVE METHODS OF OBTAINING TUBE-SEAT JOINT.

In view of the low seat pressures obtainable by the use of roller expanders, other methods of obtaining a tube-seat joint may be considered, with special reference to the seat pressures generated, as follows:-

1. Uniform Pressure Expanding.

If it were possible to expand a boiler tube joint by a uniform hydrostatic pressure, then according to the theory already outlined, seat pressures of the order of 8 Tons per sq.in. should be attainable. Relative movement between tube and seat would probably occur, however, with a consequent reduction in the seat pressure generated. A possible practical method of expanding by uniform pressure might be by the use of a tapered mandrel inserted directly and forced axially into the tube which would have to be secured relative to the boiler. In this connection Dr. W.B.Carlson of Messrs. Babcock and Wilcox has intimated that tubes have been expanded by exploding a controlled charge in the mouth of the tube, but with no apparent resulting increase in seat pressure.

2. Interference Fit.

Another practical possibility might be that of shrinking an oversize tube end(by cooling in liquid oxygen, for instance) and, having inserted the tube into the boiler, allowing it to expand. The seat pressure attainable by this method can be calculated as follows:-

Within the elastic limit, the distribution of stress and strain throughout a tube under external pressure p can be shown to be, from the Lame equations,

$$\sigma_r = - p \frac{1 - \left(r_0/r\right)^2}{1 - \left(r_0/r_1\right)^2}$$

$$\sigma_\theta = - p \frac{1 + \left(r_0/r\right)^2}{1 - \left(r_0/r_1\right)^2}$$

$$\epsilon_\theta = - \frac{p}{E\left[1 - \left(r_0/r_1\right)^2\right]}\left[(1 - \nu) + (1 + \nu)\left(\frac{r_0}{r}\right)^2\right]$$

At the outside of the tube the radial displacement is

$$u_{r_1} = - \frac{p r_1}{E}\left[\frac{1 + \left(r_0/r_1\right)^2}{1 - \left(r_0/r_1\right)^2} - \nu\right]$$

The distribution of stress and strain throughout an infinite plate having a hole expanded by a pressure p is (assuming tube and plate to be made of the same material)

$$\sigma_r = - p \left(\frac{a}{r}\right)^2$$

$$\sigma_\theta = + p \left(\frac{a}{r}\right)^2$$

$$\epsilon_\theta = \frac{1 + \nu}{E}\left(\frac{a}{r}\right)^2 p$$

At the edge of the hole the radial displacement is

$$u_a = \frac{1 + \nu}{E} pa$$

If the initial radial 'interference' is u, the tube will be compressed an amount u_{r_1} and the hole will be expanded an amount u_a such that $|u_{r_1}| + |u_a| = u$

Hence $u = \frac{2pr_1}{E} \Big/ \left[1 - \left(r_0/r_1\right)^2\right]$ (Since $r_1 \doteq a$, elastic displacements only being considered)

It is now necessary to determine the maximum seat pressure which may be attained before yielding occurs.

The von Mises criterion is, since $\sigma_z = 0$,

$$\sigma_r^2 - \sigma_r\sigma_\theta + \sigma_\theta^2 = \sigma_o^2$$

Where σ_o is the yield stress in uniaxial tension.

For the tube, this criterion reduces to

$$\frac{p^2}{\left[1 - \left(\frac{r_o}{r_i}\right)^2\right]}\left[3 + \left(\frac{r_o}{r}\right)^4\right] = \sigma_o^2$$

The left-hand side of this criterion is a maximum when $r = r_o$.

Thus the maximum allowable pressure on the tube is

$$p = \frac{\sigma_o}{2}\left[1 - \left(\frac{r_o}{r_i}\right)^2\right] \qquad \text{(Always less than } 0.5\,\sigma_o\text{)}$$

For the plate the criterion becomes

$$3p^2\left(\frac{a}{r}\right)^4 = \sigma_o^2$$

The left-hand side of this equation is a maximum when $r = a$.

Thus the maximum allowable pressure in the hole in the plate is

$$p = \frac{\sigma_o}{\sqrt{3}} = 0.5771\,\sigma_o \ .$$

Accordingly, the maximum allowable seat pressure is given by the allowable pressure on the tube. For the material used in this investigation,

$\sigma_o \doteq 16$ Tons per sq. in.

$E = 13460$ Tons per sq . in.

$\nu = 0.3$

$\frac{r_o}{r_i} = \frac{3}{4}$

Thus the maximum seat pressure which could be attained without yielding occurring at the inside of the tube would be

$$p = 8\left(1 - \frac{9}{16}\right) = 3.5 \text{ Tons per sq. in.}$$

The radial interference necessary would be such that

$$\frac{u}{r_1} = \frac{2 \times 3.5}{13460} \Big/ \frac{7}{16} = 0.00119.$$

In order to shrink the tube by an amount $\frac{u}{r_1} = 0.002$, assuming a temperature coefficient of expansion of 6.5×10^{-6} per degree Fahr., a temperature difference of 308 Fahr. degrees would be required. Assuming an ambient temperature of 68° F., this would mean lowering the temperature of the tube end to - 240° F. Since the boiling point of liquid oxygen is approx. - 300° F., a shrinkage of this amount would be practicable.

The practical difficulties in such a process could be very great, notably the difficulty of controlling the interference dimension u over the range of tolerances allowable on the tube and seat dimensions. There would also be great practical difficulties in cooling the tube end, and undesirable conditions might arise at the junction between the cooled and uncooled parts of the tube, together with unpredictable 'quenching' stresses in the tube end.

5. Tube Riveting.

Suitably controlled axial compression of the tube end would cause it to thicken and expand into the seat plate. On release of the axial load elastic recovery of the system would occur. Provided that the inward elastic radial displacement of the outside of the tube on recovery is less than the inward elastic radial displacement of the seat associated with the expanding pressure generated in the seat, a residual seat pressure would be left. This process is essentially that of riveting, and is discussed in more detail in the next section.

TUBE RIVETING EXPERIMENTS. (SPECIMENS 7 AND 8).

In order to determine the seat pressures which could be attained by riveting tubes into seat plates, several experiments were carried out by compressing short lengths of tube into seat plate discs. The specimens used consisted of tubes nominally 0.997 in. outside diameter, ⅛ in. thick, riveted into 7 inches diameter discs of the ⅜ in. boiler plate, which had centrally drilled 1 in. diameter holes. 17 x 2.5 mm., 100 ohm Tinsley strain gauges cemented with 'High Solids' Duxofix were used, disposed circumferentially across the faces of the specimens as shown in Fig. 110.

The procedure adopted was to support the plate in a suitable position between the loading platens of the Denison testing machine and to compress the tube axially until a circumferential strain of about 3% had been generated under the strain gauge adjacent to the hole. The load was then released, the specimen unwired and the projecting part of the riveted tube machined off flush with the face of the plate. The specimen was then rewired and replaced in the testing machine, and the tube pushed out in the usual way. The subsequent elastic recovery of the plate was measured by means of the strain gauges, and the seat pressure estimated. The push-out load was also recorded.

It was found that the length of the tube had a pronounced effect on the mode of its deformation under compression. Tubes 1 in. outside diameter, ⅛ in. thick, of lengths 1 in. and 2 ins. when compressed axially between unlubricated platens exhibited

the modes of deformation shown exeggersted in Fig. 111 (a and b). Accordingly, riveting of tubes into the specimens was carried out having the seat plates in the positions shown in Fig. 111 (c and d).

Two specimen seat plates were prepared (Specimens 7 and 8). Two 1 in. length tubes were successively riveted into Specimen 7, push-out tests yielding the results shown in Figs. 112 and 113. A 2 in. length tube was then riveted into this specimen as shown diagrammatically in Fig. 111d, a push-out test yielding the results shown in Fig. 114. A 1 in. length tube was riveted into Specimen 8, the results of the subsequent push-out test being shown in Fig. 115. The values of the seat pressures and coefficients of friction calculated from these results, using the theory already outlined under the section "Push-out Tests", assuming E = 13460 Tons per sq. in. and ν = 0.3, are shown on these graphs.

It can be seen from these results that much higher mean seat pressures can be generated by a riveting than by a roller expanding process, although the riveting loads required to do this are high. Also, due to unavoidable 'dishing' of the seat plate, a region of high local seat pressure appears to be developed. It appears that mean seat pressures of about 7 Tons per sq. in. can be achieved with the configuration used in these experiments, and local seat pressures of up to twice this amount can be generated. The seat pressures associated with the type of deformation shown in Fig. 111d are low, however, and therefore this 'unstable' tube compression must be avoided if the process is to be used in practice.

A POSSIBLE DESIGN OF TUBE RIVETING MACHINE.

The practical difficulties of designing a machine capable of riveting boiler tubes may prove insurmountable; a tentative design is suggested in the sketch shown in Fig. 116. Oil pressure supplied to the oil chamber of the machine would cause the riveting plate to move relative to the oil cylinder. Movement of the cylinder relative to the boiler tube could be prevented by the tapered mandrel and serrated segmental collet which would bite into the inside of the tube. To prevent excessive bulging of the tube and large movement of the tube behind the boiler, a retaining ring is positioned as shown, split for ease of assembly.

No estimate of the various forces acting has been made, but as the riveting loads required are so high, it may well be that either the axial load in the mandrel or the squeezing pressure from the collet on the tube would prove limiting factors in such a design. Such a process could be very easily and accurately controlled by the simple addition of a pressure gauge to the equipment, and, so that each tube would receive the same degree of riveting, the initial clearance between tube and seat could be closed by means of a roller type tube expander, it being remembered that close control must be kept on the initial projection of the tube (y in Fig. 116).

GENERAL CONCLUSIONS.

It is to be noted that all the joints were deliberately over-expanded, and would not be acceptable in practice. The percentage increase in inside diameter of the tubes was about 6%. Grimison and Lee (2) found in tests on ¾ ins. outside diameter tubes that the maximum seat pressure occurred for an increase in internal diameter of 2%. They managed to obtain development of the plastic zone into the plate such that the mill scale 'popped' to a distance of $\frac{r}{r_o} = 1.75$. In this research it was found necessary to give 6% increase to obtain flaking of the plumber's resin to this extent. It appears, therefore, that plumber's resin is not as sensitive an indicator as mill scale.

The researches of Grimison and Lee also showed a sharp reduction of residual seat pressure and pull-out strength beyond a certain degree of expansion, which they attributed mainly to the breaking down of the surface between tube and seat as a result of excessive extrusion. The comparison made between the experimental and theoretical axial displacements of tube and plate in this research confirm the conclusions arrived at by those investigators. It is clear that the more the relative axial movement between the tube and the seat the less does the system behave as though it were continuous. As soon as relative movement occurs, in fact, the behaviour of the joint no longer resembles that of the idealized theory, the circumferential strains in the plate fall off, and there is a consequent reduction in seat pressure.

Thus the failure of the theory to predict a maximum residual seat pressure as is observed in practice is partly due to its failure to predict the distorted shape of the principal planes. The system of principal planes which must be developed in the deformed plate of the single-hole uniform pressure theory would be of the type shown below:-

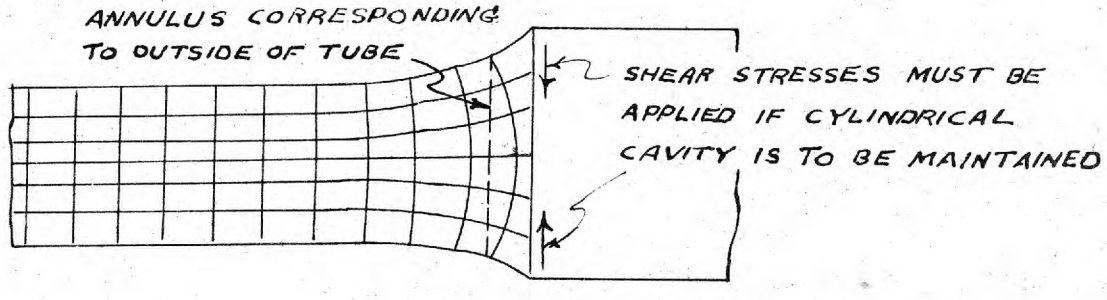

If this system could be determined, a knowledge of the shear stresses and normal stresses acting at a radius corresponding with the outside of the tube, together with an assumed value of the coefficient of friction, would allow prediction of the maximum degree of expanding which could be achieved before relative axial movement takes place.

On the face of it, therefore, it appears that such relative axial movement of the tube and plate will occur for either uniform pressure or roller type expanding, so that the high seat pressures predicted by the theory could never be generated unless relative movement be prevented by some means. From this point of view, it would seem that a rough tube and seat finish would be beneficial for producing higher seat pressures,

as would the provision of grooves along the seat length. The riveting experiments also confirm that greater circumferential strains induced in the plate during expanding lead to higher seat pressures.

In order to determine the precise difference between roller and uniform pressure expanding it would be worthwhile expanding a hole in a plate by the two methods and thereby compare the residual distributions of radial stress generated. This could be done by mensuring the elastic recovery of the plate on boring out the hole in small steps, using a strain gauge technique similar to the one outlined for the push-out tests of this research. Uniform pressure expanding of steel would be difficult to attain, but the use of a well-lubricated mandrel of very shallow taper forced into a hole of the same taper might be practicable. Such an experiment would check the theory already developed, and show whether residual stresses of the order indicated by the theory can in fact be attained, both by uniform pressure and by roller expanding. In this way it could be established whether the prevention of relative axial movement between tube and plate would ever lead to higher seat pressures.

Regarding the measurement of variables during the expanding process itself, although the results are interesting in showing the history of the torque and strain variation, it was not found possible to develop a theory suitable for making comparison with the experimental results obtained. It was at first hoped to be able to determine the complete strain path

for any particular element in the plate during expanding and removing the expanders. By plotting such strain paths on the plane of deviatoric states of stress and strain, and from a knowledge of the stress-strain curve for the steel, it would then be possible to determine the stress path for the element, having applied the Reuss equations. A simple geometrical construction which would allow this estimate to be made is outlined in Dr. R. Hill's book (6). In order to do this, however, it would be necessary to measure strains in more directions at the station considered than was done in this research, since the principal planes obviously rotate during passage of the rollers. Also, the simple construction already mentioned is not applicable to problems in which the principal planes rotate.

From the practical point of view the development of a propulsive expander which will give a controlled increase of inside diameter of the tube seems desirable. There are several criteria which may be used for the degree of expanding, but increase in inside diameter of the tube over that at tack rolling seems to be one of the easiest to control and measure, by means of mandrel travel. The tube riveting experiments show that it is possible to generate mean seat pressures of the order of 7 Tons per sq. in. Localised seat pressures of a higher value than this may be generated, and the process seems to be generally superior to the normal roller expanding process. The tube wall is thickened instead of thinned, and the end of the tube is automatically 'belled'. A close control of the process could be achieved by the provision of a pressure gauge in the equipment.

SUGGESTIONS FOR FUTURE INVESTIGATION.

It is suggested that further research into this problem should be split up into two investigations, one dealing with the more practical aspects of expanding tube joints by means of standard roller type and ball drift expanders, the other being directed towards the more fundamental aspects of forming tube joints. Included in the latter investigation could be the development of other methods of making tube joints. Specific items which require further investigation under the two general headings are as follows:-

1. Investigation of Tube Expanding by Roller and Ball Drift Expanders
   (a) Effect of second joint in close proximity to the first.
   (b) Effect of a belling roll on the stress and strain distribution in the joint.
   (c) Effect of addition of grooves in the seat on the seat pressure.
   (d) Experimental investigation of the effect of pressure on a joint in a boiler drum. A theoretical estimate of the effect of temperature could be made.
   (e) Effect of expanding another tube into a seat having had a previously expanded tube cut out.
   (f) Seat pressure distribution.
   An estimate of the seat pressure distribution along the length of the seat could be made, experimentally. One method might be by splitting the seat plate up into a

number of thin discs, each having thin circumferential strain gauges secured in shallow recesses on their faces.

(g) Ball drift expanders.

The principal factors underlying the operation of ball drift expanders should be investigated.

(h) Effect of initial clearance between tube and seat.

2. Fundamental Investigation of Forming Tube Joints.

(a) Experimental measurement of the strains and residual stress distribution existing in a plate having a hole expanded by uniform pressure, and by roller type expanders.

(b) Uniform pressure expanding of tube-plate systems, with measurement of strains and residual seat pressures induced.

(c) General experimental and theoretical consideration of other methods of making tube joints, with a view to obtaining practical methods of achieving higher seat pressures than those given by roller expanders. The observations put forward in the latter part of this thesis might serve as a basis for such an investigation.

APPENDIX 1.

A Geometrical Representation of the Relation Between the Curves Showing Variation of Strain at a Point on the Surface of the Plate, and the Circumferential Distribution of Strain at any Instant, due to the Three-roller Expanders.

Consider the strain ϵ_θ (or ϵ_r) at a particular radius in the plate at any instant, due to the localized pressure on the edge of the hole from the three rollers. If the variation of the strain ϵ_θ with θ is plotted as a polar diagram, a diagram of the type shown below would be obtained, each of the lobes of the diagram being of equal size and shape, since the system is statically determinate and there must be equal pressure on each of the three rollers. θ is measured from any arbitrary datum radius on the plate, and defines the position of any element of the plate at that radius. $0 < \theta < 360$ degrees.

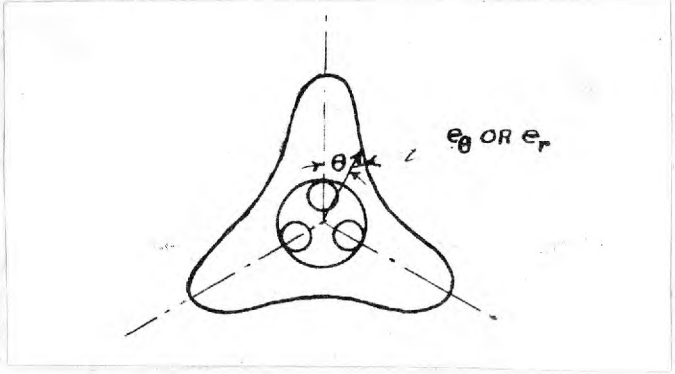

Instantaneous Polar Diagram of Strain in the Plate due to Pressure from Three Rollers, at radius r.

It should be noted that, owing to the applied torque on the rollers, a lobe of the polar diagram will not be symmetrical about the radius through the roller centre underneath it.

If the pressure on the rollers is increased, due to moving the tapered mandrel forward axially, the strains in the plate are everywhere increased, and at the particular radius r there would be an infinite number of polar diagrams, each one corresponding to a particular mandrel position and its related cage position. If these diagrams be constructed in three dimensions, in cylindrical coordinates ϵ_θ , θ, and cage rotation, a three-dimensional surface may be imagined as being generated by the above diagram rotating with the cage and enlarging or decreasing with the pressure transmitted from the mandrel.

During the expanding process the lobes of the enlarging polar diagram may be imagined as forming the threads of a right-handed three-start screw thread of enlarging outer diameter, the shape of the lobes altering continuously.

The three-dimensional diagram would be of the type shown overleaf. As an example, if the cage has rotated through 1½ revolutions, the distribution of the strain ϵ_θ at radius r in the plate would be as indicated by the dotted transverse section of the three-dimensional diagram.

A diagram of strain variation versus cage rotation at any particular angle θ for the given radius r is then given by the appropriate section through the diagram, as shown by section AA. This, then, corresponds with the various experimental graphs

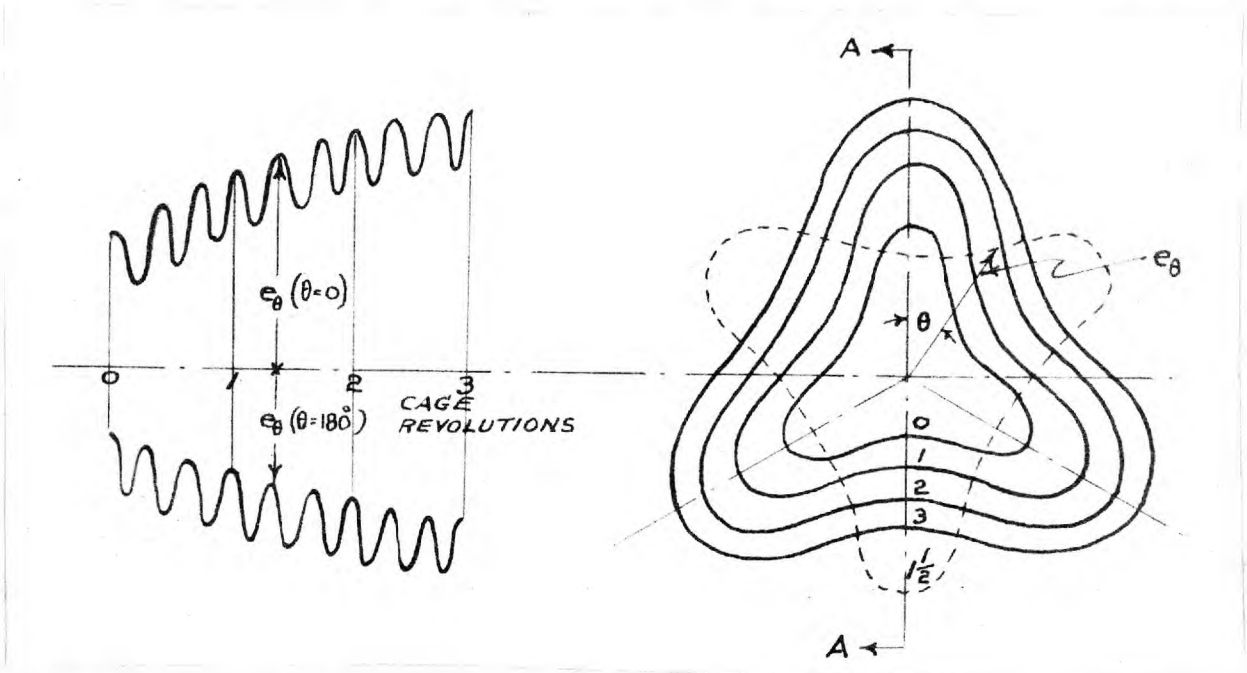

Axial Section AA at $\theta = 0$.

Transverse Sections of the Three-dimensional Diagram at various Values of Cage Revolution.

obtained showing the variation of strain with time at any particular station on the plate, since the rotational speed of the cage is approximately constant.

It can also be seen from this hypothetical three-dimensional diagram that after a given number of cage revolutions the instantaneous strain distribution round the circumference at this radius is given by the transverse cross-section through the diagram, as shown by the dotted line after 1½ cage revolutions. This indicates that the strain at any two stations on the plate 120 degrees apart must be the same, thus justifying the spacing of the radial and circumferential dynamic strain gauges at 120 degrees in these experiments.

In removing the expanders, another three-dimensional

surface may be imagined as being generated, this time by a polar diagram gradually decreasing in size, the cage rotation being in the opposite direction. Since the diagrams obtained experimentally for both and eventually showed little or no variation with cage rotation, the lobes of the generating polar diagram must have eventually disappeared, leaving a circular polar diagram, indicating that the final distribution of strain in the plate was axially symmetrical, as shown diagrammatically below:-

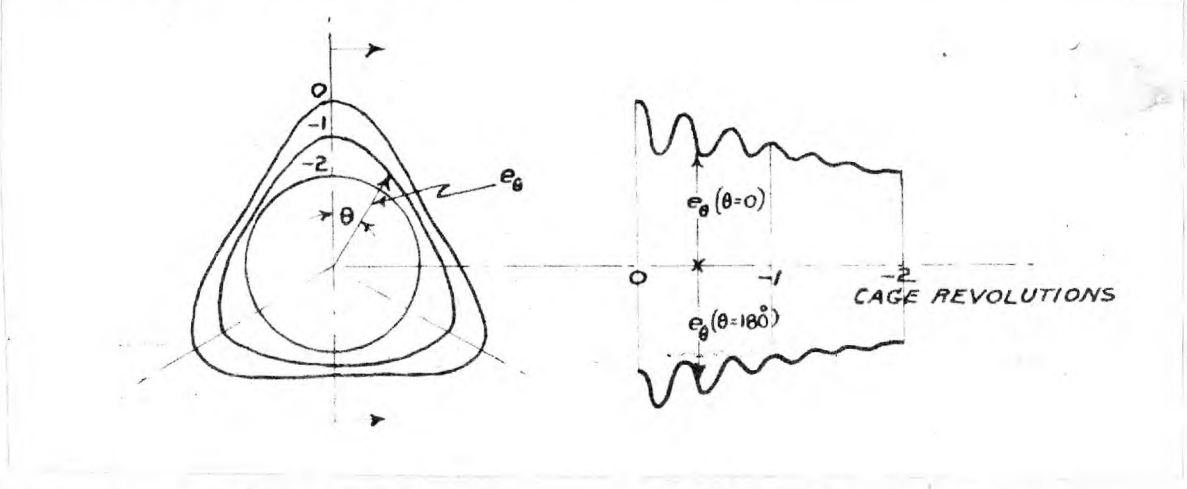

Transverse Sections of Three-dimensional Diagram.

Axial Section at $\theta = 0$.

Any theory which included the effect of the rollers in deforming the plate would have as its ultimate object the derivation of laws from which the above hypothetical three-dimensional diagrams could be constructed. It would be possible to construct a polar diagram for any particular value of cage revolution from the experimental results obtained.

APPENDIX 2.

Theoretical Distribution of Strain in the Elastic Region of a Thin Circular Finite Plate Having a Cylindrical Cavity, Expanded by an Internal Pressure Which is Afterwards Released.

Consider such a plate having a hole of radius a expanded by pressure p. Let the external radius of the plate be b, and assume that the axial stress σ_z is zero everywhere throughout the plate.

The equilibrium condition for a small element gives the equations:-

$$\sigma_r - \sigma_\theta + r\frac{\partial \sigma_r}{\partial r} = 0 \qquad \text{.....(1)}$$

Also $\epsilon_r = \frac{\partial u_r}{\partial r}$, $\epsilon_\theta = \frac{u_r}{r}$, $\epsilon_z = \frac{\partial u_z}{\partial z}$, ...(2)

and $\frac{\partial \sigma_\theta}{\partial \theta} = \frac{\partial \sigma_r}{\partial \theta} = 0$, since the system is axially symmetrical.

Now, since $\sigma_z = 0$,

$$\left.\begin{aligned} E\epsilon_z &= -\nu(\sigma_r + \sigma_\theta) \\ E\epsilon_r &= \sigma_r - \nu\sigma_\theta \\ E\epsilon_\theta &= \sigma_\theta - \nu\sigma_r \end{aligned}\right\} \qquad \text{.....(3)}$$

From Lamé's theory,

$$\left.\begin{aligned} \sigma_r &= -p\left[\left(\frac{b}{r}\right)^2 - 1\right] \Big/ \left[\left(\frac{b}{a}\right)^2 - 1\right] \\ \sigma_\theta &= p\left[\left(\frac{b}{r}\right)^2 + 1\right] \Big/ \left[\left(\frac{b}{a}\right)^2 - 1\right] \\ \sigma_z &= 0 \end{aligned}\right\} \qquad \text{.....(4)}$$

Substitution in equations (3) gives the following expressions for the strains:-

$$\left.\begin{aligned} \epsilon_r &= -\frac{p}{E\left[\left(\frac{b}{a}\right)^2-1\right]}\left[(1+\nu)\left(\frac{b}{r}\right)^2-(1-\nu)\right] \\ \epsilon_\theta &= \frac{p}{E\left[\left(\frac{b}{a}\right)^2-1\right]}\left[(1+\nu)\left(\frac{b}{r}\right)^2+(1-\nu)\right] \\ \epsilon_z &= -\frac{2\nu p}{E\left[\left(\frac{b}{a}\right)^2-1\right]} \end{aligned}\right\} \qquad \ldots\ldots(5)$$

Now plastic flow starts at the hole $r = a$, and the stresses σ_r and σ_θ must reach values such that the yield criterion of the material is satisfied. This is at a pressure p_a, say.

Using the von Mises criterion,

$(\sigma_r-\sigma_\theta)^2+(\sigma_\theta-\sigma_z)^2+(\sigma_z-\sigma_r)^2 = 2\sigma_o^2$ (where σ_o is the yield stress in uniaxial tension), and the fact that σ_z is zero gives the yield criterion as

$$\sigma_r^2-\sigma_r\sigma_\theta+\sigma_\theta^2 = \sigma_o^2 \qquad \ldots\ldots(6)$$

From equations (4), substituting the values of σ_r and σ_θ into equation (6) and writing p_a for p and a for r gives

$$p_a = \frac{\sigma_o\left[\left(\frac{b}{a}\right)^2-1\right]}{\sqrt{3\left(\frac{b}{a}\right)^4+1}} \qquad \ldots\ldots(7)$$

Similarly, if yielding continues into the plate to a radius $r = c$, the radial pressure $\sigma_r = -p_c$ at the radius $r = c$ necessary to just initiate yielding would be

$$p_c = \frac{\sigma_o\left[\left(\frac{b}{c}\right)^2-1\right]}{\sqrt{3\left(\frac{b}{c}\right)^4+1}}$$

or

$$\frac{p_c}{\left(\frac{b}{c}\right)^2-1} = \frac{\sigma_o}{\sqrt{3\left(\frac{b}{c}\right)^4+1}} \qquad \ldots\ldots(8)$$

Consequently, applying equations (5) to determine the strains in the elastic region, and using equation (8),

$$\left.\begin{aligned}
\epsilon_r &= -\frac{\sigma_o}{E\sqrt{3\left(\frac{b}{c}\right)^4+1}}\left[(1+\nu)\left(\frac{b}{r}\right)^2-(1-\nu)\right]\\
\epsilon_\theta &= +\frac{\sigma_o}{E\sqrt{3\left(\frac{b}{c}\right)^4+1}}\left[(1+\nu)\left(\frac{b}{r}\right)^2+(1-\nu)\right]\\
\epsilon_z &= -\frac{2\nu\sigma_o}{E\sqrt{3\left(\frac{b}{c}\right)^4+1}}
\end{aligned}\right\} \quad \ldots\ldots(9)$$

If the pressure at the edge of the hole causing this extent of yielding was p_x and is now decreased to zero, elastic recovery of the plate may be assumed, such that the elastic strains given by the decrease in pressure are:-

$$\left.\begin{aligned}
\epsilon_r &= +\frac{P_x}{E\left[\left(\frac{b}{a}\right)^2-1\right]}\left[(1+\nu)\left(\frac{b}{r}\right)^2-(1-\nu)\right]\\
\epsilon_\theta &= -\frac{P_x}{E\left[\left(\frac{b}{a}\right)^2-1\right]}\left[(1+\nu)\left(\frac{b}{r}\right)^2+(1-\nu)\right]\\
\epsilon_z &= +\frac{2\nu P_x}{E\left[\left(\frac{b}{a}\right)^2-1\right]}
\end{aligned}\right\} \quad \ldots\ldots(10)$$

These strains are added to the strain system existing in the plate, so that the strains remaining in the elastic region of the plate will be:-

$$\left.\begin{aligned}
\epsilon_r &= \frac{1}{E}\left[-\frac{\sigma_o}{\sqrt{3\left(\frac{b}{c}\right)^4+1}}+\frac{P_x}{\left(\frac{b}{a}\right)^2-1}\right]\left[(1+\nu)\left(\frac{b}{r}\right)^2-(1-\nu)\right]\\
\epsilon_\theta &= \frac{1}{E}\left[\frac{\sigma_o}{\sqrt{3\left(\frac{b}{c}\right)^4+1}}-\frac{P_x}{\left(\frac{b}{a}\right)^2-1}\right]\left[(1+\nu)\left(\frac{b}{r}\right)^2+(1-\nu)\right]\\
\epsilon_z &= \frac{2\nu}{E}\left[-\frac{\sigma_o}{\sqrt{3\left(\frac{b}{c}\right)^4+1}}+\frac{P_x}{\left(\frac{b}{a}\right)^2-1}\right]
\end{aligned}\right\} \ldots(11)$$

For any given expansion, E, ν, P_x, c, σ_o, a, and b are fixed, so that the residual strain distribution in the

elastic region will be given by:-

$$\left.\begin{aligned} \epsilon_r &= -\frac{k_1}{(r/a)^2} + k_2 \\ \epsilon_\theta &= +\frac{k_1}{(r/a)^2} + k_2 \\ \epsilon_z &= -k_1 \frac{2\nu}{1+\nu}\left(\frac{a}{b}\right)^2 \end{aligned}\right\} \qquad \ldots\ldots(12)$$

Where

$$\left.\begin{aligned} k_1 &= \frac{(1+\nu)\left(\frac{b}{a}\right)^2}{E}\left[\frac{\sigma_o}{\sqrt{3\left(\frac{b}{c}\right)^4+1}} - \frac{P_x}{\left(\frac{b}{a}\right)^2-1}\right] \\ k_2 &= \frac{1-\nu}{E}\left[\frac{\sigma_o}{\sqrt{3\left(\frac{b}{c}\right)^4+1}} - \frac{P_x}{\left(\frac{b}{a}\right)^2-1}\right] \end{aligned}\right\} \qquad \ldots\ldots(13)$$

Hence $k_2 = \dfrac{1-\nu}{(1+\nu)\left(\frac{b}{a}\right)^2} k_1$

At the extreme edge of the plate, where $r = b$,

$$\left.\begin{aligned} \epsilon_r &= -\frac{2\nu k_1}{(1+\nu)\left(\frac{b}{a}\right)^2} \\ \epsilon_\theta &= \frac{2k_1}{(1+\nu)\left(\frac{b}{a}\right)^2} \\ \epsilon_z &= -\frac{2\nu k_1}{(1+\nu)\left(\frac{b}{a}\right)^2} \end{aligned}\right\} \qquad \ldots\ldots(14)$$

Thus $\left.\begin{aligned} \epsilon_r &= -\nu\epsilon_\theta \\ \epsilon_z &= \epsilon_r \end{aligned}\right\}$ at the radius $r = b$ $\qquad \ldots\ldots(15)$

For these experiments, $\frac{b}{a} = 9.333 \quad \left(= \frac{b}{r_o}\right)$.

Assuming $\nu = 0.3$, then $k_2 = \dfrac{0.7}{1.3 \times 9.333} k_1 = 0.00618\, k_1$

Therefore the theoretical distribution of strain in the elastic region of the plate would be as shown in Fig. A1 . Considering the strains near the edge of the plate where $\epsilon_r \doteq -\nu\epsilon_\theta$ from Mohr's strain circle shown overleaf the normal strain ϵ is

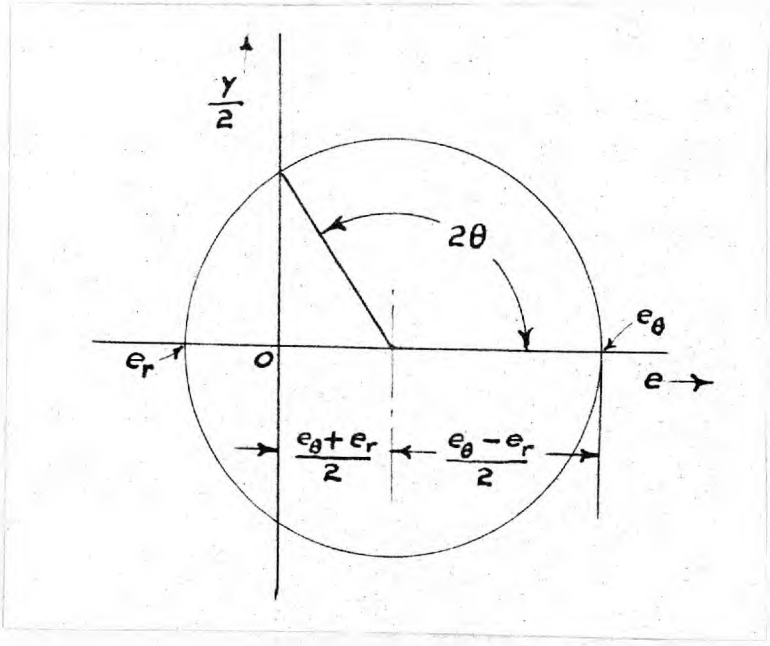

zero along lines inclined at an angle Φ with the circumferential direction, such that

$$\cos(180^\circ - 2\Phi) = \frac{\epsilon_\theta + \epsilon_r}{\epsilon_\theta - \epsilon_r} = \frac{1-\nu}{1+\nu}$$

i.e. $\cos 2\Phi = -\frac{1-\nu}{1+\nu}$. Assuming $\nu = 0.3$, $\cos 2\Phi = -\frac{0.7}{1.3}$

$= -0.539$, $\therefore 2\Phi = 180^\circ - 57.4^\circ = 122.6^\circ$

i.e. $\Phi = 61.3^\circ$ to the circumferential direction, or 28.7° to the radial direction.

APPENDIX 3.

Secondary Yielding on Releasing Expanding Pressure. (Extension of Nadai's Theory).

On the assumption that there is no thickening of the plate in the region considered and that there is no work-hardening, the stress distribution due to expanding a hole in a thin flat plate is as follows:-

Elastic Region.

$$c < r < \infty \qquad \left.\begin{aligned} \frac{\sigma_r}{\sigma_0} &= -\frac{1}{\sqrt{3}}\left(\frac{c}{r}\right)^2 \\ \frac{\sigma_\theta}{\sigma_0} &= +\frac{1}{\sqrt{3}}\left(\frac{c}{r}\right)^2 \end{aligned}\right\} \qquad \ldots\ldots(1)$$

Plastic Region.

$$a < r < c \qquad \left.\begin{aligned} \frac{\sigma_r}{\sigma_0} &= \frac{2}{\sqrt{3}}\sin\left(\theta - \frac{\pi}{6}\right) \\ \frac{\sigma_\theta}{\sigma_0} &= \frac{2}{\sqrt{3}}\sin\left(\theta + \frac{\pi}{6}\right) \\ \left(\frac{c}{r}\right)^2 &= e^{-\sqrt{3}\theta}\cos\theta \end{aligned}\right\} \qquad \ldots\ldots(2)$$

The extent of the plastic zone is given by:-

$$\left(\frac{c}{a}\right)^2 = e^{-\sqrt{3}\theta_a}\cos\theta_a \qquad \ldots\ldots(3)$$

where a is the radius of the hole and θ_a is the value of θ at the edge of the hole.

As shown by Nadai, the maximum value which θ_a can attain according to these equations is $-\frac{\pi}{3}$, giving a value of $\frac{c}{a} = 1.751$.

Releasing the expanding pressure $p = -\frac{2}{\sqrt{3}}\sigma_0 \sin\left(\theta_a - \frac{\pi}{6}\right)$ is equivalent to maintaining the pressure p and superimposing a hydrostatic tension q such that $p - q = 0$. If q is

gradually increased from zero, a state of stress is added to the above of amount:-

$$\left.\begin{aligned}\sigma_r &= q\left(\frac{a}{r}\right)^2 \\ \sigma_\theta &= -q\left(\frac{a}{r}\right)^2\end{aligned}\right\} \qquad \ldots\ldots(4)$$

until yielding again occurs at the edge of the hole.

Thus, in the plastic region:-

$$\left.\begin{aligned}\frac{\sigma_r}{\sigma_o} &= \frac{2}{\sqrt{3}}\sin\left(\theta - \frac{\pi}{6}\right) + \frac{qa^2}{\sigma_o r^2} \\ \frac{\sigma_\theta}{\sigma_o} &= \frac{2}{\sqrt{3}}\sin\left(\theta + \frac{\pi}{6}\right) - \frac{qa^2}{\sigma_o r^2}\end{aligned}\right\} \qquad \ldots\ldots(5)$$

Yielding will first occur at the edge of the hole when the stresses there satisfy the yield criterion of von Mises which may be written as:-

$$\sigma_r^2 - \sigma_r\sigma_\theta + \sigma_\theta^2 = \sigma_o^2 \qquad \ldots\ldots(6)$$

At the edge of the hole:-

$$\left.\begin{aligned}\sigma_r &= \frac{2}{\sqrt{3}}\sigma_o \sin\left(\theta_a - \frac{\pi}{6}\right) + q \\ \sigma_\theta &= \frac{2}{\sqrt{3}}\sigma_o \sin\left(\theta_a + \frac{\pi}{6}\right) - q\end{aligned}\right\} \qquad \ldots\ldots(7)$$

Substituting these values in (6) shows that

$q = \frac{2}{\sqrt{3}}\sigma_o \cos\theta_a$ is the hydrostatic tension which when superimposed on the original expanding pressure p will give secondary yielding at the edge of the hole.

Now $q \not> -p$

$\therefore \cos\theta_a \not> -\sin\left(\theta_a - \frac{\pi}{6}\right)$

$$\theta_a \not> -\frac{\pi}{6} \qquad \ldots\ldots(8)$$

From (8) it can be seen that if θ_a is algebraically greater than -30°, secondary yielding will not occur on release of the expanding pressure p.

When $\theta_a = -30^\circ$, $\left(\frac{c}{a}\right)^2 = e^{\sqrt{3}\frac{\pi}{6}} \cos\left(-\frac{\pi}{6}\right) = 2.145$

$\therefore \quad \frac{c}{a} = 1.466$,

i.e. if primary yielding exceeds a value of $\frac{c}{a} = 1.466$, secondary yielding will take place on release of the expanding pressure.

If, after initial secondary yielding at the edge of the hole due to applying the hydrostatic tension q, the tension is increased, secondary yielding will spread into the plate to a radius c'. On the radius c' the stresses will just satisfy the yield criterion, so that if q' is the hydrostatic tension transmitted across this radius and θ' is the value of θ which was attained during the expanding process at the radius c', the stresses there are given by:-

$$\left.\begin{aligned} \sigma_r &= \frac{2}{\sqrt{3}}\sigma_0 \sin\left(\theta' - \frac{\pi}{6}\right) + q' \\ \sigma_\theta &= \frac{2}{\sqrt{3}}\sigma_0 \sin\left(\theta' + \frac{\pi}{6}\right) - q' \end{aligned}\right\} \qquad \ldots\ldots(9)$$

These stresses must satisfy the yield criterion (6). In order to do so the value of q' must be given by:-

$$q' = \frac{2}{\sqrt{3}}\sigma_0 \cos\theta' .$$

Substituting this value of q' in (9) gives:-

$$\left.\begin{aligned} \frac{\sigma_r}{\sigma_0} &= \frac{2}{\sqrt{3}}\left[\sin\left(\theta' - \frac{\pi}{6}\right) + \cos\theta'\right] = \frac{2}{\sqrt{3}}\sin\left(\theta' + \frac{\pi}{6}\right) \\ \frac{\sigma_\theta}{\sigma_0} &= \frac{2}{\sqrt{3}}\left[\sin\left(\theta' + \frac{\pi}{6}\right) - \cos\theta'\right] = \frac{2}{\sqrt{3}}\sin\left(\theta' - \frac{\pi}{6}\right) \end{aligned}\right\} \ldots\ldots(10)$$

In the remainder of the primary plastic zone the stresses will, therefore, be given by:-

$$\left.\begin{aligned}\frac{\sigma_r}{\sigma_o} &= \frac{2}{\sqrt{3}}\sin\left(\theta - \frac{\pi}{6}\right) + \frac{q' c'^2}{\sigma_o r^2}\\ \frac{\sigma_\theta}{\sigma_o} &= \frac{2}{\sqrt{3}}\sin\left(\theta + \frac{\pi}{6}\right) - \frac{q' c'^2}{\sigma_o r^2}\end{aligned}\right\} \quad c' < r < c \qquad \ldots\ldots(11)$$

In the elastic region:-

$$\left.\begin{aligned}\frac{\sigma_r}{\sigma_o} &= -\frac{1}{\sqrt{3}}\left(\frac{c}{r}\right)^2 + \frac{q' c'^2}{\sigma_o r^2}\\ \frac{\sigma_\theta}{\sigma_o} &= +\frac{1}{\sqrt{3}}\left(\frac{c}{r}\right)^2 - \frac{q' c'^2}{\sigma_o r^2}\end{aligned}\right\} \quad c < r < \infty \qquad \ldots\ldots(12)$$

In the region of secondary yielding $a < r < c'$, the stresses must satisfy the von Mises yield criterion. This may be achieved by writing

$$\left.\begin{aligned}\sigma_r &= \frac{2}{\sqrt{3}}\sigma_o \sin\left(\psi + \frac{\pi}{6}\right)\\ \sigma_\theta &= \frac{2}{\sqrt{3}}\sigma_o \sin\left(\psi - \frac{\pi}{6}\right)\end{aligned}\right\} \qquad \ldots\ldots(13)$$

since substitution of these values in the left-hand side of (6) gives the value σ_o^2.

The equation of equilibrium is, as before, (neglecting thickening of the plate):-

$$\frac{d\sigma_r}{dr} = \frac{\sigma_\theta - \sigma_r}{r} \qquad \ldots\ldots(14)$$

Substitution of the values given by equation (13) into the equilibrium equation (14) leads to:-

$$r\frac{d\psi}{dr}\cos\left(\psi + \frac{\pi}{6}\right) = -\cos\psi \qquad \ldots\ldots(15)$$

Integrating this equation,

$$\frac{1}{r^2} = A^2 e^{\sqrt{3}\psi} \cos\psi \qquad \text{where } A \text{ is an arbitrary constant} \qquad \ldots\ldots(16)$$

At $r = c'$, $\psi = \psi'$, say, and comparison of the equations (13) with equations (10) shows that $\psi' = \theta'$.

Hence $\frac{1}{c'^2} = A^2 e^{\sqrt{3}\psi'} \cos\psi'$ and $A^2 = \frac{1}{c'^2 e^{\sqrt{3}\psi'} \cos\psi'}$

$$\therefore \left(\frac{c'}{r}\right)^2 = \frac{e^{\sqrt{3}\psi}\cos\psi}{e^{\sqrt{3}\psi'}\cos\psi'} = \frac{e^{\sqrt{3}\psi}\cos\psi}{e^{\sqrt{3}\theta'}\cos\theta'} \qquad \ldots\ldots(17)$$

At $r = a$, $\sigma_r = q - p$ where p was the original expanding pressure and q the superimposed hydrostatic tension.

Thus $\frac{2}{\sqrt{3}}\sigma_0 \sin(\psi_a + \frac{\pi}{6}) = q - p$ gives the value of ψ at $r = a$, i.e. ψ_a.

If $q = p$ (complete release of the expanding pressure)

$$\frac{2}{\sqrt{3}}\sigma_0 \sin(\psi_a + \frac{\pi}{6}) = 0, \quad \therefore \quad \psi_a = -\frac{\pi}{6} \qquad \ldots\ldots(18)$$

From equation (17)

$$\left(\frac{c'}{a}\right)^2 = \frac{e^{\sqrt{3}\psi_a}\cos\psi_a}{e^{\sqrt{3}\theta'}\cos\theta'} = \frac{e^{-\sqrt{3}\frac{\pi}{6}}\cos(-\frac{\pi}{6})}{e^{\sqrt{3}\theta'}\cos\theta'} \doteq \frac{0.35}{e^{\sqrt{3}\theta'}\cos\theta'}$$

Now $\left(\frac{c'}{a}\right)^2 = \left(\frac{c'}{c}\right)^2\left(\frac{c}{a}\right)^2$ and $\left(\frac{c'}{c}\right)^2 = \frac{e^{\sqrt{3}\theta'}}{\cos\theta'}$, from equations (2).

$$\therefore \frac{e^{\sqrt{3}\theta'}}{\cos\theta'}\left(\frac{c}{a}\right)^2 \doteq \frac{0.35}{e^{\sqrt{3}\theta'}\cos\theta'}$$

Hence $\theta' \doteq 0.5775 \log\frac{a}{c} - 0.3033$,

and $$\left(\frac{c'}{c}\right)^2 \doteq \frac{0.591}{\cos(0.5775\log\frac{a}{c} - 0.3033)} \qquad \ldots\ldots(19)$$

Equation (19) determines the extent of secondary yielding on release of the expanding pressure in terms of the original value of $\frac{c}{a}$ attained.

The value of $\frac{q'}{\sigma_0}$ is $\frac{2}{\sqrt{3}} \cos\psi' \simeq \frac{0.683\,\frac{a}{c}}{\left(\frac{c'}{c}\right)^2}$

Summarizing, the residual stresses are given by the following equations:-

$$\left.\begin{aligned} \frac{\sigma_r}{\sigma_0} &= \frac{2}{\sqrt{3}} \sin\left(\psi + \frac{\pi}{6}\right) \\ \frac{\sigma_\theta}{\sigma_0} &= \frac{2}{\sqrt{3}} \sin\left(\psi - \frac{\pi}{6}\right) \end{aligned}\right\} \quad a < r < c' \qquad \ldots\ldots(20)$$

Where $e^{\sqrt{3}\psi} \cos\psi \simeq 0.35\left(\frac{a}{r}\right)^2$. $\ldots\ldots(21)$

$$\left.\begin{aligned} \frac{\sigma_r}{\sigma_0} &= \frac{2}{\sqrt{3}} \sin\left(\theta - \frac{\pi}{6}\right) + \frac{0.683\,\frac{a}{c}}{\left(\frac{r}{c}\right)^2} \\ \frac{\sigma_\theta}{\sigma_0} &= \frac{2}{\sqrt{3}} \sin\left(\theta + \frac{\pi}{6}\right) - \frac{0.683\,\frac{a}{c}}{\left(\frac{r}{c}\right)^2} \end{aligned}\right\} \quad c' < r < c \qquad \ldots\ldots(22)$$

Where $\frac{e^{\sqrt{3}\theta}}{\cos\theta} = \left(\frac{r}{c}\right)^2$. $\ldots\ldots(23)$

$$\left.\begin{aligned} \frac{\sigma_r}{\sigma_0} &= \left[-0.5771 + 0.683\,\frac{a}{c}\right]\left(\frac{c}{r}\right)^2 \\ \frac{\sigma_\theta}{\sigma_0} &= \left[+0.5771 - 0.683\,\frac{a}{c}\right]\left(\frac{c}{r}\right)^2 \end{aligned}\right\} \quad c < r < \infty \qquad \ldots\ldots(24)$$

Example. If $\frac{c}{a} = 1.751$ (Maximum extent of primary yielding before thickening of the plate becomes appreciable), then:-

$$\frac{c'}{c} = 0.646\,, \quad 0.683\,\frac{a}{c} = 0.39\,, \quad 0.35\left(\frac{a}{r}\right)^2 = \frac{0.143}{\left(\frac{r}{c}\right)^2}$$

Neglecting secondary yielding on release of the expanding pressure, if $\frac{c}{a} = 1.751$, the residual stresses would be given by:-

Plastic Region.

$$\left.\begin{aligned}\frac{\sigma_r}{\sigma_o} &= \frac{2}{\sqrt{3}}\left[\sin\left(\theta - \frac{\pi}{6}\right) + \left(\frac{a}{r}\right)^2\right] = \frac{2}{\sqrt{3}}\sin\left(\theta - \frac{\pi}{6}\right) + 0.3765\left(\frac{a}{r}\right)^2 \\ \frac{\sigma_\theta}{\sigma_o} &= \frac{2}{\sqrt{3}}\left[\sin\left(\theta + \frac{\pi}{6}\right) - \left(\frac{a}{r}\right)^2\right] = \frac{2}{\sqrt{3}}\sin\left(\theta + \frac{\pi}{6}\right) - 0.3765\left(\frac{a}{r}\right)^2\end{aligned}\right\} \ldots (25)$$

Where $\frac{e^{\sqrt{3}\theta}}{\cos\theta} = \left(\frac{r}{c}\right)^2$ as before. $\qquad a < r < c$

Elastic Region.

$$\left.\begin{aligned}\frac{\sigma_r}{\sigma_o} &= (-0.5771 + 0.3765)\left(\frac{a}{r}\right)^2 = -0.2006\left(\frac{a}{r}\right)^2 \\ \frac{\sigma_\theta}{\sigma_o} &= (+0.5771 - 0.3765)\left(\frac{a}{r}\right)^2 = +0.2006\left(\frac{a}{r}\right)^2\end{aligned}\right\} \quad c < r < \infty \quad \ldots (26)$$

Tables A1 and A2, and Fig. A2 show the difference between the residual stress distribution on taking secondary yielding into account and that on neglecting secondary yielding.

BIBLIOGRAPHY.

1. The Expansion of Boiler Tubes into Tube Plates.
   Baxter, A.M.,
   Report No. 5, R.B. 110, (1947), The British Shipbuilding Research Association.

2. An Experimental Investigation of Tube Expanding.
   Grimison, E.D. and Lee, G.H.,
   Trans. A.S.M.E., Vol. 65 (1943) p.497.

3. Expanded Tube Joints in Boiler Drums, with Special Reference to the Battersea High Pressure Boilers.
   Shannon, W.B., Pratt, C.W., Webb, T.B., and Carlson, W.B.,
   Proc. Inst. Mech. Engrs. 154 (1946) p. 52.

4. A Theory of the Expanding of Boiler and Condenser Tube Joints Through Rolling.
   Nadai, A.,
   Trans. A.S.M.E., Vol. 65 (1943) p.865.

   Also

   Theory of Flow and Fracture of Solids, Vol.1
   Nadai, A.,
   McGraw Hill Book Co. Inc., New York, N.Y.,(1950) p.476.

5. The Holding Power and Hydraulic Tightness of Expanded Tube Joints.
   Goodier, J.N., and Schoessow, G.J.,
   Trans. A.S.M.E., Vol. 65 (1943) p.489.

6. The Mathematical Theory of Plasticity.
   Hill, R.,
   Oxford Clarendon Press.

7. Resistance Strain Gauges for the Measurment of Roll Force, Torque, and Strip Tension.
   Rankine, Batley, and Stanton.
   Journal Iron and Steel Institute, Vol. 160, (Dec.1948)p.381.

8. The Bonded Wire Gauge Torquemeter.
   Huge, A.C.,
   Proceedings Society of Experimental Stress Analysis, Vol. 1 No. 2, p.68 (1944).

9. The Use of Plumber's Resin to Determine the Occurrence of Yield.
   Blair, J.S.,
   W.E.P. No. 51, Proc. Inst. Mech. Engrs. Vol. 161 (1949).

10. Minimising Zero Drift in Electrical Strain Gauge Bridges.
Urwin and Swainger,
Journal Roy. Aero. Soc. (Nov.1947).

11. The Formation and Enlargement of a Circular Hole in a Thin Plastic Sheet.
Taylor, G.I.,
Quart. Journ. Mech. App. Math. 1 (1948) p.103.

12. The Hardening of Metals, p.165.
Tabor, D.
Oxford University Press. (1951).

ZERO DRIFT TEST ON SPECIMEN NO. 2.

All gauges zeroed after a period of 3 hours warming-up.

Bridge voltage:- 6V.

Gauges 33 to 37 on separate piece of boiler plate clamped to boiler plate specimen, connected into active side of static strain recorder.

Figures shown in the table below are % Fractional Resistance Change x 1000 (= 100,000k).

Time in hours	0	1	2	3	6	21
Temp. °C.	20	22.4	25	25.2	21.8	16.1
Channel No. 1	ALL GAUGES ZEROED	8	4½	2½	-3½	-5½
2		7½	3	1	-4	-5½
3		7½	4	2	-4½	-5½
4		7½	4	2	-3½	-5½
5		7½	4	2	-4	-4½
6		8	4	2½	-2½	-5
7		7½	4	2	-3½	-5
8		7½	4	2	-4	-5
9		7½	3½	2	-3½	-4½
10		8	3½	2	-3	-4½
11		7½	3½	1½	-3	-5
12		7½	3½	2	-4	-5
13		7½	3½	2	-4½	-5½
14		8	3½	2	-3½	-5½
15		7½	3½	2½	-2½	-4½
16		7½	3½	1½	-3	-5
17		7½	3½	1½	-3½	-5½
18		7½	4	2½	-4	-5½
19		7½	4	2½	-4½	-5½
20		7½	3½	1½	-4½	-5½
21		7½	3½	2	-4	-5½
22		7½	3½	2	-4	-4½
23		7½	3½	2½	-4	-5
24		7½	3½	1½	-4	-5
25		7½	3½	1½	-4	-5
26		7½	3½	1½	-4	-5
27		6½	2½	1½	-4	-5
28		7½	3½	2	-3½	-5½
29		7½	3½	2	-4	-5½
30		7½	3½	1½	-4	-5
31		7½	3½	1½	-3½	-5
32		7½	3½	1½	-4½	-5½
33		7½	3½	1½	-4½	-5
34		7½	3½	1½	-4	-5
35		7½	2½	2	-4½	-4½
36		7	3	2	-4	-5
37		8	4	2	-4	-4½

TABLE 1.

EXPERIMENT NO. 2.

$\frac{T}{M}$ = 4.26. Final Ratio $\frac{\text{Back Extrusion}}{\text{Total Extrusion}} = \frac{0.069}{0.1617} = 0.427$

Cage Revolutions		Total Extrusion ins.	Back Extrusion ins.	Torque (from spring balance) T lb.ft.	Torque in equivalent microamps. M
0	↑ First Expanding	0	0	0	0
0.5		0	0	0.5	0.117
1.0		0.0002	0.0001	1.75	0.411
1.5		0.0003	0.0002	2.0	0.47
2.0		0.0005	0.0002	3.0	0.704
2.5		0.0007	0.0001	4.0	0.94
3.0		0.0014	0.0002	5.75	1.35
3.5		0.0018	0.0004	6.25	1.47
4.0		0.0037	0.0012	6.75	1.585
4.5		0.0046	0.0013	8.0	1.88
5.0		0.0062	0.0027	8.75	2.05
5.5		0.0081	0.0033	10.25	2.41
6.0		0.0106	0.0052	16.75	3.93
6.5		0.0166	0.0069	30.5	7.17
7.0		0.0237	0.0111	47.0	11.04
7.5		0.0347	0.0152	61.2	14.37
8.0		0.0439	0.0201	75.5	17.73
8.5	↓	0.0561	0.0248	93.0	21.84
8.556		0.0564	0.0248	-	-
8.5		0.0568	0.0251	-	-
8.0		0.0607	0.0270	-	-
7.5		0.0623	0.0277	-	-
7.0		0.0626	0.0275	-	-
6.5		0.0626	0.0275	-	-
6.0	↓	0.0626	0.0275	-	-
0		0.0626	0.0270	8.75	2.05
0.5		0.0674	0.0269	23.0	5.4
1.0		0.0731	0.0281	42.8	9.95
1.5		0.0817	0.0282	58.0	13.62
2.0		0.0913	0. 0339	79.5	18.67
2.5		0.1026	0.0367	90.0	21.13
3.0		0.1160	0.0441	100.5	23.6
3.5		0.1280	0.0491	100.0	23.5
4.0		0.1391	0.0551	104.6	24.55
4.5	Second Expanding	0.1499	0.0621	122.0	28.6
4.75		0.1524	0.0638	-	-
4.5	↑	0.1552	0.0668	-	-
4.0		0.1593	0.0686	-	-
3.5		0.1610	0.0692	-	-
3.0		0.1617	0.0693	-	-
2.5		0.1617	0.0692	-	-
2.0		0.1617	0.0692	-	-
1.5		0.1617	0.0692	-	-
1.0		0.1617	0.0691	-	-
0.5		0.1617	0.0691	-	-
0		0.1617	0.0690	-	-

TABLE 2.

EXPERIMENT NO. 2.

Final Readings on the Microammeters, Extent of Yielding as Indicated by Plumber's Resin, and Back Gauge.

R means radial strain gauge.

C means circumferential strain gauge.

e = 0.0027 M. M = Microammeter Reading, e = % strain.

See Fig. 33 for details of the positions of the strain gauges.

Zero drift correction approximately +0.01% strain.

Circuit	$\frac{r}{r_o}$	R or C	Reading M Microamps.	%e	Corrected %e
1	2.5	R	-20.9	-0.0565	-0.0465
2	5.0	R	-2.6	-0.007	+0.003
3	2.5	C	+2.5	+0.0068	+0.0168
4	5.0	C	+0.4	+0.0011	+0.0111
5	2.5	R	-32.3	-0.0872	-0.0772
6	5.0	R	-5.8	-0.0157	-0.0057
7	2.5	C	+8.6	+0.0232	+0.0332
8	5.0	C	+1.9	+0.0051	+0.0151

Plumber's resin indicated yielding to $\frac{r}{r_o}$ = 1.54 on front of plate.

" " " " " $\frac{r}{r_o}$ = 1.74 " back " "

" " " " " approximately 0.563 in.

from the back of the plate along the outside of the tube.

Back Gauge = 2.083 ins. diameter.

TABLE 3.

EXPERIMENT NO. 2.

Residual Strains on the Plate Immediately After Experiment 2.

R means radial, C means circumferential strain gauge.
S" = 2.084 . Gauges 33 to 37 cemented to separate piece of boiler plate clamped to the specimen.
Order in which results are tabulated is order in which the readings were taken.
See Fig. 33 for details of the positions of the strain gauges.

Channel	r/r₀	R or C	% k	Zero Drift Correction	Corrected % k	k/2.084 = % e
33	-	-	-0.0034			
34	-	-	-0.003	Mean		
35	-	-	-0.003	Correction		
36	-	-	-0.0032	= +0.0033		
37	-	-	-0.0038			
1	1.75	R	> -1.0	+0.0033	> -1.0	> -0.48
2	2.58	R	-0.0792	+0.0033	-0.0759	-0.0364
3	3.42	R	-0.0238	+0.0033	-0.0205	-0.0098
4	4.25	R	-0.0160	+0.0033	-0.0127	-0.0061
5	5.08	R	-0.0134	+0.0034	-0.0100	-0.0048
6	5.91	R	-0.0108	+0.0034	-0.0074	-0.0036
7	6.75	R	-0.0094	+0.0034	-0.0060	-0.0029
8	7.59	R	-0.0088	+0.0034	-0.0054	-0.0026
9	1.75	C	+0.0948	+0.0035	+0.0983	+0.0471
10	2.58	C	+0.0243	+0.0035	+0.0278	+0.0133
11	3.42	C	+0.0093	+0.0035	+0.0128	+0.0061
12	4.25	C	+0.0044	+0.0035	+0.0079	+0.0038
13	5.08	C	+0.0016	+0.0036	+0.0052	+0.0026
14	5.91	C	-0.0004	+0.0036	+0.0032	+0.0015
15	6.75	C	-0.0015	+0.0036	+0.0021	+0.0010
16	7.59	C	-0.0012	+0.0036	+0.0024	+0.0011
17	1.75	R	-0.473	+0.0037	-0.4693	-0.2252
18	2.58	R	-0.107	+0.0037	-0.1033	-0.0494
19	3.42	R	-0.0386	+0.0037	-0.0349	-0.0167
20	4.25	R	-0.0283	+0.0037	-0.0246	-0.0118
21	5.08	R	-0.0206	+0.0038	-0.0168	-0.0081
22	5.91	R	-0.017	+0.0038	-0.0132	-0.0063
23	6.75	R	-0.0134	+0.0038	-0.0096	-0.0046
24	7.59	R	-0.0113	+0.0038	-0.0075	-0.0036
25	1.75	C	+0.345	+0.0039	+0.3489	+0.1674
26	2.58	C	+0.0727	+0.0039	+0.0766	+0.0367
27	3.42	C	+0.0353	+0.0039	+0.0392	+0.0188
28	4.25	C	+0.023	+0.0039	+0.0269	+0.0129
29	5.08	C	+0.014	+0.0040	+0.0180	+0.0086
30	5.91	C	+0.0102	+0.0040	+0.0142	+0.0068
31	6.75	C	+0.0072	+0.0040	+0.0112	+0.0054
32	7.59	C	+0.0051	+0.0041	+0.0092	+0.0044
33	-	-	-0.0042			
34	-	-	-0.0038	Mean		
35	-	-	-0.0038	Correction		
36	-	-	-0.0040	= +0.0041		
37	-	-	-0.0046			

TABLE 4.

EXPERIMENT NO. 1 (TRIAL EXPERIMENT).

$\frac{T}{M} = 1.8$. Final Ratio $\frac{\text{Back Extrusion}}{\text{Total Extrusion}} = \frac{0.0531}{0.1280} = 0.415$

Cage Revolutions		Total Extrusion ins.	Back Extrusion ins.	Torque (from spring balance) T lb.ft.	Torque in equivalent microamps.
0	First Expanding ↑	0	Unstable ↑	0.63	0.35
1		0.0012		2.0	1.11
2		0.0023		2.75	1.53
3		0.0028		3.13	1.74
4		0.0035		3.25	1.81
5		0.0046		3.38	1.88
6		0.0048		3.38	1.88
7		0.0060		3.88	2.15
8		0.0078		3.98	2.21
9		0.0089		4.12	2.29
10		0.0106		5.5	3.06
11		0.0117		6.25	3.47
12		0.0218		11.76	6.53
13	↓	0.0398	↓	42.5	23.60
13		0.0558	0.0117	-	-
12		0.0579	0.0125	-	-
11		0.0579	0.0125	-	-
10		0.0572	0.0125	-	-
9	↓	0.0572	0.0125	-	-
0	Second Expanding	0.0572	0.0122	0	0
1		0.0589	0.0121	15.0	8.33
2		0.0711	0.0135	52.5	29.2
3		0.0874	0.0219	89.5	49.7
4		0.1086	0.0284	124.3	69.0
4	↑	0.1248	0.0515	-	-
3		0.1282	0.0532	-	-
2		0.1282	0.0531	-	-
1		0.1280	0.0531	-	-

TABLE 5.

EXPERIMENT NO. 1 (TRIAL EXPERIMENT).

Final Readings on the Microammeters. Extent of Yielding as Indicated by Plumber's Resin, and Back Gauge.

R means radial strain gauge.

C means circumferential strain gauge.

e = 0.001969 M. M = Microammeter Reading. e = % strain.

See Fig. 32 for details of the positions of the strain gauges.

No zero drift correction.

Circuit	$\frac{r}{r_o}$	R or C	Reading M Microamps.	% e
1	2.5	R	-22.5	-0.0443
2	4.42	C	+5.0	+0.0098
3	2.5	C	+13.5	+0.0266
4	4.42	R	-2.0	-0.0039
5	2.5	R	-41.0	-0.0807
6	4.42	C	+5.0	+0.0098
7	2.5	C	+14.5	+0.0286
8	4.42	R	-3.4	-0.0067

Plumber's resin indicated yielding to $\frac{r}{r_o}$ = 1.67 on front of plate.

" " " " " $\frac{r}{r_o}$ = 1.75 " back " "

" " " " " approximately 0.375 in.

from the back of the plate along the outside of the tube.

Back Gauge = 2.063 ins. diameter.

TABLE 6.

EXPERIMENT NO. 1 (TRIAL EXPERIMENT).

Residual Strains on the Plate Immediately After Experiment 1.

R means radial, C means circumferential strain gauge.
S" = 1.732 . Since gauges 8, 16, 24, and 32 were measuring strains which were almost negligible, they may be used to give an estimate of the general zero drift of all the gauges.
Thus, mean zero drift =(0.0192 + 0.0091 + 0.0243 + 0.0145)/ 4
= +0.0168 % strain.
See Fig. 32 for details of the positions of the strain gauges.

Channel	$\frac{r}{r_o}$	R or C	% k	k/1.732 = % e	Corrected % e
1	1.75	R	-0.3	-0.1732	-0.19
2	2.92	C	+0.061	+0.0352	+0.0184
3	3.67	R	+0.0063	+0.0036	-0.0132
4	4.83	C	+0.04	+0.0231	+0.0063
5	5.58	R	+0.0222	+0.0128	-0.004
6	6.75	C	+0.0338	+0.0195	+0.0027
7	7.5	R	+0.0263	+0.0152	-0.0016
8	8.67	C	+0.0333	+0.0193	+0.0025
9	1.75	C	+0.18	+0.104	+0.0872
10	2.92	R	-0.0062	-0.0036	-0.0204
11	3.67	C	+0.0462	+0.0267	+0.0099
12	4.83	R	+0.019	+0.011	-0.0058
13	5.58	C	+0.0404	+0.0233	+0.0065
14	6.75	R	+0.0402	+0.0232	+0.0064
15	7.5	C	+0.0255	+0.0147	-0.0021
16	8.67	R	+0.0157	+0.0091	-0.0077
17	1.75	R	> -1	> -0.577	> -0.594
18	2.92	C	+0.0764	+0.0441	+0.0273
19	3.67	R	+0.0107	+0.0062	-0.0106
20	4.83	C	+0.052	+0.03	+0.0132
21	5.58	R	+0.016	+0.0092	-0.0076
22	6.75	C	+0.02	+0.0115	-0.0053
23	7.5	R	+0.0466	+0.0268	+0.01
24	8.67	C	+0.0421	+0.0243	+0.0075
25	1.75	C	+0.397	+0.229	+0.2122
26	2.92	R	-0.006	-0.0035	-0.0203
27	3.67	C	+0.0562	+0.0325	+0.0157
28	4.83	R	+0.022	+0.0127	-0.0041
29	5.58	C	+0.04	+0.0231	+0.0063
30	6.75	R	+0.0232	+0.0134	-0.0034
31	7.5	C	+0.0375	+0.0216	+0.0048
32	8.67	R	+0.0252	+0.0145	-0.0023

TABLE 7.

EXPERIMENT NO. 3.

$\frac{T}{M}$ = 1.42. Final Ratio $\frac{\text{Back Extrusion}}{\text{Total Extrusion}} = \frac{0.0334}{0.0810} = 0.412$

Cage Revolutions	Total Extrusion ins.	Back Extrusion ins.	Torque (from spring balance) T lb.ft.	Torque in equivalent microamps. M
0	0	0	0	0
0.5	0.0016	0.0004	3.0	2.11
1.0	0.0037	0.0008	4.75	3.34
1.5	0.0062	0.0014	5.0	3.52
2.0	0.0083	0.0016	3.75	2.64
2.5	0.0097	0.0024	3.0	2.11
3.0	0.0104	0. 0041	3.5	2.46
3.5	0.0117	0.0045	3.13	2.2
4.0	0.0129	0.0050	3.38	2.38
4.5	0.0145	0.0057	3.5	2.46
5.0	0. 0163	0.0066	4.75	3.34
5.5	0.0188	0.0078	5.0	3.52
6.0	0.0223	0.0087	6.5	4.57
6.5	0.0258	0.0101	7.0	4.94
7.0	0.0301	0.0109	7.5	5.28
7.5	0.0343	0.0130	8.13	5.72
8.0	0.0389	0.0137	8.25	5.81
8.5	0.0414	0.0156	9.5	6.69
9.0	0.0467	0.0166	10.5	7.4
9.5	0.0480	0.0186	11.88	8.36
10.0	0.0524	0.0204	12.0	8.45
10.5	0.0557	0.0224	12.25	8.62
11.0	0.0617	0.0244	12.5	8.8
11.5	0.0644	0.0264	12.5	8.8
12.0	0.0699	0.0284	11.63	8.18
12.5	0.0741	0.0300	11.75	8.27
13.0	0.0770	0.0322	11.26	7.93
13.5	0.0805	0.0330	10.25	7.92
13.58	0. 0806	0.0332	-	-
13.5	0.0807	0.0333	-	-
13.0	0.0810	0.0334	-	-
12.5	0.0810	0.0334	-	-
12.0	0.0810	0.0334	-	-

TABLE 8.

EXPERIMENT NO. 3.

Final Readings on the Micrammeters. Extent of Yielding as Indicated by Plumber's Resin, and Back Gauge.

R means radial strain gauge.

C means circumferential strain gauge.

e = 0.0027 M. M = Micrammeter Reading, e = % strain.

See Fig. 34 for details of the positions of the strain gauges.

Zero drift correction approximately +0.006% strain.

Circuit	$\frac{r}{r_o}$	R or C	Reading M Microamps.	%e	Corrected %e
1	2.5	R	> -50	> -0.135	> -0.129
2	5.0	R	-2.0	-0.0054	+0.0006
3	2.5	C	-1.6	-0.0043	+0.0023
4	5.0	C	0	0	+0.006
5	2.5	R	> -50	> -0.135	> -0.129
6	5.0	R	-5.6	-0.0151	-0.0091
7	2.5	C	+12.1	+0.0327	+0.0387
8	5.0	C	+2.0	+0.0054	+0.0114

Plumber's resin indicated yielding to $\frac{r}{r_o}$ = 1.35 on front of plate.

" " " " " $\frac{r}{r_o}$ = 1.75 " " " "

" " " " " approximately 0.563 ins.

from the back of the plate along the outside of the tube.

Back Gauge = 1.037 ins.

TABLE 9.

EXPERIMENT NO. 3.

Residual Strains on the Plate Immediately After Experiment 3.

R means radial, C means circumferential strain gauge.
S^n = 2.084 . Gauges 21 to 25 cemented to separate piece of boiler plate clamped to the specimen.
Order in which results are tabulated is order in which the readings were taken.
See Fig. 34 for details of the positions of the strain gauges.

Channel	$\frac{r}{r_o}$	R or C	% k	Zero Drift Correction	Corrected % k	k/2.084 = % e
21	-	-	-0.0030			
22	-	-	-0.0028	Mean		
23	-	-	-0.0030	Correction		
24	-	-	-0.0030	= +0.0030		
25	-	-	-0.0032			
1	2.167	R	-0.1000	+0.0030	-0.0970	-0.0465
2	3.167	R	-0.0071	+0.0030	-0.0041	-0.0020
3	4.167	R	-0.0036	+0.0030	-0.0006	-0.0003
4	5.167	R	-0.0038	+0.0030	-0.0008	-0.0004
5	6.167	R	-0.0048	+0.0030	-0.0018	-0.0009
6	2.167	C	+0.0208	+0.0030	+0.0238	+0.0114
7	3.167	C	-0.0018	+0.0030	+0.0012	+0.0006
8	4.167	C	-0.001	+0.0029	+0.0019	+0.0009
9	5.167	C	-0.0017	+0.0029	+0.0012	+0.0006
10	6.167	C	-0.0017	+0.0029	+0.0012	+0.0006
11	2.167	R	-0.286	+0.0029	-0.2831	-0.1357
12	3.167	R	-0.0666	+0.0029	-0.0637	-0.0306
13	4.167	R	-0.0288	+0.0029	-0.0259	-0.0124
14	5.167	R	-0.017	+0.0029	-0.0141	-0.0068
15	6.167	R	-0.0128	+0.0028	-0.0100	-0.0048
16	2.167	C	+0.127	+0.0028	+0.1298	+0.0623
17	3.167	C	+0.0482	+0.0028	+0.0510	+0.0245
18	4.167	C	+0.0254	+0.0028	+0.0282	+0.0135
19	5.167	C	+0.0164	+0.0028	+0.0192	+0.0092
20	6.167	C	+0.0122	+0.0028	+0.0150	+0.0072
21	-	-	-0.0028			
22	-	-	-0.0022	Mean		
23	-	-	-0.0028	Correction		
24	-	-	-0.0028	= +0.0027		
25	-	-	-0.0028			

TABLE 10.

EXPERIMENT NO. 4.

Final Ratio $\frac{\text{Back Extrusion}}{\text{Total Extrusion}} = \frac{0.0518}{0.1387} = 0.373$

Cage Revolutions		Total Extrusion ins.	Back Extrusion ins.
0	First Reading	0	0
0.5		0.0005	0
1.0		0.0007	-0.0003
1.5		0.0021	-0.0005
2.0		0.0023	-0.0008
2.5		0.0044	-0.0009
3.0		0.0039	-0.0009
3.5		0.0060	-0.0009
4.0		0.0062	-0.0007
4.5		0.0074	-0.0006
5.0		0.0076	0
5.5		0.0090	0.0004
6.0		0.0092	0.0008
6.5		0.0106	0.0017
7.0		0.0113	0.0027
7.5		0.0133	0.0037
8.0		0.0140	0.0045
8.5		0.0166	0.0050
9.0		0.0170	0.0060
9.5		0.0195	0.0070
10.00		0.0202	0.0078
10.5		0.0235	0.0087
11.0		0.0244	0.0098
11.5		0. 0274	0.0110
12.0		0.0290	0.0120
12.5		0.0318	0.0130
13.0		0.0351	0.0139
13.5		0.0359	0.0149
14.0		0.0370	0.0159
14.5		0.0400	0.0168
15.0		0.0410	0.0179
15.5		0.0441	0.0185
16.0		0.0453	0.0197
16.5		0.0480	0.0204
17.0		0.0494	0.0213
17.5		0.0499	0.0220
17.79		0.0499	0.0220
17.5		0.0504	0.0221
17.0		0.0506	0.0221
16.5		0.0506	0.0221
16.9		0.0506	0.0221

CONTINUED OVERLEAF

TABLE 11.

Cage Revolutions		Total Extrusion ins.	Back Extrusion ins.
0		0.0506	0.0221
0.5		0.0513	0.0218
1.0		0.0527	0.0206
1.5		0.0534	0.0216
2.0	Second Expanding	0.0798	0.0239
2.5		0.1000	0.0274
2.5		0.1035	0.0345
2.0		0.1081	0.0368
1.5		0.1118	0.0396
1.0		0.1120	0.0401
0.5		0.1123	0.0403
0		0.1123	0.0403
-0.5		0.1123	0.0403
-1.0		0.1123	0.0404
-1.5		0.1123	0.0404
0		0.1123	0.0404
0.5		0.1178	0.0433
0.69	Third Expanding	0.1281	0.0454
0.5		0.1317	0.0470
0		0.1366	0.0506
-0.5		0.1390	0.0514
-1.0		0.1391	0.0519
-1.5		0.1391	0.0518
-2.0		0.1391	0.0518
-2.5		0.1390	0.0518
-3.0		0.1390	0.0518
-3.5		0.1387	0.0518
-4.0		0.1387	0.0518
-4.5		0.1387	0.0518

TABLE 11 (CONTINUED).

EXPERIMENT NO. 4.

Final Readings on the Micrometers. Extent of Yielding as Indicated by Plumber's Resin, and Back Gauge.

R means radial strain gauge.

C means circumferential strain gauge.

e = 0.002943 M. M = Micrometer Reading, e = % strain.

See Fig. 35 for details of the positions of the strain gauges.

Zero drift correction approximately +0.007 % strain.

Circuit	$\frac{r}{r_o}$	R or C	Reading M Microamps.	% e	Corrected % e
1	2.5	R	-20.2	-0.0594	-0.0524
2	2.0	C	+32	+0. 0941	+0.1011
3	2.5	C	+12.3	+0.0362	+0.0432
4	2.0	R	> -50	>-0.147	>-0.147
5	2.5	R	-6.0	-0.0176	-0.0106
6	2.0	C	+3.3	+0.0097	+0.0167
7	2.5	C	+0.2	+0.0006	+0.0076
8	2.0	R	-10.3	-0.0303	-0.0233

Plumber's resin indicated yielding to $\frac{r}{r_o}$ = 1.48 on front of plate.

" " " " " $\frac{r}{r_o}$ = 1.35 " back " "

" " " " " approximately 0.063 in.

from the back of the plate along the outside of the tube.

Back Gauge = 4.024 ins. diameter.

TABLE 12.

EXPERIMENT NO. 4.

Residual Strains on the Plate Immediately After Experiment 4.

R means radial, C means circumferential strain gauge.
S" = 1.972 for strain gauges 1 to 5 and 23 to 27.
S" = 2.10 for all other gauges.
Gauges 45 to 50 cemented to separate piece of boiler plate clamped to the specimen.
Gauges 1 to 5, 23 to 27, and 45 to 47 Tinsley 8 x 1.5 mm., all other gauges being Tinsley 17 x 2.5 mm.
Order in which results are tabulated is order in which the readings were taken.
See Fig. 35 for details of the positions of the strain gauges.

Channel	$\frac{r}{r_o}$	R or C	% k	Zero Drift Correction	Corrected % k	% e
45	-	-	-0.0045	Mean =		
46	-	-	-0.0049	+0.0047		
47	-	-	-0.0047			
48	-	-	+0.0019	Mean =		
49	-	-	+0.0017	-0.0017		
50	-	-	+0.0015			
1	1.5	R	> -1.0	+0.0047	> -1.0	>-0.51
2	1.916	R	-0.506	+0.0047	-0.5013	-0.2544
3	2.333	R	-0.110	+0.0047	-0.1053	-0.0533
4	2.75	R	-0.0535	+0.0047	-0.0488	-0.0247
5	3.17	R	-0.045	+0.0047	-0.0403	-0.0204
6	3.833	R	-0.033	-0.0017	-0.0347	-0.0165
7	4.5	R	-0.0165	-0.0017	-0.0182	-0.0087
8	5.17	R	-0.0094	-0.0017	-0.0111	-0.0053
9	5.833	R	-0.0116	-0.0017	-0.0133	-0.0063
10	6.5	R	-0.0075	-0.0017	-0.0092	-0.0044
11	7.17	R	+0.0027	-0.0017	+0.0010	+0.0005
12	1.5	C	+0.485	-0.0017	+0.4833	+0.23
13	1.916	C	+0.175	-0.0017	+0.1733	+0.0825
14	2.333	C	+0.0995	-0.0017	+0.0978	+0.0465
15	2.75	C	+0.075	-0.0017	+0.0733	+0.0349
16	3.17	C	+0.0407	-0.0017	+0.039	+0.0185
17	3.833	C	+0.042	-0.0017	+0.0403	+0.0192
18	4.5	C	+0.037	-0.0017	+0.0353	+0.0168
19	5.17	C	+0.029	-0.0017	+0.0273	+0.0130
20	5.833	C	+0.0255	-0.0017	+0.0238	+0.0113
21	6.5	C	+0.0196	-0.0017	+0.0179	+0.0085
22	7.17	C	+0.0062	-0.0017	+0.0045	+0.0021
23	1.5	R	-0.0666	+0.0047	-0.0619	(-0.0314)
24	1.916	R	-0.078	+0.0047	-0.0733	-0.0371
25	2.333	R	-0.037	+0.0047	-0.0323	-0.0164

CONTINUED OVERLEAF

TABLE 13.

Channel	$\frac{L}{r_o}$	R or C	% k	Zero Drift Correction	Corrected % k	% e
26	2.75	R	-0.0216	+0.0047	-0.0169	-0.0086
27	3.17	R	-0.0068	+0.0047	-0.0021	-0.0011
28	3.833	R	+0.0044	-0.0017	+0.0027	+0.0013
29	4.5	R	0	-0.0017	-0.0017	-0.0008
30	5.17	R	-0.006	-0.0017	-0.0077	-0.0037
31	5.833	R	+0.001	-0.0017	-0.0007	-0.0003
32	6.5	R	+0.0035	-0.0017	+0.0018	+0.0009
33	7.17	R	+0.0015	-0.0017	-0.0002	-0.0001
34	1.5	C	+0.147	-0.0017	+0.1453	+0.0691
35	1.916	C	+0.050	-0.0017	+0.0483	+0.023
36	2.333	C	+0.0145	-0.0017	+0.0128	+0.0061
37	2.75	C	+0.0118	-0.0017	+0.0101	+0.0048
38	3.17	C	+0.003	-0.0017	+0.0013	+0.0006
39	3.833	C	+0.007	-0.0017	+0.0053	+0.0025
40	4.5	C	+0.0025	-0.0017	+0.0008	+0.0004
41	5.17	C	+0.001	-0.0017	-0.0007	-0.0003
42	5.833	C	+0.001	-0.0017	-0.0007	-0.0003
43	6.5	C	+0.0038	-0.0017	+0.0021	+0.0010
44	7.17	C	+0.0074	-0.0017	+0.0057	+0.0027
45	-	-	-0.0046	Mean =		
46	-	-	-0.0050	+0.0047		
47	-	-	-0.0044			
48	-	-	+0.0020	Mean =		
49	-	-	+0.0018	-0.0017		
50	-	-	+0.0013			

TABLE 13 (CONTINUED).

EXPERIMENT NO. 4a.

Final Ratio $\frac{\text{Back Extrusion}}{\text{Total Extrusion}} = \frac{0.1186}{0.3973} = 0.299$

Cage Revolutions		Total Extrusion ins.	Back Extrusion ins.
0	Fourth Expanding	0.1367	0.0518
0.5		0.1390	0.0518
1.0		0.141	0.0515
1.5		0.1466	0.0517
2.0		0.1681	0.0539
2.5		0.1811	0.0553
3.0		0.2101	0.0617
3.5		0.2272	0.0687
3.972		0.2518	0.0760
3.5		0.2607	0.0814
3.0		0.2652	0.0870
2.5		0.2652	0.0873
2.0		0.2657	0.0877
1.5		0.2655	0.0876
1.0		0.2655	0.0876
0	Fifth Expanding	0.2655	0.0876
0.5		0.2703	0.0863
1.0		0.2780	0.0867
1.5		0.2935	0.0876
2.0		0.3086	0.0843
2.5		0.3455	0.0900
3.0		0.3740	0.0967
3.222		0.3767	0.1045
3.0		0.3852	0.1053
2.5		0.3946	0.1145
2.0		0.3978	0.1180
1.5		0.3978	0.1185
1.0		0.3976	0.1186
0.5		0.3973	0.1186
0		0.3973	0.1186
-0.5		0.3973	0.1186
-1.0		0.3973	0.1186
-1.5		0.3973	0.1186
-2.0		0.3973	0.1186
-2.5		0.3973	0.1186
-3.0		0.3973	0.1186
-3.5		0.3973	0.1186

TABLE 14.

EXPERIMENT NO. 4a.

Final Readings on the Microammeters. Extent of Yielding as Indicated by Plumber's Resin, and Back Gauge.

R means radial strain gauge.

C means circumferential strain gauge.

e = 0.002943 M. M = Microammeter Reading, e = % strain.

See Fig. 35 for details of the positions of the strain gauges.

Negligible zero drift.

Circuit	$\frac{r}{r_o}$	R or C	Reading M Microamps.	% e
1	2.5	R	> -50	> -0.147
2	2.0	C	+23.3	+0.0685
3	2.5	C	+15.2	+0.0447
4	2.0	R	> -50	> -0.147
5	2.5	R	-25.5	-0.075
6	2.0	C	+21.7	+0.0638
7	2.5	C	+6.5	+0.0191
8	2.0	R	> -50	> -0.147

Plumber's resin indicated yielding to $\frac{r}{r_o}$ = 1.75 on front of plate.

" " " " " $\frac{r}{r_o}$ = 1.35 " back " "

" " " " " approximately 0.219 in.

from the back of the plate along the outside of the tube.

Back Gauge = 4.028 ins.

TABLE 15.

EXPERIMENT NO. 4a.

Residual Strains on the Plate Immediately After Experiment 4a.

R means radial, C means circumferential strain gauge.
S" = 1.972 for strain gauges 1 to 5 and 23 to 27.
S" = 2.10 for all other gauges.
Gauges 45 to 50 cemented to separate piece of boiler plate clamped to the specimen.
Gauges 1 to 5, 23 to 27, and 45 to 47 Tinsley 8 x 1.5 mm., all other gauges being Tinsley 17 x 2.5 mm.
See Fig. 35 for details of the positions of the strain gauges.

Channel	$\frac{r}{r_o}$	R or C	% k	Zero Drift Correction	Corrected % k	% e
1	1.5	R	> -1.0	+0.02	> -1.0	> - 0.51
2	1.916	R	> -1.0	+0.02	> -1.0	> -0.51
3	2.333	R	-0.3395	+0.02	-0.3395	-0.1725
4	2.75	R	-0.1510	+0.02	-0.1310	-0.0665
5	3.17	R	-0.1109	+0.02	-0.0909	-0.0461
6	3.833	R	-0.0573	+0.0034	-0.0539	-0.0257
7	4.5	R	-0.0341	+0.0034	-0.0307	-0.0146
8	5.17	R	-0.0217	+0.0034	-0.0183	-0.0087
9	5.833	R	-0.0143	+0.0034	-0.0109	-0.0052
10	6.5	R	-0.0042	+0.0034	-0.0008	-0.0004
11	7.17	R	-0.0038	+0.0034	-0.0004	-0.0002
12	1.5	C	> +1.0	+0.0034	> +1.0	> +0.476
13	1.916	C	+0.2106	+0.0034	+0.2140	+0.1020
14	2.333	C	+0.1058	+0.0034	+0.1092	+0.0520
15	2.75	C	+0.0727	+0.0034	+0.0761	+0.0362
16	3.17	C	+0.0491	+0. 0034	+0.0525	+0.0250
17	3.833	C	+0.0428	+0.0034	+0.0462	+0.0221
18	4.5	C	+0.0350	+0.0034	+0.0384	+0.0183
19	5.17	C	+0.0302	+0.0034	+0.0336	+0.0160
20	5.833	C	+0.0239	+0.0034	+0.0273	+0.0130
21	6.5	C	+0.0159	+0.0034	+0.0193	+0.0092
22	7.17	C	+0.0140	+0.0034	+0.0174	+0.0083
23	1.5	R	-0.1107	+0.02	-0.0907	-0.0460
24	1.916	R	-0.6370	+0.02	-0.6170	-0.3130
25	2.333	R	-0.2407	+0.02	-0.2207	-0.1120
26	2.75	R	-0.0871	+0.02	-0.0671	-0.0340
27	3.17	R	-0.0456	+0.02	-0.0256	-0.0130
28	3.833	R	-0.0139	+0.0034	-0.0105	-0.0050
29	4.5	R	-0.0057	+0.0034	-0.0023	-0.0011
30	5.17	R	-0.0034	+0.0034	0	0
31	5.833	R	-0.0126	+0.0034	-0.0092	-0.0044
32	6.5	R	-0.0046	+0.0034	-0.0012	-0.0006
33	7.17	R	-0.0034	+0.0034	0	0

CONTINUED OVERLEAF

TABLE 16.

Channel	$\frac{r}{r_o}$	R or C	% k	Zero Drift Correction	Corrected % k	% e
34	1.5	C	+0.4600	+0.0034	+0.4634	+0.2200
35	1.916	C	+0.1726	+0.0034	+0.1760	+0.0840
36	2.333	C	+0.0492	+0.0034	+0.0526	+0.0250
37	2.75	C	+0.0218	+0.0034	+0.0252	+0.0120
38	3.17	C	+0.0156	+0.0034	+0.0190	+0.0090
39	3.833	C	+0.0092	+0.0034	+0.0126	+0.0060
40	4.5	C	+0.0050	+0.0034	+0.0084	+0.0040
41	5.17	C	-0.0034	+0.0034	0	0
42	5.833	C	-0.0030	+0.0034	+0.0004	+0.0002
43	6.5	C	-0.0007	+0.0034	+0.0027	+0.0013
44	7.17	C	+0.0014	+0.0034	+0.0048	+0.0023
45	-	-	-0.0190	Mean =		
46	-	-	-0.0210	+0.0200		
47	-	-	-0.0200			
48	-	-	-0.0050	Mean =		
49	-	-	-0.0022	+0.0034		
50	-	-	-0.0030			

TABLE 16 (CONTINUED).

EXPERIMENT NO. 5. (RETRACTIVE EXPANDERS).

Final Ratio $\frac{\text{Back Extrusion}}{\text{Total Extrusion}} = \frac{0.1205}{0.3040} = 0.396$

Cage Revolutions		Total Extrusion ins.	Back Extrusion ins.
0	↑	0	0
0.5		0	0.0013
1.0		0.0055	0.0086
1.5		0.0110	0.0119
2.0		0.0140	0.0147
2.5		0.0163	0.0160
3.0		0.0191	0.0183
3.5		0.0216	0.0193
4.0		0.0239	0.0212
4.5		0.0262	0.0223
5.0		0.0288	0.0243
5.5		0.0317	0.0253
6.0		0.0343	0.0273
6.5		0.0370	0.0285
7.0		0.0398	0.0303
7.5		0.0430	0.0315
8.0		0.0460	0.0334
8.5		0.0488	0.0345
9.0		0.0518	0.0364
9.5		0.0552	0.0377
10.0		0.0584	0.0394
10.5		0.0621	0.0405
11.0		0.0655	0.0423
11.5		0.0690	0.0433
12.0		0.0720	0.0449
12.5		0.0759	0.0460
13.0		0.0791	0.0477
13.5		0.0830	0.0486
14.0		0.0870	0.0502
14.5		0.0911	0.0511
15.0		0.0956	0.0528
15.5		0.0996	0.0538
16.0		0.1043	0.0567
16.5		0.1090	0.0584
17.0		0.1130	0.0593
17.5		0.1187	0.0607
18.0		0.1235	0.0617
18.5		0.1282	0.0627
19.0		0.1327	0.0628
19.5		0.1385	0.0633
20.0		0.1456	0.0633
20.5		0.152	0.0633
21.0		0.1597	0.0634
21.5		0.1647	0.0635
22.0		0.1700	0.0636
22.5		0.1740	0.0636
23.0		0.1774	0.0637
23.5	↓	0.1750	0.0637

First Expanding

TABLE 17. (CONTINUED OVERLEAF).

Cage Revolutions		Total Extrusion ins.	Back Extrusion ins.
0	↑	0.1750	0.0637
0.5		0.1755	0.0683
1.0		0.1795	0.0747
1.5		0.1860	0.0833
2.0		0.1916	0.0865
2.5		0.1960	0.0901
3.0		0.2000	0.0923
3.5		0.2035	0.0953
4.0		0.2070	0.0971
4.5		0.2105	0.0996
5.0		0.2140	0.1012
5.5		0.2174	0.1032
6.0		0.2210	0.1046
6.5		0.2250	0.1066
7.0		0.2285	0.1083
7.5		0.2330	0.1099
8.0		0.2353	0.1109
8.5		0.2405	0.1127
9.0		0.2435	0.1137
9.5		0.2480	0.1150
10.0		0.2520	0.1162
10.5		0.2560	0.1174
11.0		0.2590	0.1182
11.5		0.2660	0.1189
12.0		0.2690	0.1195
12.5		0.2740	0.1198
13.0		0.2780	0.1199
13.5		0.2840	0.1199
14.0		0.2890	0.1200
14.5		0.2960	0.1201
15.0		0.2980	0.1202
15.5		0.3026	0.1202
16.0		0.3030	0.1203
16.5		0.3040	0.1204
17.0	↓	0.3040	0.1205

Second Expanding

TABLE 17 (CONTINUED).

EXPERIMENT NO. 5.

Residual Strains on the Plate Immediately After Experiment 5.

All gauges circumferential, except gauges 14 and 28, which were radial gauges positioned at the extreme edge of the plate.
$s'' = 2.084$.
The column headed % k has been corrected for zero drift as in the previous experiments.
See Fig. 36 for details of the positions of the strain gauges.

Channel	$\frac{r}{r_o}$	Corrected % k	k/2.084 = % e	$\left(\frac{r_o''}{r''}\right)^2$
1	1.46	Gauge Failed	-	0.5260
2	1.71	0.188	0.0902	0.3860
3	1.96	0.112	0.0537	0.2930
4	2.21	0.081	0.0389	0.2310
5	2.46	0.062	0.0297	0.1860
6	2.71	0.047	0.0225	0.1540
7	2.96	0.038	0.0182	0.1283
8	3.21	0.035	0.0168	0.1093
9	3.46	0.030	0.0144	0.0940
10	3.71	0.022	0.0105	0.0817
11	3.96	0.019	0.0091	0.0718
12	4.21	0.015	0.0072	0.0635
13	4.45	0.010	0.0048	0.0567
14	4.50	-0.014	-0.0067	0.0556
15	1.46	Gauge Failed	-	0.5260
16	1.71	0.223	0.1070	0.3860
17	1.96	0.117	0.0561	0.2930
18	2.21	0.091	0.0437	0.2310
19	2.46	0.073	0.0350	0.1860
20	2.71	0.054	0.0259	0.1540
21	2.96	0.041	0.0197	0.1283
22	3.21	0.033	0.0158	0.1093
23	3.46	0.029	0.0139	0.0940
24	3.71	0.025	0.0120	0.0817
25	3.96	0.018	0.0086	0.0718
26	4.21	0.021	0.0101	0.0635
27	4.45	0.014	0.0067	0.0567
28	4.50	-0.011	-0.0053	0.0556

TABLE 18.

EXPERIMENT NO. 5.

Residual Strains on the Plate Immediately After Experiment 5, as Determined from the Punch Marks.

FRONT

$\frac{r''}{r''_o}$	$\left(\frac{r''_o}{r''}\right)^2$	$\% \, e_\theta$
1.306	0.587	0.314
1.342	0.555	0.241
1.376	0.529	0.208
1.412	0.501	0.193
1.451	0.475	0.171
1.493	0.449	0.141
1.529	0.428	0.122
1.570	0.406	0.103
1.608	0.387	0.093
1.645	0.369	0.083
1.682	0.354	0.074
1.721	0.337	0.065
1.761	0.322	0.056
1.803	0.308	0.055
1.841	0.295	0.054
1.883	0.282	0.046
1.922	0.271	0.032
1.961	0.260	0.031
2.0	0.250	0.031
2.037	0.241	0.041
2.073	0.233	0.030
2.114	0.224	0.041

BACK

$\frac{r''}{r''_o}$	$\left(\frac{r''_o}{r''}\right)^2$	$\% \, e_\theta$
1.306	0.587	0.506
1.344	0.553	0.398
1.38	0.525	0.324
1.419	0.497	0.289
1.457	0.471	0.239
1.498	0.445	0.199
1.541	0.421	0.177
1.578	0.401	0.157
1.620	0.381	0.147
1.653	0.366	0.135
1.693	0.349	0.125
1.732	0.333	0.108
1.772	0.318	0.105
1.808	0.306	0.082
1.850	0.292	0.074
1.892	0.279	0.066
1.927	0.269	0.058
1.969	0.258	0.057
2.003	0.249	0.056
2.040	0.240	0.042
2.078	0.231	0.036
2.120	0.222	0.023

TABLE 19.

Results of the Push-out Tests on Specimens Expanded with Roller Type Tube Expanders.

Specimen	1	2	3	5
r_o'' ins.	0.7904	0.7945	0.3990	1.590
a'' ins.	1.0175	1.0155	0.508	2.0255
b ins.	7.0	7.0	3.5	7.0
h ins.	1.211	1.13	0.564	2.435
β 1/in.	0.2923	0.293	0.586	0.143
$\frac{E\left[1-\left(\frac{a''}{b}\right)^2\right]}{10^5(1+\nu)}$	0.1013	0.1013	0.1013	0.09484
$10^5 k_2$ Front	35.5	19.3	30.0	27.2
$10^5 k_2$ Back	40.0	31.3	40.5	27.2
p_F T/in.^{2}	3.6	1.956	3.04	2.76
p_B T/in.^{2}	4.055	3.17	4.1	2.76
$\bar{p}$ T/in.^{2}	3.828	2.563	3.57	2.76
F Tons	6.47	3.97	1.205	29.75
μ	0.211	0.207	0.175	0.328

TABLE 20.

Numerical Solution for Plate in which $h_i = mr_i$

ρ	$\Delta\theta$	$10^3\Delta v$	$10^3\Delta\epsilon_z$	$\Delta\bar{\sigma}$ T/in.^{2}
1.0	-0.0213	0.0874	0.0308	0.0944
0.98	-0.0218	0.0938	0.0350	0.0989
0.96	-0.0223	0.10	0.0393	0.1046
0.94	-0.0228	0.1078	0.0449	0.1105
0.92	-0.0233	0.1157	0.0506	0.1172
0.90	-0.0237	0.1246	0.0573	0.1249
0.88	-0.0241	0.1350	0.0657	0.1330
0.86	-0.0244	0.1466	0.0753	0.1433
0.84	-0.0249	0.1602	0.0871	0.1527
0.82	-0.0251	0.1757	0.1013	0.1653
0.80	-0.0252	0.1931	0.1180	0.1785
0.78	-0.0254	0.2133	0.1379	0.1931
0.76	-0.0252	0.2375	0.1629	0.210
0.74	-0.0246	0.2640	0.1921	0.2293
0.72	-0.0247	0.2976	0.2293	0.2493
0.70	-0.0236	0.336	0.2746	0.2725
0.68	-0.0226	0.3823	0.3318	0.3027
0.66	-0.0211	0.4360	0.40	0.3343
0.64	-0.0183	0.4970	0.4805	0.3760
0.62	-0.0155	0.570	0.5820	0.420
0.60	-0.0133	0.6520	0.6989	0.4730
0.58	-0.0081	0.748	0.837	0.527
0.56	-0.0041	0.859	1.007	0.588
0.54	-0.0001	0.984	1.198	0.656
0.52	+0.0033	1.125	1.423	0.731
0.50	+0.0054	1.285	1.686	0.807
0.48	+0.0075	1.480	2.018	0.889
0.46	+0.0084	1.70	2.404	0.974
0.44	+0.0092	1.967	2.897	1.067
0.42	+0.0082	2.283	3.517	1.153
0.40	+0.0072	2.693	4.360	1.240
0.38	+0.0068	3.185	5.446	1.344
0.36	+0.0032	3.820	6.940	1.409
0.34	+0.0019	4.66	9.17	1.483
0.32	+0.0015	5.76	12.35	1.563
0.30	+0.0020	7.22	17.15	1.612
0.28	+0.0063	9.08	24.07	1.703
0.26	+0.0163	11.5	34.75	1.802
0.24	+0.0336	14.4	50.88	1.94
0.22	+0.0787	17.3	73.0	2.90
0.20	+0.1217	19.7	101.3	4.86
0.18	+0.1790	20.9	140.2	10.77
0.16	+0.181	9.3	80.3	18.23
0.151				

CONTINUED OVERLEAF

TABLE 21.

Numerical Solution for Plate in which $h_i = mr_i$

ρ	θ	$10^3 v$	$10^3 \epsilon_z$	$\bar{\sigma}$ T/in.^{2}
1.0	-0.2025	1.7480	0.1437	16.0
0.98	-0.2238	1.8345	0.1745	16.09
0.96	-0.2456	1.9292	0.2095	16.19
0.94	-0.2679	2.0292	0.2488	16.30
0.92	-0.2907	2.1370	0.2937	16.41
0.90	-0.3140	2.2527	0.3443	16.53
0.88	-0.3377	2.3773	0.4016	16.65
0.86	-0.3618	2.5123	0.4673	16.78
0.84	-0.3862	2.659	0.5426	16.93
0.82	-0.4111	2.819	0.6297	17.08
0.80	-0.4362	2.995	0.7310	17.24
0.78	-0.4614	3.188	0.8490	17.42
0.76	-0.4868	3.401	0.9869	17.62
0.74	-0.5120	3.639	1.1498	17.83
0.72	-0.5366	3.903	1.3419	18.06
0.70	-0.5613	4.20	1.571	18.31
0.68	-0.5849	4.536	1.846	18.58
0.66	-0.6075	4.919	2.178	18.88
0.64	-0.6286	5.355	2.578	19.21
0.62	-0.6469	5.852	3.058	19.59
0.60	-0.6624	6.422	3.64	20.01
0.58	-0.6737	7.074	4.339	20.48
0.56	-0.6818	7.822	5.176	21.01
0.54	-0.6859	8.681	6.183	21.60
0.52	-0.6860	9.665	7.381	22.25
0.50	-0.6827	10.79	8.804	22.99
0.48	-0.6773	12.08	10.49	23.79
0.46	-0.6698	13.56	12.51	24.68
0.44	-0.6614	15.26	14.91	25.66
0.42	-0.6522	17.22	17.81	26.72
0.40	-0.6440	19.51	21.33	27.88
0.38	-0.6368	22.20	25.69	29.12
0.36	-0.630	25.38	31.13	30.46
0.34	-0.6268	29.20	38.07	31.87
0.32	-0.6249	33.86	47.24	33.35
0.30	-0.6234	39.62	59.59	34.91
0.28	-0.6214	46.84	76.74	36.53
0.26	-0.6151	55.92	100.8	38.23
0.24	-0.5988	67.42	135.6	40.02
0.22	-0.5652	81.82	186.4	41.97
0.20	-0.4865	99.12	259.4	44.87
0.18	-0.3648	118.8	360.7	49.73
0.16	-0.1858	139.7	500.9	60.5
0.151	-0.0048	149.0	581.2	78.73

CONTINUED OVERLEAF

TABLE 21(CONTINUED).

Numerical Solution for Plate in which $h_i = mr_i$

ϕ	σ_r T/in.^{2}	σ_θ T/in.^{2}	$10^3 \epsilon_\theta$	$\frac{h}{mc} = \phi \exp(\epsilon_z - \epsilon_\theta)$
1.0	-12.27	+5.83	0.7065	0.9994
0.98	-12.63	+5.49	0.7431	0.9794
0.96	-13.01	+5.13	0.7832	0.9594
0.94	-13.38	+4.76	0.8271	0.9395
0.92	-13.8	+4.38	0.8754	0.9195
0.90	-14.19	+3.97	0.9285	0.8995
0.88	-14.59	+3.55	0.9872	0.8795
0.86	-15.0	+3.12	1.052	0.8595
0.84	-15.42	+2.68	1.124	0.8395
0.82	-15.84	+2.21	1.204	0.8195
0.80	-16.31	+1.74	1.293	0.7996
0.78	-16.77	+1.25	1.392	0.7796
0.76	-17.24	+0.75	1.504	0.7596
0.74	-17.7	+0.24	1.629	0.7396
0.72	-18.19	-0.27	1.772	0.7197
0.70	-18.7	-0.8	1.933	0.6997
0.68	-19.22	-1.32	2.118	0.6798
0.66	-19.72	-1.65	2.330	0.6599
0.64	-20.26	-2.12	2.576	0.6400
0.62	-20.81	-2.78	2.861	0.6201
0.60	-21.4	-3.2	3.194	0.6003
0.58	-22.0	-3.54	3.586	0.5804
0.56	-22.64	-3.82	4.051	0.5606
0.54	-23.34	-4.03	4.605	0.5409
0.52	-24.02	-4.15	5.269	0.5211
0.50	-24.8	-4.21	6.072	0.5014
0.48	-25.6	-4.2	7.047	0.4817
0.46	-26.5	-4.15	8.239	0.4620
0.44	-27.45	-4.07	9.710	0.4423
0.42	-28.43	-3.95	11.54	0.4226
0.40	-29.6	-3.87	13.82	0.4030
0.38	-30.8	-3.79	16.72	0.3834
0.36	-32.17	-3.74	20.44	0.3639
0.34	-33.6	-3.79	25.27	0.3444
0.32	-35.13	-3.89	31.66	0.3250
0.30	-36.7	-4.01	40.33	0.3058
0.28	-38.4	-4.11	52.42	0.2869
0.26	-40.0	-4.02	69.85	0.2682
0.24	-41.65	-3.47	96.07	0.2497
0.22	-42.96	-2.02	137.9	0.2309
0.20	-43.93	+1.93	210.3	0.2101
0.18	-44.55	+9.09	351.6	0.1817
0.16	-45.5	+23.13	729.3	0.1273
0.151	-45.8	+45.1	1475.0	0.0618
			$\downarrow$	$\downarrow$
			∞	0

TABLE 21 (CONTINUED).

Numerical Solution for Flat Plate. (h: constant).

ϕ	$\Delta\theta$	$10^3\Delta v$	$10^3\Delta\epsilon_z$	$\Delta\bar{\sigma}$ T/in.^{2}
1.0	-0. 0206	0.0714	0.0153	0.0760
0.98	-0.0212	0.0756	0.0174	0.0797
0.96	-0.0218	0.0804	0.0197	0.0830
0.94	-0.0223	0.0851	0.0223	0.0890
0.92	-0.0228	0.0905	0.0251	0.0940
0.90	-0.0234	0.0964	0.0285	0.0991
0.88	-0.0239	0.1032	0.0329	0.1055
0.86	-0.0245	0.1108	0.0378	0.1126
0.84	-0.0252	0.1195	0.0438	0.1195
0.82	-0.0257	0.1288	0. 0506	0.1282
0.80	-0.0263	0.1399	0.0593	0.1372
0.78	-0.0269	0.1527	0.0698	0.1476
0.76	-0.0274	0.1660	0.0809	0.1608
0.74	-0.0280	0.1828	0.0962	0.1737
0.72	-0.0284	0. 2016	0.1143	0.1891
0.70	-0.0288	0. 2240	0.1369	0. 2060
0.68	-0.0292	0. 251	0.1657	0. 225
0.66	-0.0294	0. 282	0. 2009	0. 245
0.64	-0.0290	0. 318	0. 2441	0. 273
0.62	-0.0288	0. 362	0. 299	0. 301
0.60	-0.0276	0. 414	0. 368	0. 337
0.58	-0.0257	0. 476	0. 453	0. 384
0.56	-0.0244	0. 552	0. 564	0. 424
0.54	-0.0196	0. 640	0. 698	0. 499
0.52	-0.0161	0. 740	0. 856	0. 566
0.50	-0.0118	0. 868	1. 065	0. 643
0.48	-0.0063	1. 016	1. 317	0. 737
0.46	-0.0023	1. 187	1. 623	0. 839
0.44	+0.0019	1. 385	1. 984	0. 940
0.42	+0.0038	1. 621	2. 443	1. 038
0.40	+0.0064	1. 913	3. 03	1. 160
0.38	+0.0069	2. 268	3. 781	1. 278
0.36	+0.0054	2. 707	4. 786	1. 386
0.34	+0.0033	3. 283	6. 201	1. 486
0.32	+0.0027	4. 06	8. 307	1. 598
0.30	-0.0006	5. 05	11. 27	1. 673
0.28	+0.0019	6. 44	15. 99	1. 792
0.26	+0.0052	8. 30	23. 19	1. 89
0.24	+0.0114	10. 79	34. 75	1. 95
0.22	+0.034	13. 9	52. 77	2. 17
0.20	+0.076	17. 16	79. 18	3. 02
0.18	+0.141	19. 85	115. 9	5. 67
0.16	+0.230	21. 2	173. 6	14. 82
0.14	+0.145	4. 04	37. 3	17. 73
0.136				

CONTINUED OVERLEAF

TABLE 22.

Numerical Solution for Flat Plate. (h_i constant).

ϕ	θ	$10^3 v$	$10^3 \epsilon_z$	$\bar{\sigma}$ T/in.^{2}
1.0	0	1.785	0	16.0
0.98	-0.0206	1.856	0.0153	16.08
0.96	-0.0418	1.932	0.0327	16.16
0.94	-0.0636	2.012	0.0524	16.24
0.92	-0.0859	2.098	0.0747	16.33
0.90	-0.1087	2.188	0.0998	16.42
0.88	-0.1321	2.284	0.1283	16.52
0.86	-0.1560	2.388	0.1612	16.63
0.84	-0.1805	2.498	0.1990	16.74
0.82	-0.2057	2.618	0.2428	16.86
0.80	-0.2314	2.747	0.2934	16.99
0.78	-0.2577	2.887	0.3527	17.12
0.76	-0.2846	3.039	0.4225	17.27
0.74	-0.3120	3.205	0.5034	17.43
0.72	-0.3400	3.388	0.5996	17.61
0.70	-0.3684	3.590	0.7139	17.8
0.68	-0.3972	3.814	0.8508	18.0
0.66	-0.4264	4.065	1.017	18.23
0.64	-0.4558	4.347	1.217	18.47
0.62	-0.4848	4.665	1.462	18.74
0.60	-0.5136	5.027	1.761	19.05
0.58	-0.5412	5.441	2.129	19.38
0.56	-0.5669	5.917	2.582	19.77
0.54	-0.5913	6.469	3.146	20.19
0.52	-0.6109	7.109	3.844	20.69
0.50	-0.627	7.849	4.70	21.26
0.48	-0.6388	8.717	5.765	21.90
0.46	-0.6451	9.733	7.082	22.64
0.44	-0.6474	10.92	8.705	23.46
0.42	-0.6455	12.31	10.69	24.4
0.40	-0.6417	13.93	13.13	25.44
0.38	-0.6353	15.84	16.16	26.6
0.36	-0.6284	18.11	19.94	27.88
0.34	-0.623	20.81	24.73	29.27
0.32	-0.6197	24.1	30.93	30.75
0.30	-0.6170	28.16	39.24	32.35
0.28	-0.6176	33.21	50.51	34.02
0.26	-0.6157	39.65	66.5	35.82
0.24	-0.6105	47.95	89.69	37.71
0.22	-0.5991	58.74	124.4	39.66
0.20	-0.5651	72.64	177.2	41.83
0.18	-0.4891	89.8	256.4	44.85
0.16	-0.3481	109.7	372.3	50.52
0.14	-0.1181	130.9	545.9	65.34
0.136	40.027	134.9	583.2	83.07

CONTINUED OVERLEAF

TABLE 22 (CONTINUED).

Numerical Solution for Flat Plate. (h_i constant).

ϕ	σ_r T/in.^{2}	σ_θ T/in.^{2}	$10^3\epsilon_\theta$	$\frac{h}{h_i} = \exp \epsilon_z$
1.0	-9.24	+9.24	0.893	1.00000
0.98	-9.61	+8.95	0.93	1.00001
0.96	-10.0	+8.65	0.97	1.00003
0.94	-10.4	+8.337	1.014	1.00005
0.92	-10.81	+8.0	1.062	1.00007
0.90	-11.22	+7.64	1.114	1.00010
0.88	-11.63	+7.283	1.17	1.00013
0.86	-12.07	+6.905	1.232	1.00016
0.84	-12.51	+6.51	1.3	1.00020
0.82	-12.98	+6.09	1.375	1.00024
0.80	-13.44	+5.647	1.457	1.00029
0.78	-13.91	+5.2	1.547	1.00035
0.76	-14.4	+4.72	1.647	1.00042
0.74	-14.96	+4.226	1.759	1.00050
0.72	-15.48	+3.713	1.883	1.00060
0.70	-15.97	+3.177	2.022	1.00071
0.68	-16.56	+2.618	2.179	1.00085
0.66	-17.12	+2.043	2.355	1.00102
0.64	-17.71	+1.445	2.555	1.00122
0.62	-18.32	+0.844	2.785	1.00146
0.60	-18.94	+0.218	3.047	1.00176
0.58	-19.58	-0.3903	3.351	1.00213
0.56	-20.26	-0.989	3.704	1.00258
0.54	-20.92	-1.579	4.118	1.00315
0.52	-21.66	-2.084	4.608	1.00384
0.50	-22.42	-2.56	5.192	1.0047
0.48	-23.2	-2.903	5.892	1.0058
0.46	-24.1	-3.175	6.743	1.0071
0.44	-24.97	-3.345	7.787	1.0087
0.42	-25.96	-3.425	9.078	1.0107
0.40	-27.0	-3.462	10.69	1.0132
0.38	-28.17	-3.423	12.73	1.0163
0.36	-29.41	-3.365	15.33	1.0201
0.34	-30.84	-3.359	18.69	1.0250
0.32	-32.3	-3.4	23.11	1.0314
0.30	-33.93	-3.482	29.04	1.0400
0.28	-35.74	-3.686	37.21	1.0518
0.26	-37.57	-3.81	48.73	1.0688
0.24	-39.46	-3.782	65.73	1.0938
0.22	-41.34	-3.463	91.96	1.1325
0.20	-42.82	-2.01	135.3	1.1938
0.18	-43.9	+1.779	214.4	1.292
0.16	-44.63	+10.17	381.0	1.451
0.14	-45.07	+29.76	918.0	1.726
0.136	-45.75	+50.16	1666.0	1.792
			∞	

TABLE 22 (CONTINUED).

Comparative Results for the Three Sizes of Specimen.

Specimen	3	2	4
Maximum value of e_θ attained at $r/r_o = 2.5$ on the face exhibiting maximum yielded zone. % strain	0.054	0.053	0.077
Maximum torque attained during expanding. T_1 lb.ft.	13.5	100	1600
Initial torque to release expanders after final expanding T_2 lb.ft.	-5.1	-56	-800
$\frac{T_2}{T_1}$	-0.378	-0.56	-0.5
Total extrusion ins.	0.081	0.1617	0.3973
Back extrusion ins.	0.0334	0.069	0.1186
Final ratio $\frac{\text{Back extrusion}}{\text{Total extrusion}}$	0.412	0.427	0.299
Total number of cage revolutions during expanding. N_1	13.85	13.6	28.57
Total number of mandrel revolutions during expanding N_2	64.0	66.0	130.7
$\frac{N_2}{N_1}$	4.62	4.85	4.58
Total work done in expanding ft.lb.	2920	14,900	214,000
Ratios of work done to that on Specimen 3	1	5.1	73.3
Ratios of maximum torques attained to that on Specimen 3	1	7.41	118

TABLE 23.

Calculation of the Residual Circumferential Strains at the Inside Diameters of the Tubes.

Specimen	1	2	3	5
r_o ins.	0.748	0.750	0.3735	1.5055
r_i ins.	1.01	1.01	0.4085	2.0105
a ins.	1.0125	1.0125	0.5	2.0155
r'_o ins.	0.7514	0.7534	0.3755	1.5125
r''_o ins.	0.7904	0.7945	0.399	1.59
u_o ins.	0.039	0.0411	0.0235	0.0775
$\frac{u_o}{r'_o}$	0.0519	0.0546	0.0626	0.0512
$\log(1 + \frac{u_o}{r'_o})$	0.0506	0.05318	0.06076	0.04993
$\left(\frac{r''_o}{a''}\right)^2$	0.603	0.612	0.618	0.616

TABLE 24.

Theoretical Distribution of Residual Circumferential Strain for $\frac{r_o}{c} = 0.247$.

$\left(\frac{r_o}{r}\right)^2$	$\frac{r_2}{r}$	$\frac{r}{c} = \frac{0.247}{r_o/r}$	Expanded ϵ_θ	Released ϵ_θ	Residual ϵ_θ
0	0	∞	0	0	0
0.061	0.247	1.0	0.00089	0.00023	0.00066
0.1	0.316	0.781	0.00155	0.00038	0.00117
0.2	0.447	0.552	0.00391	0.00075	0.00316
0.3	0.548	0.451	0.00726	0.00113	0.00613
0.4	0.632	0.391	0.01171	0.00151	0.0102
0.5	0.707	0.349	0.0175	0.00189	0.01561
0.6	0.775	0.319	0.0232	0.00226	0.02094
0.7	0.837	0.295	0.031	0.00264	0.02836
0.8	0.894	0.276	0.0395	0.00302	0.03648
0.9	0.949	0.26	0.0487	0.00339	0.04531
1.0	1.0	0.247	0.05862	0.00377	0.05485

TABLE 25.

Residual Stress Distribution for $\frac{c}{t} = 1.751$.

Secondary Yielding Taken into Account.

$\frac{r}{c}$	$\frac{e^{\sqrt{3}\psi}\cos\psi}{(r/c)^2} = 0.1143$			Residual $\frac{\sigma_r}{\sigma_o} = \frac{2}{\sqrt{3}}\sin(\psi + \frac{\pi}{6})$	Residual $\frac{\sigma_\theta}{\sigma_o} = \frac{2}{\sqrt{3}}\sin(\psi - \frac{\pi}{6})$
0.5711	0.35	-30.0		0	-1.0
0.58	0.339	-30.7		-0.0141	-1.007
0.59	0.328	-31.5		-0.0302	-1.015
0.60	0.317	-32.4		-0.0484	-1.023
0.61	0.307	-33.1		-0.0625	-1.030
0.62	0.297	-33.9		-0.0785	-1.037
0.63	0.288	-34.7		-0.0946	-1.043
0.64	0.279	-35.4		-0.1087	-1.050
0.645	0.2745	-35.8		-0.1168	-1.053
$\frac{r}{c}$	$\frac{2}{\sqrt{3}}\sin(\theta - \frac{\pi}{6})$	$\frac{2}{\sqrt{3}}\sin(\theta + \frac{\pi}{6})$	$\frac{0.39}{(r/c)^2}$	Residual $\frac{\sigma_r}{\sigma_o}$	Residual $\frac{\sigma_\theta}{\sigma_o}$
0.65	-1.047	-0.1007	0.922	-0.125	-1.022
0.66	-1.033	-0.0706	0.895	-0.138	-0.9656
0.67	-1.017	-0.0343	0.869	-0.148	-0.9033
0.68	-1.002	-0.0061	0.843	-0.159	-0.8491
0.69	-0.989	+0.0222	0.819	-0.170	-0.7968
0.70	-0.974	+0.0503	0.796	-0.178	-0.7457
0.80	-0.83	+0.2795	0.61	-0.22	-0.3305
0.90	-0.7	+0.4455	0.482	-0.218	-0.0365
1.0	-0.5771	+0.5771	0.39	-0.1871	+0.1871
1.1				-0.154	+0.154
1.2				-0.1295	+0.1295

TABLE A1.

Residual Stress Distribution for $\frac{\ell}{a} = 1.751$.

Secondary Yielding Neglected.

$\frac{r}{c}$	$e^{-\sqrt{3}\theta} \cos\theta = \left(\frac{\ell}{r}\right)^2$	θ°	$\sqrt{\frac{2}{3}}\sin(\theta-\frac{\pi}{6})$	$\sqrt{\frac{2}{3}}\sin(\theta+\frac{\pi}{6})$	$\frac{0.3705}{(r/c)^2}$	Residual $\frac{\sigma_r}{\sigma_o}$	Residual $\frac{\sigma_\theta}{\sigma_o}$
0.5711	3.06	-60.0	-1.155	-0.5771	1.155	0	-1.732
0.58	2.97	-52.1	-1.143	-0.4343	1.118	-0.025	-1.556
0.59	2.87	-48.4	-1.131	-0.3643	1.083	-0.048	-1.447
0.60	2.775	-45.4	-1.117	-0.3067	1.047	-0.07	-1.354
0.61	2.685	-42.9	-1.103	-0.258	1.013	-0.09	-1.271
0.62	2.6	-40.8	-1.09	-0.2166	0.981	-0.109	-1.198
0.63	2.515	-38.8	-1.077	-0.1767	0.95	-0.127	-1.127
0.64	2.44	-37.0	-1.063	-0.1408	0.921	-0.142	-1.062
0.65	2.36	-35.0	-1.047	-0.1007	0.892	-0.155	-0.9927
0.66	2.295	-33.5	-1.033	-0.0706	0.867	-0.166	-0.9376
0.67	2.22	-31.7	-1.017	-0.0343	0.84	-0.177	-0.8743
0.68	2.16	-30.3	-1.002	-0.0061	0.817	-0.185	-0.8231
0.69	2.10	-28.9	-0.989	+0.0222	0.792	-0.197	-0.7698
0.70	2.04	-27.5	-0.974	+0.0503	0.77	-0.204	-0.7197
0.80	1.56	-16.0	-0.83	+0.2795	0.589	-0.241	-0.3095
0.90	1.235	-7.3	-0.7	+0.4455	0.465	-0.235	-0.0195
1.0	1.0	0	-0.5771	+0.5771	0.3765	-0.2006	+0.2006
1.1						-0.166	+0.166
1.2						-0.1397	+0.1397

TABLE A2.

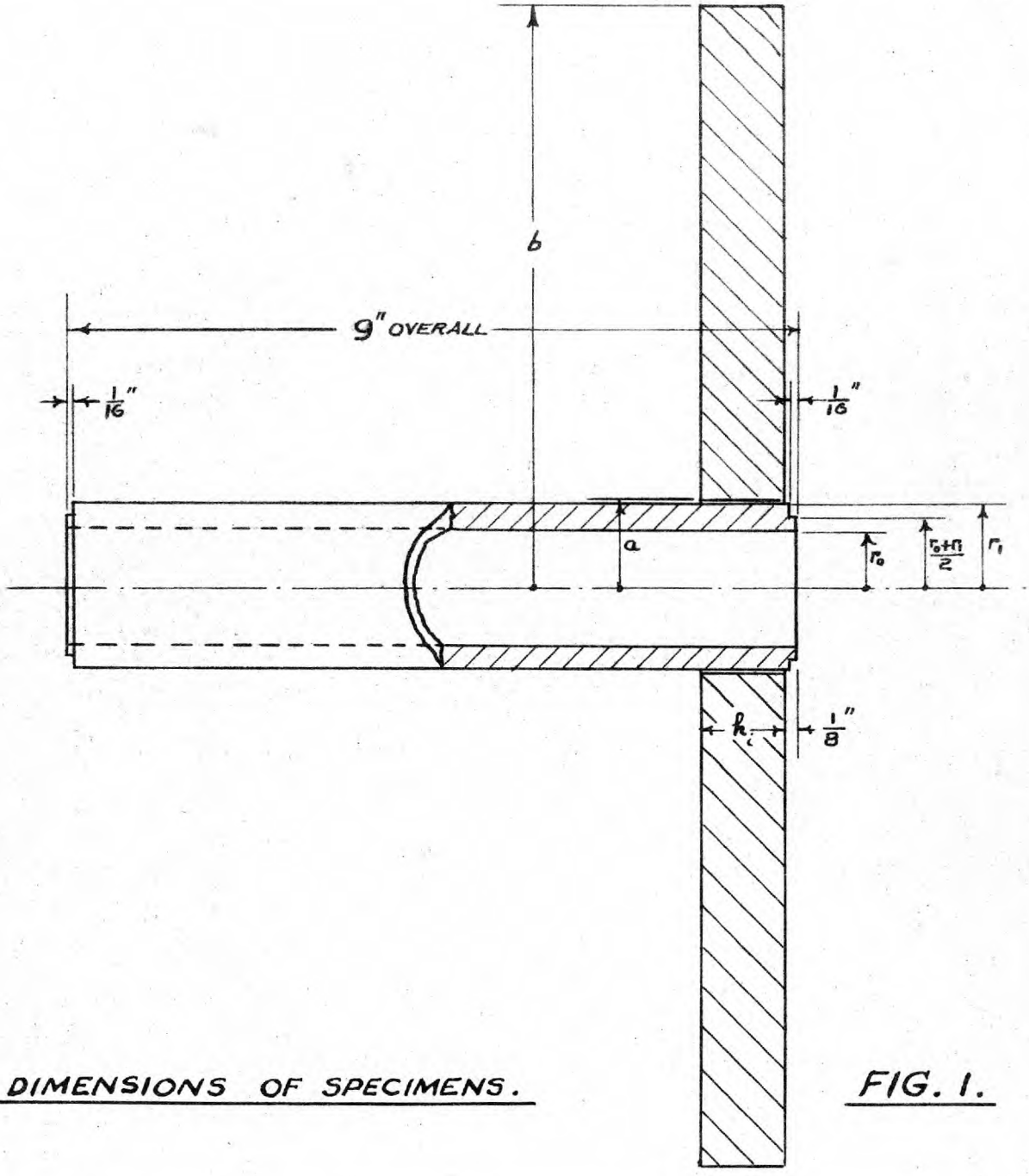

DIMENSIONS OF SPECIMENS.

FIG. 1.

SPECIMEN NUMBER	TUBE INSIDE DIA: $2r_0$ INS:	TUBE OUTSIDE DIA: $2r_1$ INS:	PLATE HOLE DIA: $2a$ INS:	PLATE OUTSIDE DIA: $2b$ INS:	PLATE THICKNESS h INS:	CLEARANCE ON DIA: $2(a-r_1)$ INS:
1 (TRIAL EXPT:)	1·496	2·020	2·025	14	1·211	0·005
2	1·500	2·020	2·025	14	1·13	0·005
3	0·747	0·997	1·000	7	0·564	0·003
4	3·004	4·020	4·030	28	2·26	0·010
5	3·011	4·021	4·031	14	2·435	0·010
6	3·004	4·020	4·030	28	2·26	0·010

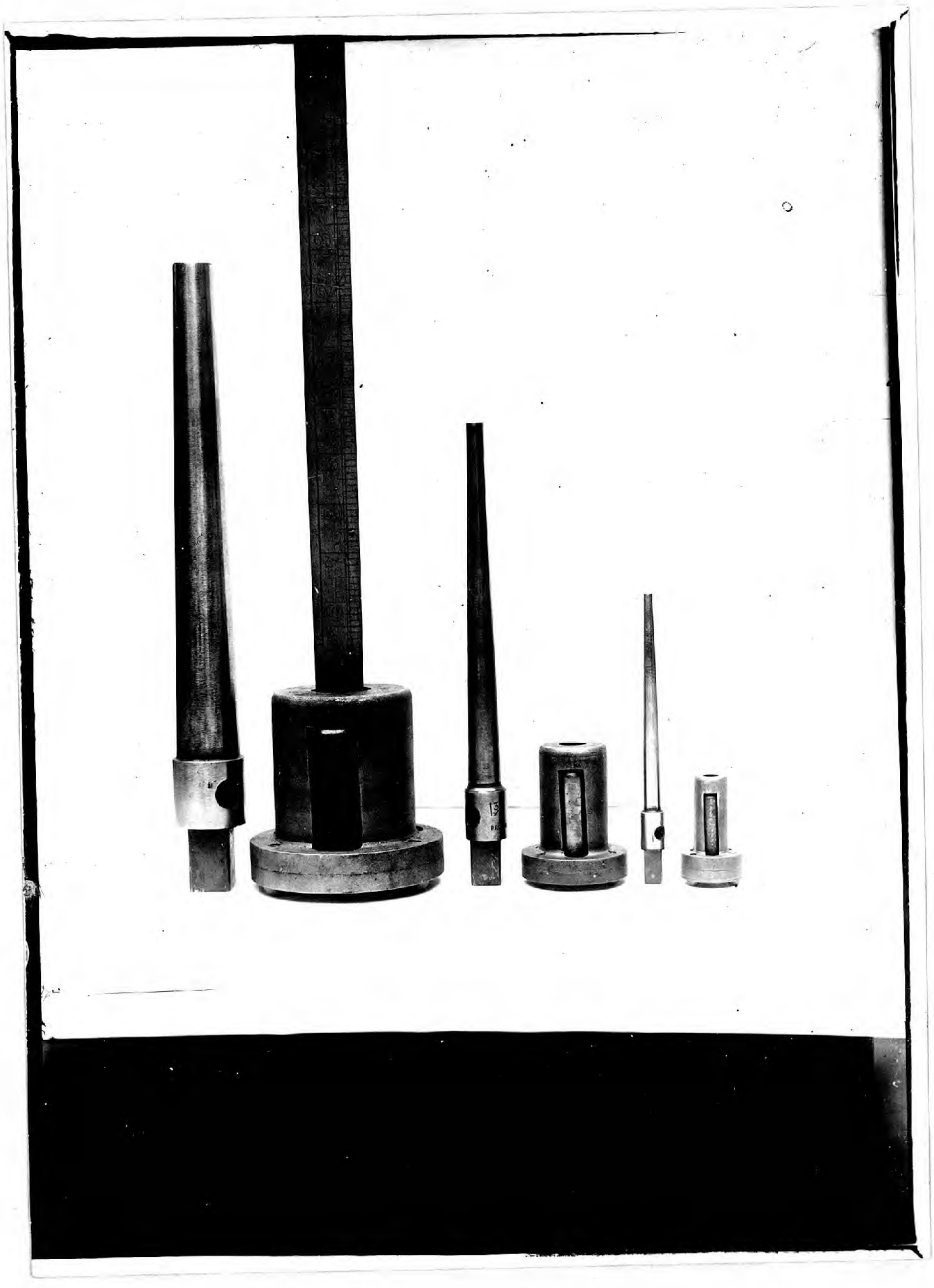

FIG. 2.

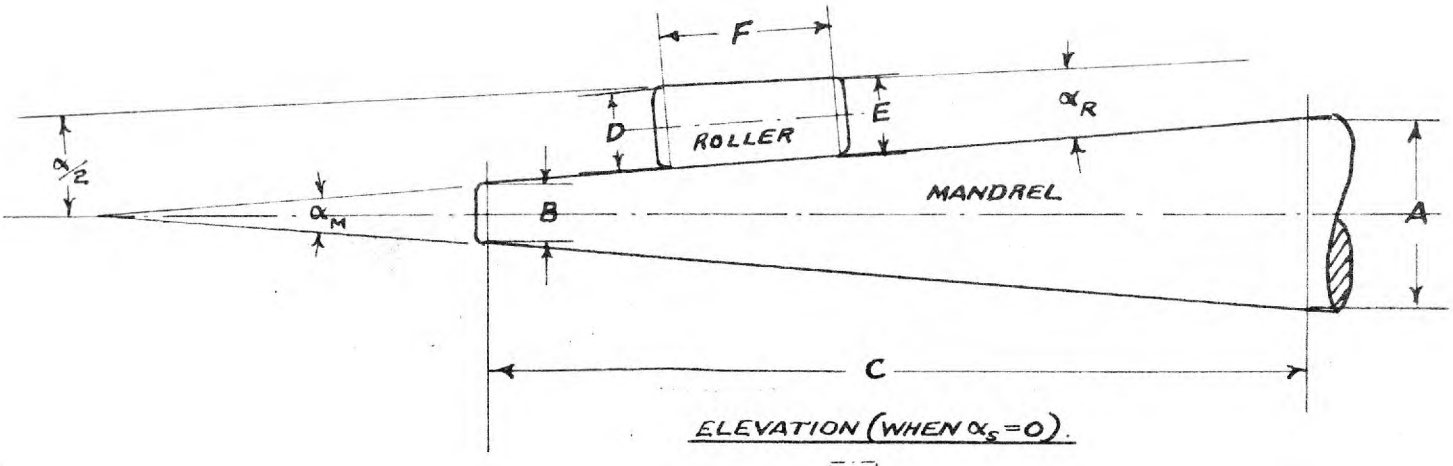

ELEVATION (WHEN $\alpha_S = 0$).

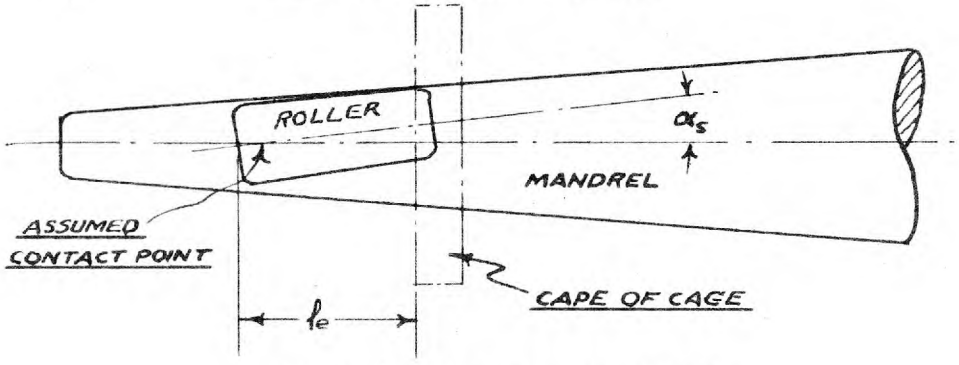

PLAN (IN WORKING POSITION).

NOTE:- $\alpha = \alpha_M - 2\alpha_R$ = CONE ANGLE SWEPT OUT BY ROLLERS IF THE AXES OF THE ROLLERS LIE IN THE SAME PLANE AS THE MANDREL AXIS, I.E. WHEN α_S IS ZERO.

TO EXPAND FROM DIA: INS:	MANDREL				ROLLERS.						
	A INS:	B INS:	C INS:	α_M°	D INS:	E INS:	F INS:	α_R°	α°	α_S°	l_e INS:
0·75	0·364	0·185	3·5	4·58	0·281	0·253	1·35	1·19	2·2	1·7	1·188
1·5	0·684	0·378	7·3	2·4	0·571	0·535	1·8	1·145	0·11	2·1	1·625
3·0	1·346	0·842	9·9	2·91	1·116	1·068	2·625	1·05	0·81	1·7	2·375

DIMENSIONS OF EXPANDERS.

(PROPULSIVE TYPE).

FIG. 3.

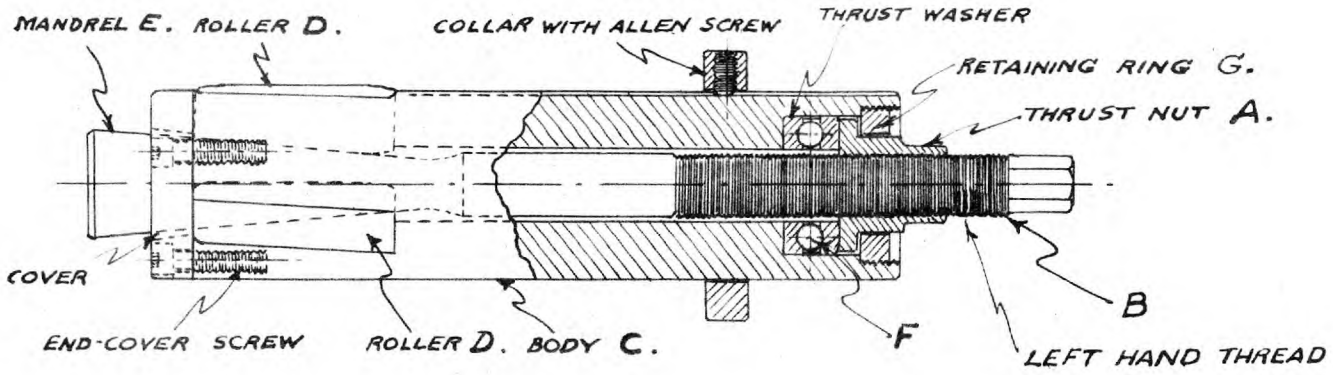

TYPICAL RETRACTIVE EXPANDER.

FIG. 4.

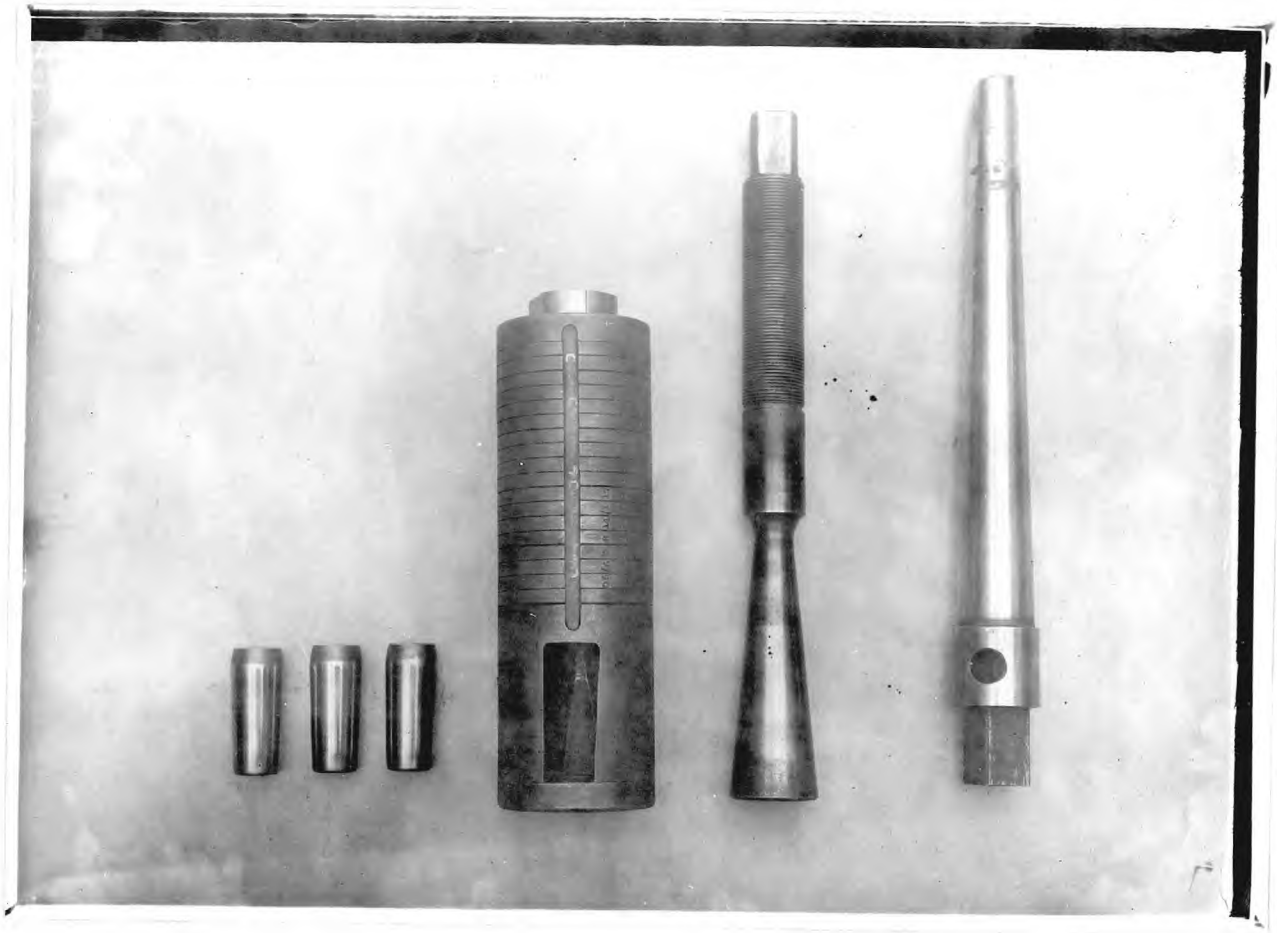

RETRACTIVE EXPANDER SET.

MANDREL OF PROPULSIVE EXPANDER.

FIG. 5.

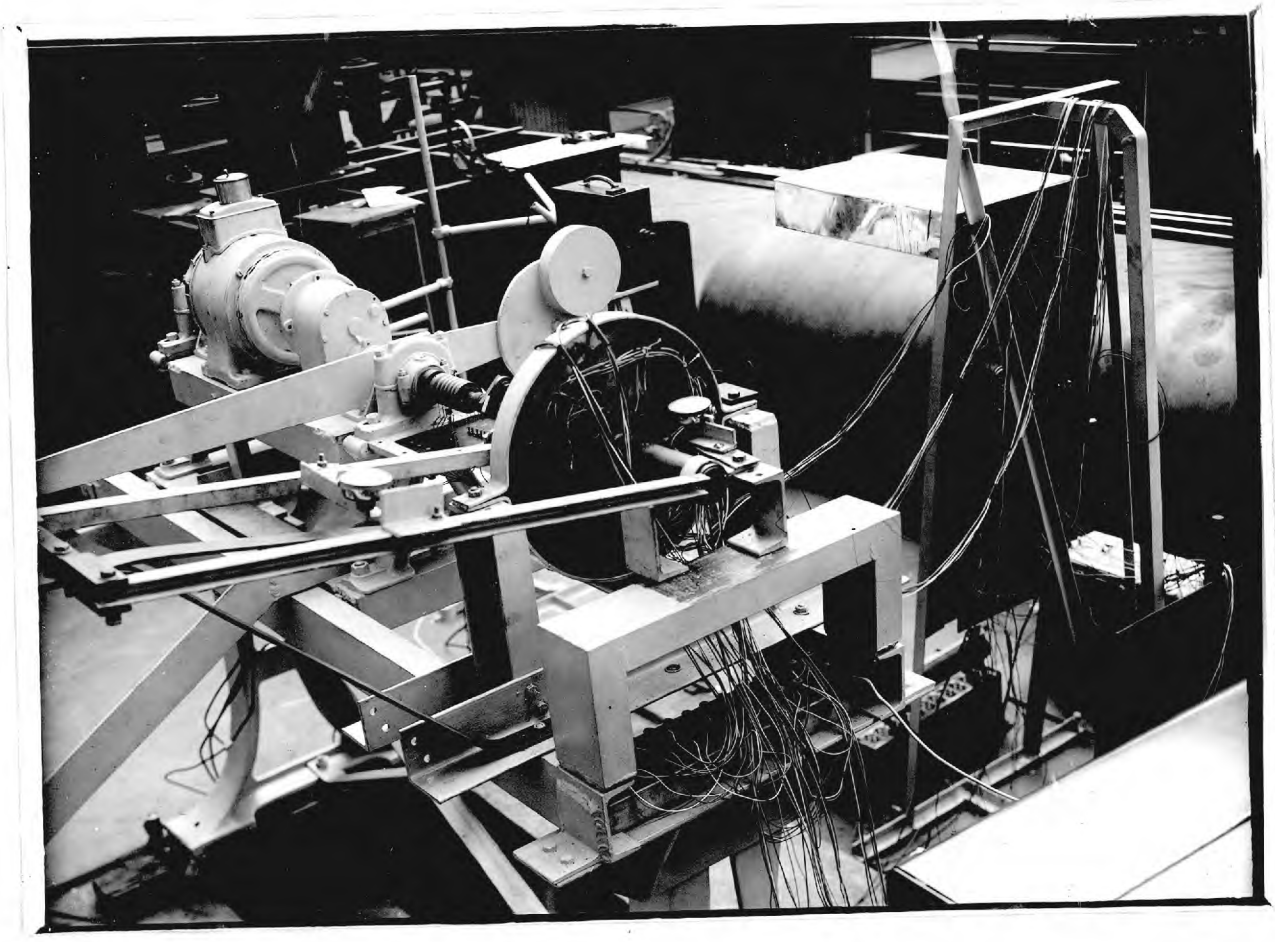

FIG. 6.

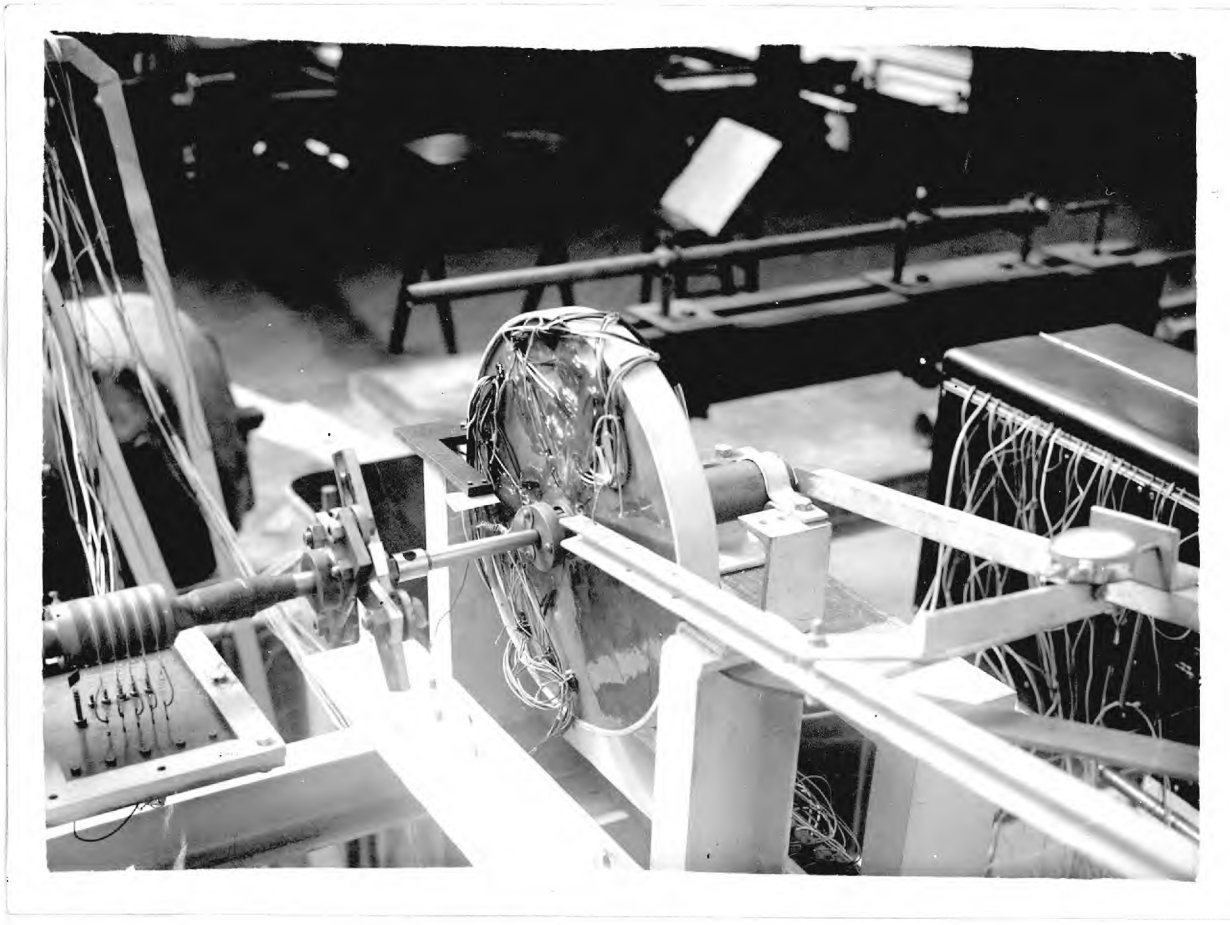

FIG. 7.

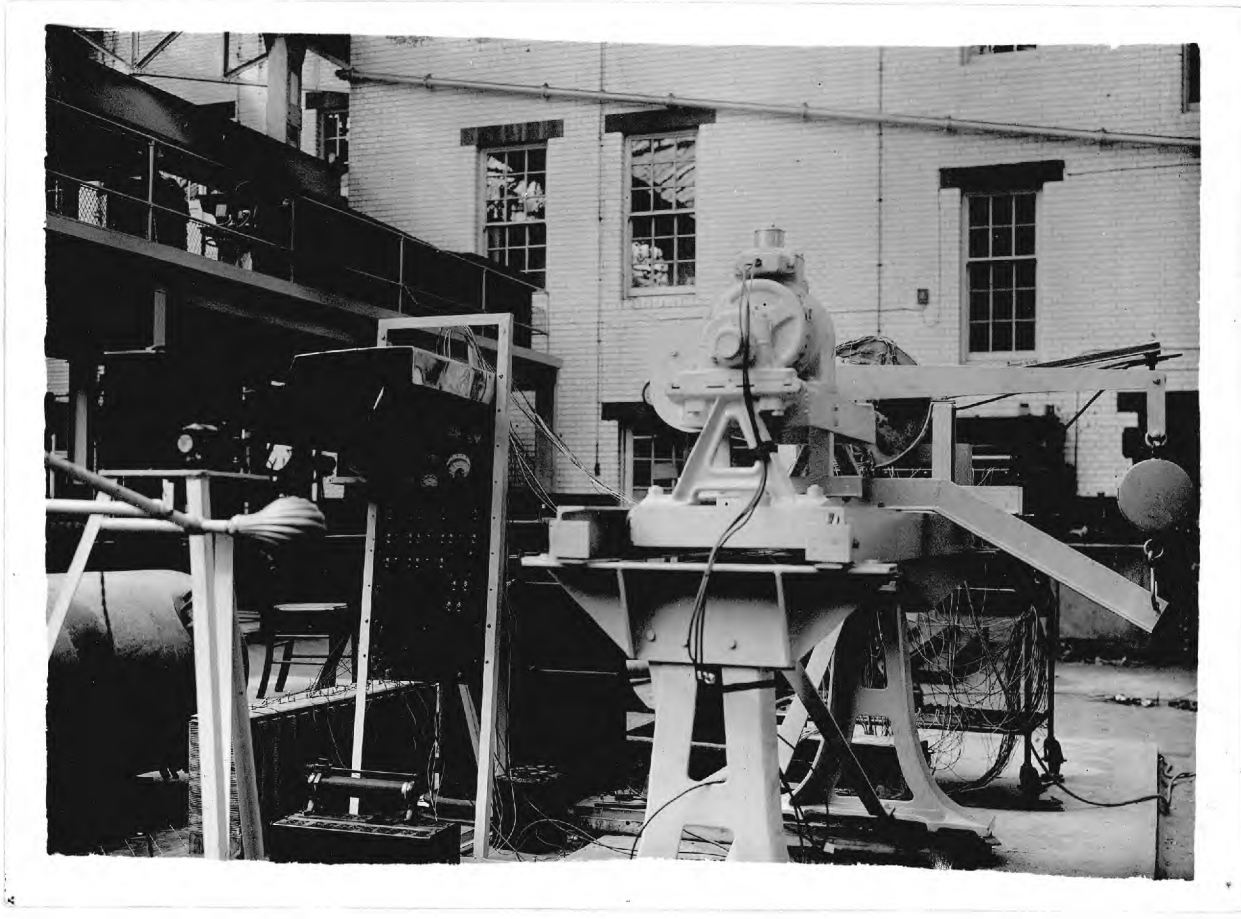

FIG. 8.

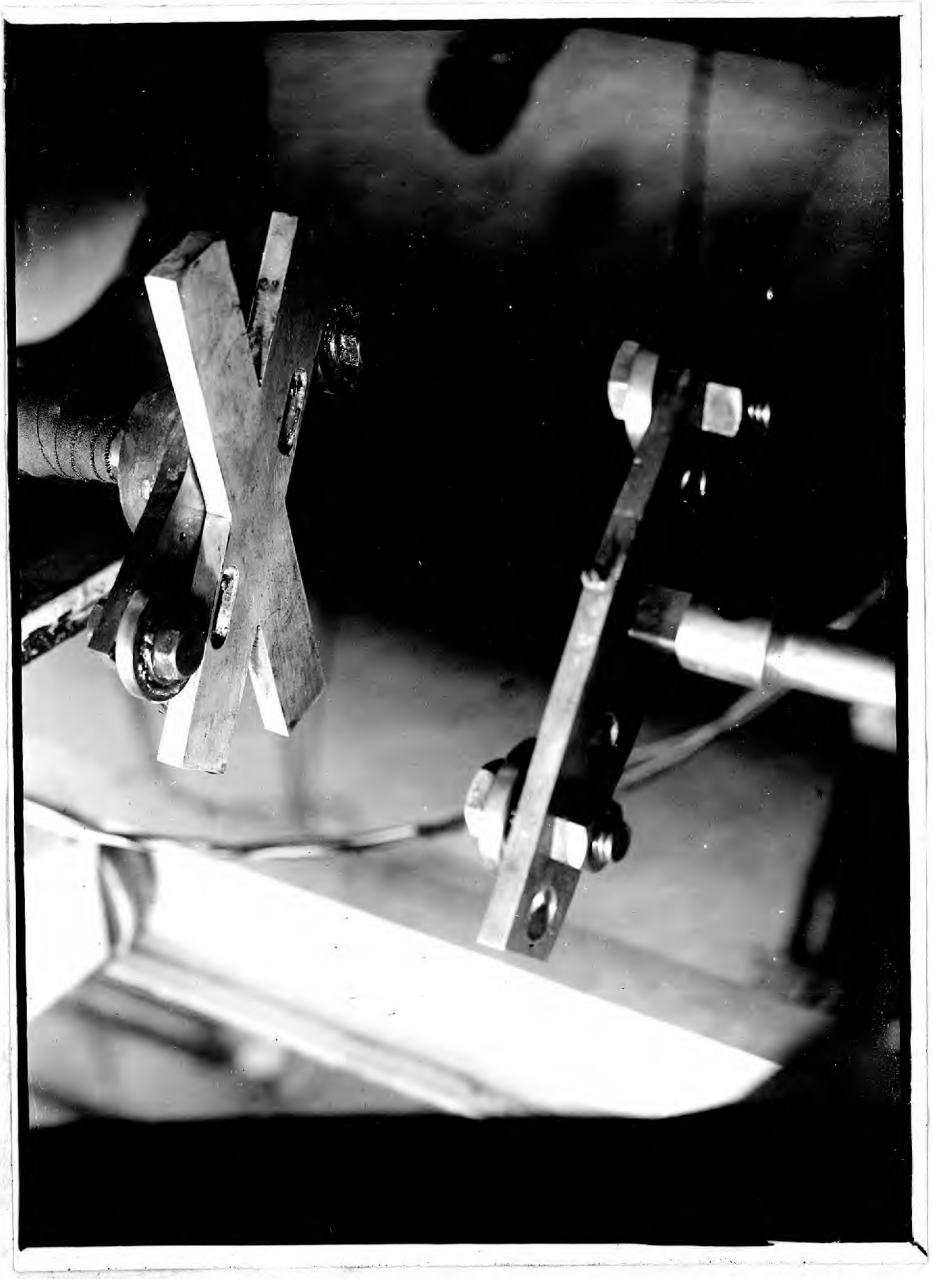

FIG. 9.

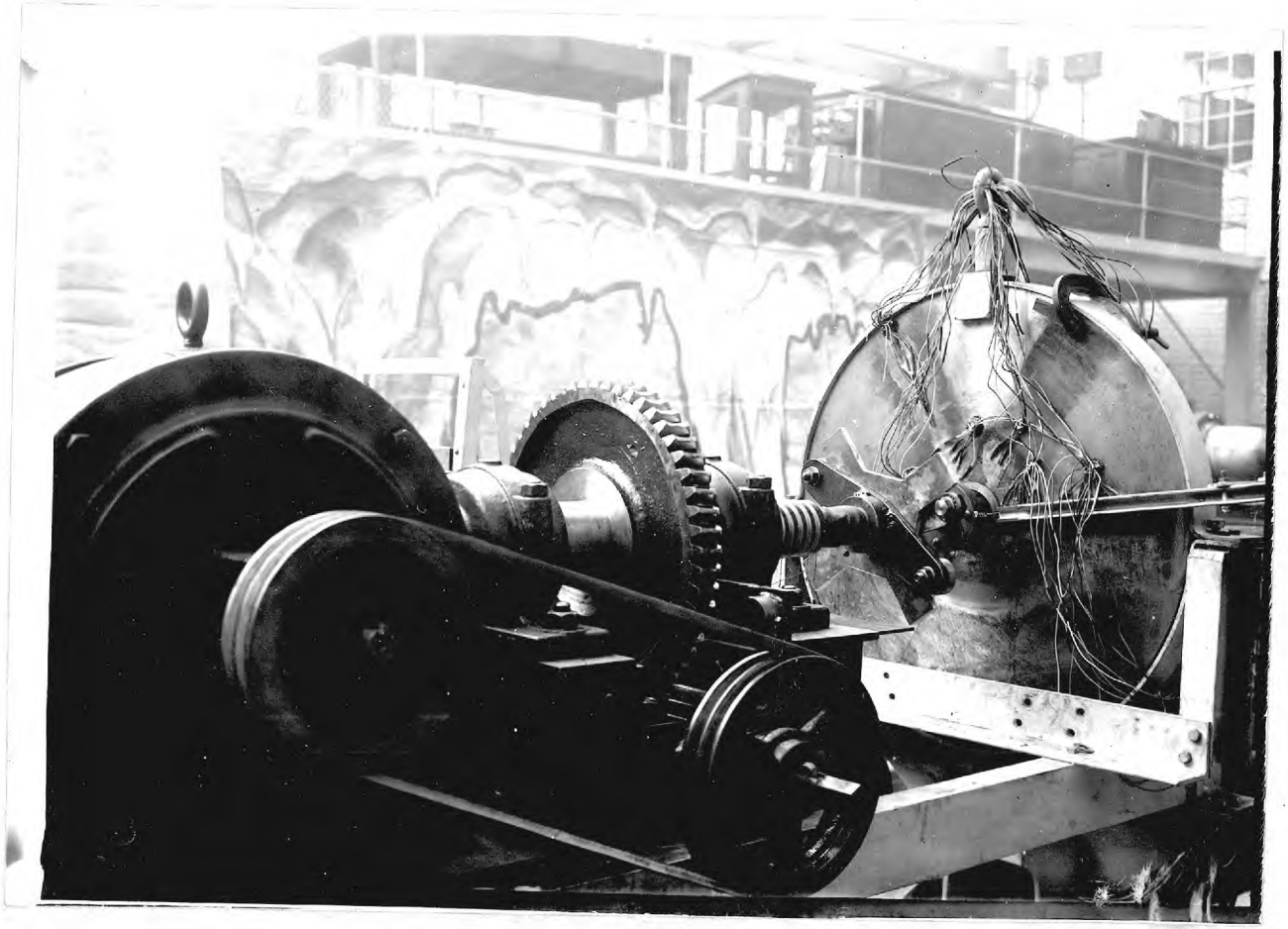

FIG. 10.

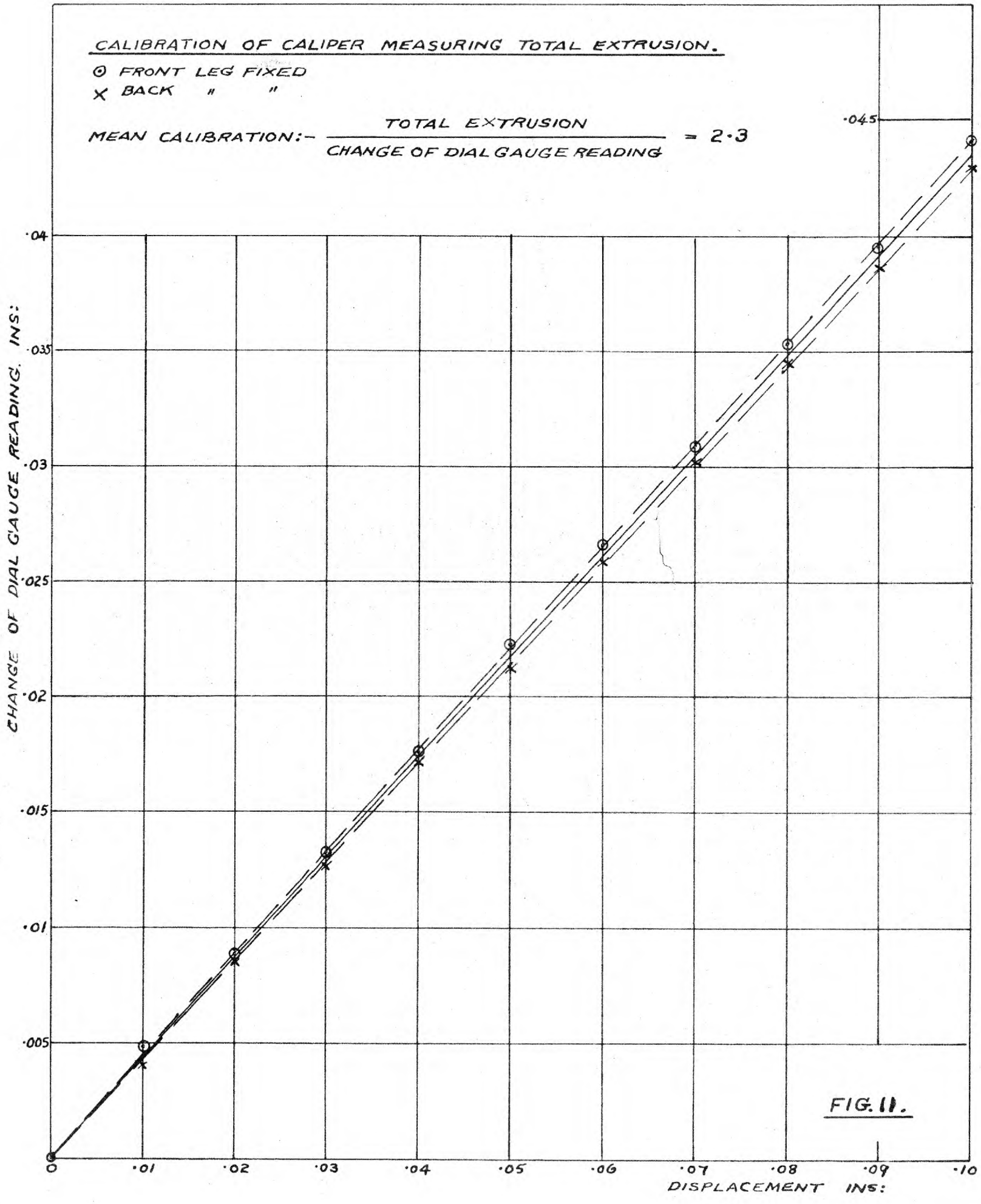
CALIBRATION OF CALIPER MEASURING TOTAL EXTRUSION.
⊙ FRONT LEG FIXED
× BACK " "
MEAN CALIBRATION:- TOTAL EXTRUSION / CHANGE OF DIAL GAUGE READING = 2·3
·045
·04
·035
·03
·025
·02
·015
·01
·005
CHANGE OF DIAL GAUGE READING. INS:
0
·01
·02
·03
·04
·05
·06
·07
·08
·09
·10
DISPLACEMENT INS:

FIG. 11.

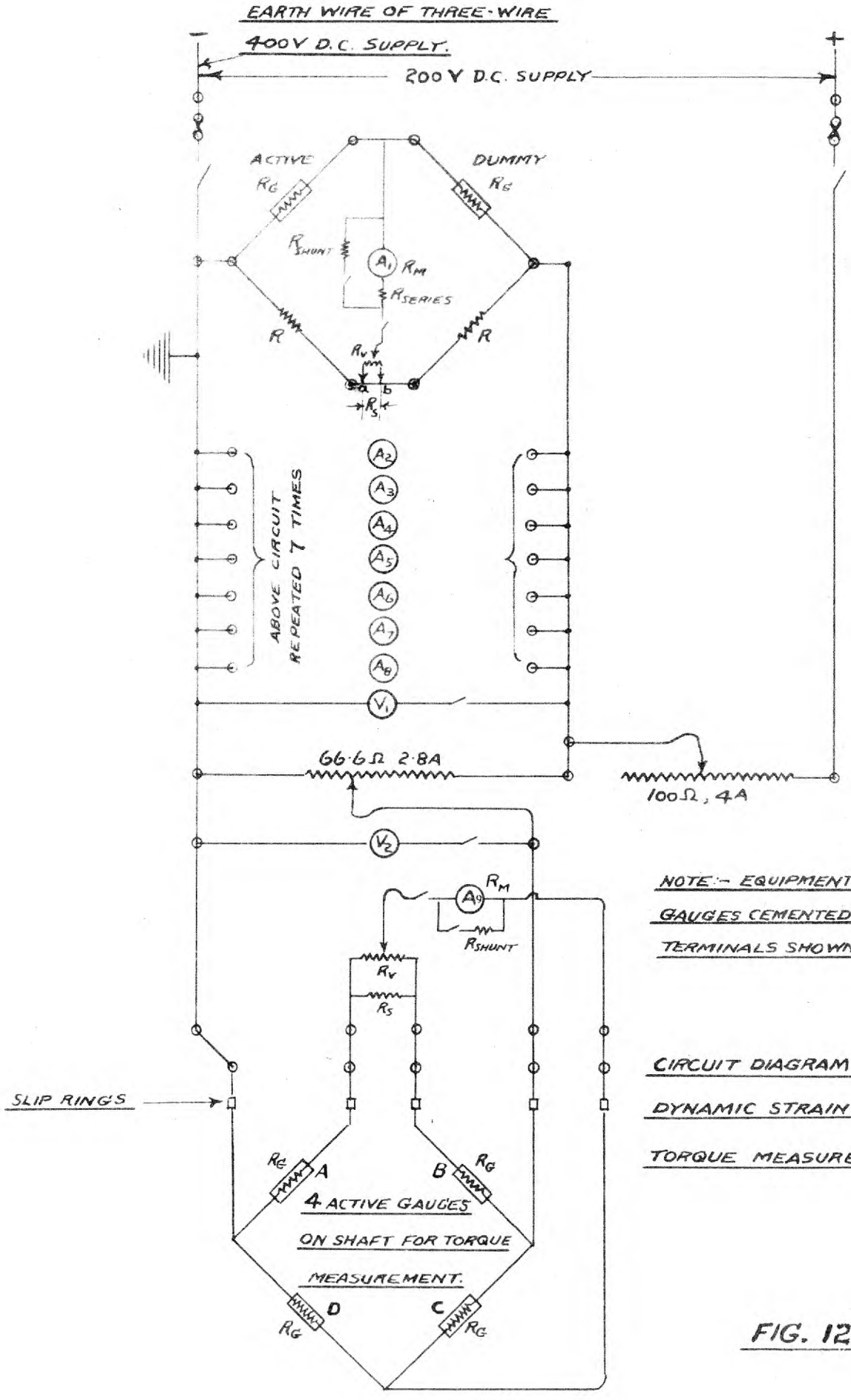

NOTE:- EQUIPMENT ON WHICH GAUGES CEMENTED EARTHED. TERMINALS SHOWN THUS:- ⊙

CIRCUIT DIAGRAM FOR DYNAMIC STRAIN AND TORQUE MEASUREMENT.

FIG. 12.

CALIBRATION OF TORSION METER.
(FOR EXPERIMENT 2).
50-0-50 μA 172·9 Ω MICROAMMETER.
APPLIED VOLTAGE 10 V.
INCREASING TORQUE ⊙
DECREASING " +
$\frac{T}{M}$ = 4·26 LB. FT./μA

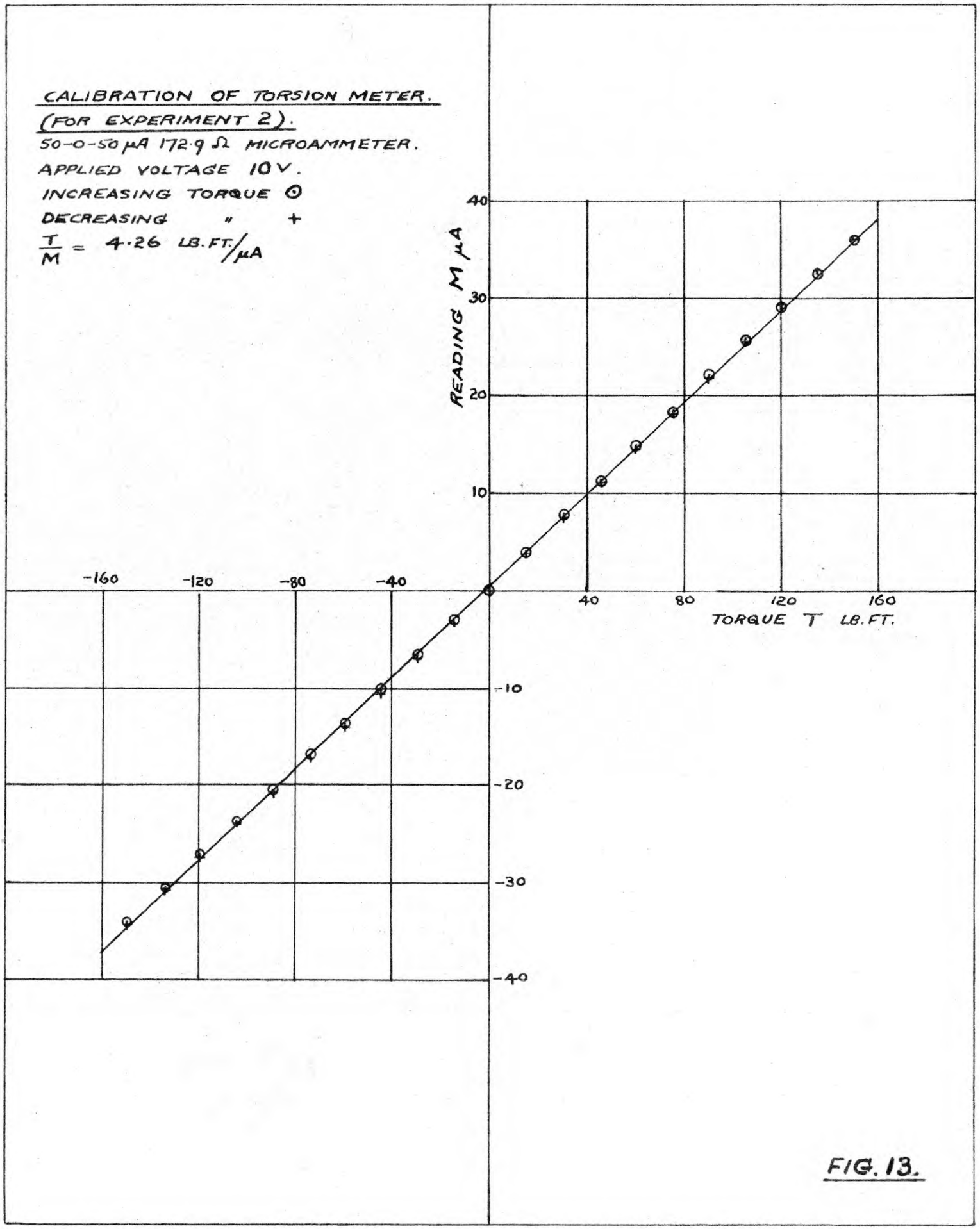

FIG. 13.

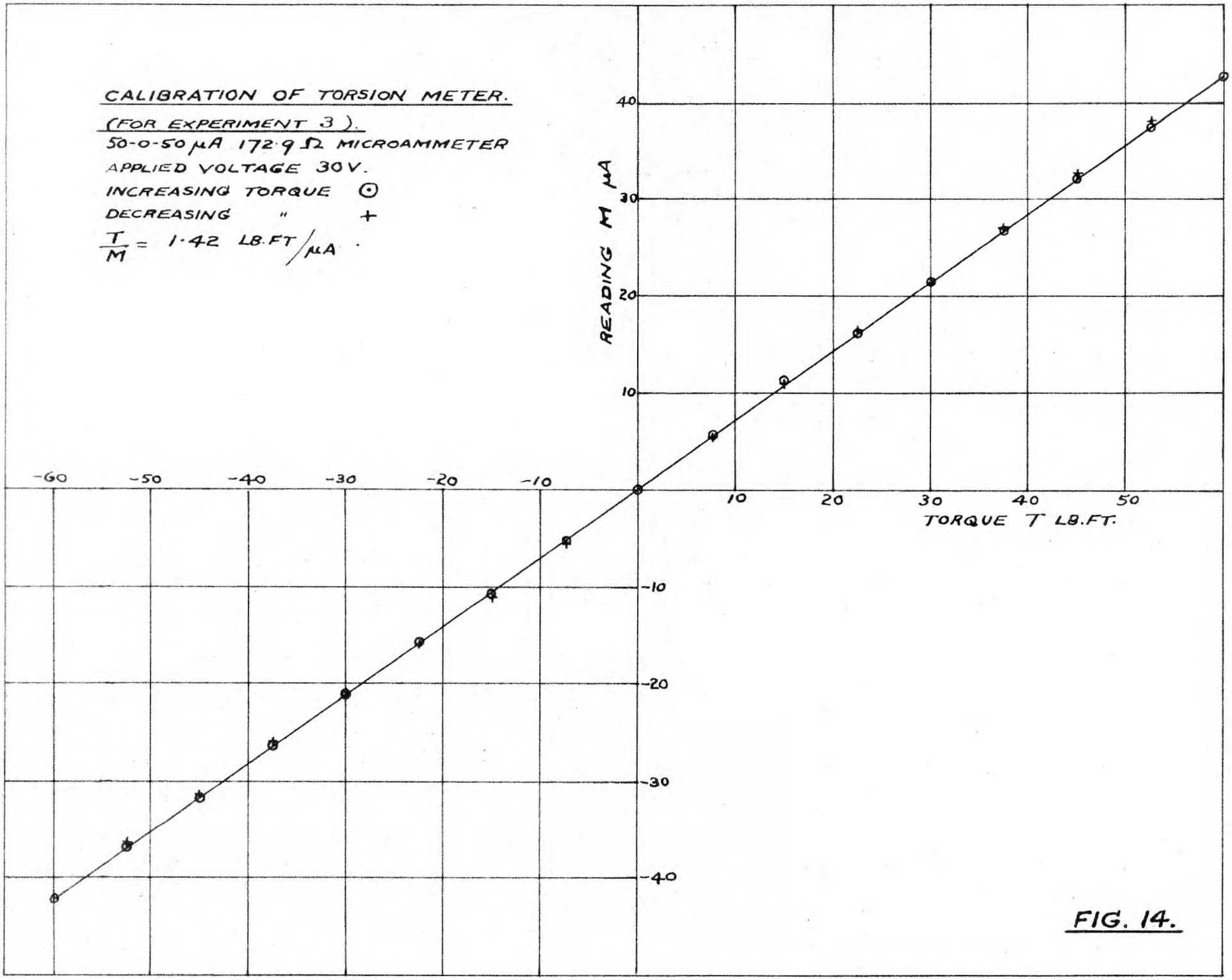
CALIBRATION OF TORSION METER.
(FOR EXPERIMENT 3).
50-0-50 μA 172·9 Ω MICROAMMETER
APPLIED VOLTAGE 30 V.
INCREASING TORQUE ⊙
DECREASING " +
T/M = 1·42 LB.FT/μA .
READING M μA
TORQUE T LB.FT.
40
30
20
10
-10
-20
-30
-40
-60
-50
-40
-30
-20
-10
10
20
30
40
50

FIG. 14.

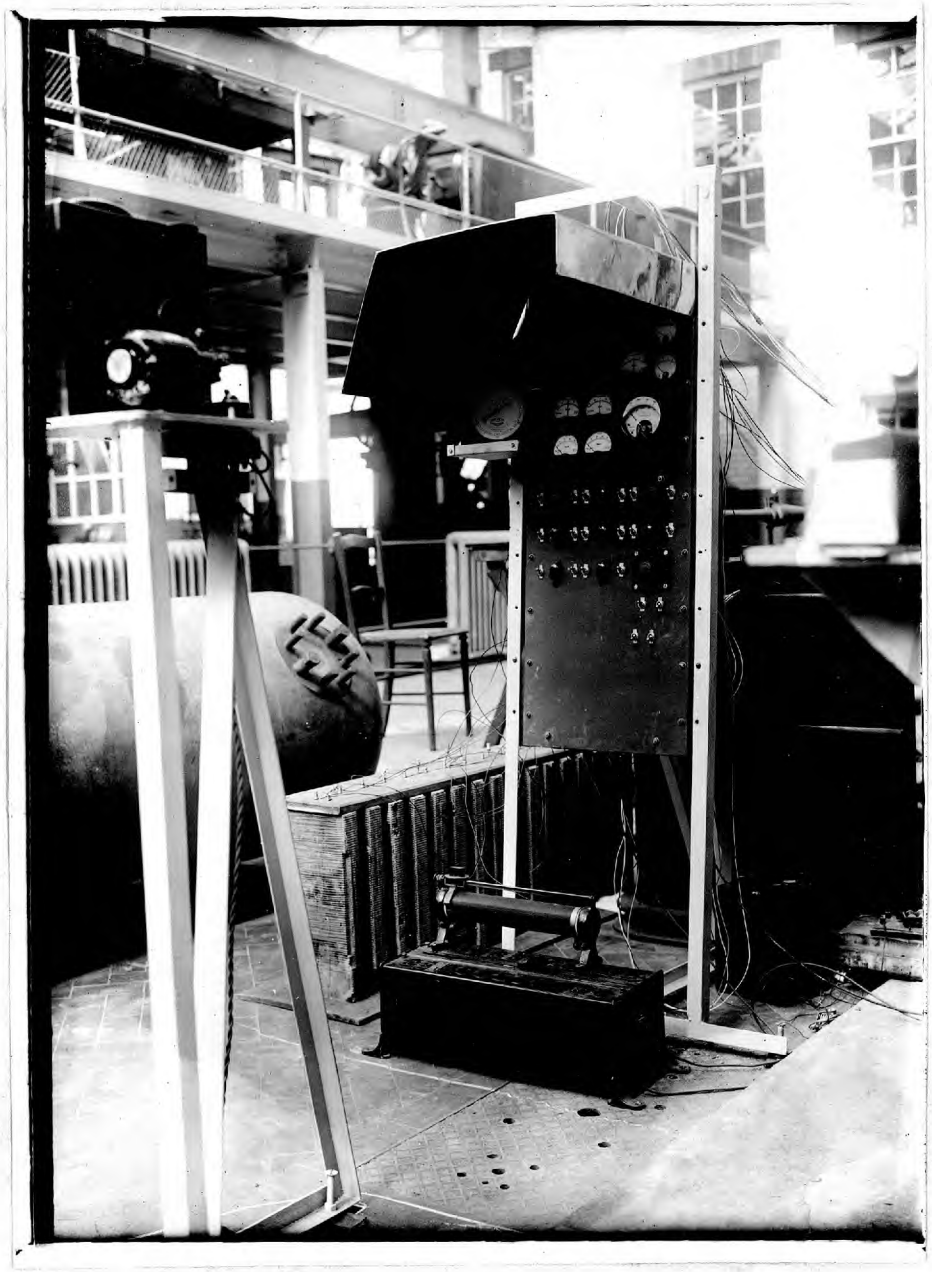

FIG. 15.

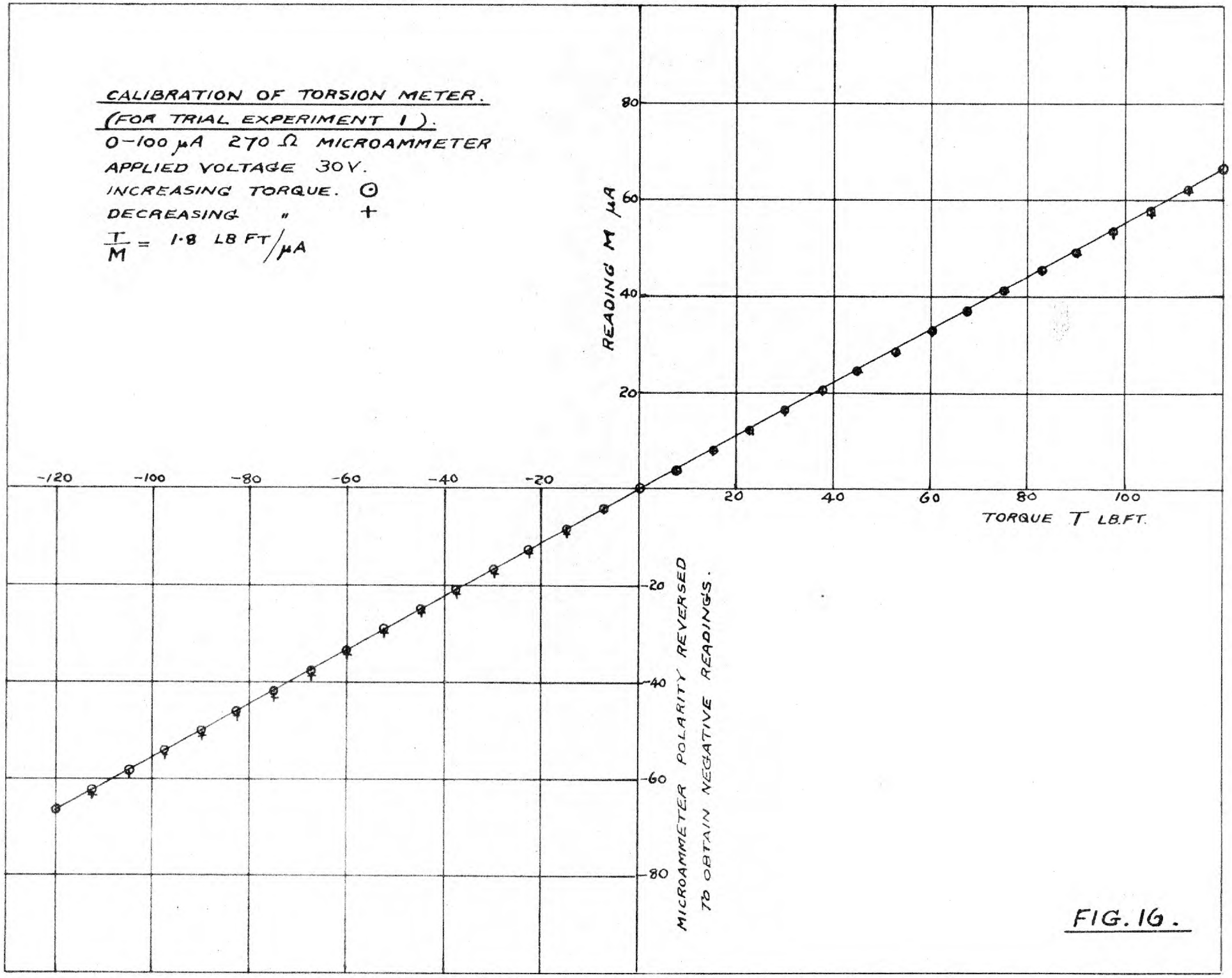
CALIBRATION OF TORSION METER.
(FOR TRIAL EXPERIMENT 1).
0–100 μA 270 Ω MICROAMMETER
APPLIED VOLTAGE 30V.
INCREASING TORQUE. ⊙
DECREASING " +
T/M = 1·8 LB FT/μA
READING M μA
80
60
40
20
20
40
60
80
100
TORQUE T LB.FT.
-120
-100
-80
-60
-40
-20
-20
-40
-60
-80
MICROAMMETER POLARITY REVERSED
TO OBTAIN NEGATIVE READINGS.

FIG. 16.

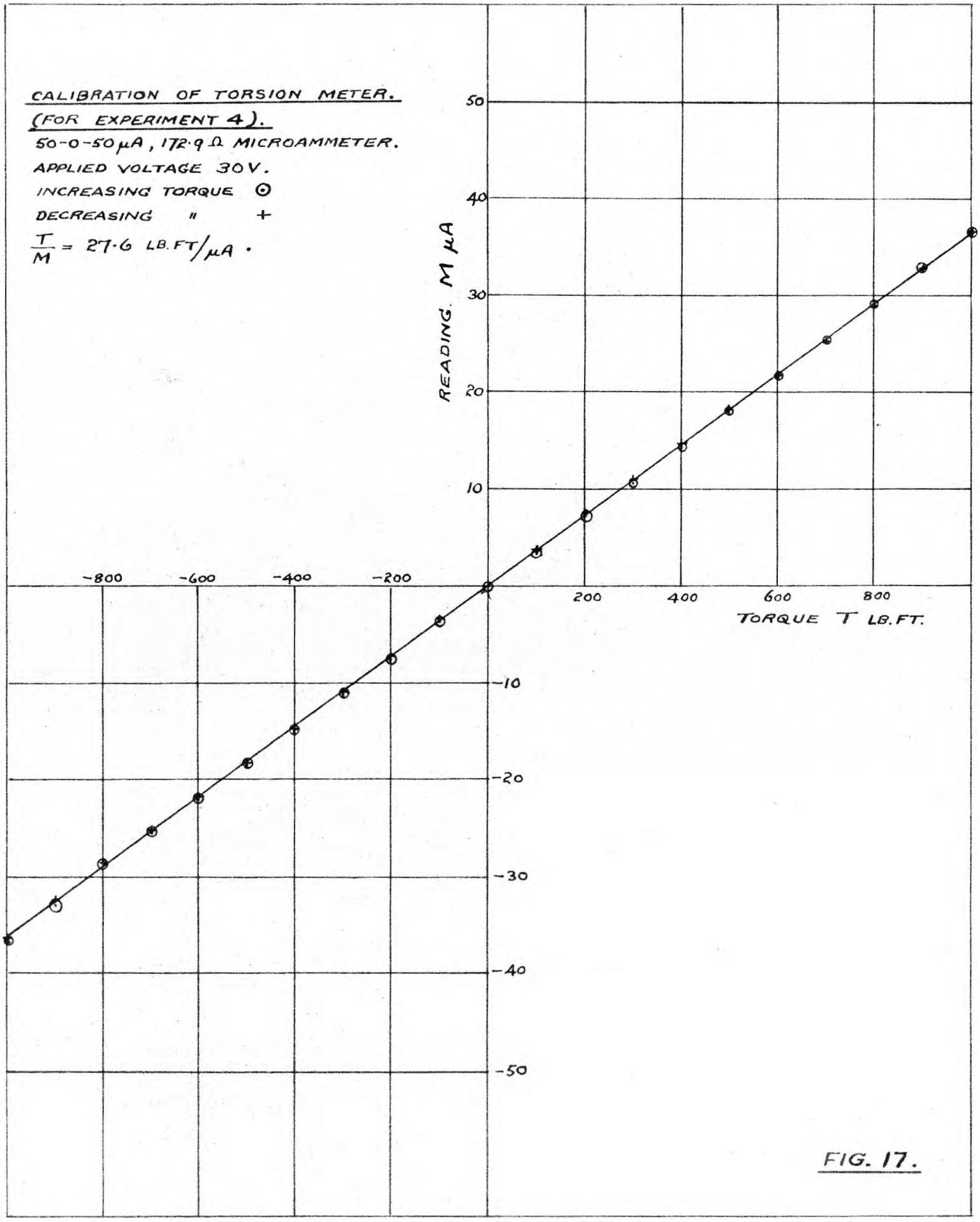
CALIBRATION OF TORSION METER.
(FOR EXPERIMENT 4).
50-0-50 μA, 172·9 Ω MICROAMMETER.
APPLIED VOLTAGE 30V.
INCREASING TORQUE ⊙
DECREASING " +
T/M = 27·6 LB.FT/μA.
READING. M μA
50
40
30
20
10
-10
-20
-30
-40
-50
-800
-600
-400
-200
200
400
600
800
TORQUE T LB.FT.

FIG. 17.

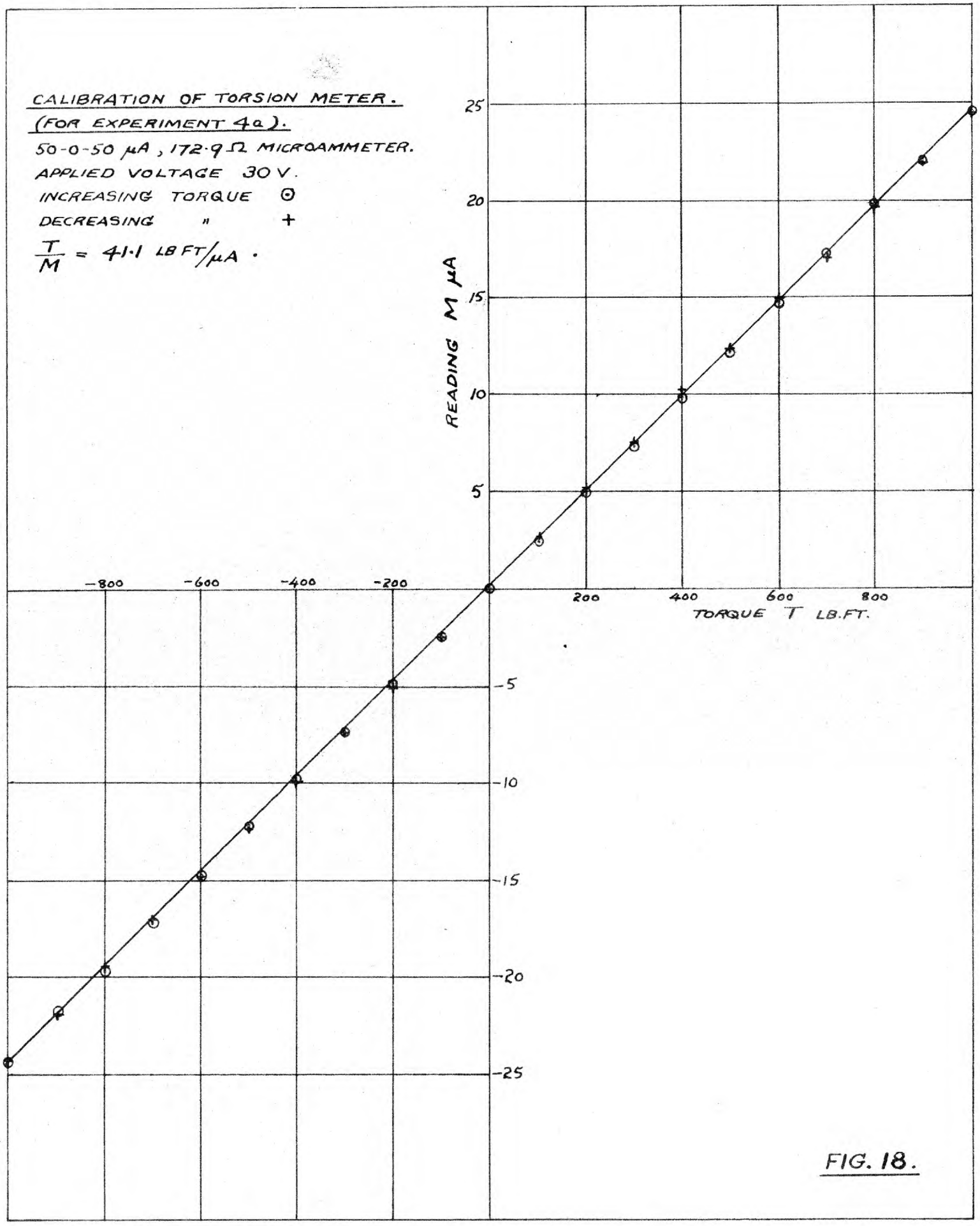
CALIBRATION OF TORSION METER.
(FOR EXPERIMENT 4a).
50-0-50 μA, 172·9 Ω MICROAMMETER.
APPLIED VOLTAGE 30 V.
INCREASING TORQUE ⊙
DECREASING " +
T/M = 41·1 LB FT/μA.
READING M μA
25
20
15
10
5
-5
-10
-15
-20
-25
-800
-600
-400
-200
200
400
600
800
TORQUE T LB.FT.

FIG. 18.

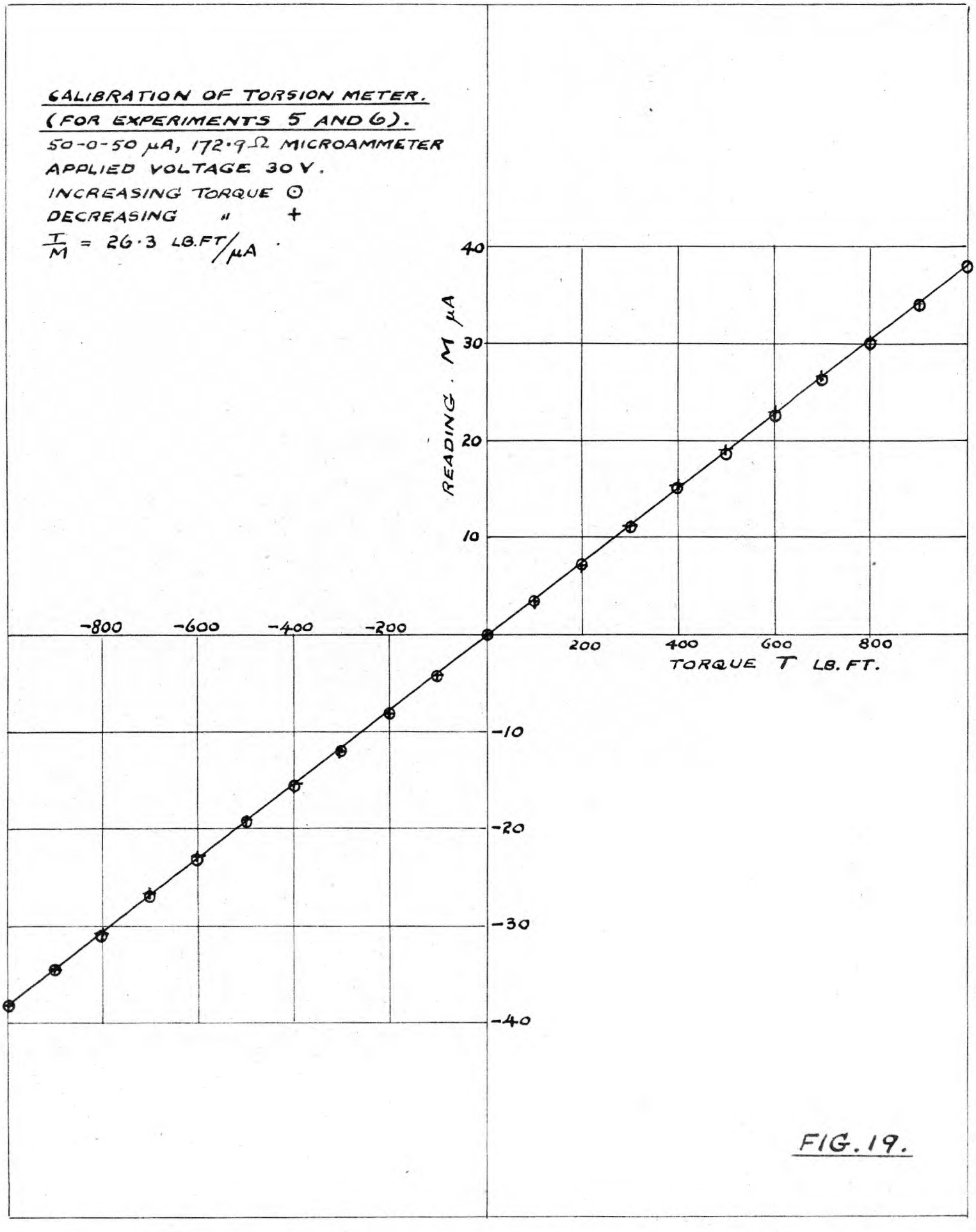
CALIBRATION OF TORSION METER.
(FOR EXPERIMENTS 5 AND 6).
50-0-50 μA, 172·9 Ω MICROAMMETER
APPLIED VOLTAGE 30 V.
INCREASING TORQUE ⊙
DECREASING " +
I/M = 26·3 LB.FT/μA.
READING. M μA
40
30
20
10
-10
-20
-30
-40
-800
-600
-400
-200
200
400
600
800
TORQUE T LB. FT.

FIG. 19.

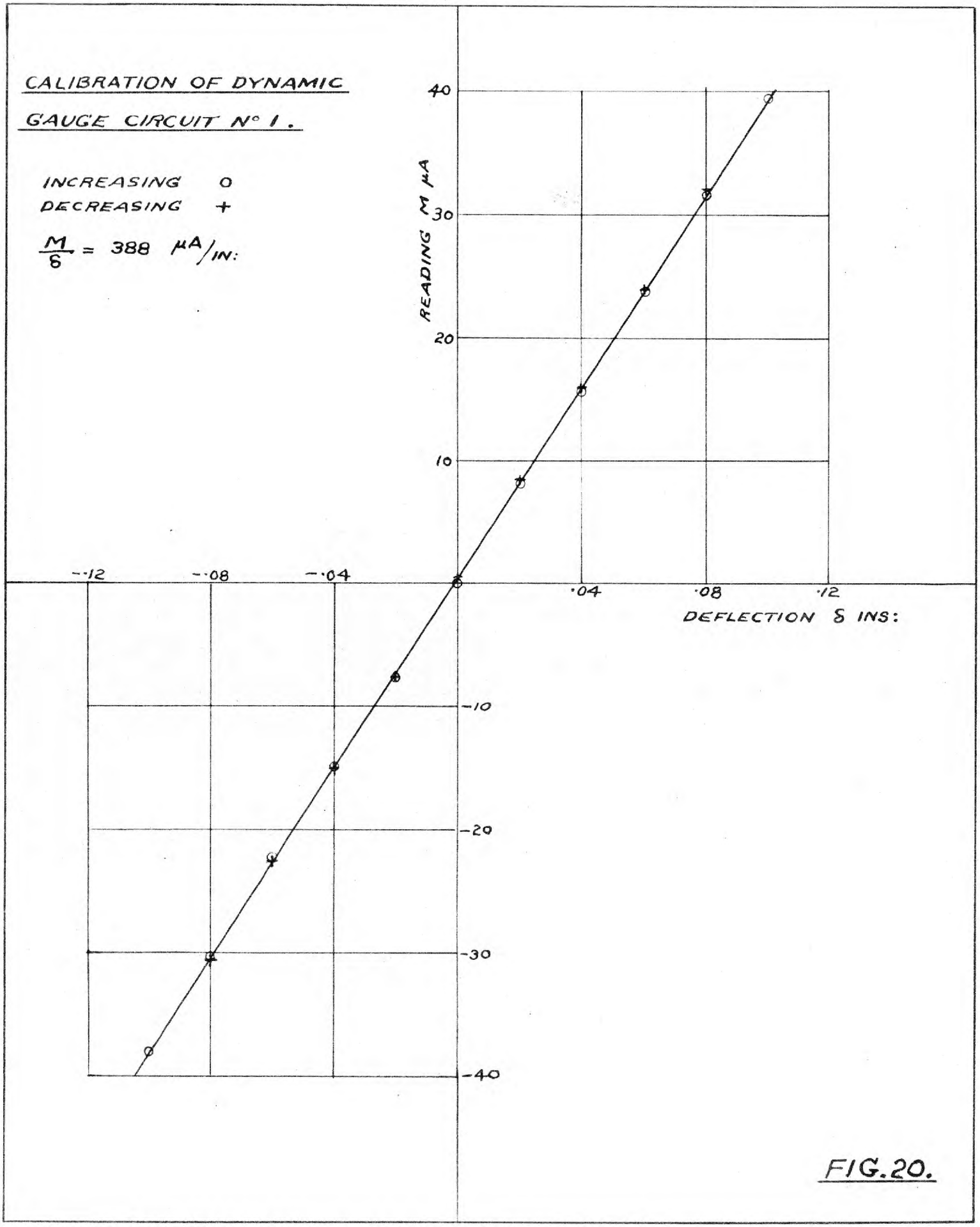
CALIBRATION OF DYNAMIC
GAUGE CIRCUIT N° 1.
INCREASING o
DECREASING +
M/δ = 388 μA/IN:
READING M μA
40
30
20
10
-10
-20
-30
-40
-·12
-·08
-·04
·04
·08
·12
DEFLECTION δ INS:

FIG.20.

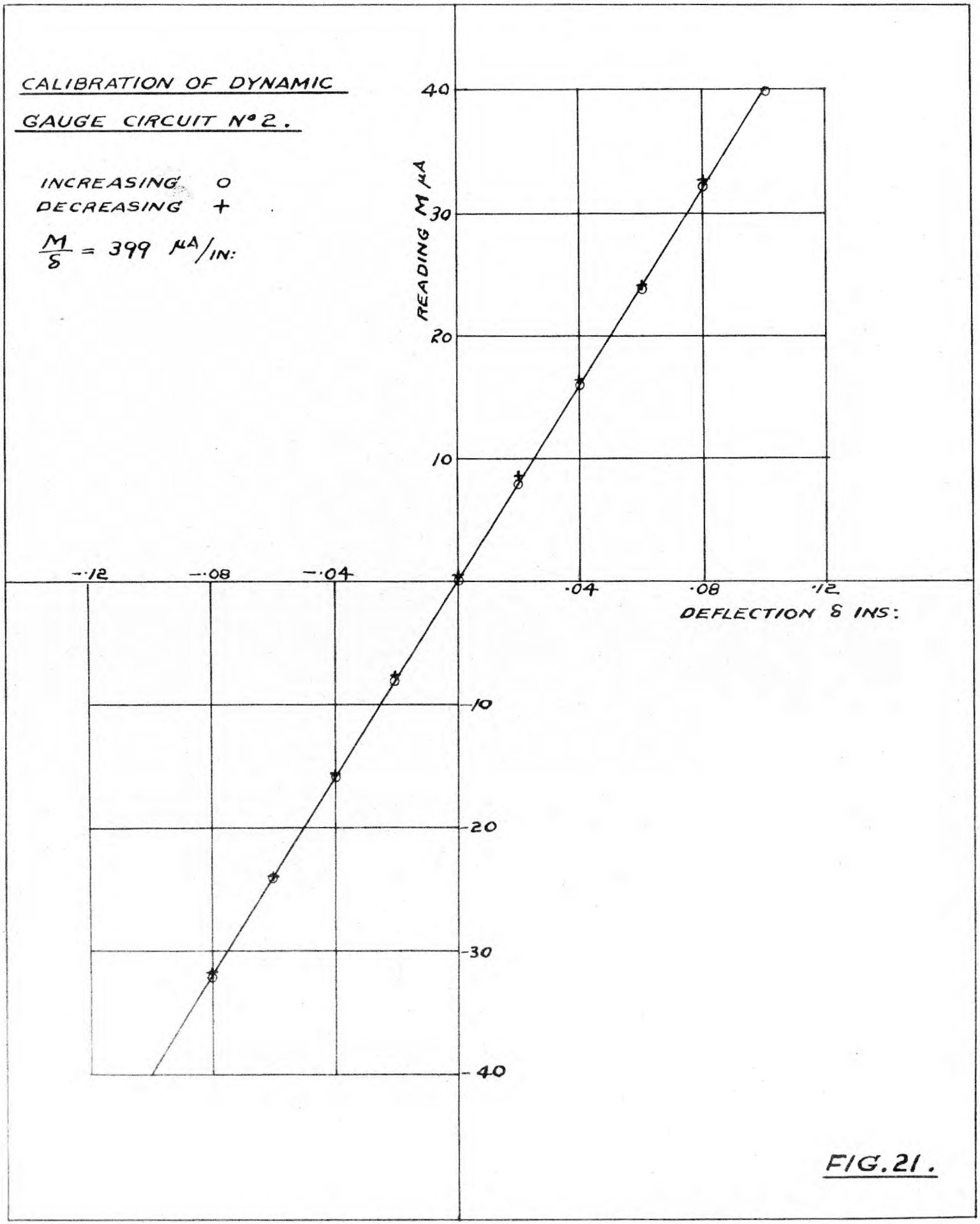
CALIBRATION OF DYNAMIC
GAUGE CIRCUIT N° 2.
INCREASING o
DECREASING +
M/δ = 399 μA/IN:
READING M μA
40
30
20
10
-·12
-·08
-·04
·04
·08
·12
DEFLECTION δ INS:
-10
-20
-30
-40

FIG. 21.

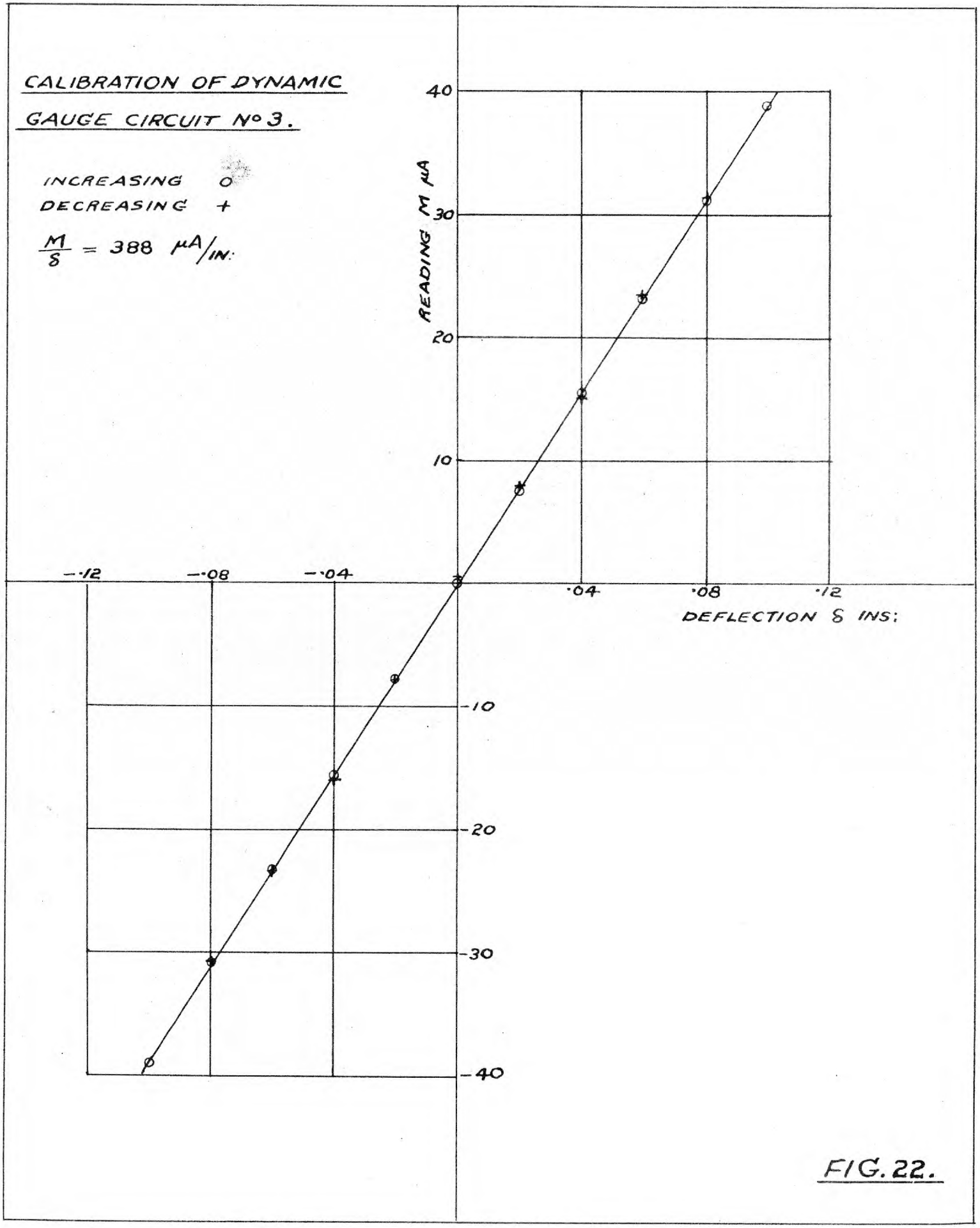
CALIBRATION OF DYNAMIC
GAUGE CIRCUIT No 3.
INCREASING O
DECREASING +
M/δ = 388 μA/IN.
READING M μA
40
30
20
10
-10
-20
-30
-40
-·12
-·08
-·04
·04
·08
·12
DEFLECTION δ INS:

FIG. 22.

CALIBRATION OF DYNAMIC GAUGE CIRCUIT No 4.

INCREASING o
DECREASING +

$\frac{M}{\delta} = 397\ \mu A/IN.$

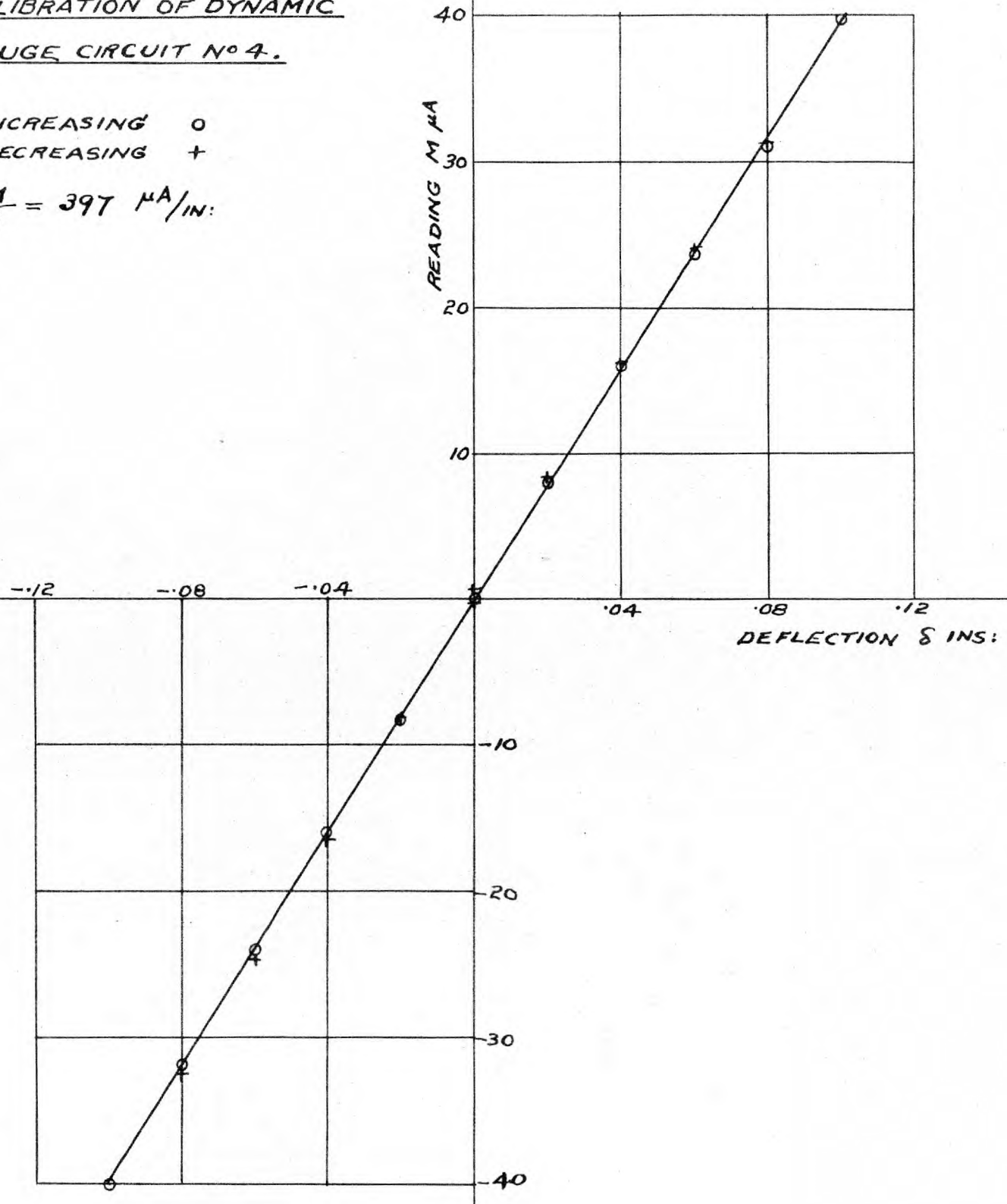

FIG.23.

CALIBRATION OF DYNAMIC GAUGE CIRCUIT No 5.

INCREASING O
DECREASING +

$\frac{M}{\delta}$ = 387 μA/IN:

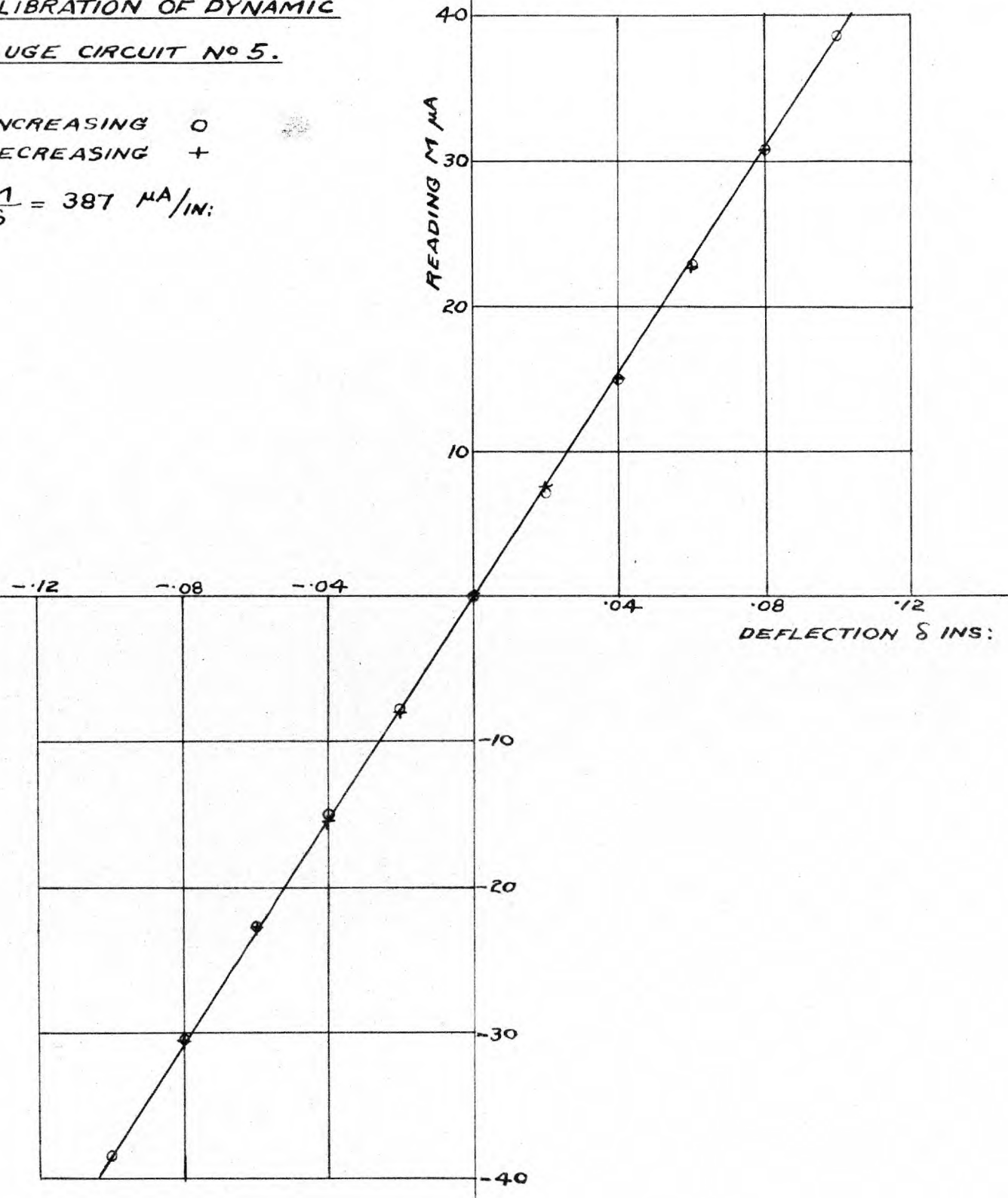

FIG. 24.

CALIBRATION OF DYNAMIC GAUGE CIRCUIT Nº 6.

INCREASING 0
DECREASING +

$\frac{M}{\delta}$ = 390 μA/IN.

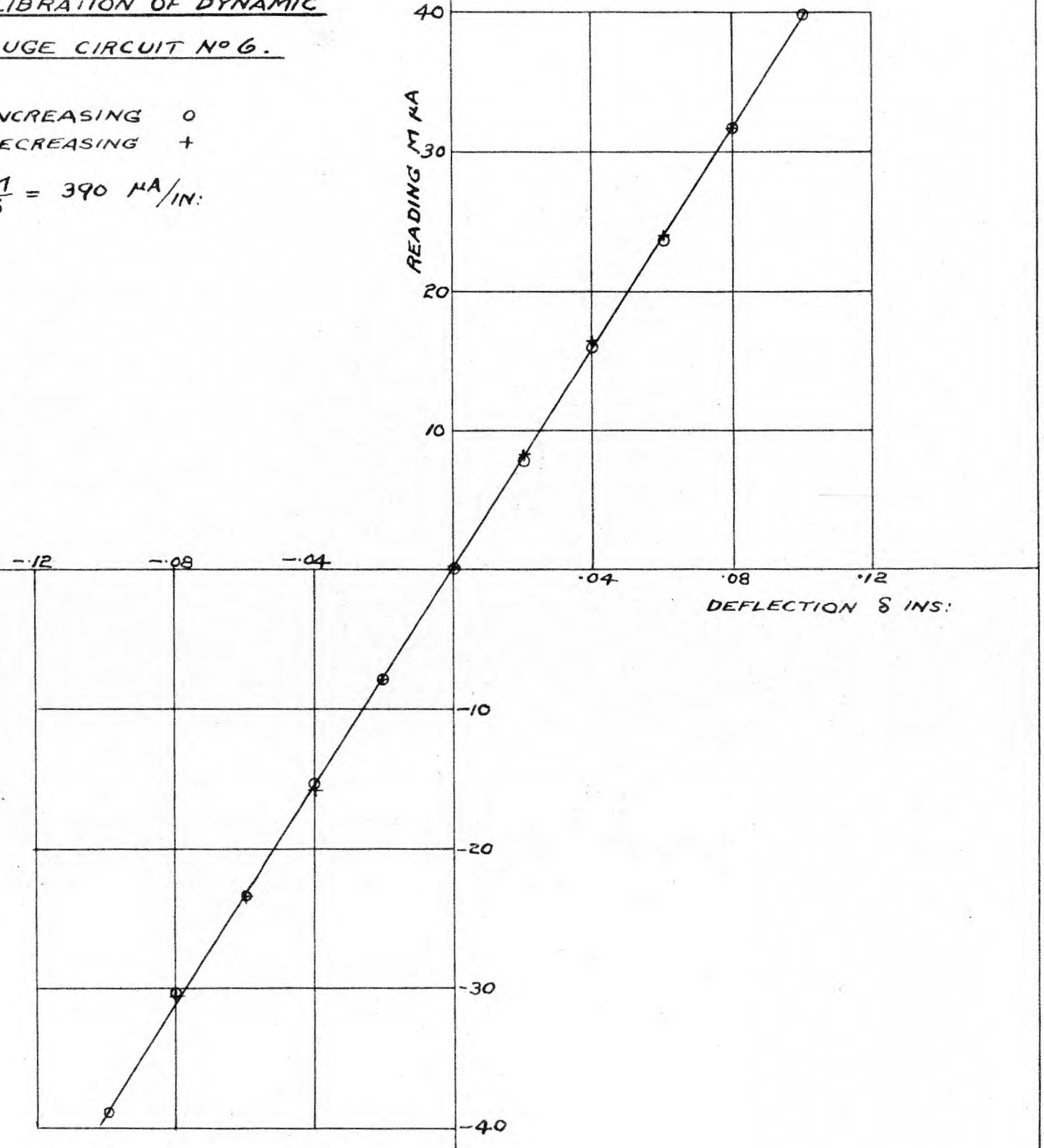

FIG. 25.

CALIBRATION OF DYNAMIC GAUGE CIRCUIT No 7.

INCREASING o
DECREASING +

$\frac{M}{\delta} = 388\ \mu A/IN.$

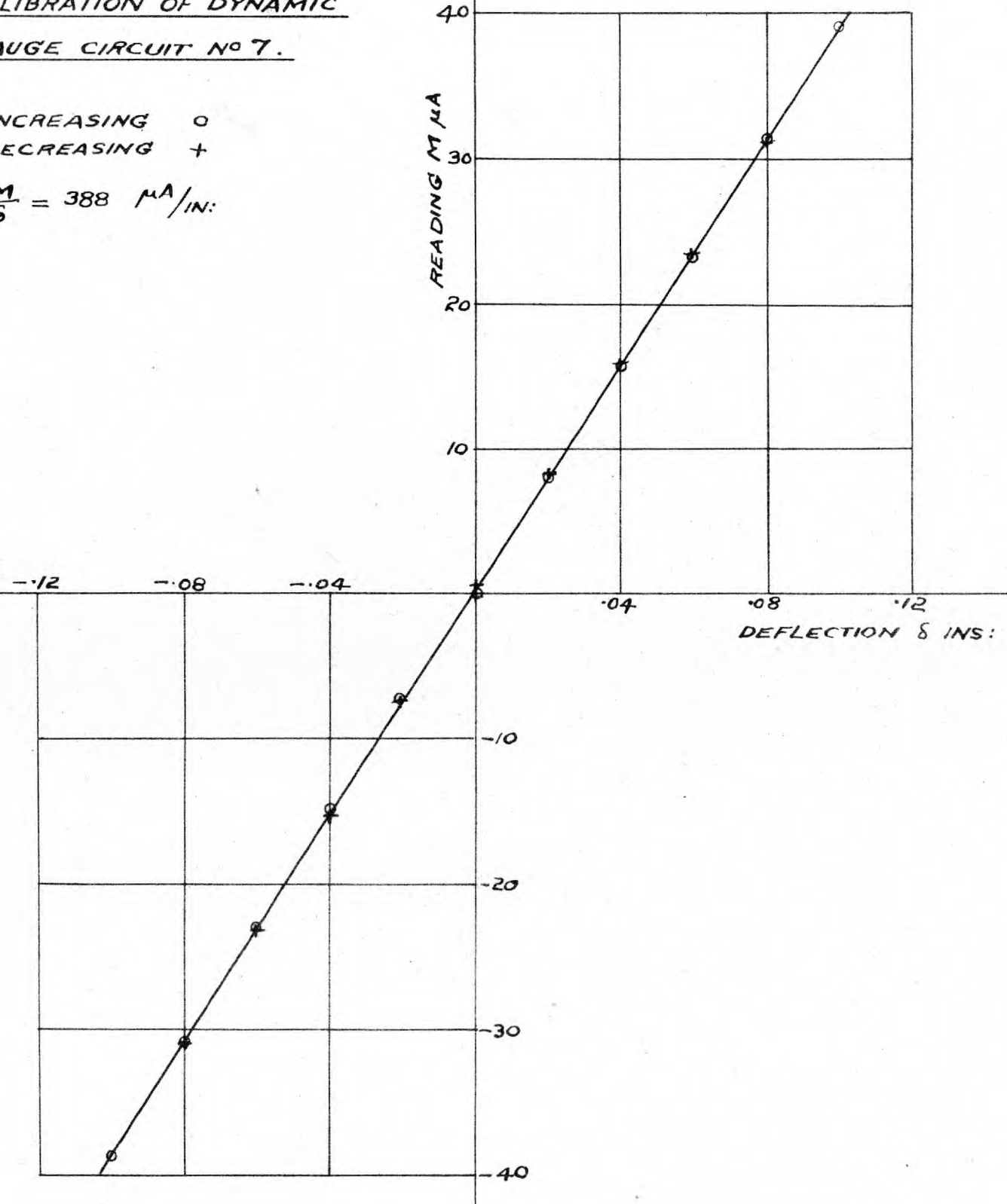

FIG. 26.

CALIBRATION OF DYNAMIC GAUGE CIRCUIT N° 8.

INCREASING o
DECREASING +

$\frac{M}{\delta} = 396\ \mu A/IN.$

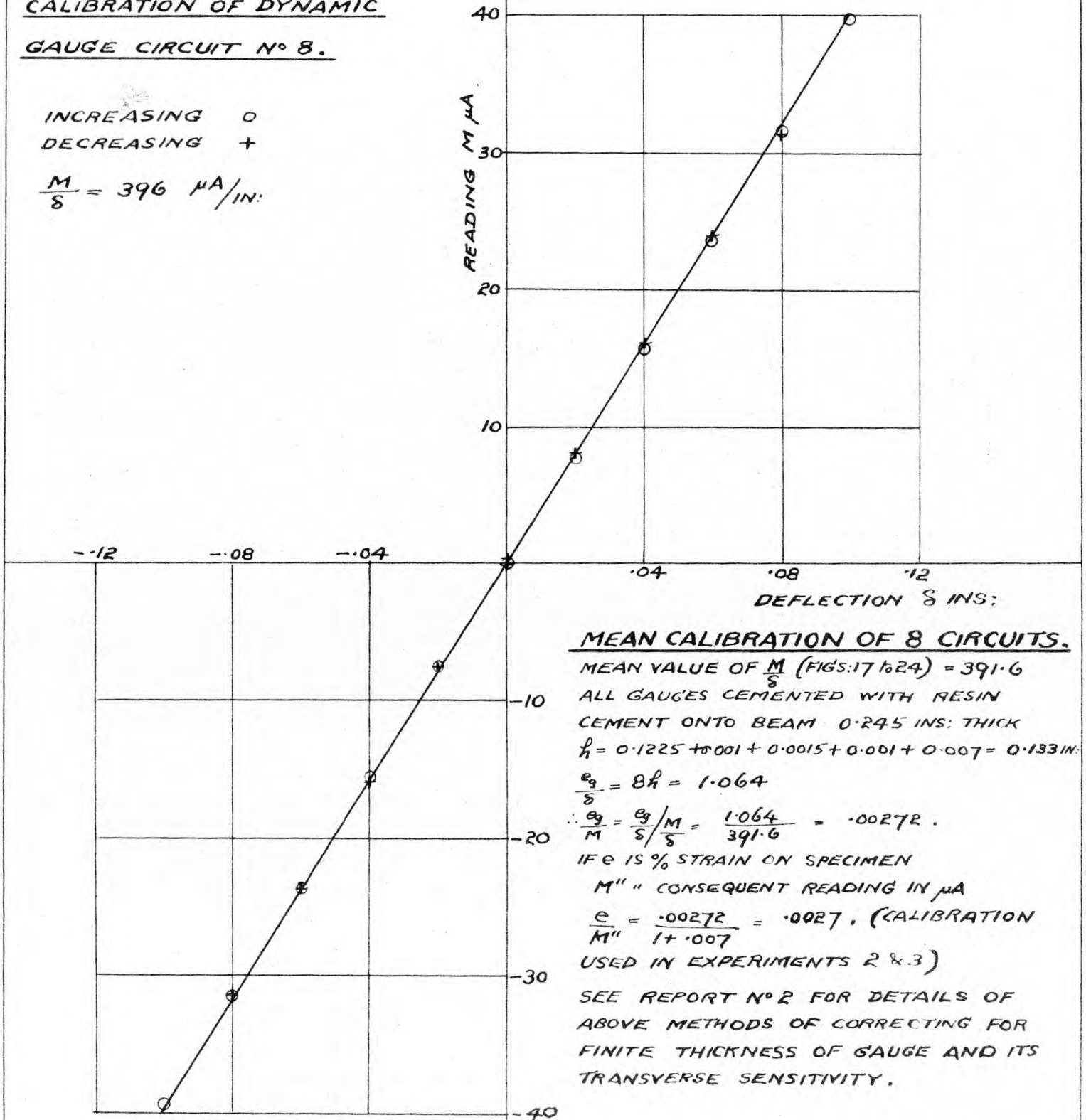

MEAN CALIBRATION OF 8 CIRCUITS.

MEAN VALUE OF $\frac{M}{\delta}$ (FIGS: 17 to 24) = 391·6

ALL GAUGES CEMENTED WITH RESIN CEMENT ONTO BEAM 0·245 INS: THICK

$h = 0.1225 + 0.001 + 0.0015 + 0.001 + 0.007 = 0.133$ IN.

$\frac{e_g}{\delta} = 8h = 1.064$

$\therefore \frac{e_g}{M} = \frac{e_g}{\delta} \Big/ \frac{M}{\delta} = \frac{1.064}{391.6} = .00272.$

IF e IS % STRAIN ON SPECIMEN
M" " CONSEQUENT READING IN μA

$\frac{e}{M''} = \frac{.00272}{1 + .007} = .0027.$ (CALIBRATION USED IN EXPERIMENTS 2 & 3)

SEE REPORT N° 2 FOR DETAILS OF ABOVE METHODS OF CORRECTING FOR FINITE THICKNESS OF GAUGE AND ITS TRANSVERSE SENSITIVITY.

FIG. 27.

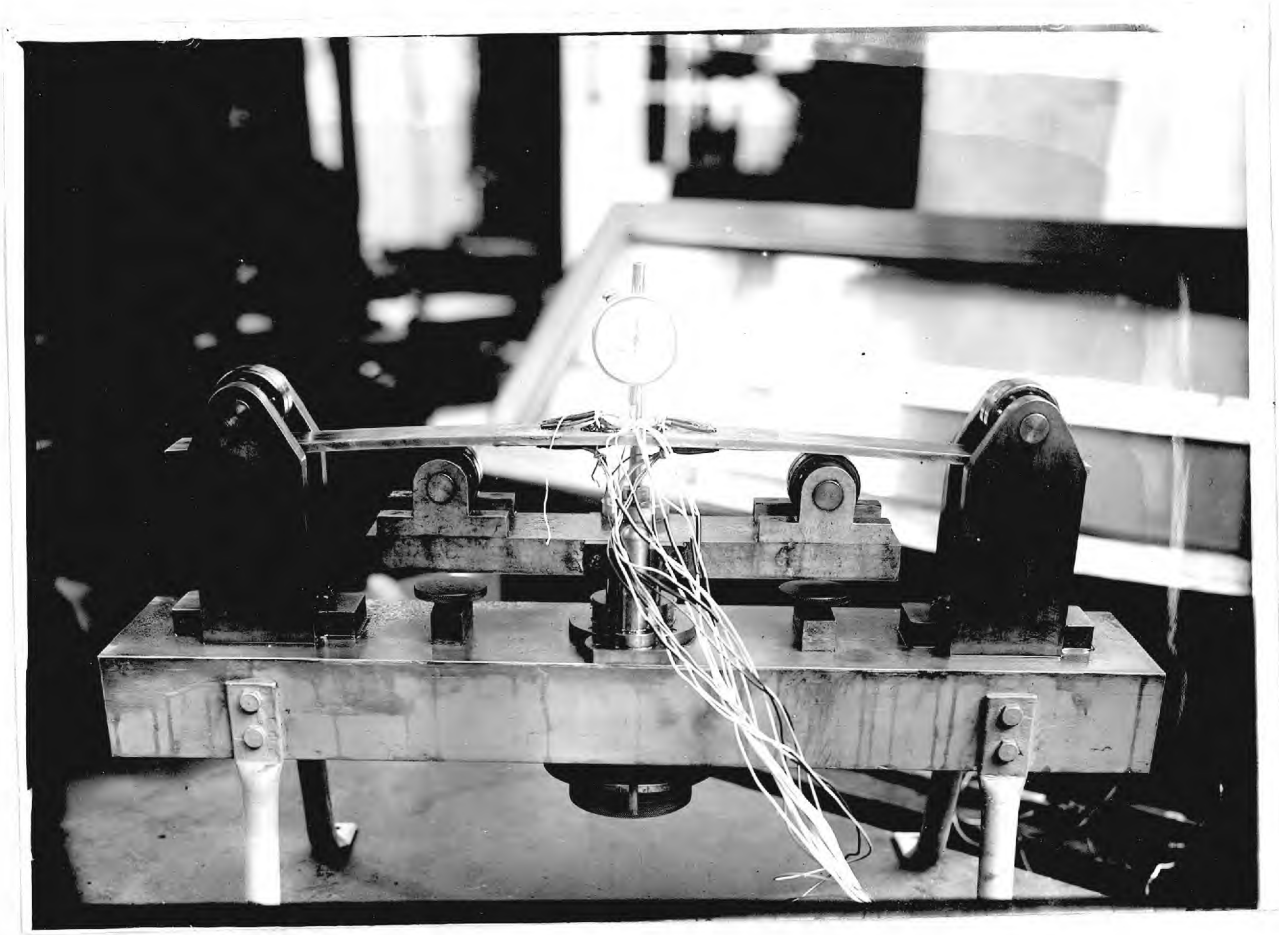

FIG. 28.

FIG. 29.

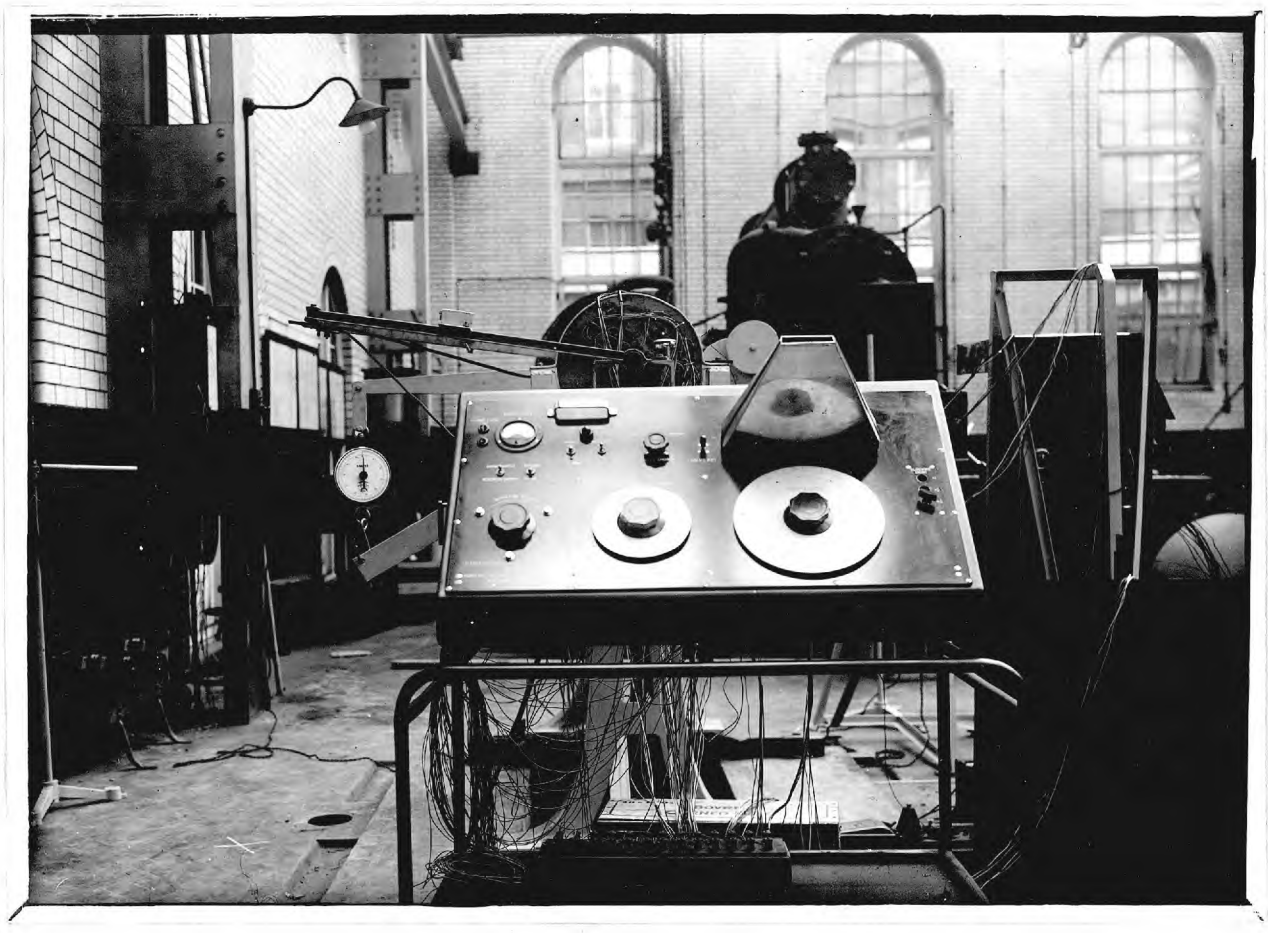

FIG. 30.

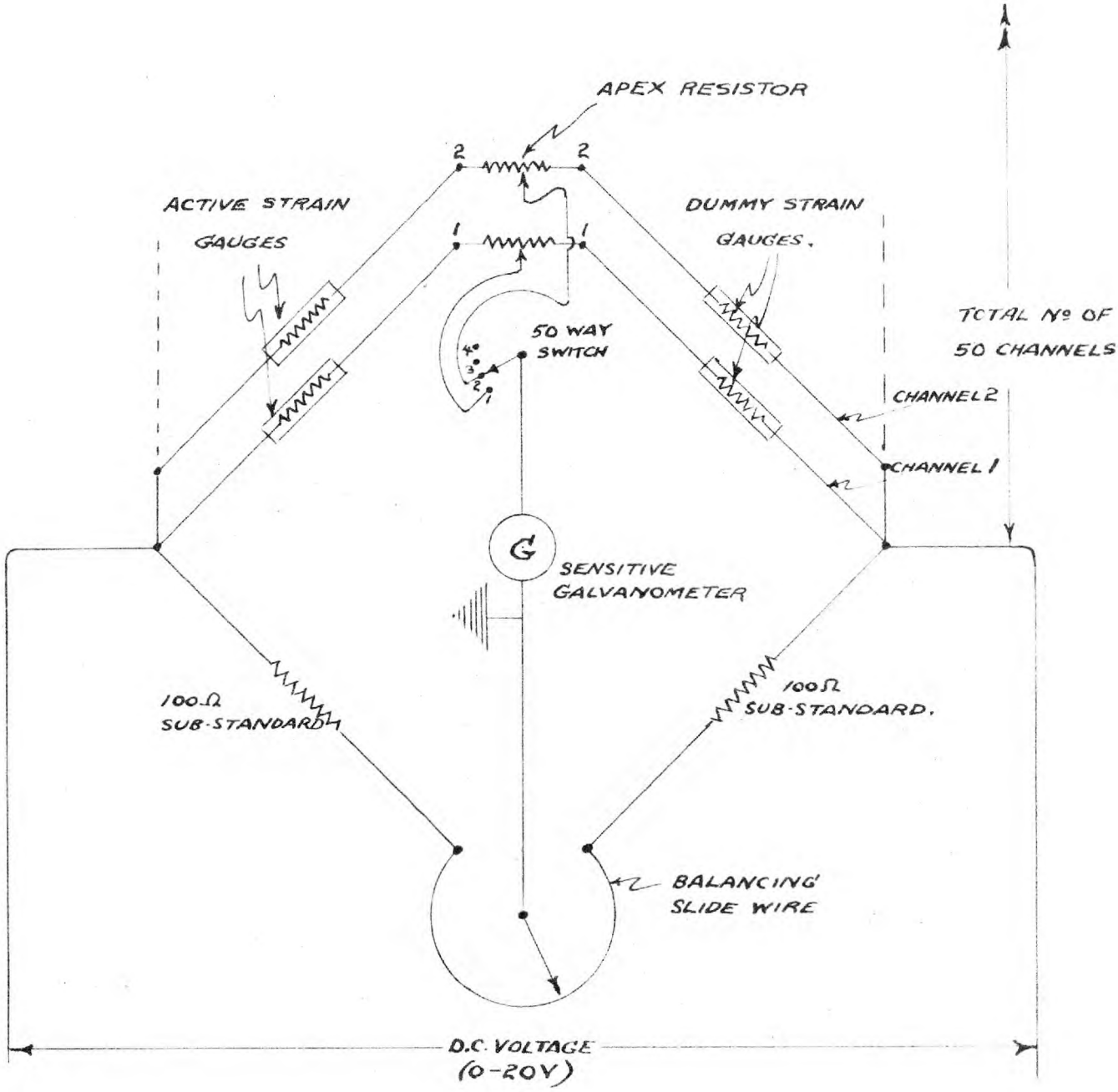

SIMPLIFIED CIRCUIT DIAGRAM FOR SAVAGE AND PARSONS STATIC STRAIN RECORDER.

FIG. 31.

POSITIONS OF STRAIN GAUGES ON SPECIMEN Nº 1. (TRIAL EXPERIMENT Nº 1).

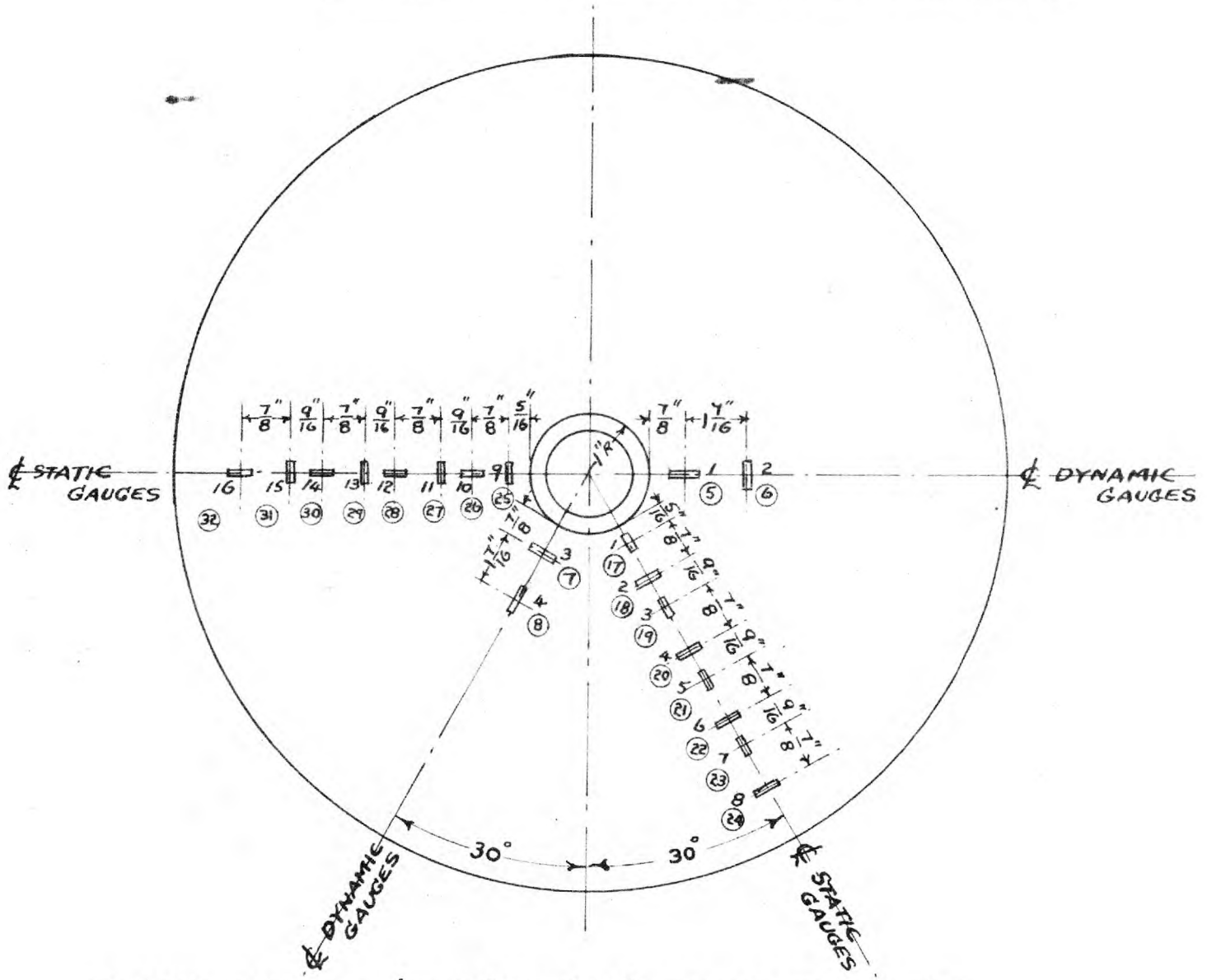

DYNAMIC GAUGES:– $\frac{1}{2}$ IN. × 4MM., 400 Ω BRITISH THERMOSTAT.

STATIC " :– $\frac{1}{4}$ IN. × 4MM., 200 Ω " " .

ALL CEMENTED WITH 'HIGH SOLIDS DUROFIX' NITRO-CELLULOSE CEMENT.

FRONT OF SPECIMEN SHOWN, ALL GAUGES BEING DUPLICATED ON THE BACK.

NUMBERS REFER TO CHANNEL OR CIRCUIT IN WHICH GAUGE IS CONNECTED.

THE NUMBERS OF THE GAUGES ON THE BACK OF THE SPECIMEN ARE CIRCLED.

FIG. 32.

POSITIONS OF STRAIN GAUGES ON SPECIMEN Nº 2. (EXPERIMENT Nº 2).

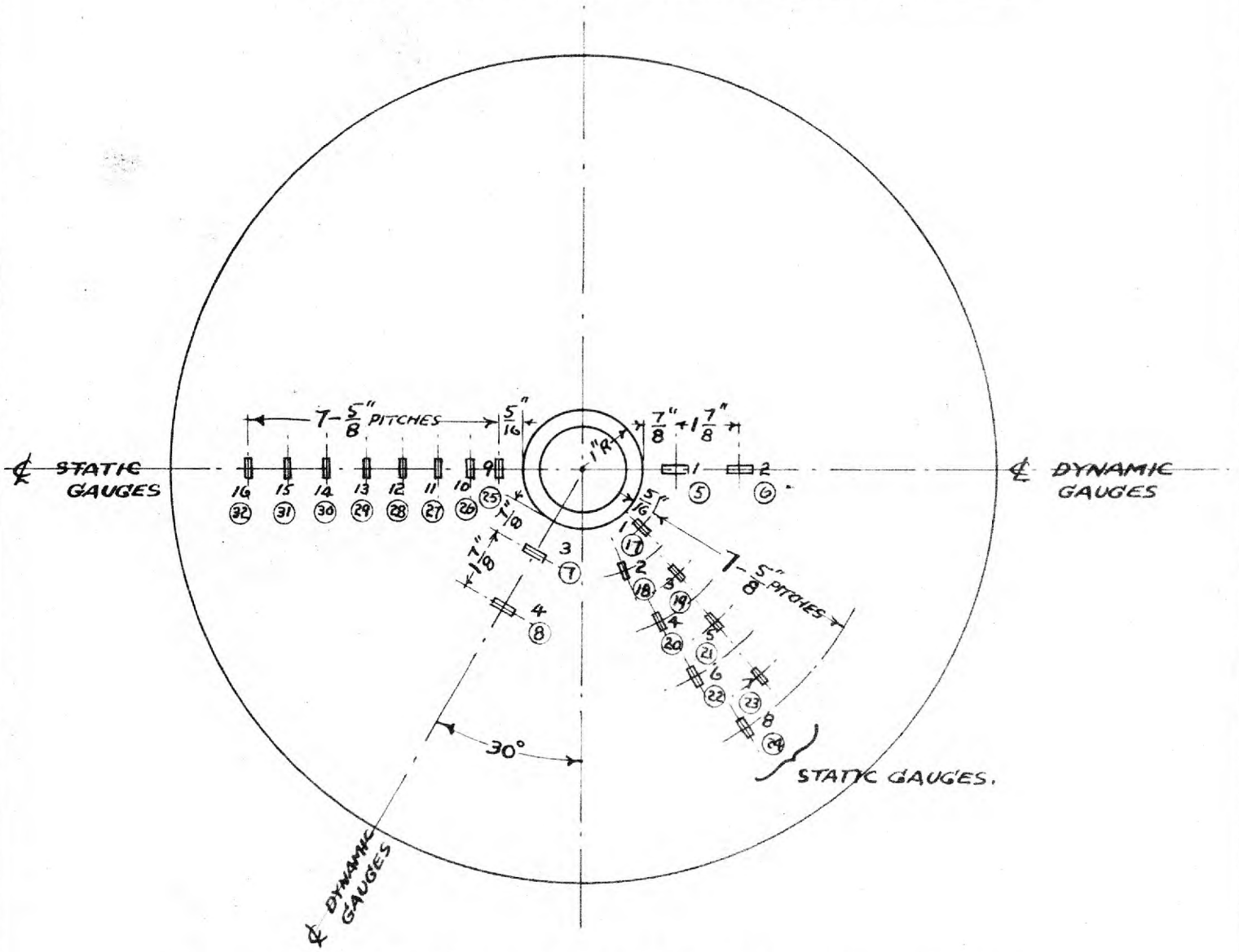

DYNAMIC GAUGES:- $\frac{1}{2}$ IN. x 4MM., 400Ω BRITISH THERMOSTAT.

STATIC " :- $\frac{1}{4}$ IN. x 4MM., 200Ω " "

ALL CEMENTED WITH 'ROCKITE' PHENOL-FORMALDEHYDE RESIN CEMENT.

FRONT OF SPECIMEN SHOWN, ALL GAUGES DUPLICATED ON BACK.

NUMBERS REFER TO CHANNEL OR CIRCUIT IN WHICH GAUGE IS CONNECTED.

THE NUMBERS OF THE GAUGES ON THE BACK OF THE SPECIMEN ARE CIRCLED.

FIG. 33.

POSITIONS OF STRAIN GAUGES ON

SPECIMEN No 3 (EXPERIMENT No 3).

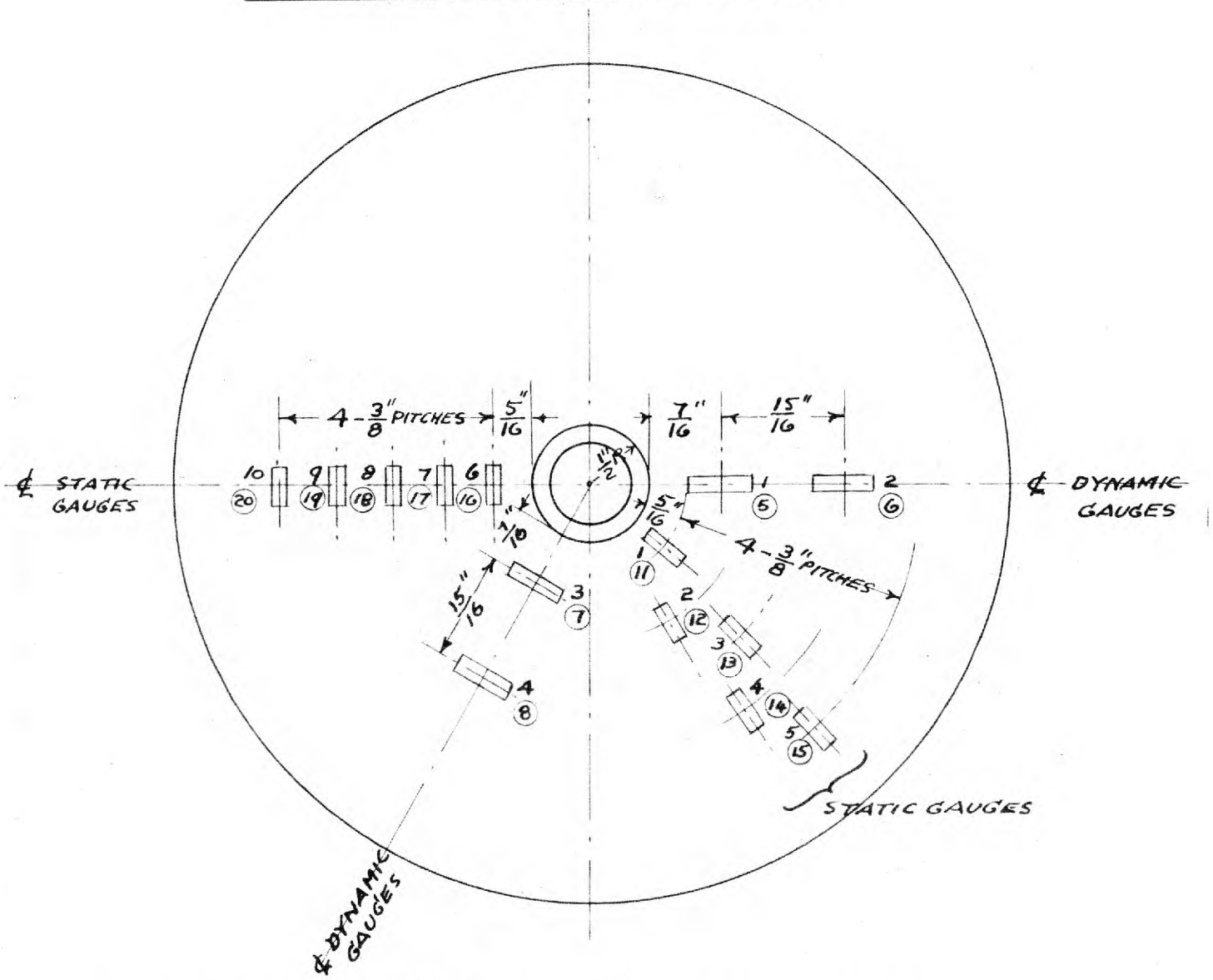

DYNAMIC GAUGES:- $\frac{1}{2}$" × 4 MM.; 400 Ω BRITISH THERMOSTAT.

STATIC GAUGES:- $\frac{1}{4}$" × 4 MM.; 200 Ω " " .

ALL CEMENTED WITH 'ROCKITE' PHENOL FORMALDEHYDE RESIN CEMENT.

FRONT OF SPECIMEN SHOWN, ALL GAUGES BEING DUPLICATED ON THE BACK.

NUMBERS REFER TO CHANNEL OR CIRCUIT IN WHICH GAUGE IS CONNECTED.

THE NUMBERS OF THE GAUGES ON THE BACK OF THE SPECIMEN ARE CIRCLED.

FIG. 34.

POSITIONS OF STRAIN GAUGES ON SPECIMEN

Nº 4. (EXPERIMENTS Nos 4 & 4a).

(ALSO DYNAMIC GAUGES ON SPECIMEN Nº 6).

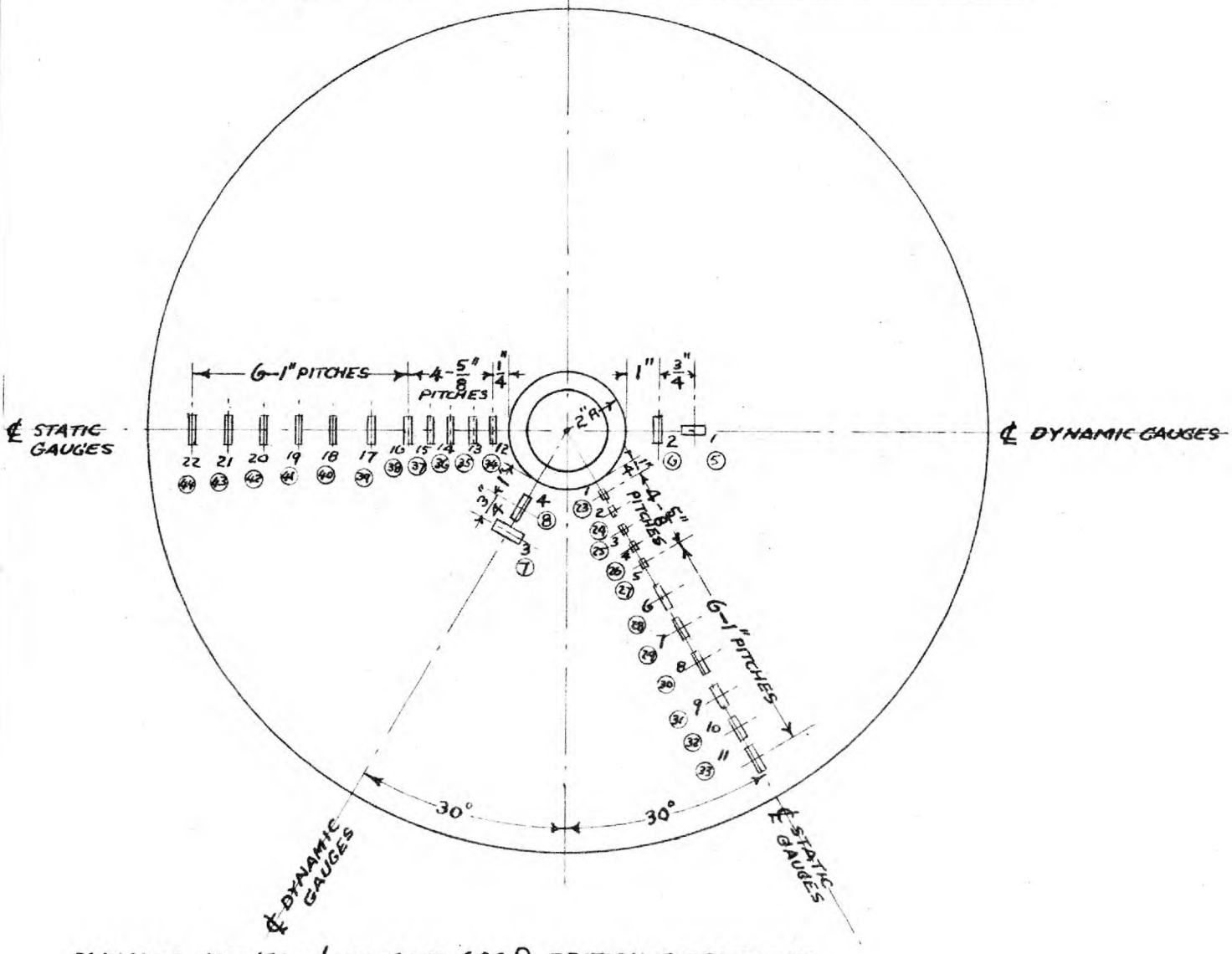

DYNAMIC GAUGES:- $\frac{1}{2}$ IN: × 4 MM., 400 Ω BRITISH THERMOSTAT.

STATIC GAUGES:- Nos 1 to 5, 23 to 27 :- 8 × 1·5 MM:, 50 Ω TINSLEY.

REMAINDER :- 17 × 2·5 MM:, 100 Ω " .

ALL CEMENTED WITH 'HIGH SOLIDS DUROFIX' NITRO-CELLULOSE CEMENT.

FRONT OF SPECIMEN SHOWN, ALL GAUGES BEING DUPLICATED ON THE BACK.

NUMBERS REFER TO CHANNEL OR CIRCUIT IN WHICH GAUGE IS CONNECTED.

THE NUMBERS OF THE GAUGES ON THE BACK OF THE SPECIMEN ARE CIRCLED.

FIG. 35.

DETAILS OF SPECIMEN 5.

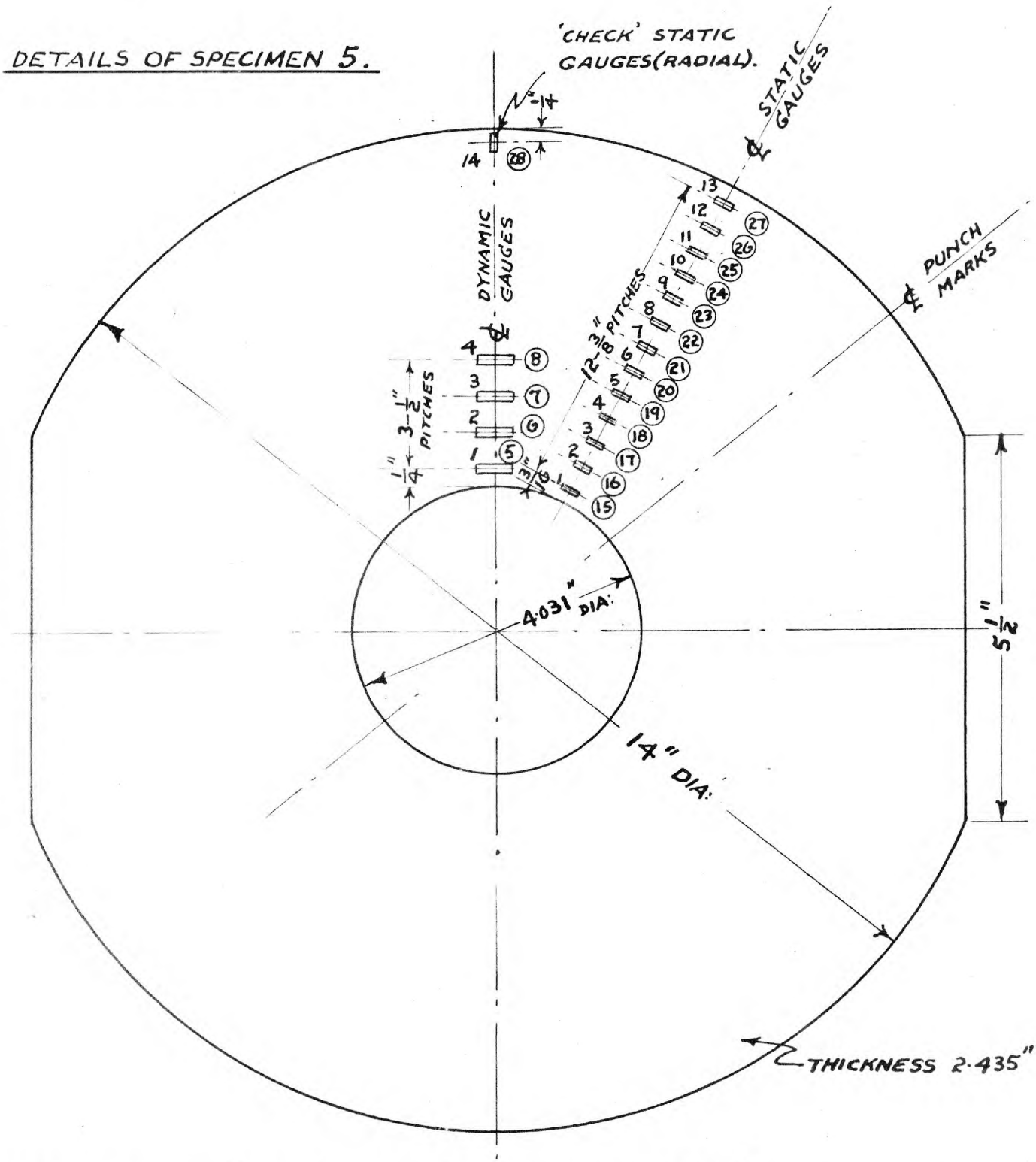

DYNAMIC GAUGES:- $\frac{1}{2}$ IN. × 4MM., 400 Ω BRITISH THERMOSTAT. } ALL BAKED ON.
STATIC GAUGES:- $\frac{1}{4}$ IN. × 4MM., 200 Ω " "

FRONT OF SPECIMEN SHOWN, NUMBERS OF GAUGES ON BACK ARE CIRCLED.

TUBE OUTSIDE DIA: 4·021 IN., INSIDE DIA: 3·011 IN.

FIG. 36.

CALIBRATION OF BRITISH THERMOSTAT GAUGES.

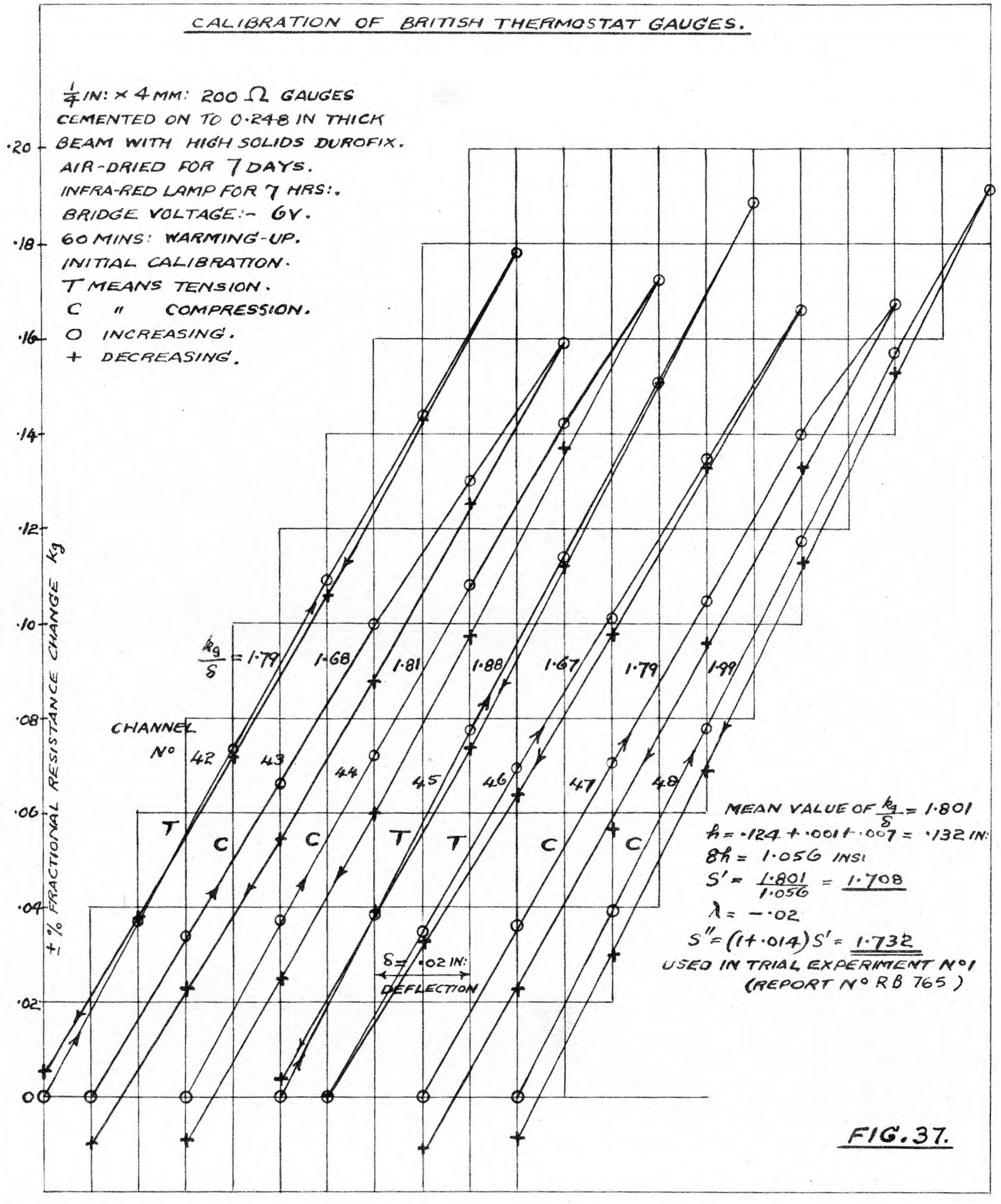

FIG. 37.

CALIBRATION OF BRITISH THERMOSTAT GAUGES.

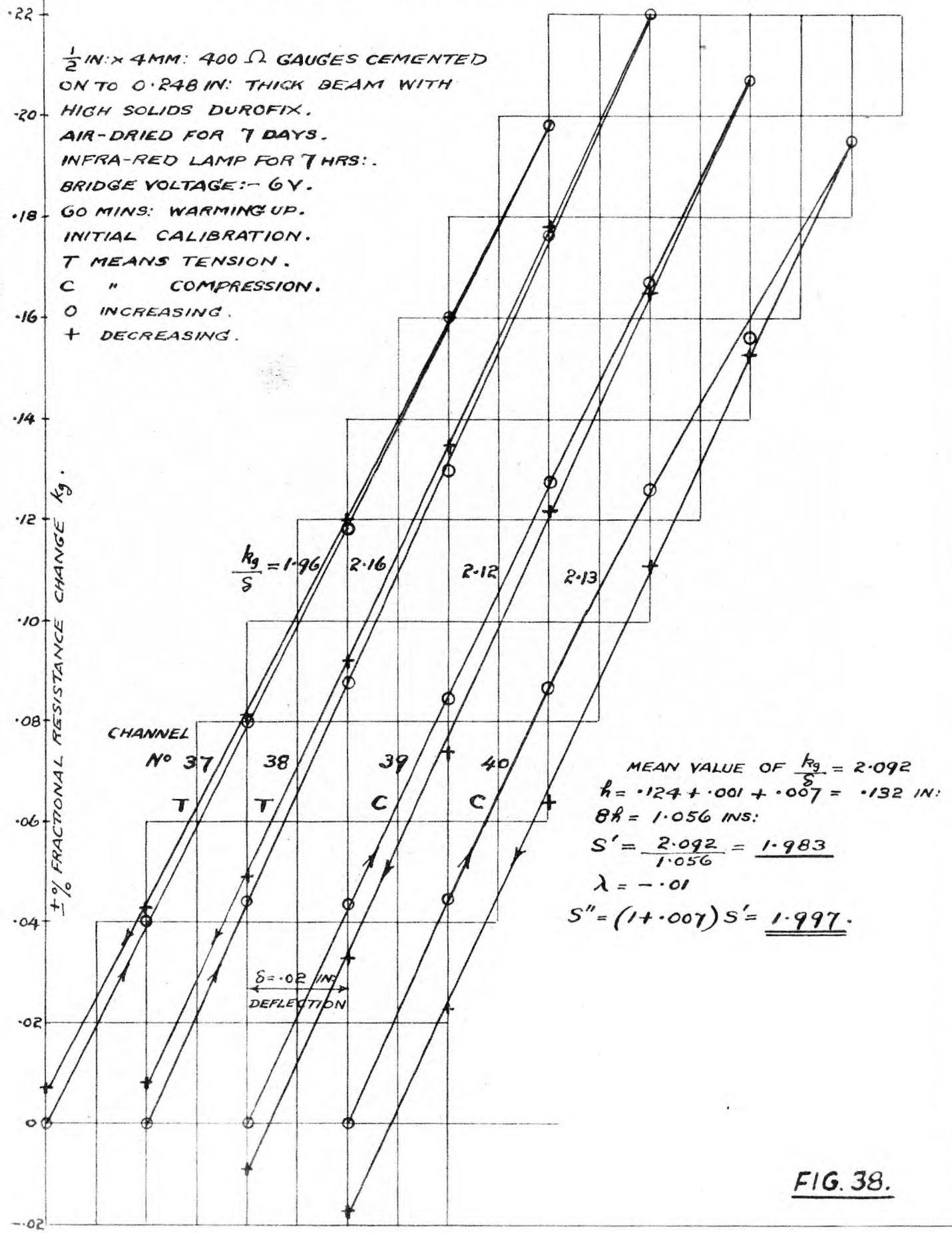

FIG. 38.

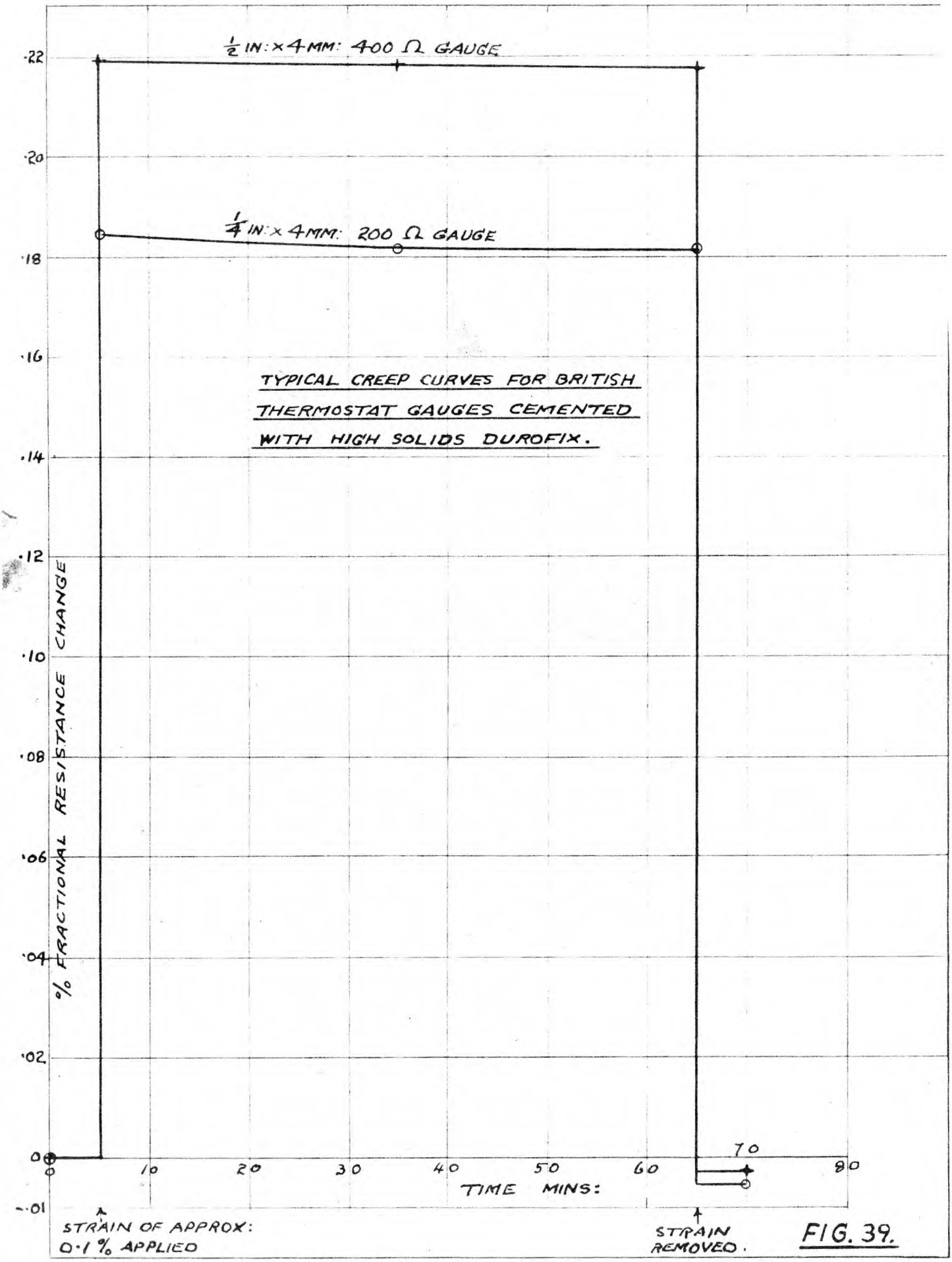
½ IN: x 4MM: 400 Ω GAUGE
¼ IN: x 4MM: 200 Ω GAUGE
TYPICAL CREEP CURVES FOR BRITISH THERMOSTAT GAUGES CEMENTED WITH HIGH SOLIDS DUROFIX.
% FRACTIONAL RESISTANCE CHANGE
·22
·20
·18
·16
·14
·12
·10
·08
·06
·04
·02
0
-·01
0
10
20
30
40
50
60
70
80
TIME MINS:
STRAIN OF APPROX: 0·1 % APPLIED
STRAIN REMOVED.

FIG. 39.

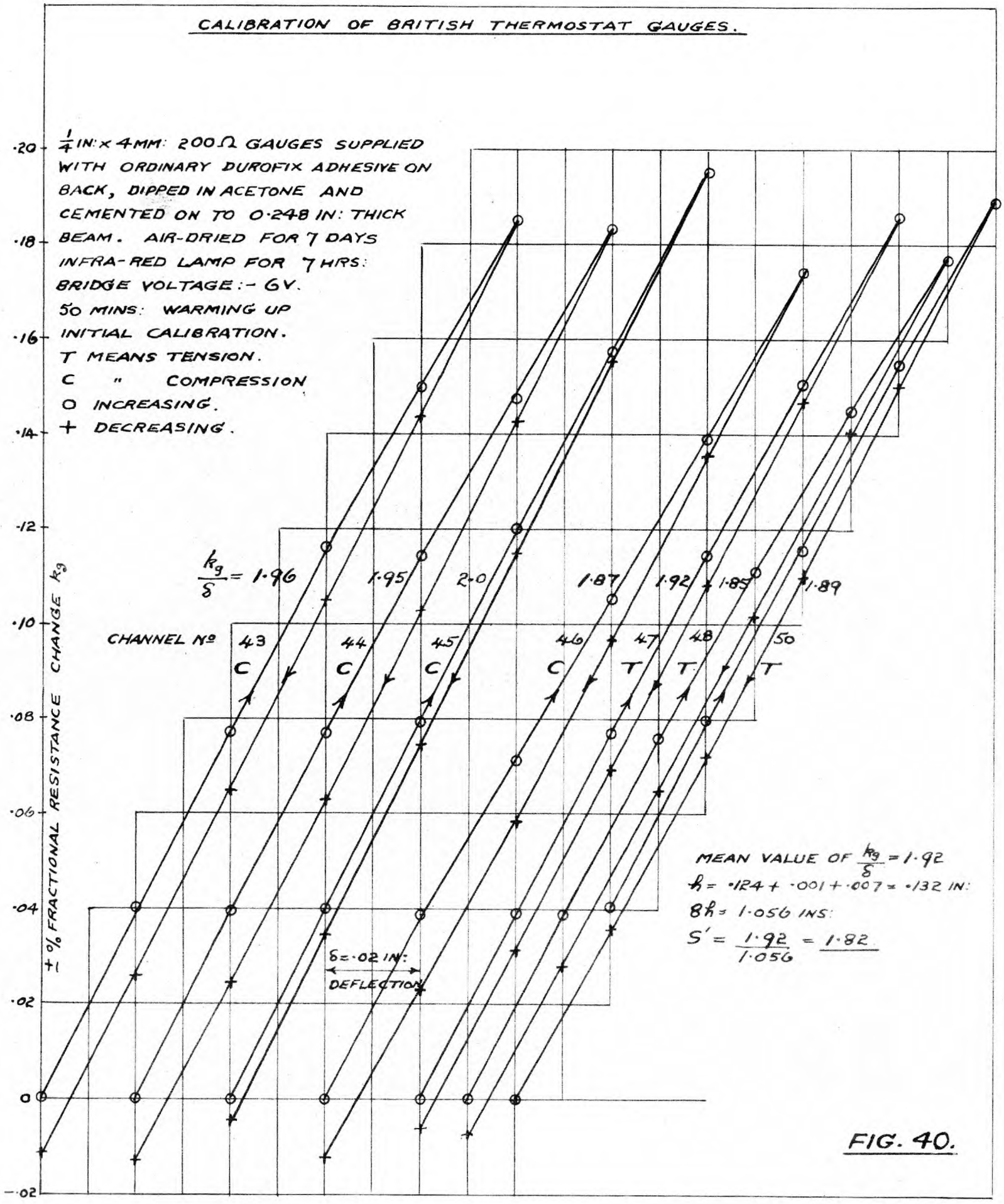
CALIBRATION OF BRITISH THERMOSTAT GAUGES.
1/4 IN: x 4MM: 200Ω GAUGES SUPPLIED WITH ORDINARY DUROFIX ADHESIVE ON BACK, DIPPED IN ACETONE AND CEMENTED ON TO 0·248 IN: THICK BEAM. AIR-DRIED FOR 7 DAYS INFRA-RED LAMP FOR 7 HRS: BRIDGE VOLTAGE:- 6V. 50 MINS: WARMING UP INITIAL CALIBRATION.
T MEANS TENSION.
C " COMPRESSION
O INCREASING.
+ DECREASING.
± % FRACTIONAL RESISTANCE CHANGE kg
·20
·18
·16
·14
·12
·10
·08
·06
·04
·02
0
-·02
kg/δ = 1·96 1·95 2·0 1·87 1·92 1·85 1·89
CHANNEL Nº 43 44 45 46 47 48 50
C C C C T T T
δ=·02 IN: DEFLECTION
MEAN VALUE OF kg/δ = 1·92
h = ·124 + ·001 + ·007 = ·132 IN:
8h = 1·056 INS:
S' = 1·92/1·056 = 1·82

FIG. 40.

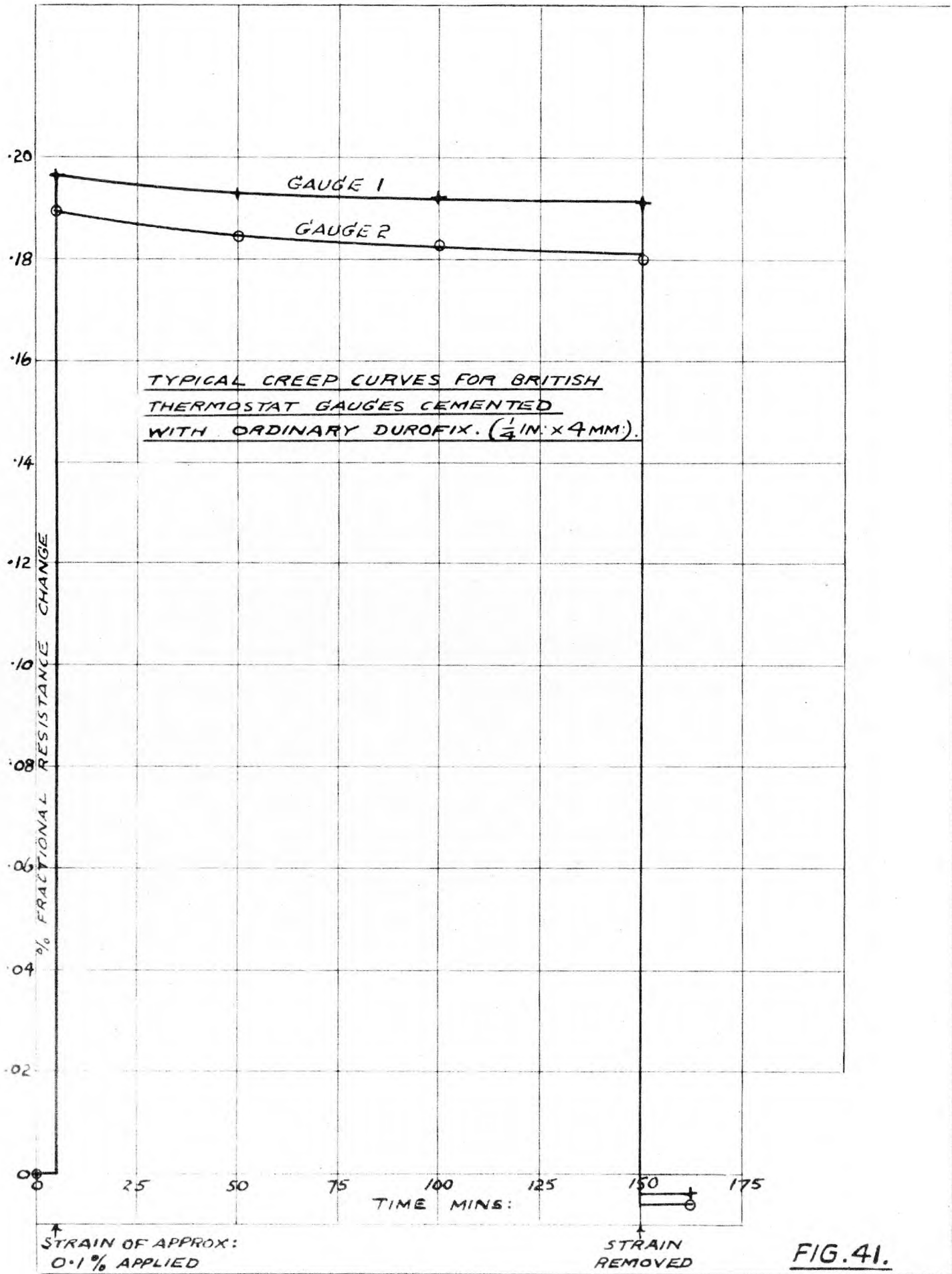
·20
·18
·16
·14
·12
·10
·08
·06
·04
·02
0
GAUGE 1
GAUGE 2
TYPICAL CREEP CURVES FOR BRITISH THERMOSTAT GAUGES CEMENTED WITH ORDINARY DUROFIX. (1/4 IN. x 4 MM.).
% FRACTIONAL RESISTANCE CHANGE
0
25
50
75
100
125
150
175
TIME MINS:
STRAIN OF APPROX: 0·1 % APPLIED
STRAIN REMOVED

FIG. 41.

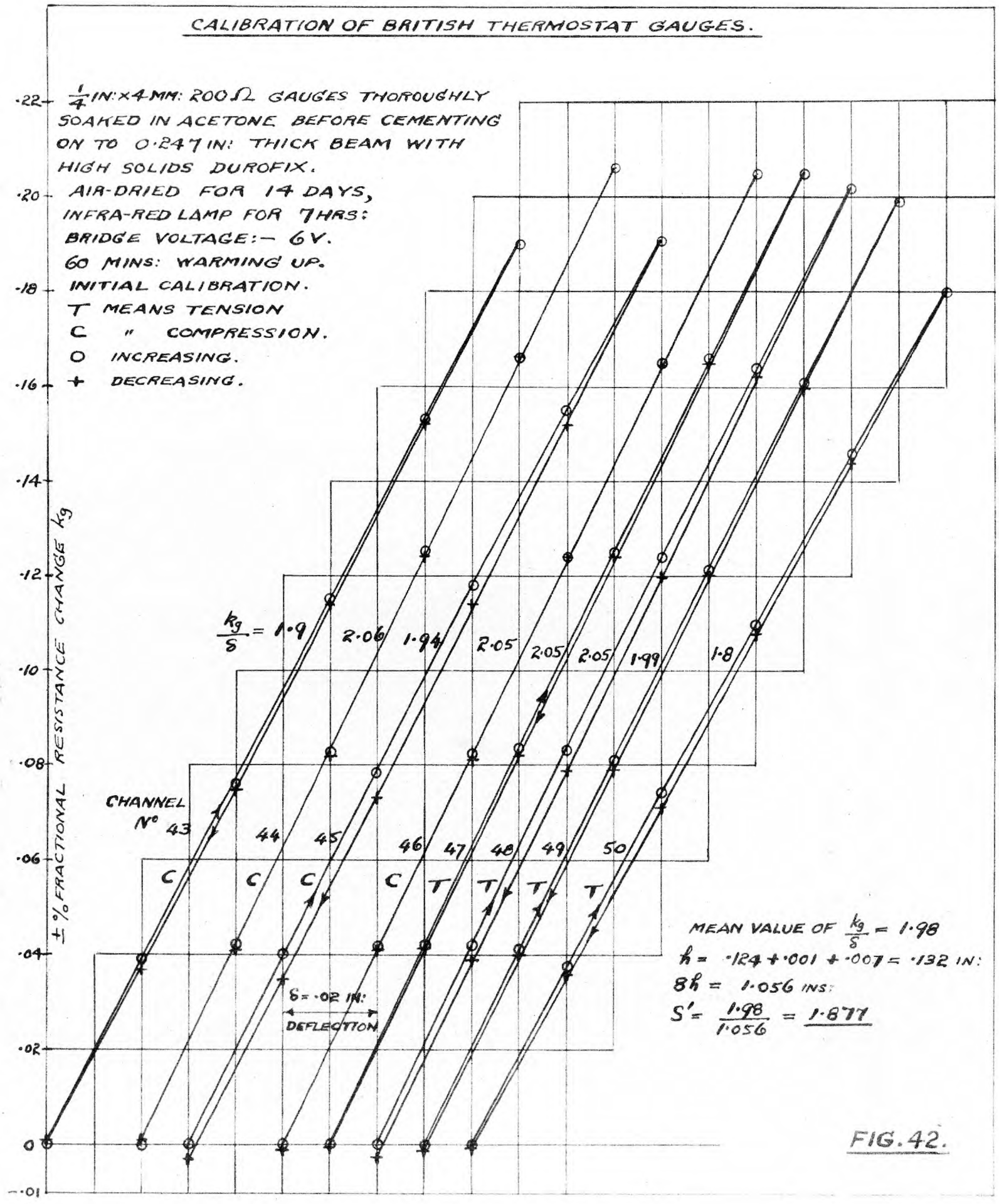
CALIBRATION OF BRITISH THERMOSTAT GAUGES.
1/4 IN: x 4 MM: 200 Ω GAUGES THOROUGHLY SOAKED IN ACETONE BEFORE CEMENTING ON TO 0·247 IN: THICK BEAM WITH HIGH SOLIDS DUROFIX.
AIR-DRIED FOR 14 DAYS, INFRA-RED LAMP FOR 7 HRS:
BRIDGE VOLTAGE:— 6V.
60 MINS: WARMING UP.
INITIAL CALIBRATION.
T MEANS TENSION
C " COMPRESSION.
O INCREASING.
+ DECREASING.
± % FRACTIONAL RESISTANCE CHANGE kg
·22
·20
·18
·16
·14
·12
·10
·08
·06
·04
·02
0
-·01
kg/δ = 1·9 2·06 1·94 2·05 2·05 2·05 1·99 1·8
CHANNEL N° 43 44 45 46 47 48 49 50
C C C C T T T T
δ = ·02 IN:
DEFLECTION
MEAN VALUE OF kg/δ = 1·98
h = ·124 + ·001 + ·007 = ·132 IN:
8h = 1·056 INS:
S' = 1·98/1·056 = 1·877

FIG. 42.

CALIBRATION OF BRITISH THERMOSTAT GAUGES.

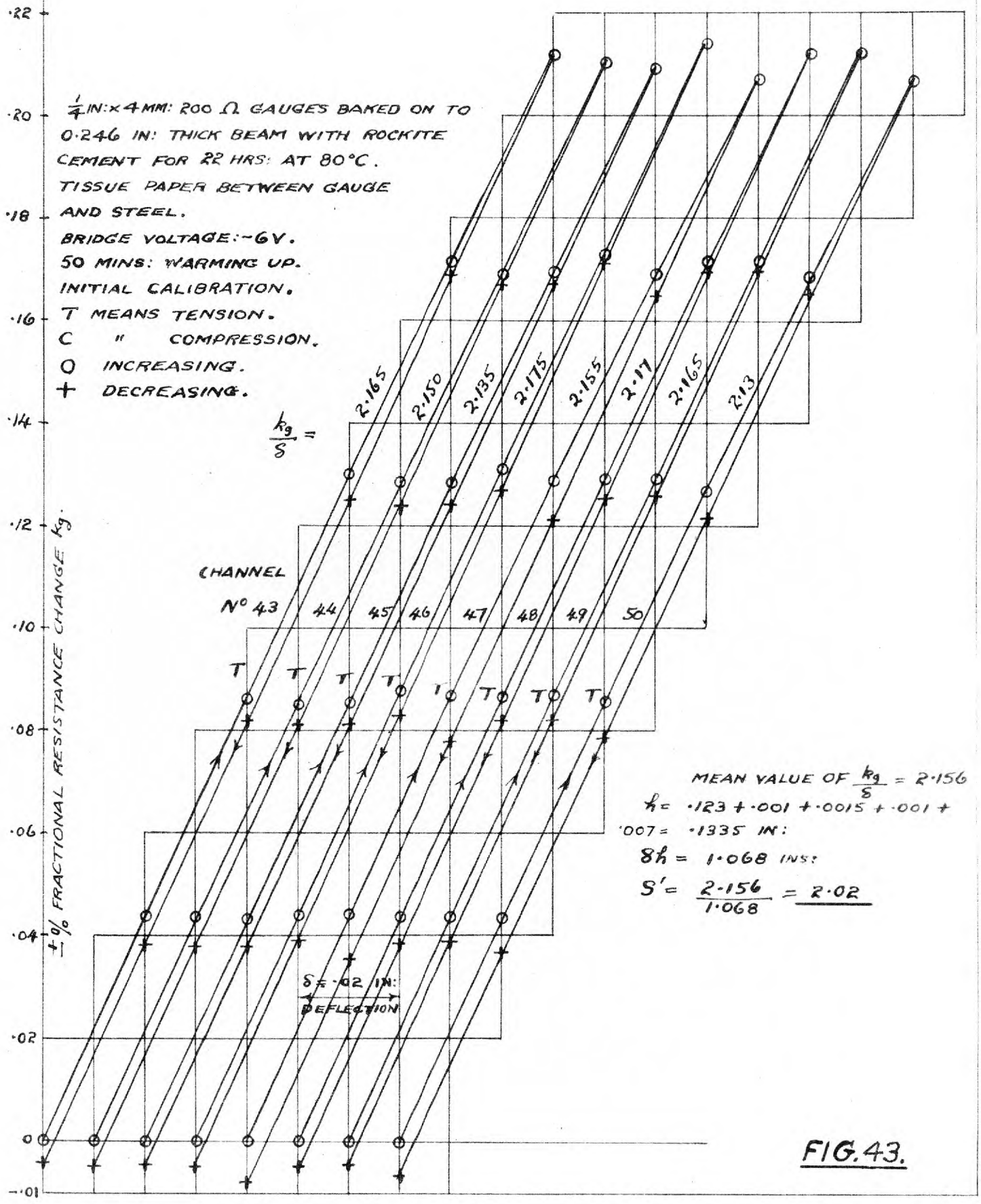

FIG. 43.

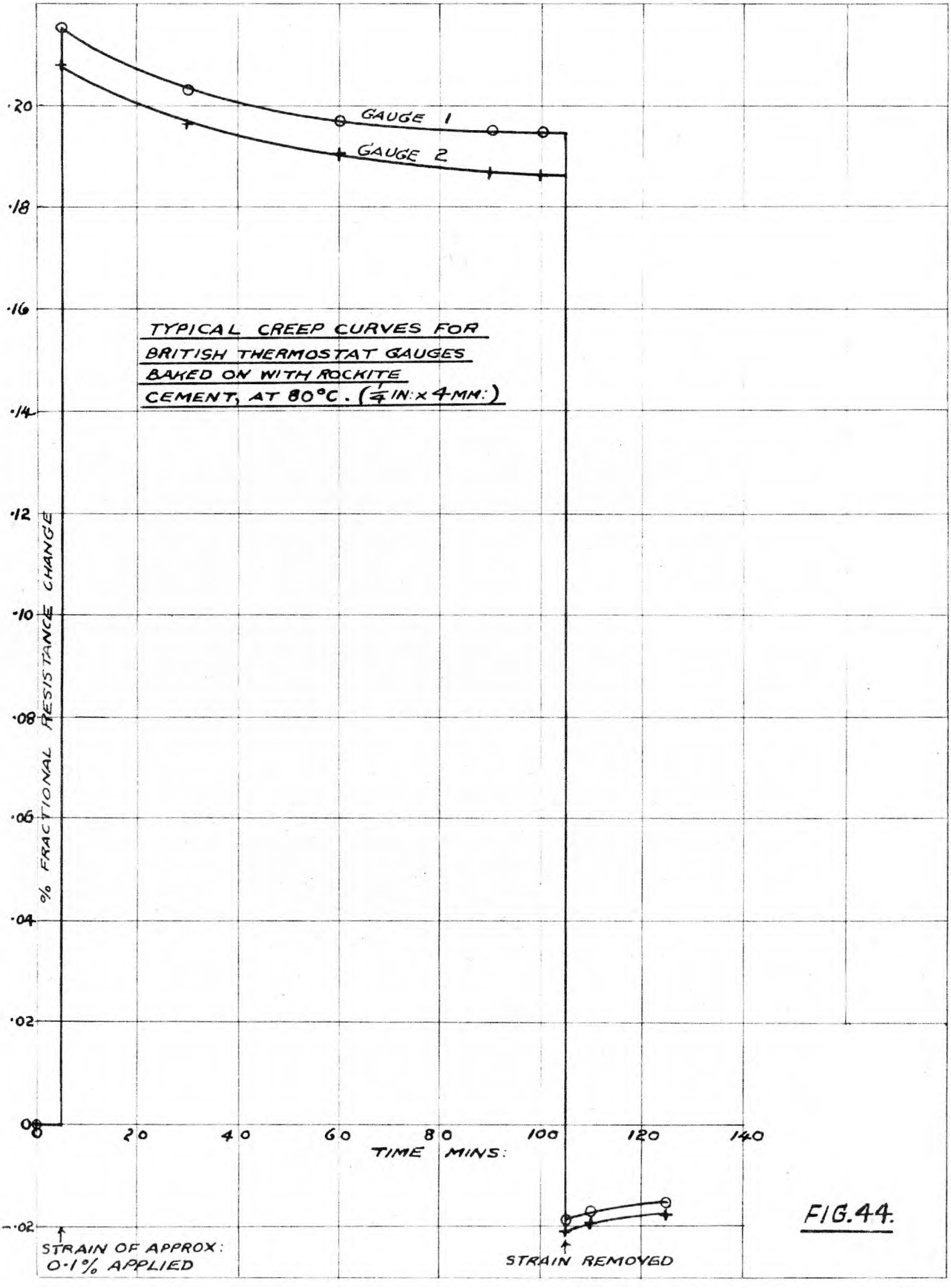
·20
·18
·16
·14
·12
·10
·08
·06
·04
·02
0
-·02
% FRACTIONAL RESISTANCE CHANGE
GAUGE 1
GAUGE 2
TYPICAL CREEP CURVES FOR BRITISH THERMOSTAT GAUGES BAKED ON WITH ROCKITE CEMENT, AT 80°C. (¼ IN. x 4 MM.)
0
20
40
60
80
100
120
140
TIME MINS.
STRAIN OF APPROX: 0·1% APPLIED
STRAIN REMOVED

FIG.44.

CALIBRATION OF BRITISH THERMOSTAT GAUGES.

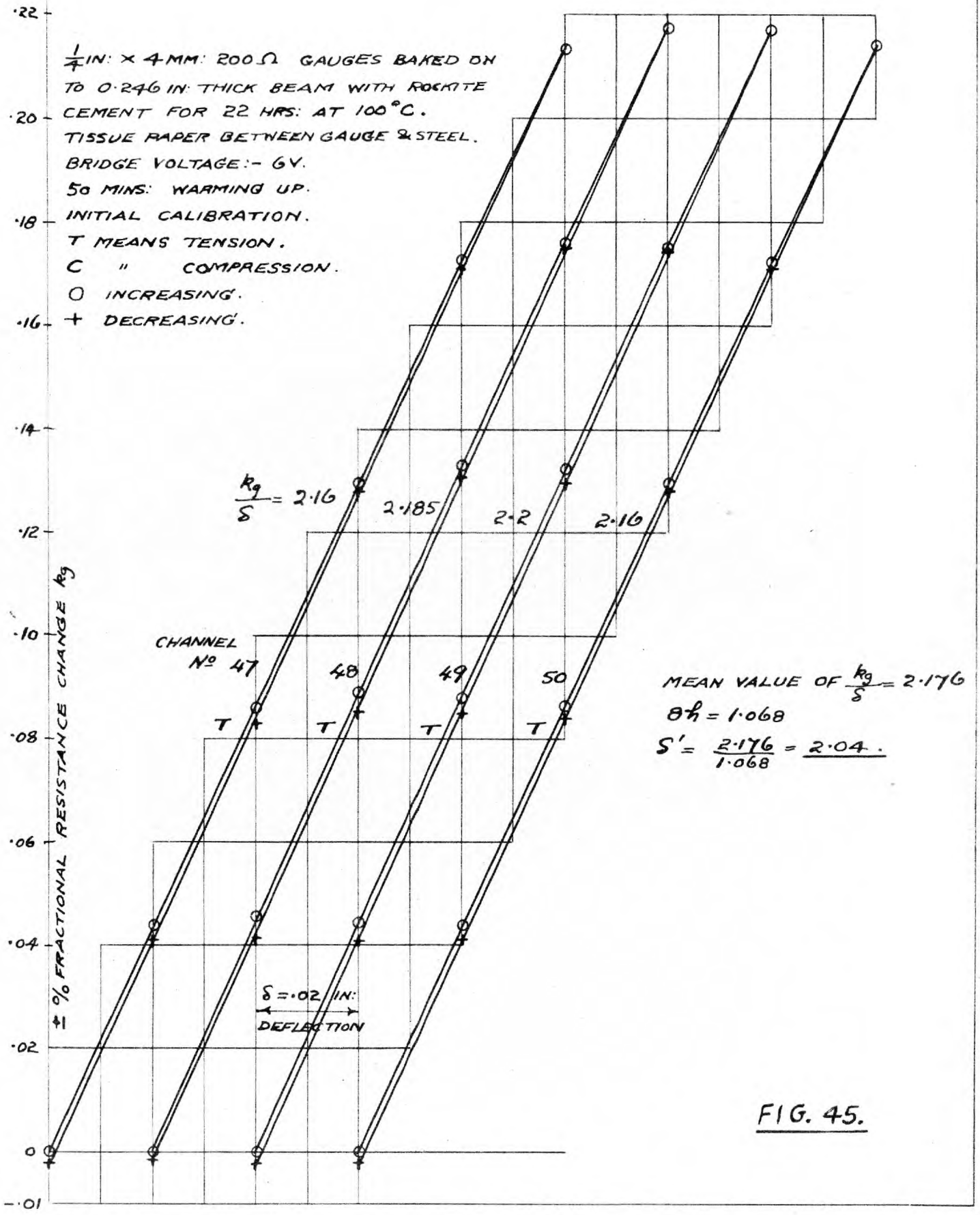

FIG. 45.

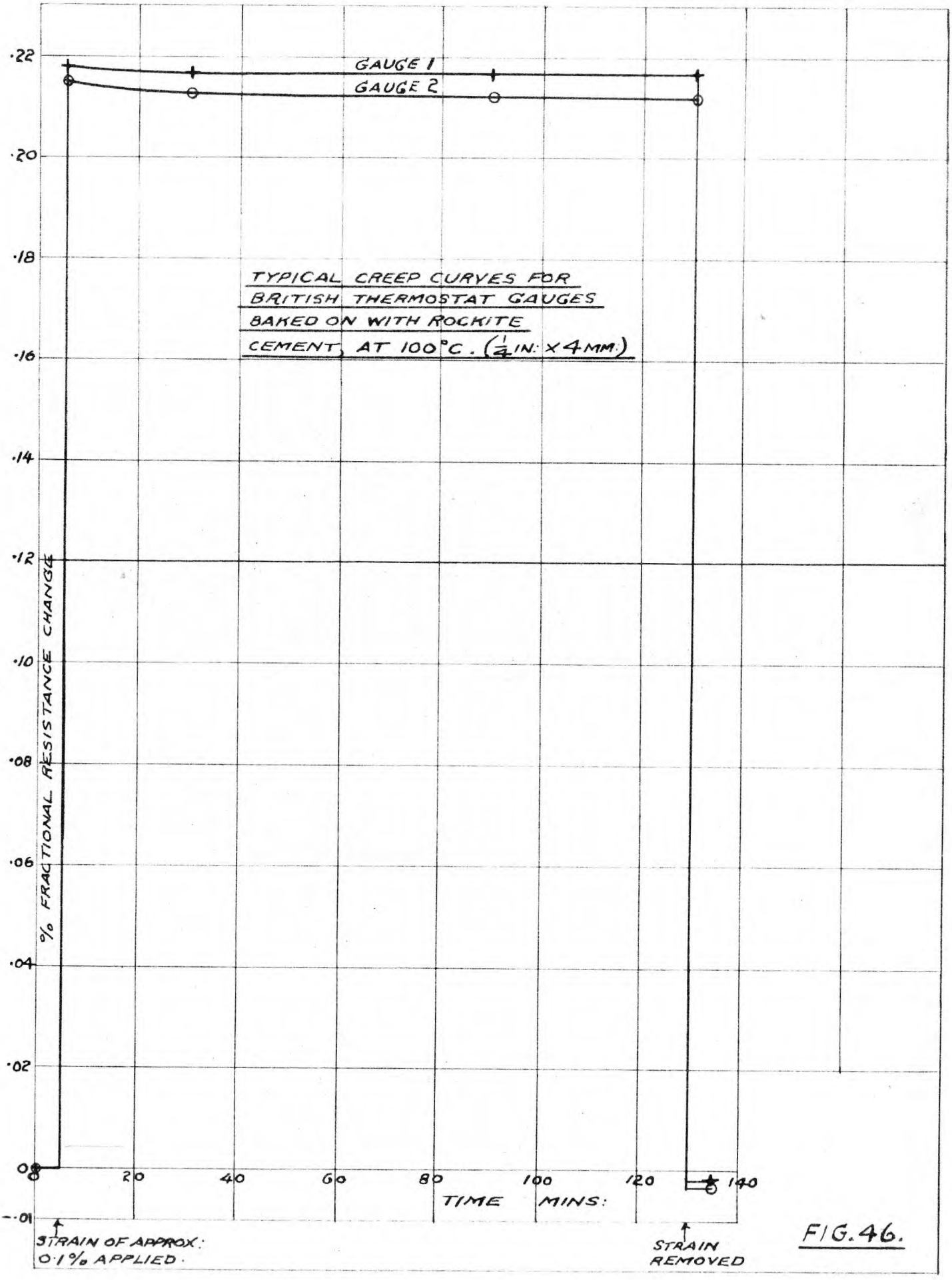
GAUGE 1
GAUGE 2
TYPICAL CREEP CURVES FOR BRITISH THERMOSTAT GAUGES BAKED ON WITH ROCKITE CEMENT, AT 100°C. (1/4 IN. x 4 MM.)
% FRACTIONAL RESISTANCE CHANGE
·22
·20
·18
·16
·14
·12
·10
·08
·06
·04
·02
0
-·01
20
40
60
80
100
120
140
TIME MINS.
STRAIN OF APPROX. 0·1% APPLIED.
STRAIN REMOVED

FIG. 46.

CALIBRATION OF BRITISH THERMOSTAT GAUGES.

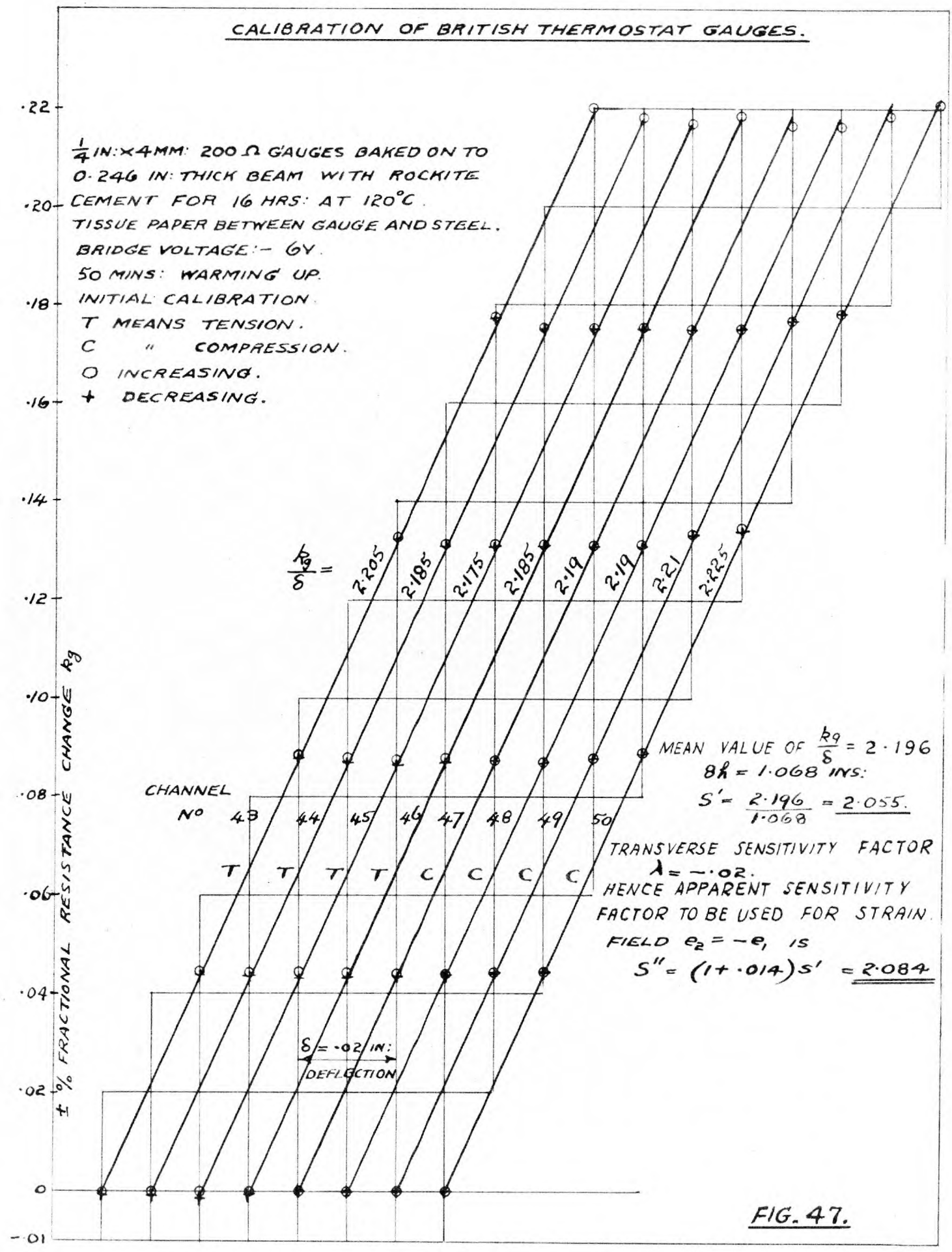

FIG. 47.

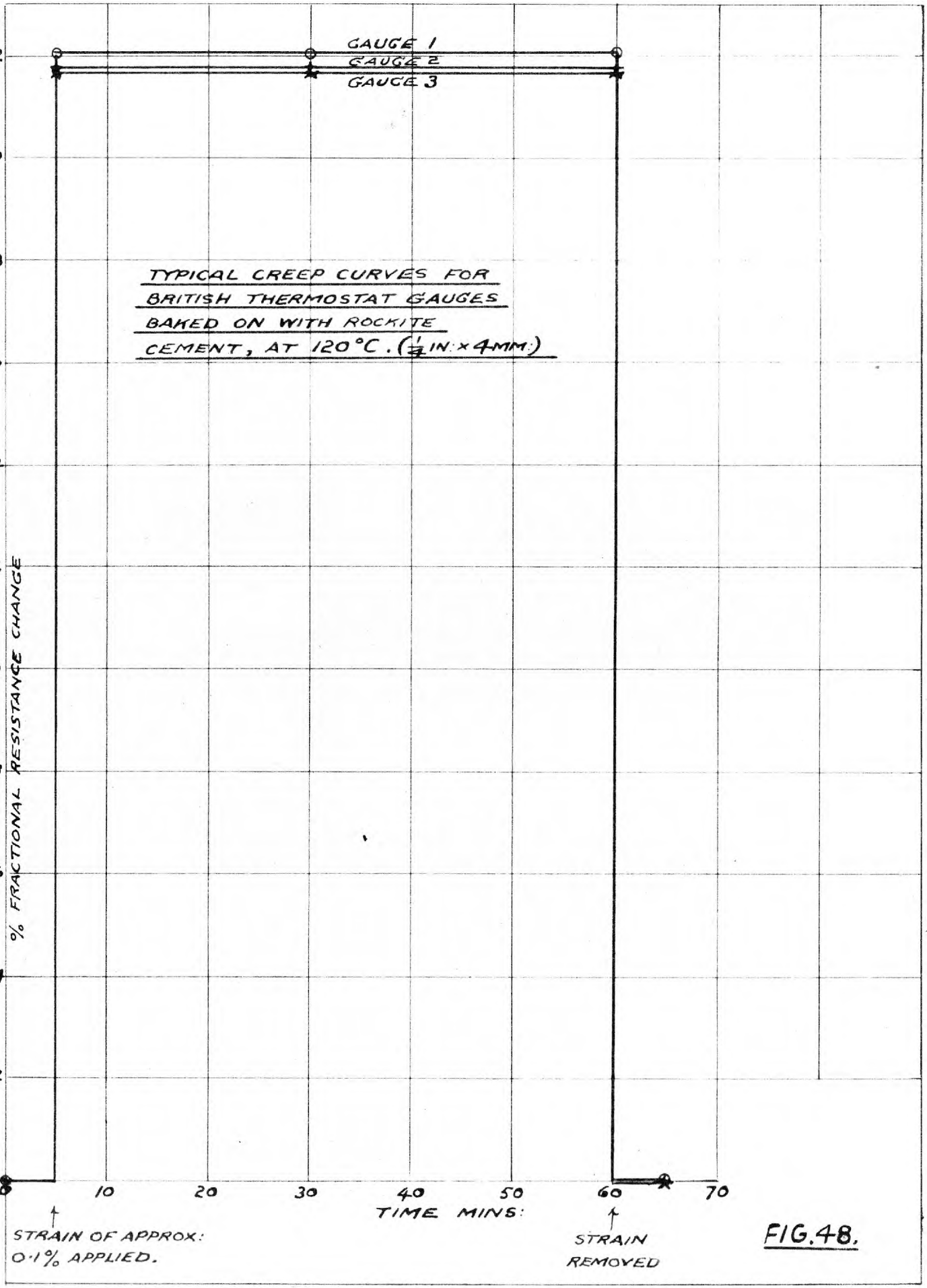
GAUGE 1
GAUGE 2
GAUGE 3
TYPICAL CREEP CURVES FOR BRITISH THERMOSTAT GAUGES BAKED ON WITH ROCKITE CEMENT, AT 120°C. (1/4 IN. x 4MM.)
·22
·20
·18
·16
·14
·12
·10
·08
·06
·04
·02
0
% FRACTIONAL RESISTANCE CHANGE
0
10
20
30
40
50
60
70
TIME MINS.
STRAIN OF APPROX: 0·1% APPLIED.
STRAIN REMOVED

FIG.48.

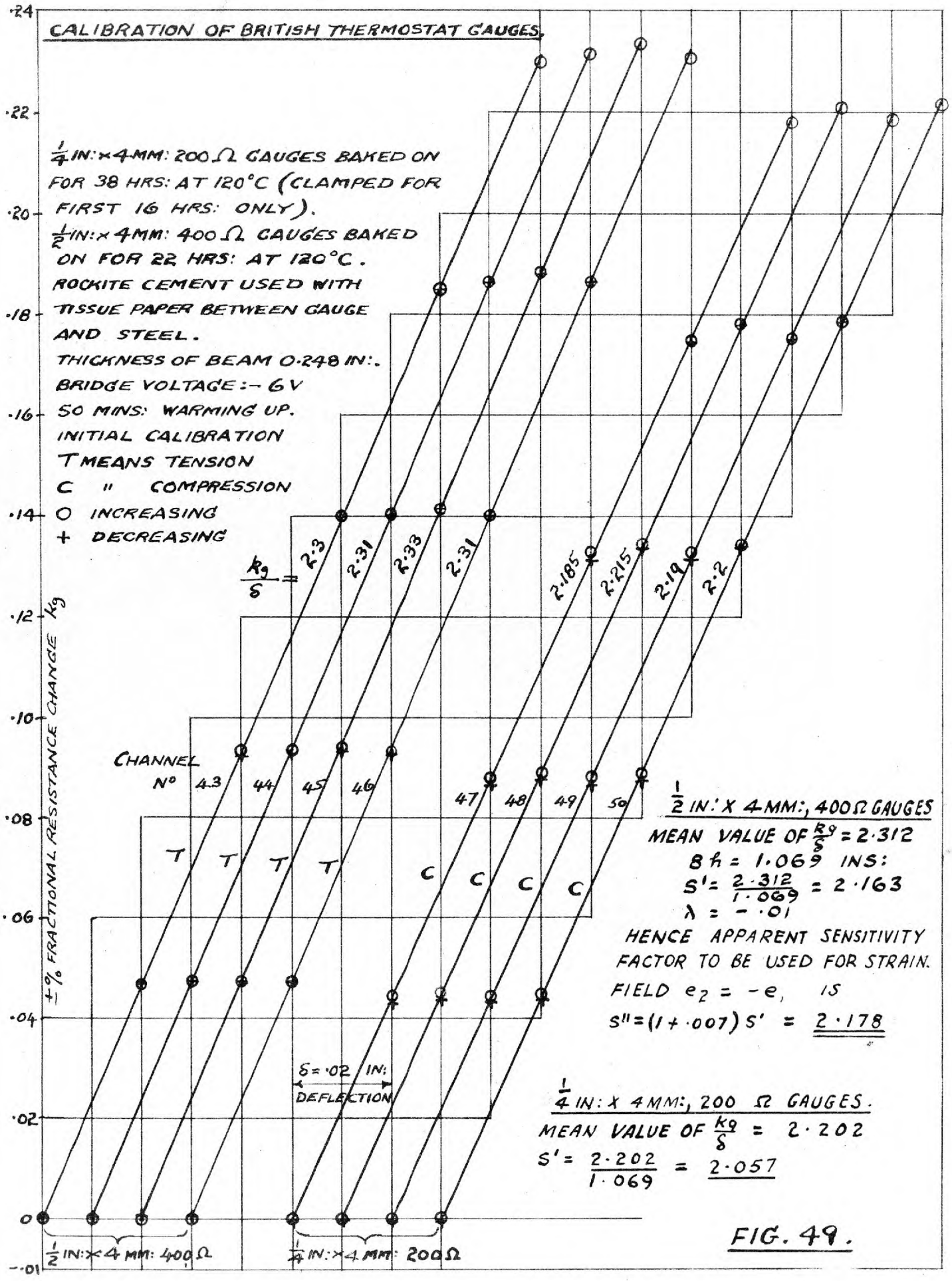
CALIBRATION OF BRITISH THERMOSTAT GAUGES.
¼ IN: × 4 MM: 200 Ω GAUGES BAKED ON FOR 38 HRS: AT 120°C (CLAMPED FOR FIRST 16 HRS: ONLY).
½ IN: × 4 MM: 400 Ω GAUGES BAKED ON FOR 22 HRS: AT 120°C.
ROCKITE CEMENT USED WITH TISSUE PAPER BETWEEN GAUGE AND STEEL.
THICKNESS OF BEAM 0·248 IN:.
BRIDGE VOLTAGE:- 6 V
50 MINS: WARMING UP.
INITIAL CALIBRATION
T MEANS TENSION
C " COMPRESSION
O INCREASING
+ DECREASING
$\frac{k_g}{\delta}$ = 2·3 2·31 2·33 2·31 2·185 2·215 2·19 2·2
CHANNEL N° 43 44 45 46 47 48 49 50
T T T T C C C C
± % FRACTIONAL RESISTANCE CHANGE k_g
·24 ·22 ·20 ·18 ·16 ·14 ·12 ·10 ·08 ·06 ·04 ·02 0 -·01
δ = ·02 IN: DEFLECTION
½ IN: × 4 MM: 400 Ω
¼ IN: × 4 MM: 200 Ω
½ IN: X 4 MM:, 400 Ω GAUGES
MEAN VALUE OF $\frac{k_g}{\delta}$ = 2·312
8h = 1·069 INS:
S' = $\frac{2·312}{1·069}$ = 2·163
λ = - ·01
HENCE APPARENT SENSITIVITY FACTOR TO BE USED FOR STRAIN. FIELD $e_2 = -e_1$ IS
S'' = (1 + ·007) S' = 2·178
¼ IN: X 4 MM:, 200 Ω GAUGES.
MEAN VALUE OF $\frac{k_g}{\delta}$ = 2·202
S' = $\frac{2·202}{1·069}$ = 2·057

FIG. 49.

CALIBRATION OF TINSLEY GAUGES.

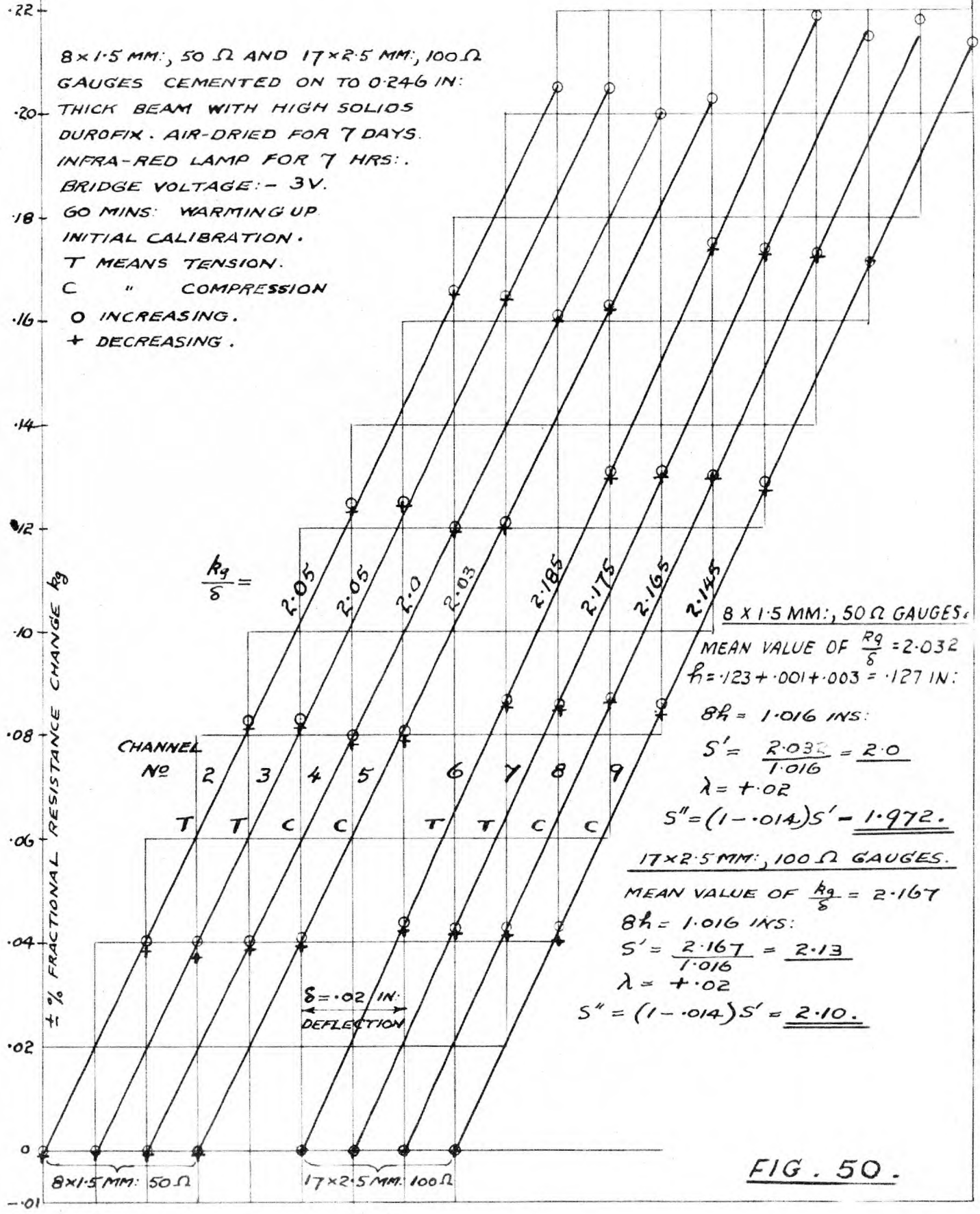

8 X 1·5 MM:, 50 Ω GAUGES.

MEAN VALUE OF $\frac{Rg}{\delta}$ = 2·032

h = ·123 + ·001 + ·003 = ·127 IN:

$8h$ = 1·016 INS:

$S' = \frac{2·032}{1·016} = \underline{2·0}$

λ = +·02

$S'' = (1 - ·014)S' = \underline{1·972.}$

17×2·5 MM:, 100 Ω GAUGES.

MEAN VALUE OF $\frac{kg}{\delta}$ = 2·167

$8h$ = 1·016 INS:

$S' = \frac{2·167}{1·016} = \underline{2·13}$

λ = +·02

$S'' = (1 - ·014)S' = \underline{2·10.}$

FIG. 50.

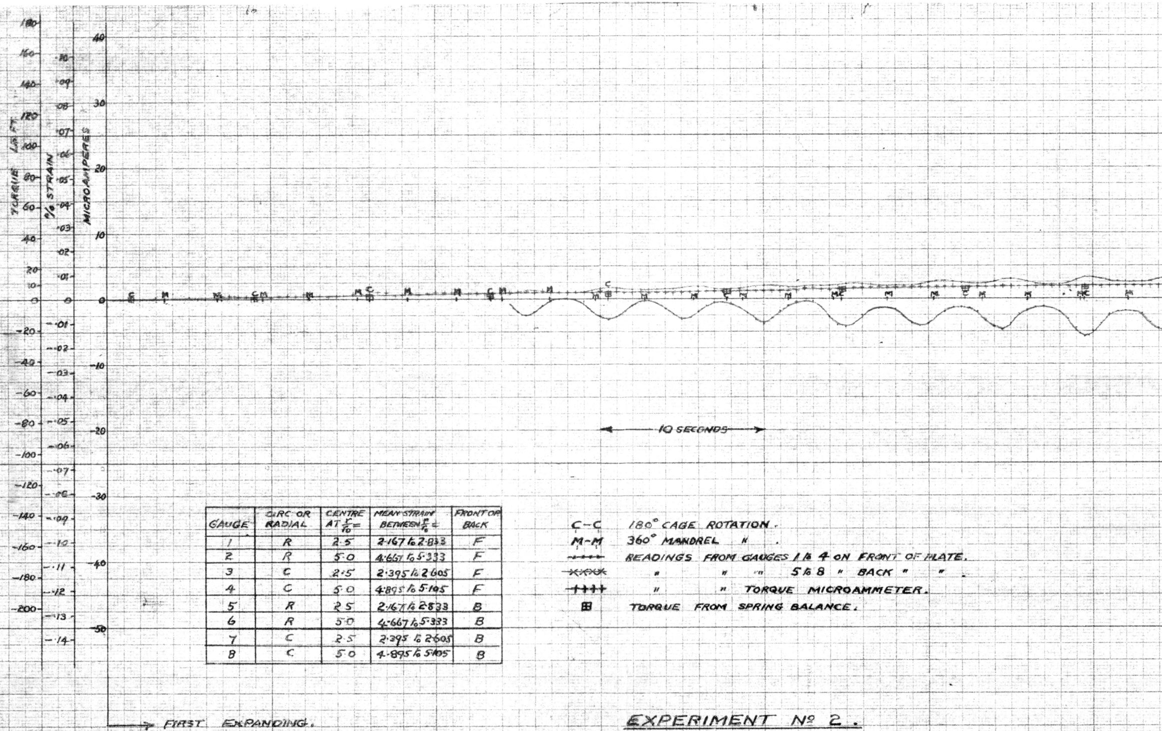

GAUGE	CIRC OR RADIAL	CENTRE AT $\frac{r}{r_0}$=	MEAN STRAIN BETWEEN $\frac{r}{r_0}$ =	FRONT OR BACK
1	R	2·5	2·167 to 2·833	F
2	R	5·0	4·667 to 5·333	F
3	C	2·5	2·395 to 2·605	F
4	C	5·0	4·895 to 5·105	F
5	R	2·5	2·167 to 2·833	B
6	R	5·0	4·667 to 5·333	B
7	C	2·5	2·395 to 2·605	B
B	C	5·0	4·895 to 5·105	B

C–C 180° CAGE ROTATION.
M–M 360° MANDREL " .
–•–•–•– READINGS FROM GAUGES 1 to 4 ON FRONT OF PLATE.
–×–×–×– " " " 5 to 8 " BACK " " .
–+–+–+– " " TORQUE MICROAMMETER.
⊞ TORQUE FROM SPRING BALANCE.

EXPERIMENT Nº 2.

FIG. 51.

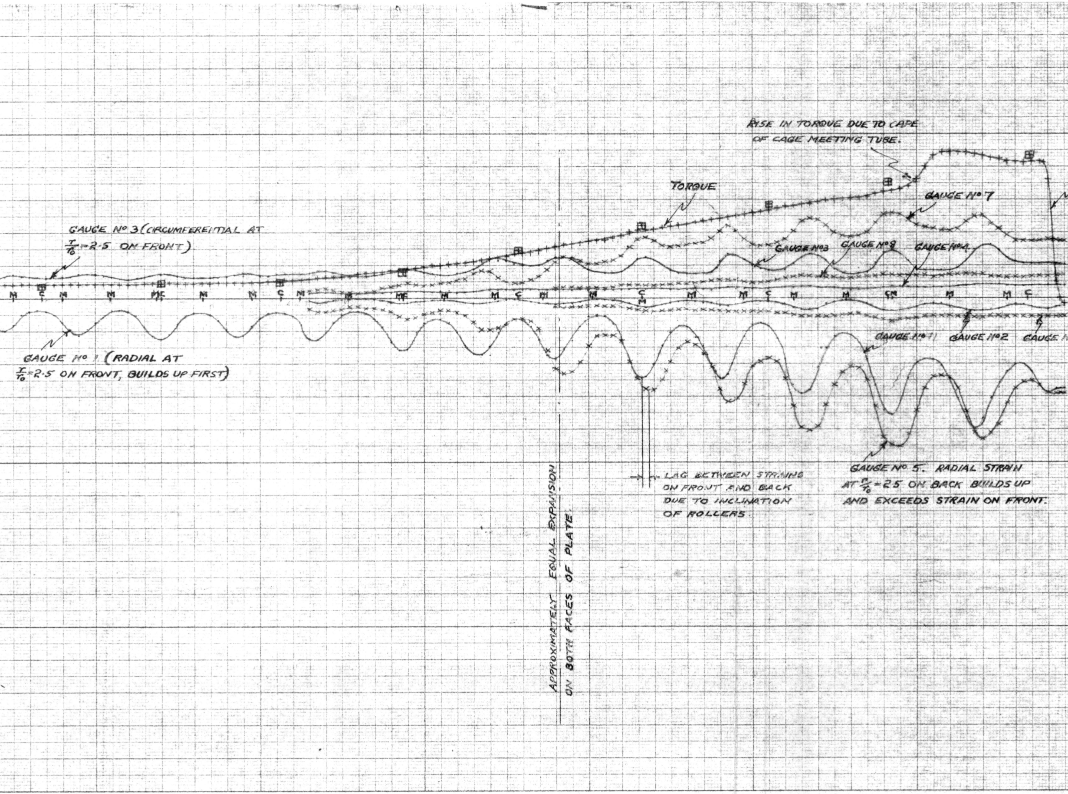

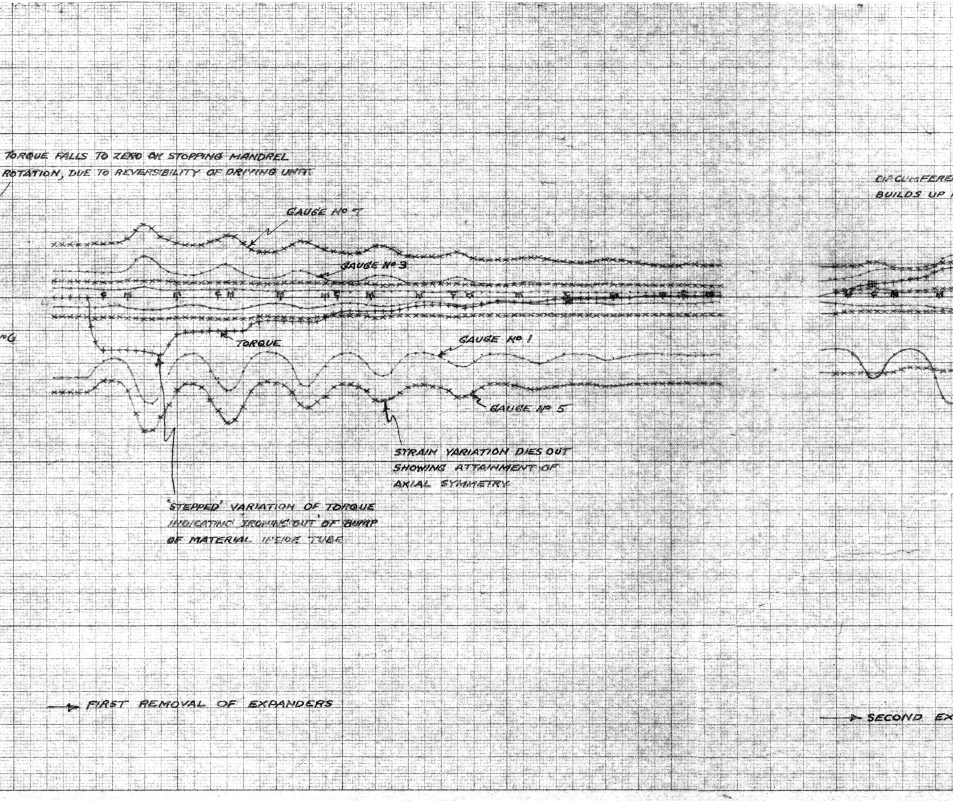

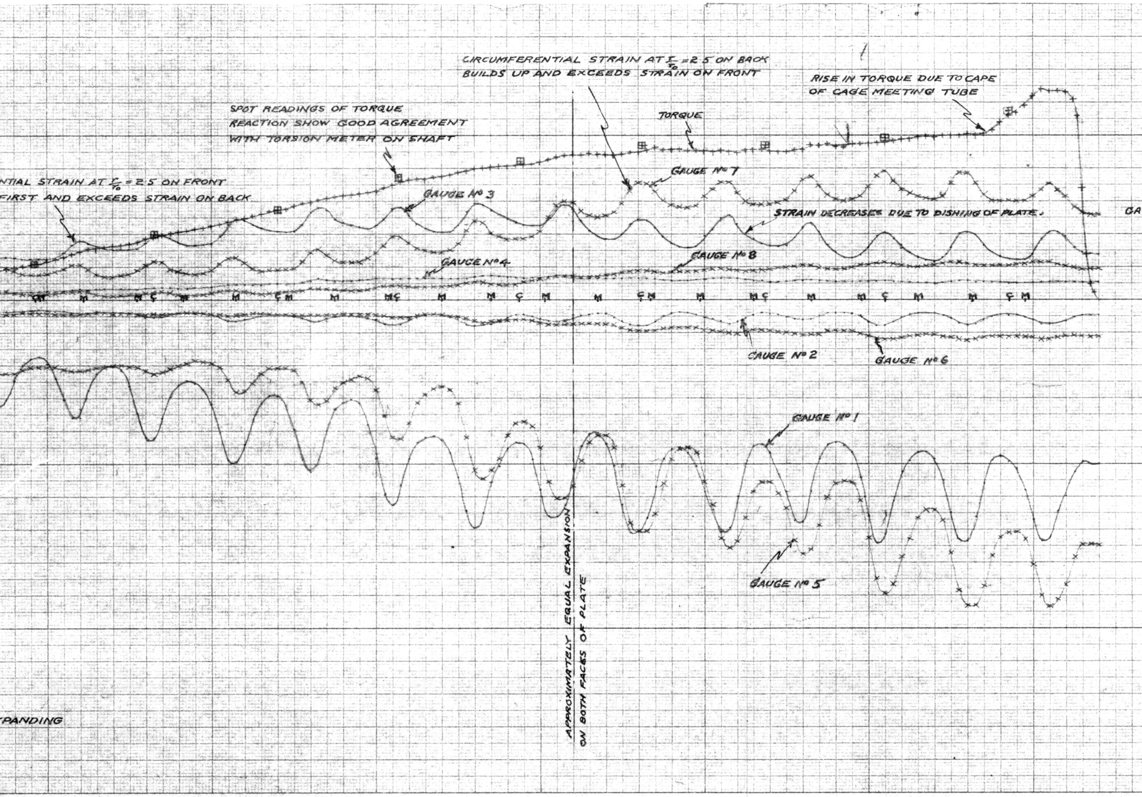

→ SECOND REMOVAL OF EXPANDERS

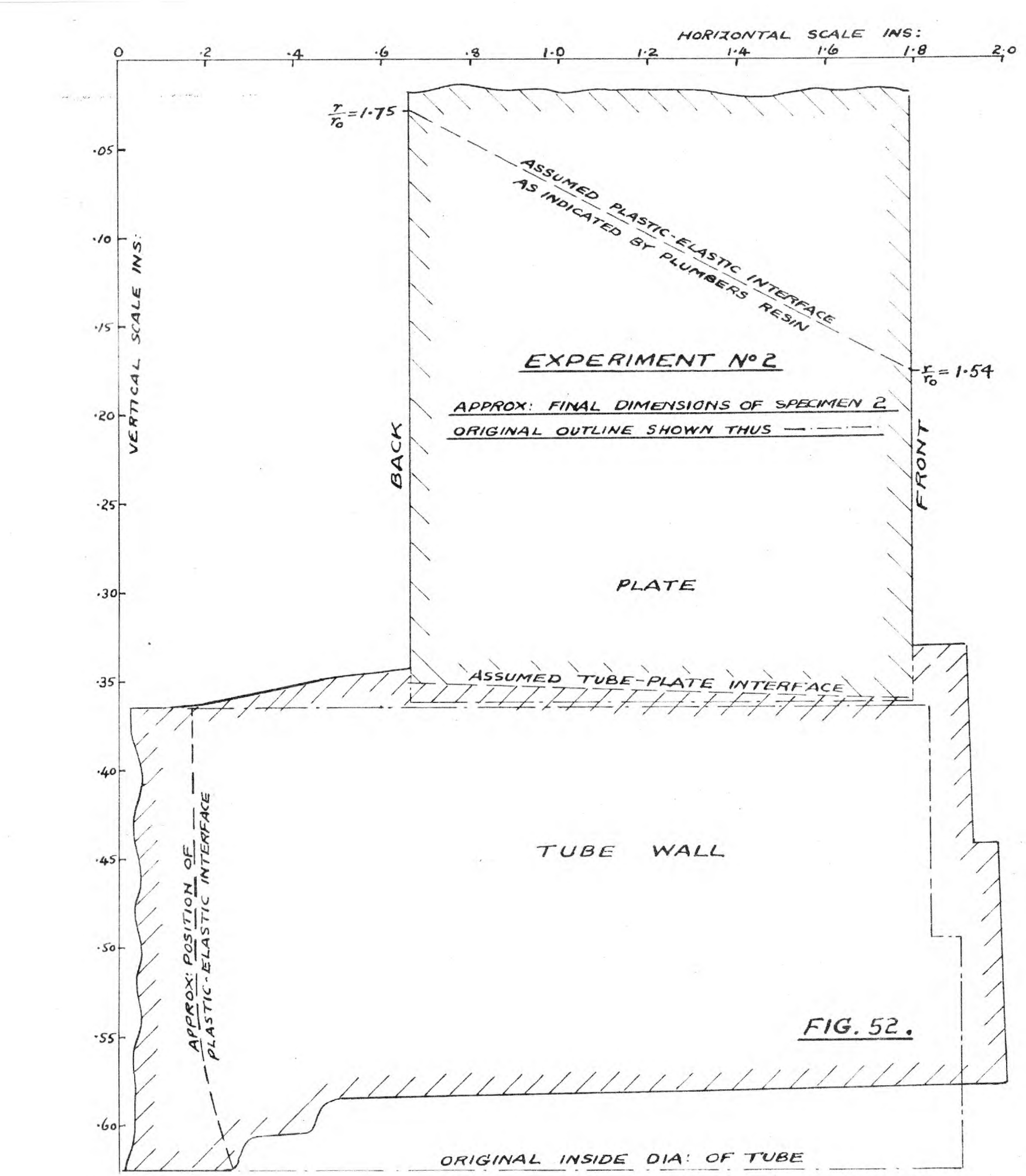
HORIZONTAL SCALE INS:
0
·2
·4
·6
·8
1·0
1·2
1·4
1·6
1·8
2·0
VERTICAL SCALE INS:
·05
·10
·15
·20
·25
·30
·35
·40
·45
·50
·55
·60
r/r0 = 1·75
ASSUMED PLASTIC-ELASTIC INTERFACE AS INDICATED BY PLUMBERS RESIN
r/r0 = 1·54
EXPERIMENT Nº 2
APPROX: FINAL DIMENSIONS OF SPECIMEN 2
ORIGINAL OUTLINE SHOWN THUS
BACK
FRONT
PLATE
ASSUMED TUBE-PLATE INTERFACE
TUBE WALL
APPROX: POSITION OF PLASTIC-ELASTIC INTERFACE
ORIGINAL INSIDE DIA: OF TUBE

FIG. 52.

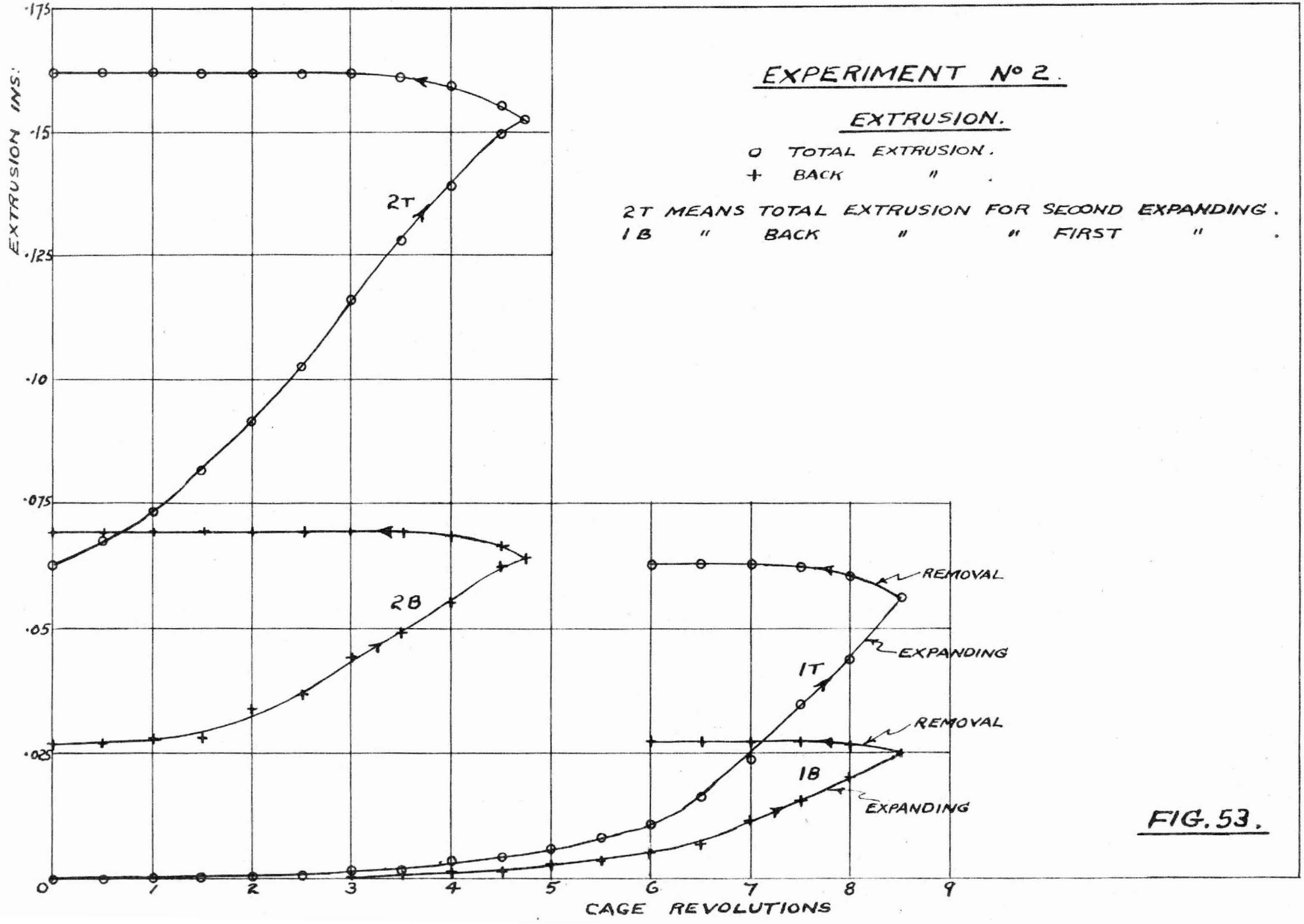
EXPERIMENT Nº 2.
EXTRUSION.
o TOTAL EXTRUSION.
+ BACK " .
2T MEANS TOTAL EXTRUSION FOR SECOND EXPANDING.
1B " BACK " " FIRST " .
EXTRUSION INS.
·175
·15
·125
·10
·075
·05
·025
0
1
2
3
4
5
6
7
8
9
CAGE REVOLUTIONS
2T
2B
1T
1B
REMOVAL
EXPANDING
REMOVAL
EXPANDING

FIG. 53.

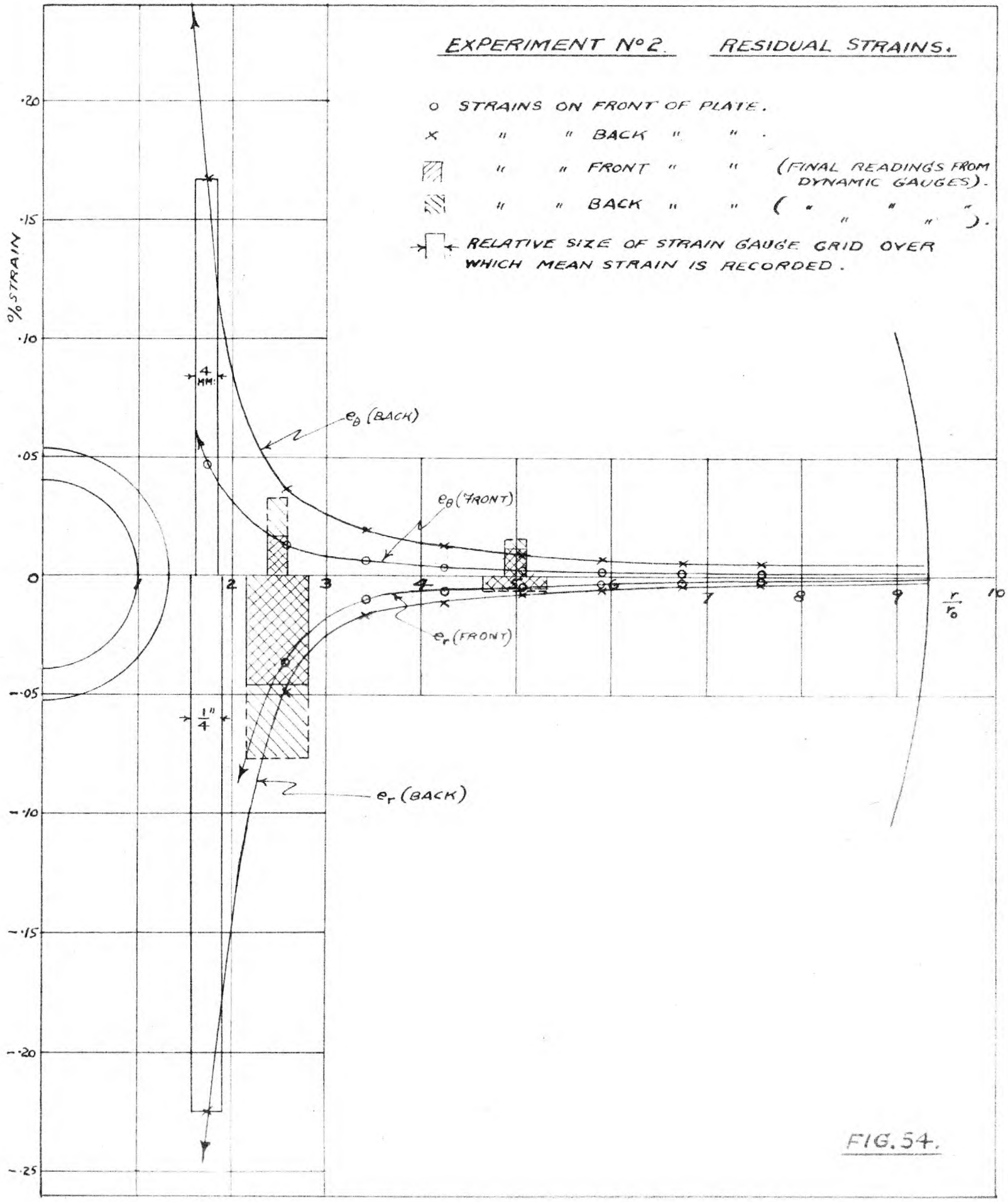
EXPERIMENT Nº 2. RESIDUAL STRAINS.
o STRAINS ON FRONT OF PLATE.
× " " BACK " " .
" " FRONT " " (FINAL READINGS FROM DYNAMIC GAUGES).
" " BACK " " (" " " ").
RELATIVE SIZE OF STRAIN GAUGE GRID OVER WHICH MEAN STRAIN IS RECORDED.
% STRAIN
·20
·15
·10
·05
0
-·05
-·10
-·15
-·20
-·25
4 MM.
1/4"
e_θ (BACK)
e_θ (FRONT)
e_r (FRONT)
e_r (BACK)
1
2
3
4
5
6
7
8
9
10
$\frac{r}{r_0}$

FIG. 54.

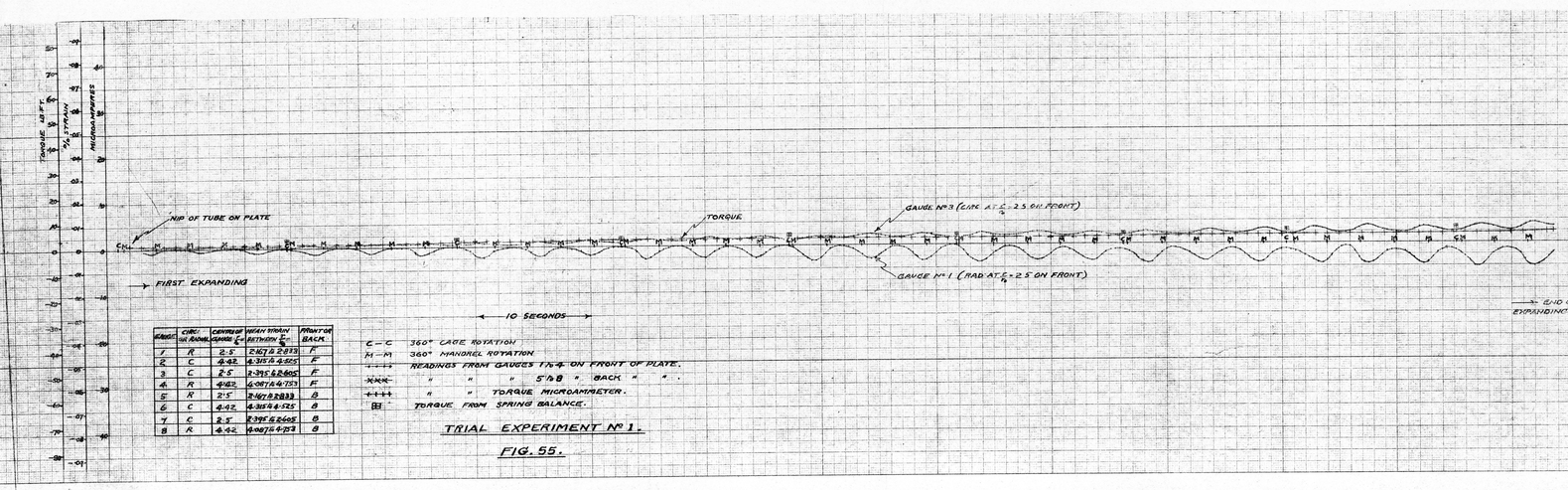

GAUGE	CIRC. OR RADIAL	CENTRE OF GAUGE $\frac{r}{t}$	MEAN STRAIN BETWEEN $\frac{r}{t}$=	FRONT OR BACK
1	R	2.5	2.967 & 2.833	F
2	C	4.42	4.315 & 4.605	F
3	C	2.5	2.315 & 2.605	F
4	R	4.42	4.087 & 4.733	F
5	R	2.5	2.467 & 2.833	B
6	C	4.42	4.315 & 4.525	B
7	C	2.5	2.395 & 2.605	B
8	R	4.42	4.087 & 4.273	B

C–C 360° CAGE ROTATION
M–M 360° MANDREL ROTATION
1 2 3 4 READINGS FROM GAUGES 1 TO 4 ON FRONT OF PLATE.
X X X " " " 5 TO 8 " BACK " " .
+ + + + " " TORQUE MICROAMMETER.
⊞ TORQUE FROM SPRING BALANCE.

TRIAL EXPERIMENT No 1.

FIG. 55.

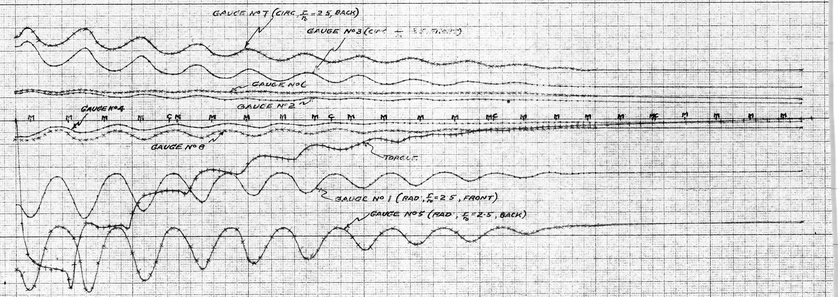

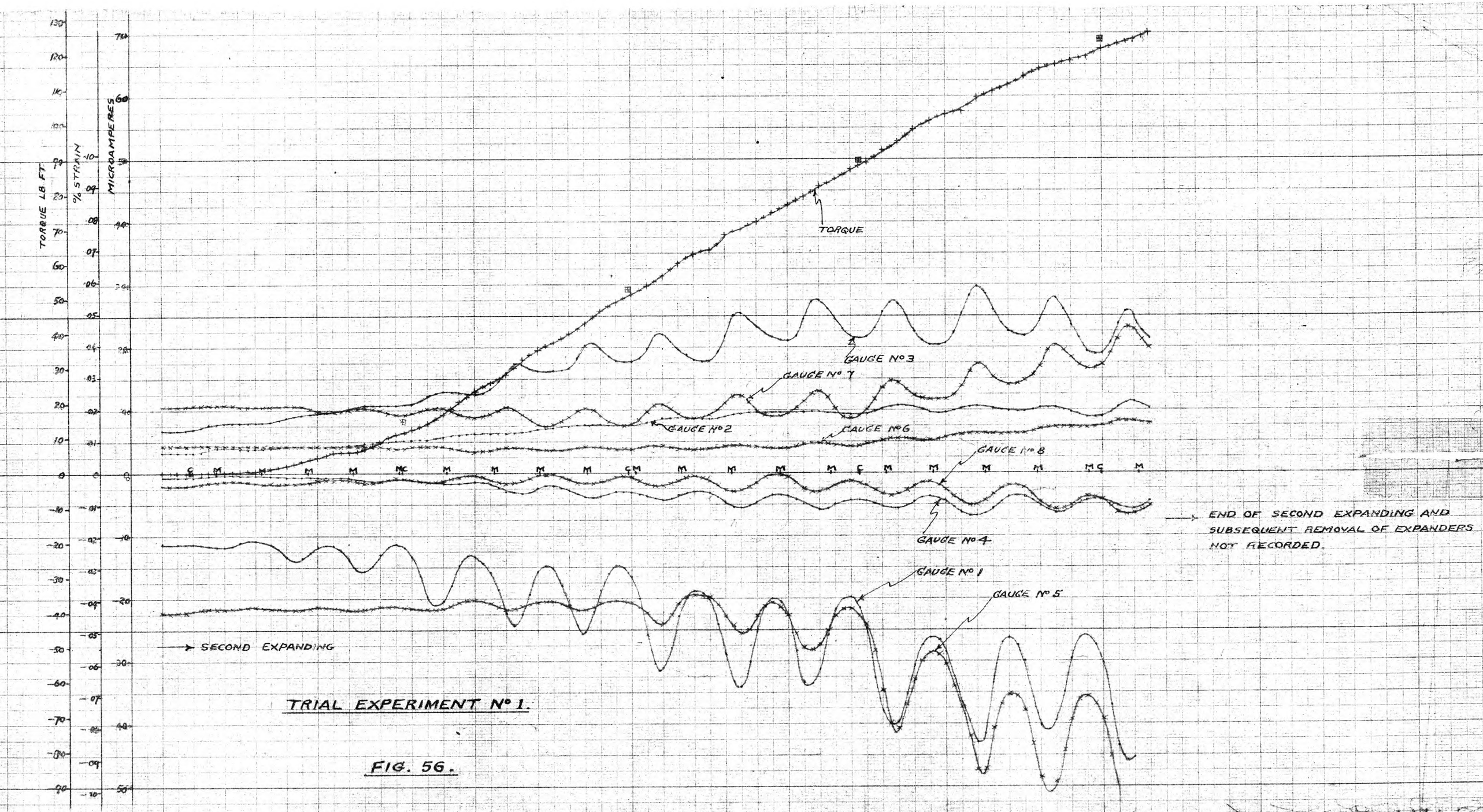

TRIAL EXPERIMENT No 1.

FIG. 56.

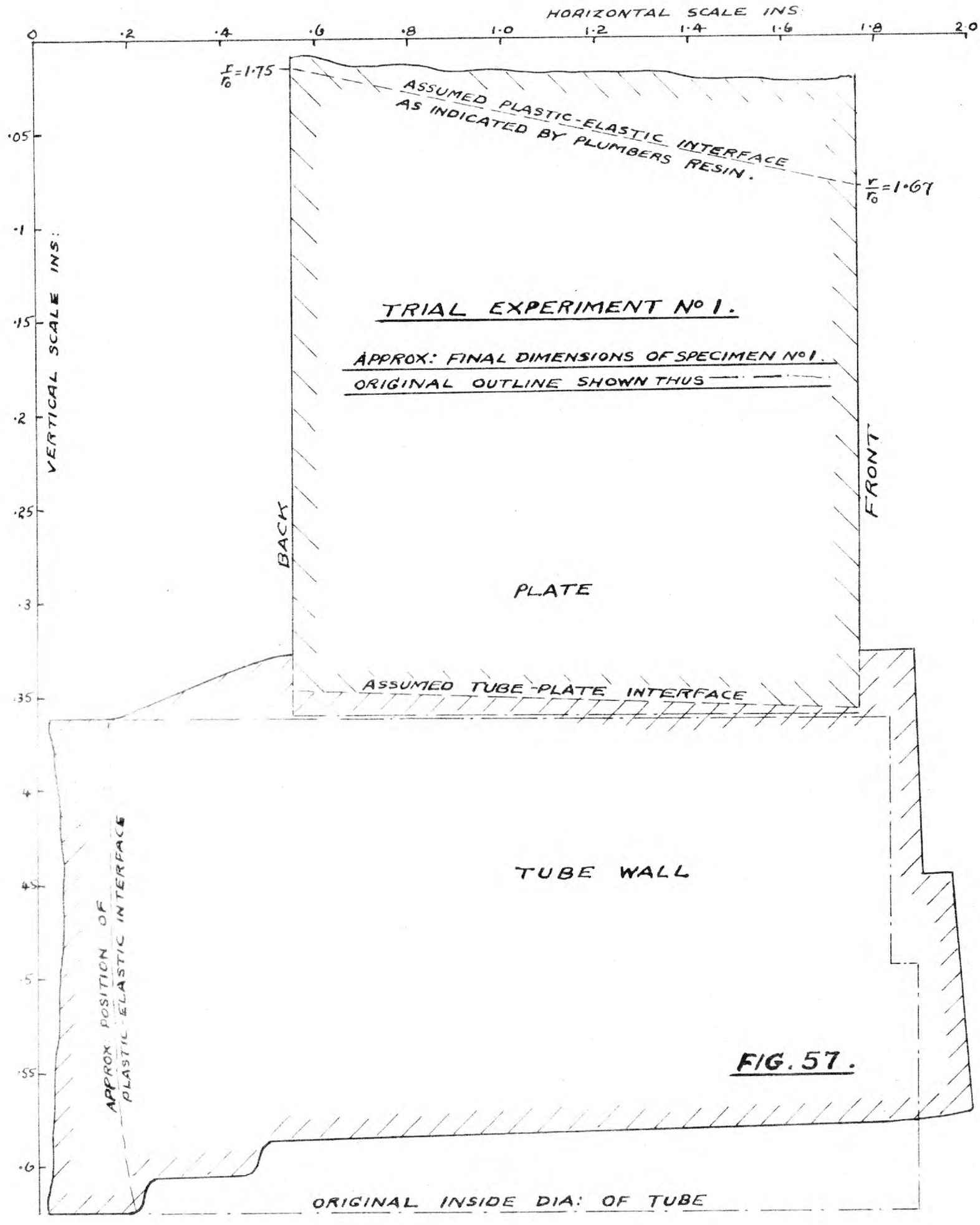
HORIZONTAL SCALE INS:
0
·2
·4
·6
·8
1·0
1·2
1·4
1·6
1·8
2·0
VERTICAL SCALE INS:
·05
·1
·15
·2
·25
·3
·35
·4
·45
·5
·55
·6
r/r0 = 1·75
ASSUMED PLASTIC-ELASTIC INTERFACE AS INDICATED BY PLUMBERS RESIN.
r/r0 = 1·67
TRIAL EXPERIMENT No 1.
APPROX: FINAL DIMENSIONS OF SPECIMEN No 1.
ORIGINAL OUTLINE SHOWN THUS
BACK
FRONT
PLATE
ASSUMED TUBE-PLATE INTERFACE
TUBE WALL
APPROX POSITION OF PLASTIC-ELASTIC INTERFACE
ORIGINAL INSIDE DIA: OF TUBE

FIG. 57.

TRIAL EXPERIMENT Nº 1.

EXTRUSION.

o TOTAL EXTRUSION.
\+ BACK " .

1T MEANS TOTAL EXTRUSION FOR FIRST EXPANDING.
2B " BACK " " SECOND " .

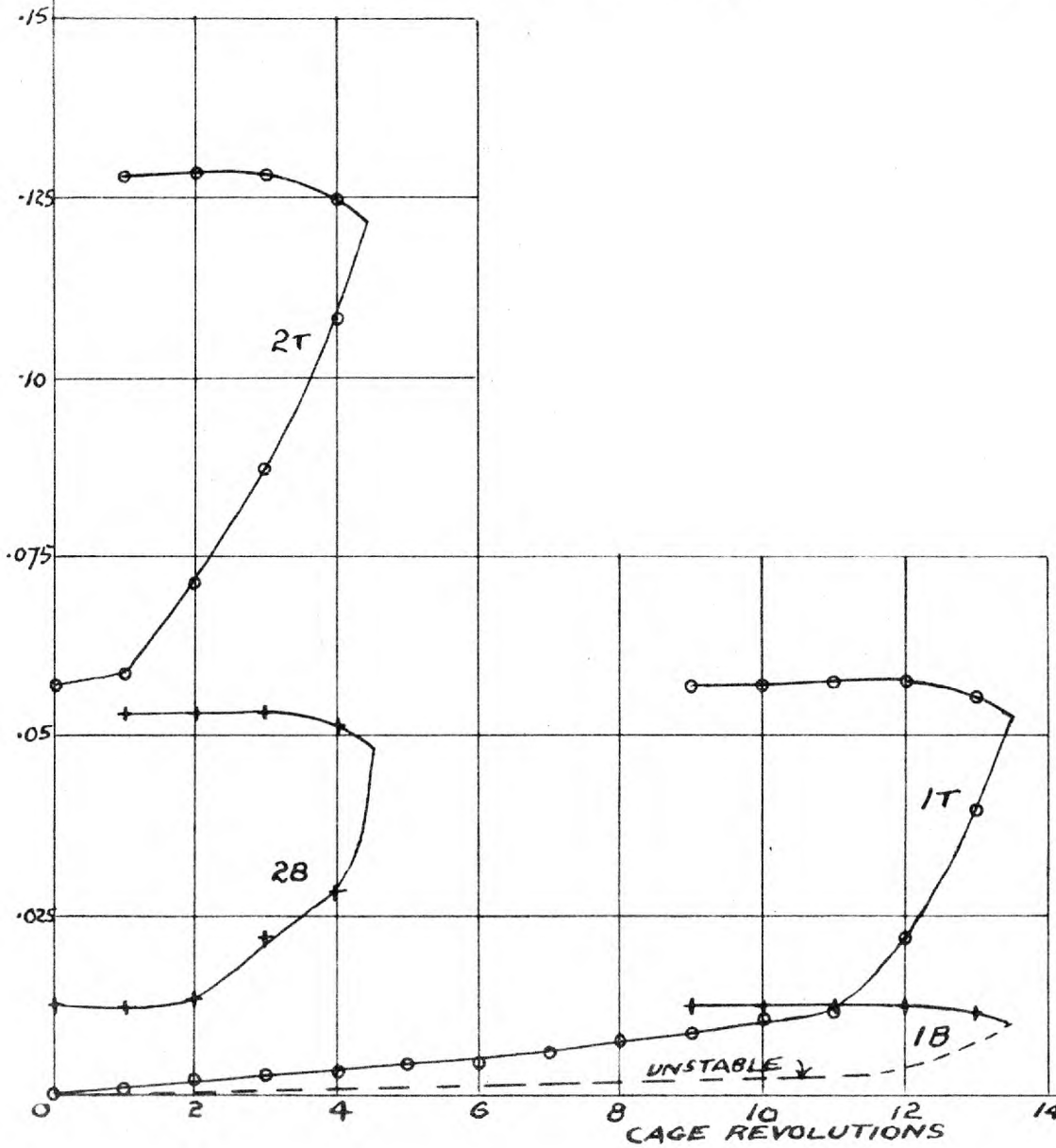

FIG.58.

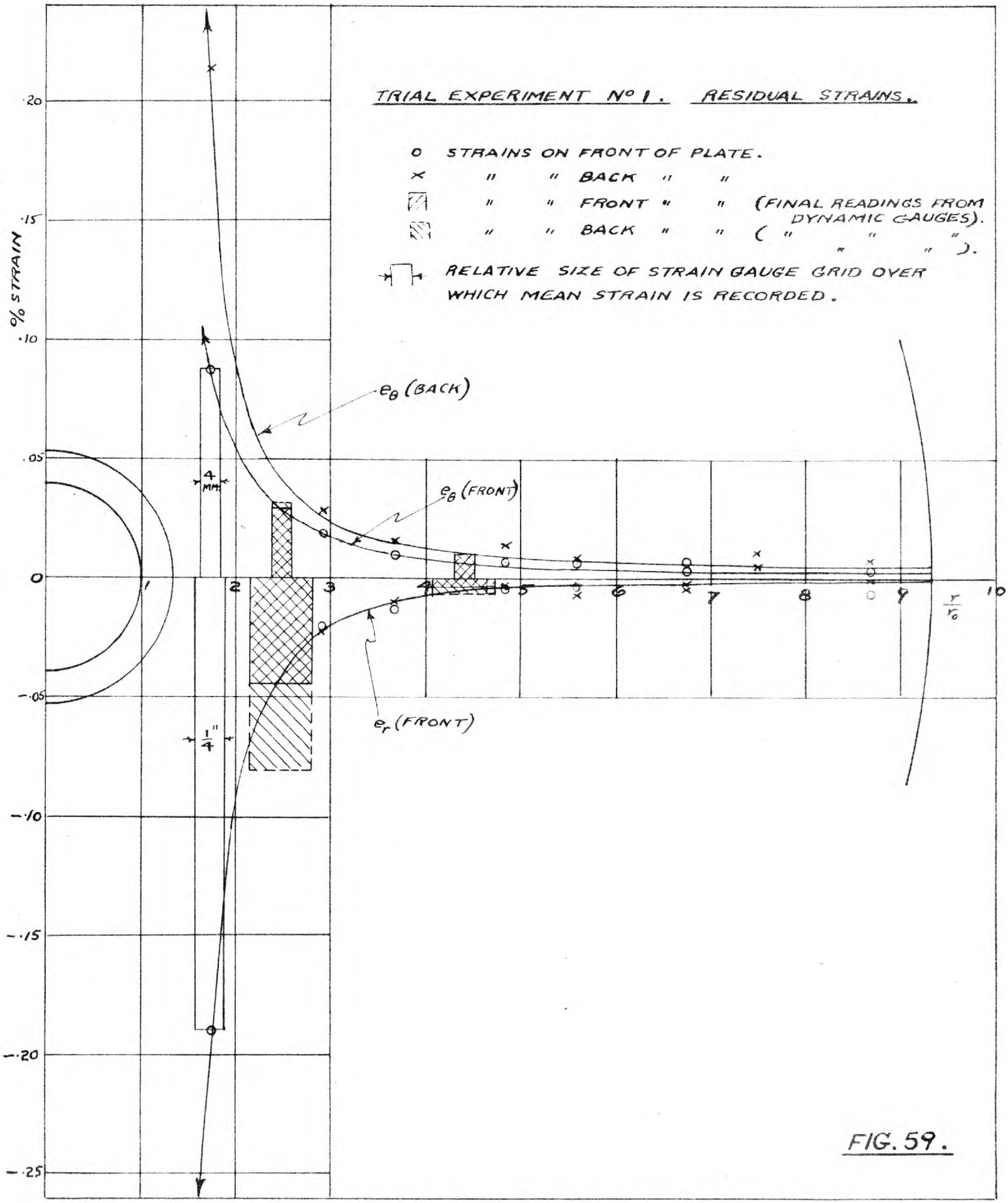
TRIAL EXPERIMENT Nº 1. RESIDUAL STRAINS.
o STRAINS ON FRONT OF PLATE.
× " " BACK " "
" " FRONT " " (FINAL READINGS FROM DYNAMIC GAUGES).
" " BACK " " (" " " ").
RELATIVE SIZE OF STRAIN GAUGE GRID OVER WHICH MEAN STRAIN IS RECORDED.
% STRAIN
·20
·15
·10
·05
0
-·05
-·10
-·15
-·20
-·25
e_θ (BACK)
e_θ (FRONT)
e_r (FRONT)
4 MM.
1/4"
1
2
3
4
5
6
7
8
9
10
$\frac{r}{r_0}$

FIG. 59.

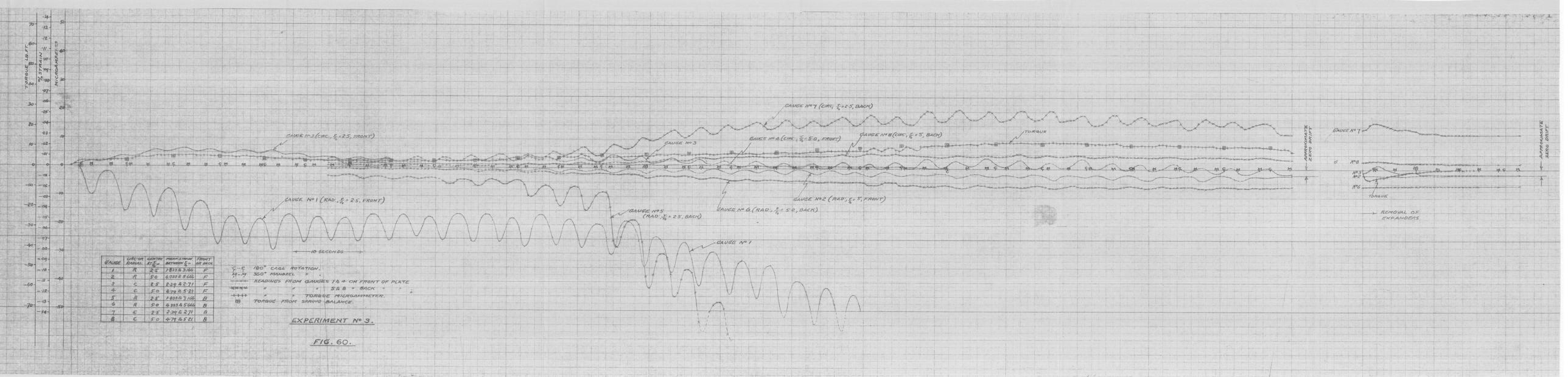

GAUGE	CIRC OR RADIAL	CENTRE r/t =	FROM STRAIN BETWEEN r/t =	FRONT OR BACK
1	R	2·5	1·8338 & 3·146	F
2	R	5·0	4·0338 & 6·66	F
3	C	2·5	2·39 & 2·71	F
4	C	5·0	4·79 & 5·21	F
5	R	2·5	1·8338 & 3·166	B
6	R	5·0	4·0338 & 5·66	B
7	C	2·5	2·39 & 2·71	B
8	C	5·0	4·79 & 5·21	B

C–C 180° CAGE ROTATION.
M–M 360° MANDREL "
READINGS FROM GAUGES 1 & 4 ON FRONT OF PLATE
" " " 5 & 8 " BACK " "
" " " TORQUE MICROAMMETER.
TORQUE FROM SPRING BALANCE.

EXPERIMENT No 3.

FIG. 60.

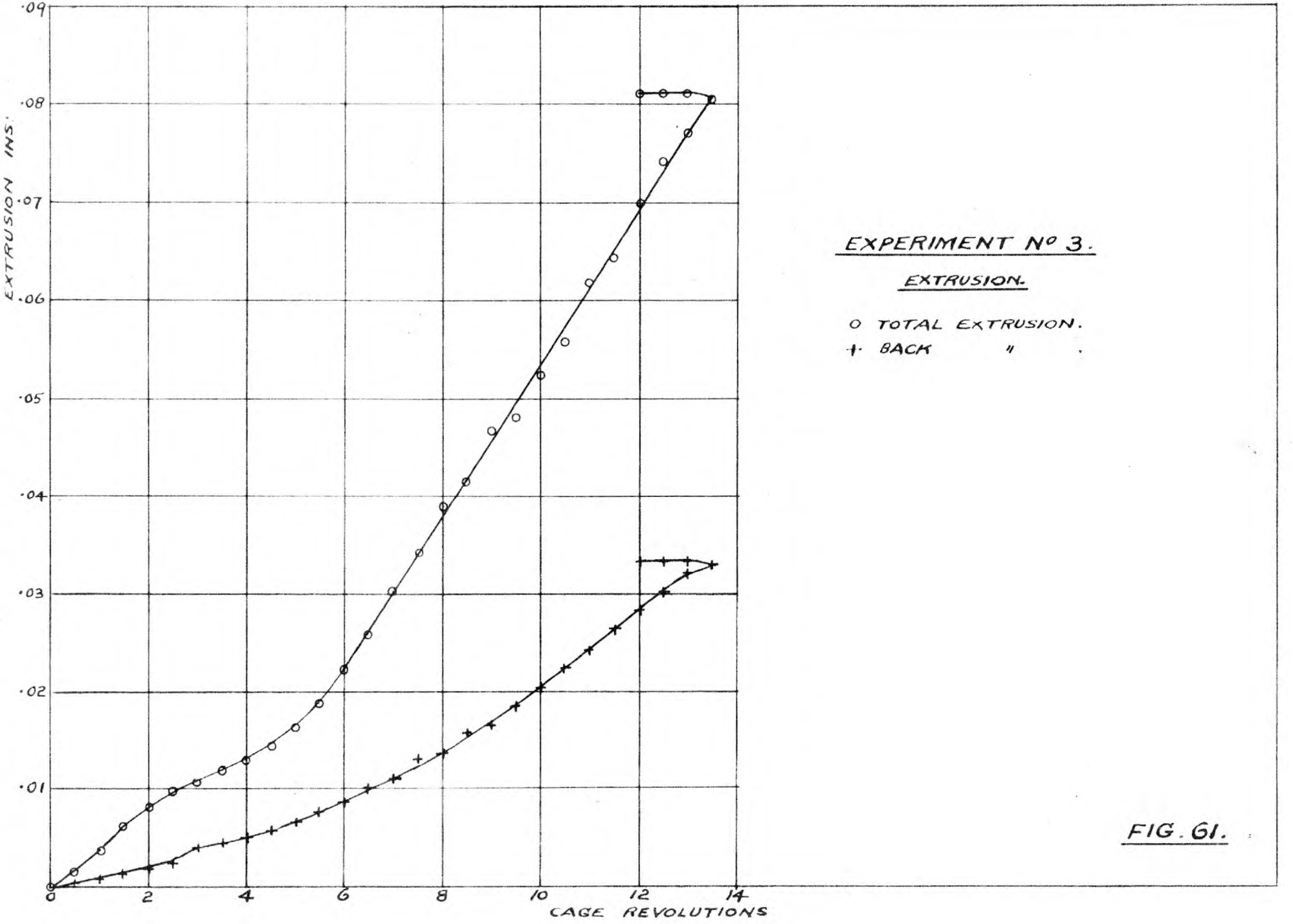

EXPERIMENT Nº 3.

EXTRUSION.

o TOTAL EXTRUSION.

+ BACK " .

FIG. 61.

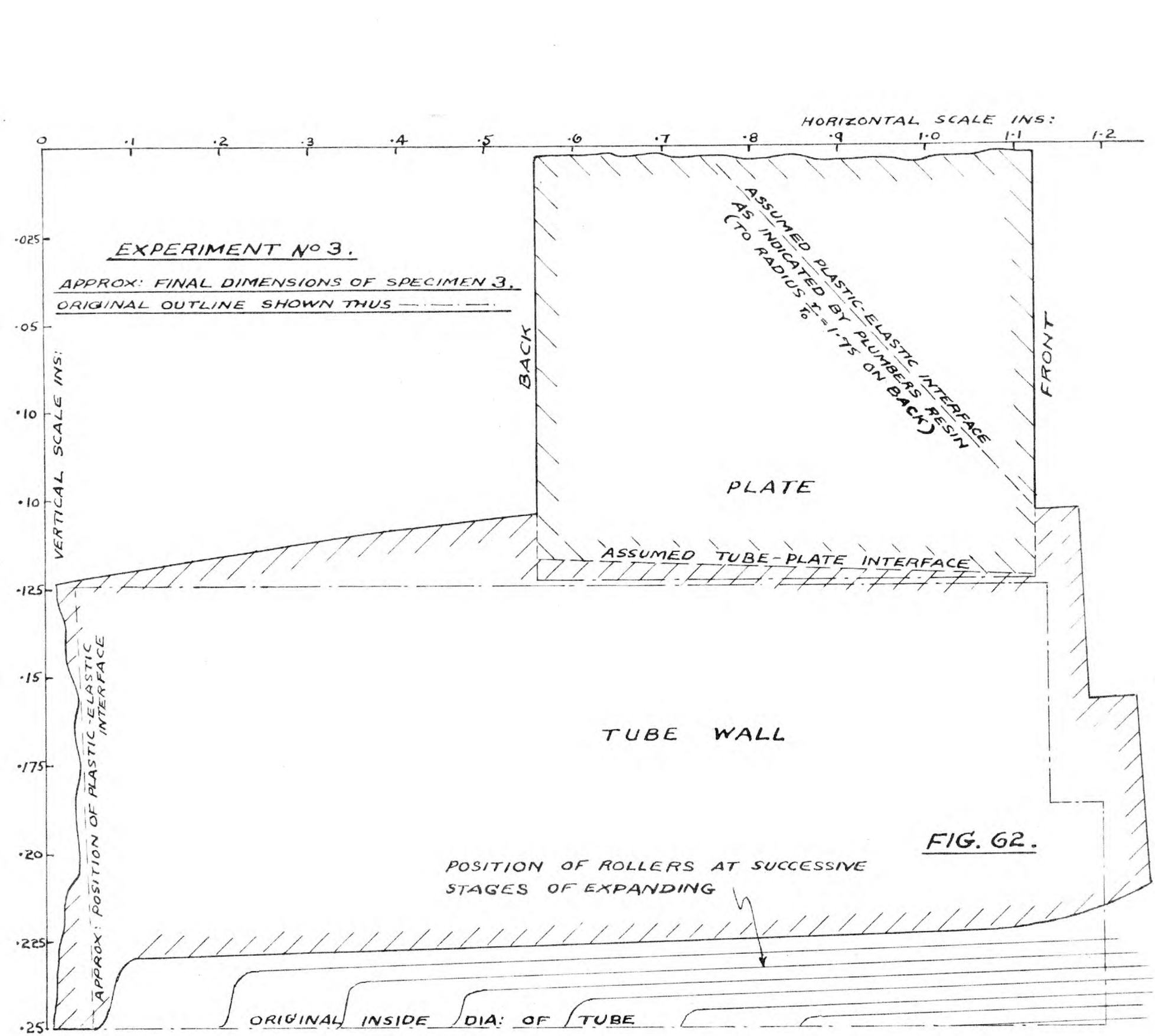
HORIZONTAL SCALE INS:
0
·1
·2
·3
·4
·5
·6
·7
·8
·9
1·0
1·1
1·2
EXPERIMENT No 3.
APPROX: FINAL DIMENSIONS OF SPECIMEN 3.
ORIGINAL OUTLINE SHOWN THUS
VERTICAL SCALE INS:
·025
·05
·10
·10
·125
·15
·175
·20
·225
·25
BACK
FRONT
ASSUMED PLASTIC-ELASTIC INTERFACE AS INDICATED BY PLUMBERS RESIN (TO RADIUS r/r0 = 1·75 ON BACK)
PLATE
ASSUMED TUBE-PLATE INTERFACE
TUBE WALL
APPROX: POSITION OF PLASTIC-ELASTIC INTERFACE
POSITION OF ROLLERS AT SUCCESSIVE STAGES OF EXPANDING
ORIGINAL INSIDE DIA: OF TUBE

FIG. 62.

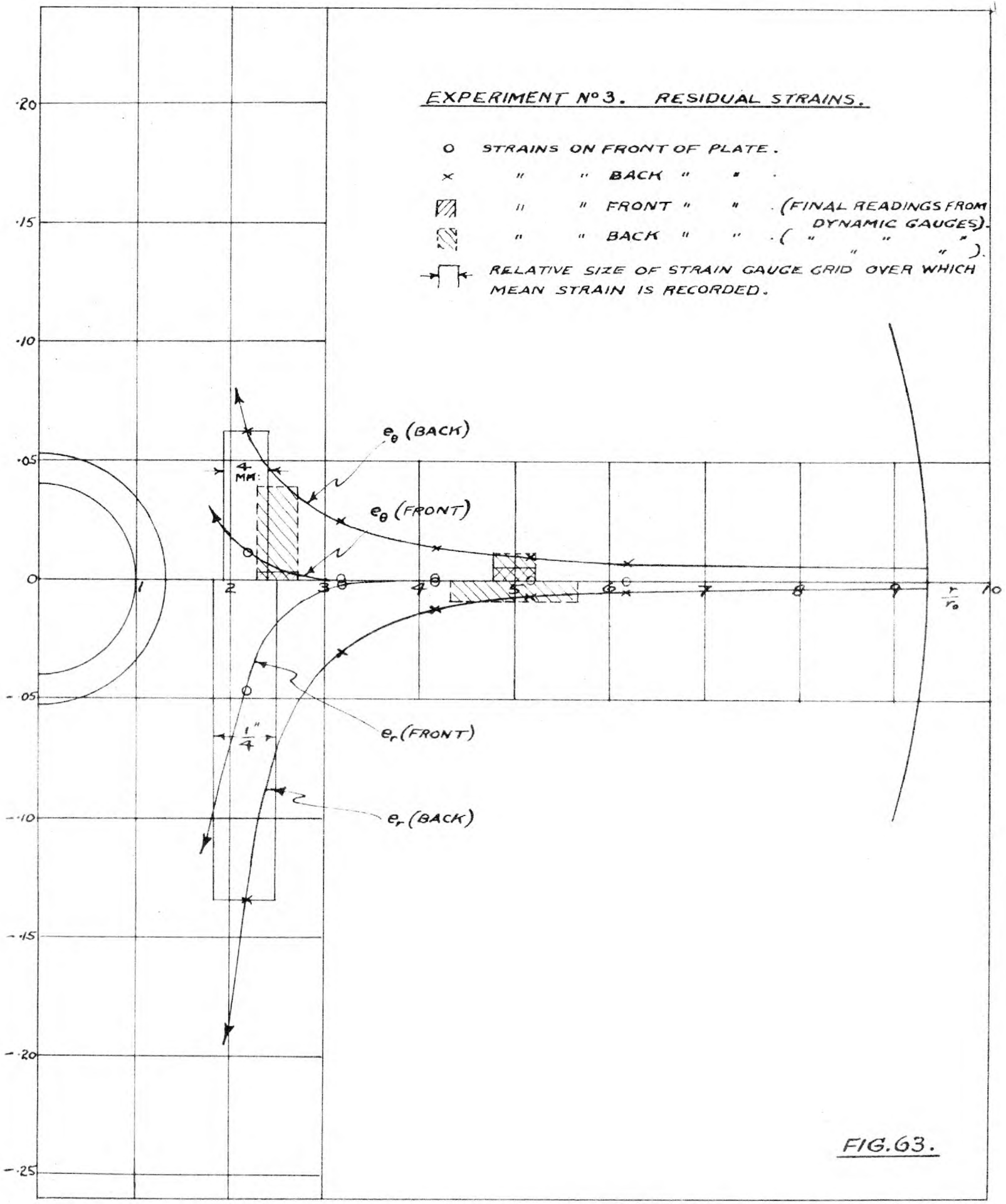
EXPERIMENT Nº 3. RESIDUAL STRAINS.
O STRAINS ON FRONT OF PLATE.
× " " BACK " " .
" " FRONT " " . (FINAL READINGS FROM DYNAMIC GAUGES).
" " BACK " " . (" " " ").
RELATIVE SIZE OF STRAIN GAUGE GRID OVER WHICH MEAN STRAIN IS RECORDED.
·20
·15
·10
·05
0
- ·05
- ·10
- ·15
- ·20
- ·25
1
2
3
4
5
6
7
8
9
10
r/r0
4 MM.
1/4"
eθ (BACK)
eθ (FRONT)
er (FRONT)
er (BACK)

FIG. 63.

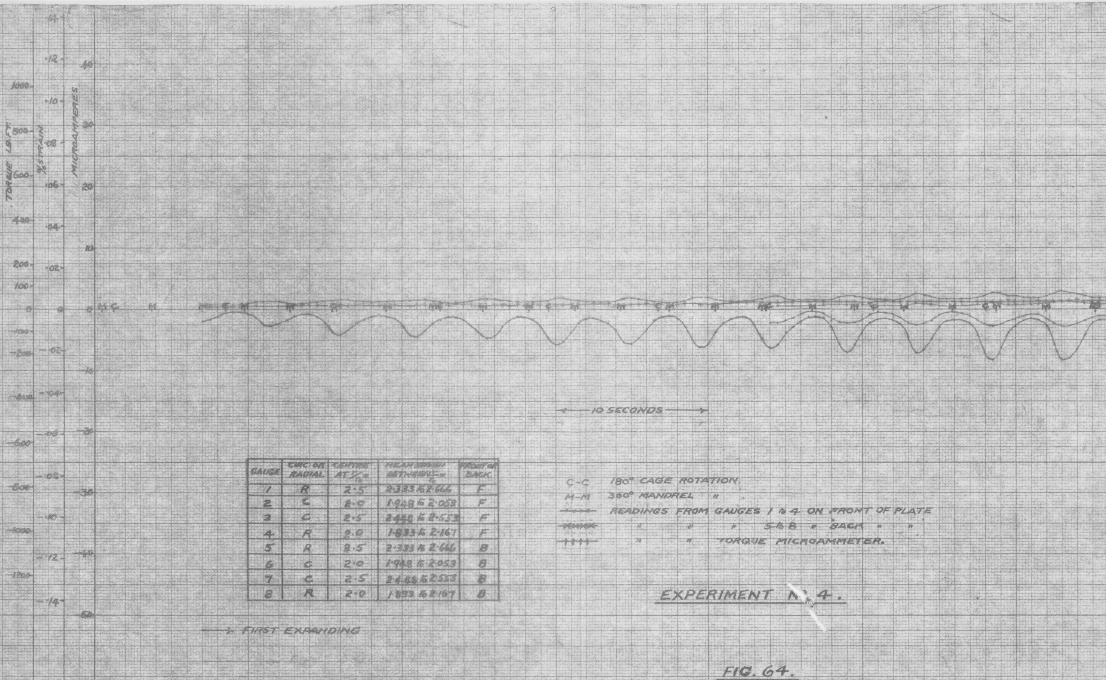

GAUGE	CIRC. OR RADIAL	CENTRE AT r/r_0 =	MEAN STRAIN BETWEEN r/r_0 =	FRONT OR BACK.
1	R	2·5	2·333 to 2·666	F
2	C	2·0	1·948 to 2·053	F
3	C	2·5	2·448 to 2·553	F
4	R	2·0	1·833 to 2·167	F
5	R	2·5	2·333 to 2·666	B
6	C	2·0	1·948 to 2·053	B
7	C	2·5	2·448 to 2·553	B
8	R	2·0	1·833 to 2·167	B

C–C 180° CAGE ROTATION.
M–M 360° MANDREL "
–•–•– READINGS FROM GAUGES 1 to 4 ON FRONT OF PLATE
–×–×– " " " 5 to 8 " BACK " "
–+–+– " " TORQUE MICROAMMETER.

EXPERIMENT No. 4.

FIG. 64.

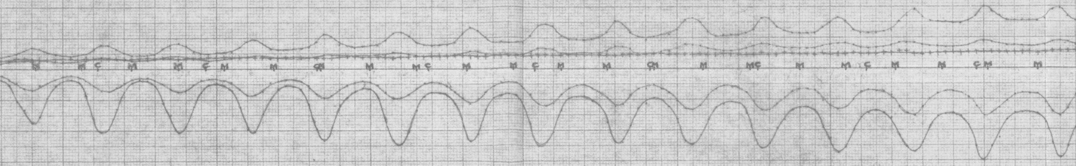

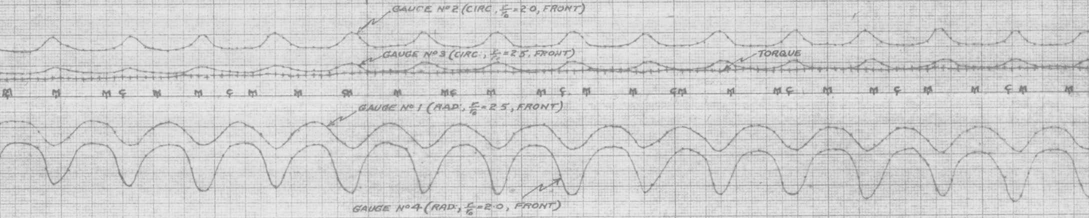

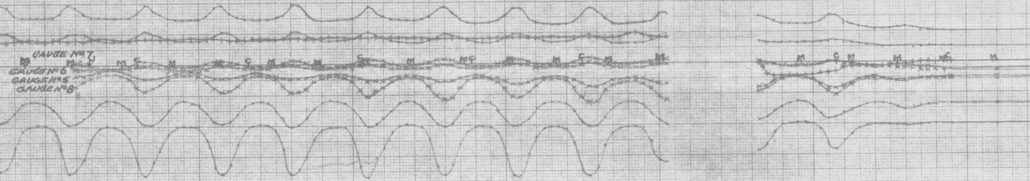

→ FIRST REMOVAL OF EXPANDERS

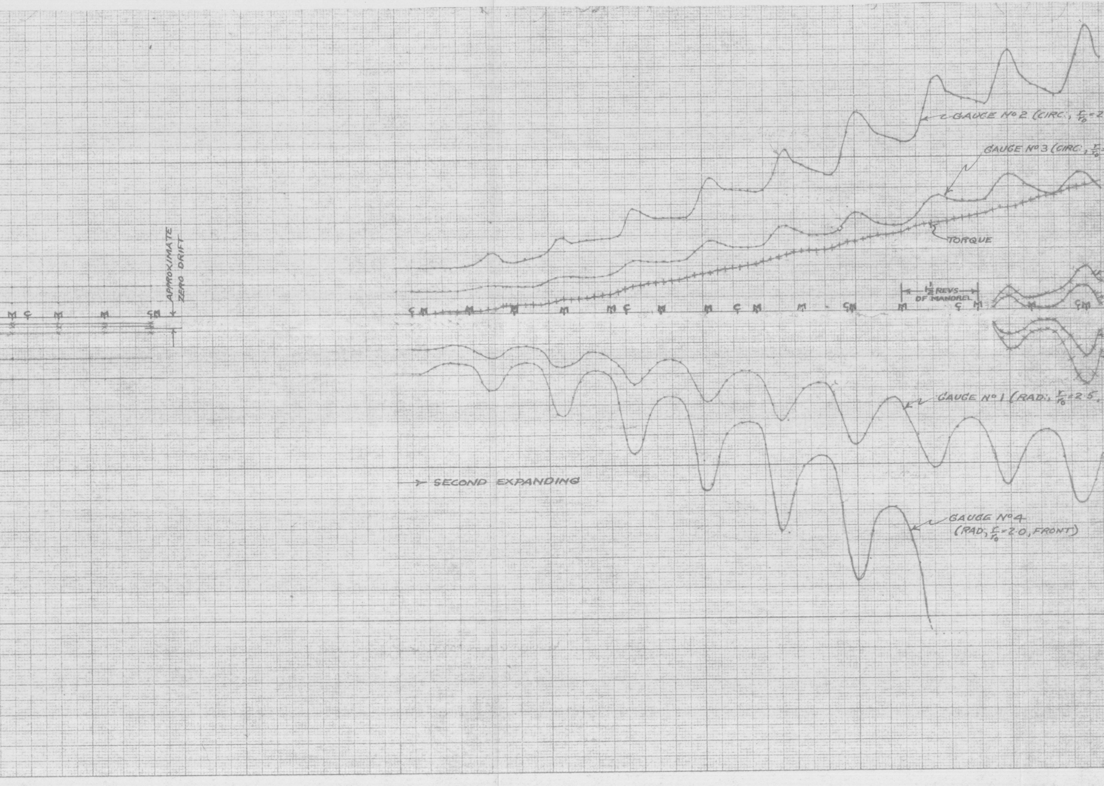

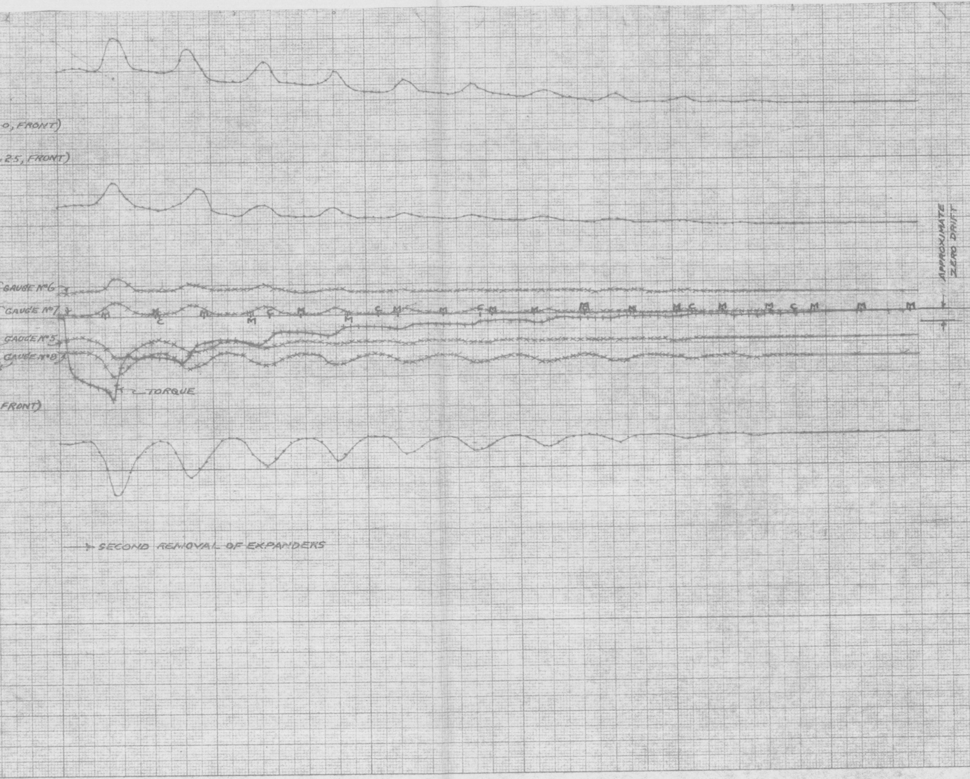

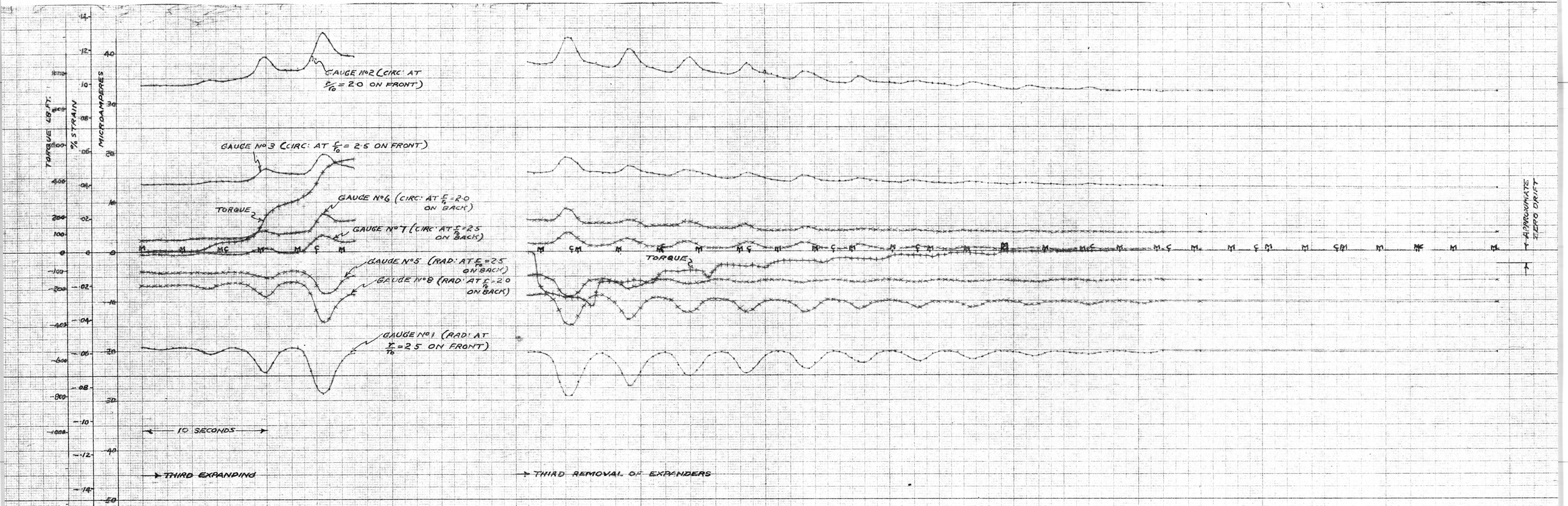

EXPERIMENT No 4.

FIG. 65.

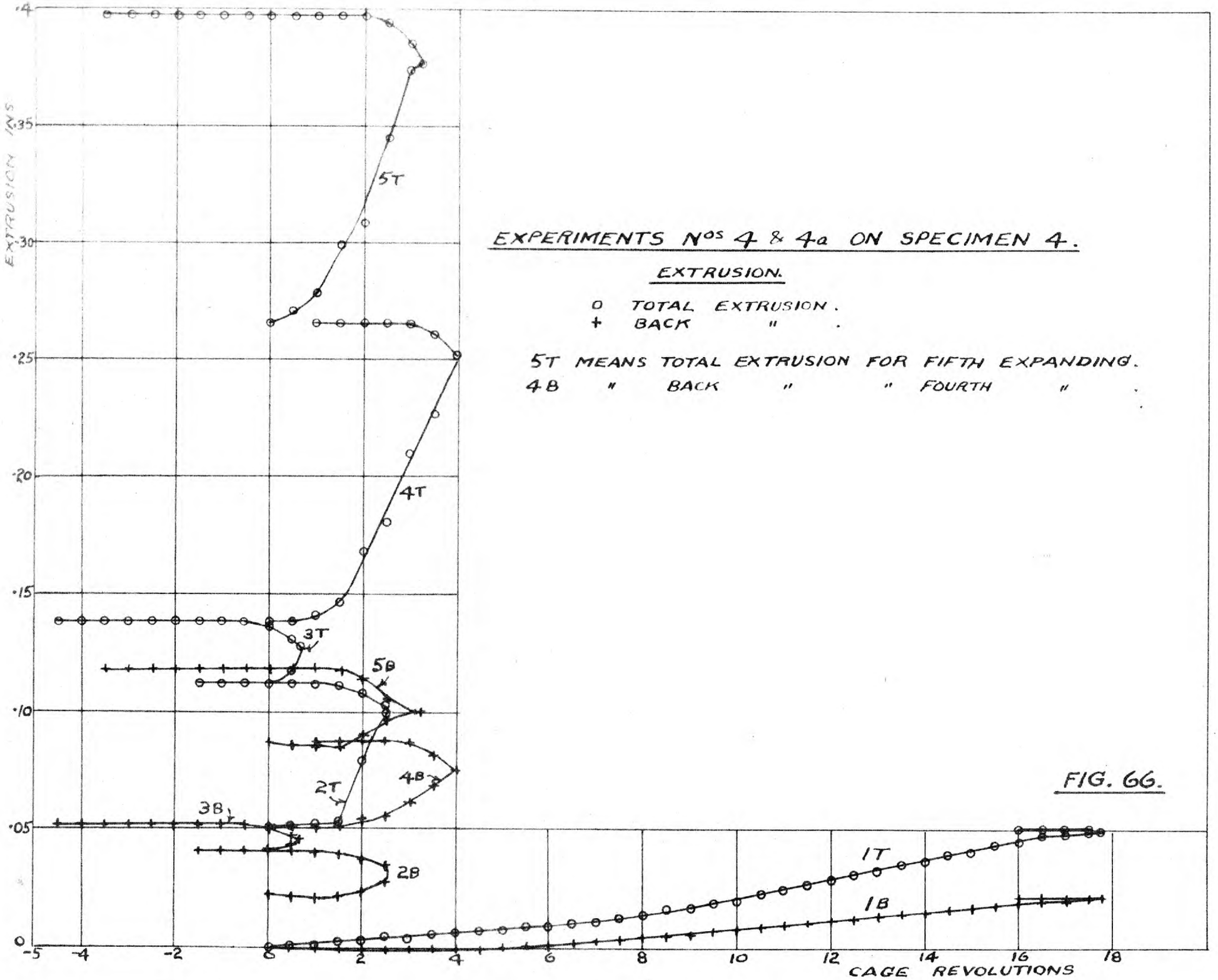
EXPERIMENTS Nos 4 & 4a ON SPECIMEN 4.
EXTRUSION.
o TOTAL EXTRUSION.
+ BACK "
5T MEANS TOTAL EXTRUSION FOR FIFTH EXPANDING.
4B " BACK " " FOURTH "
EXTRUSION INS
·4
·35
·30
·25
·20
·15
·10
·05
0
5T
4T
3T
5B
4B
2T
3B
2B
1T
1B
-5
-4
-2
0
2
4
6
8
10
12
14
16
18
CAGE REVOLUTIONS

FIG. 66.

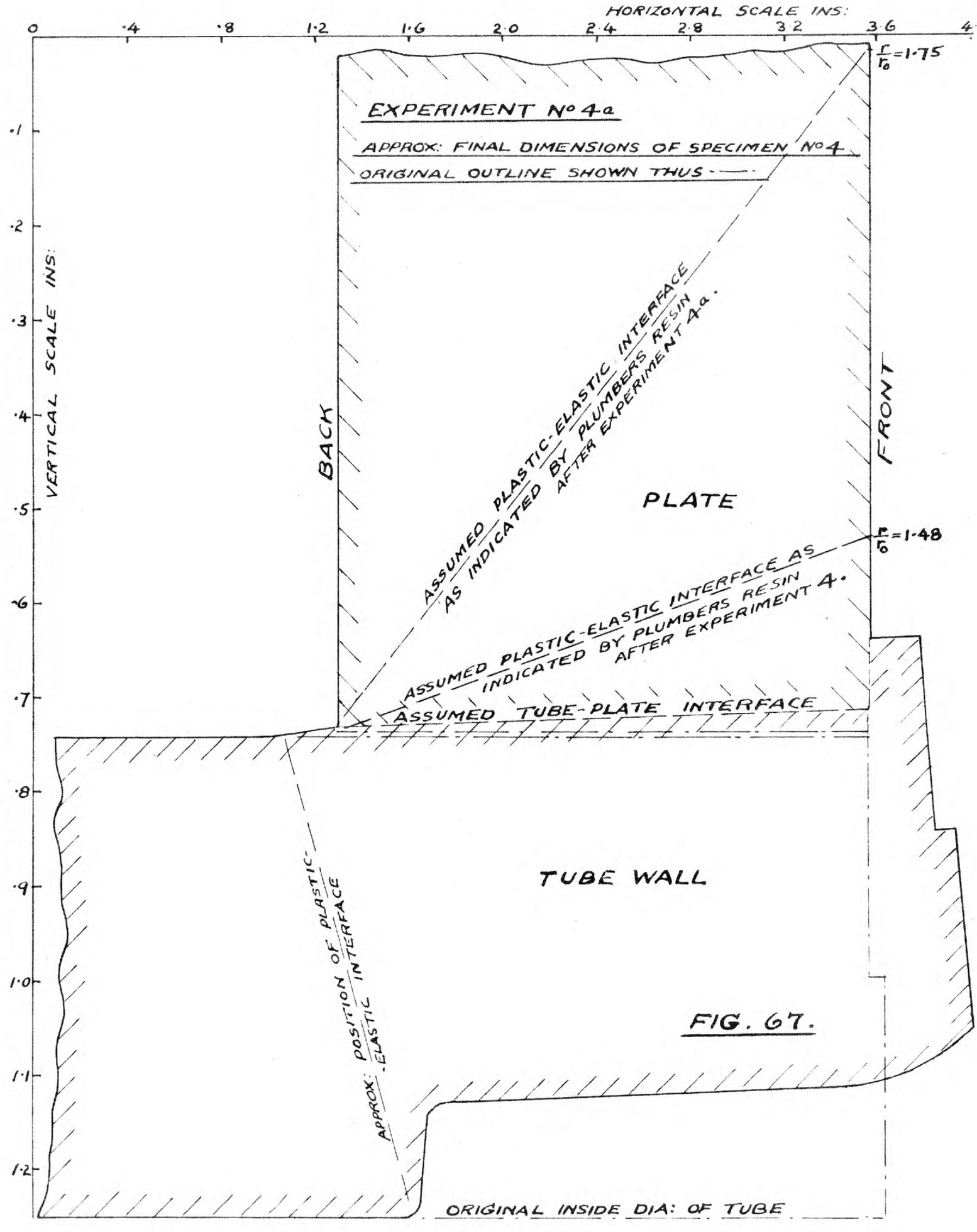
HORIZONTAL SCALE INS:
0
·4
·8
1·2
1·6
2·0
2·4
2·8
3·2
3·6
4·0
VERTICAL SCALE INS:
·1
·2
·3
·4
·5
·6
·7
·8
·9
1·0
1·1
1·2
EXPERIMENT No 4a
APPROX: FINAL DIMENSIONS OF SPECIMEN No 4.
ORIGINAL OUTLINE SHOWN THUS - - —
BACK
FRONT
PLATE
TUBE WALL
r/r0 = 1·75
r/r0 = 1·48
ASSUMED PLASTIC-ELASTIC INTERFACE AS INDICATED BY PLUMBERS RESIN AFTER EXPERIMENT 4a.
ASSUMED PLASTIC-ELASTIC INTERFACE AS INDICATED BY PLUMBERS RESIN AFTER EXPERIMENT 4.
ASSUMED TUBE-PLATE INTERFACE
APPROX: POSITION OF PLASTIC-ELASTIC INTERFACE
ORIGINAL INSIDE DIA: OF TUBE

FIG. 67.

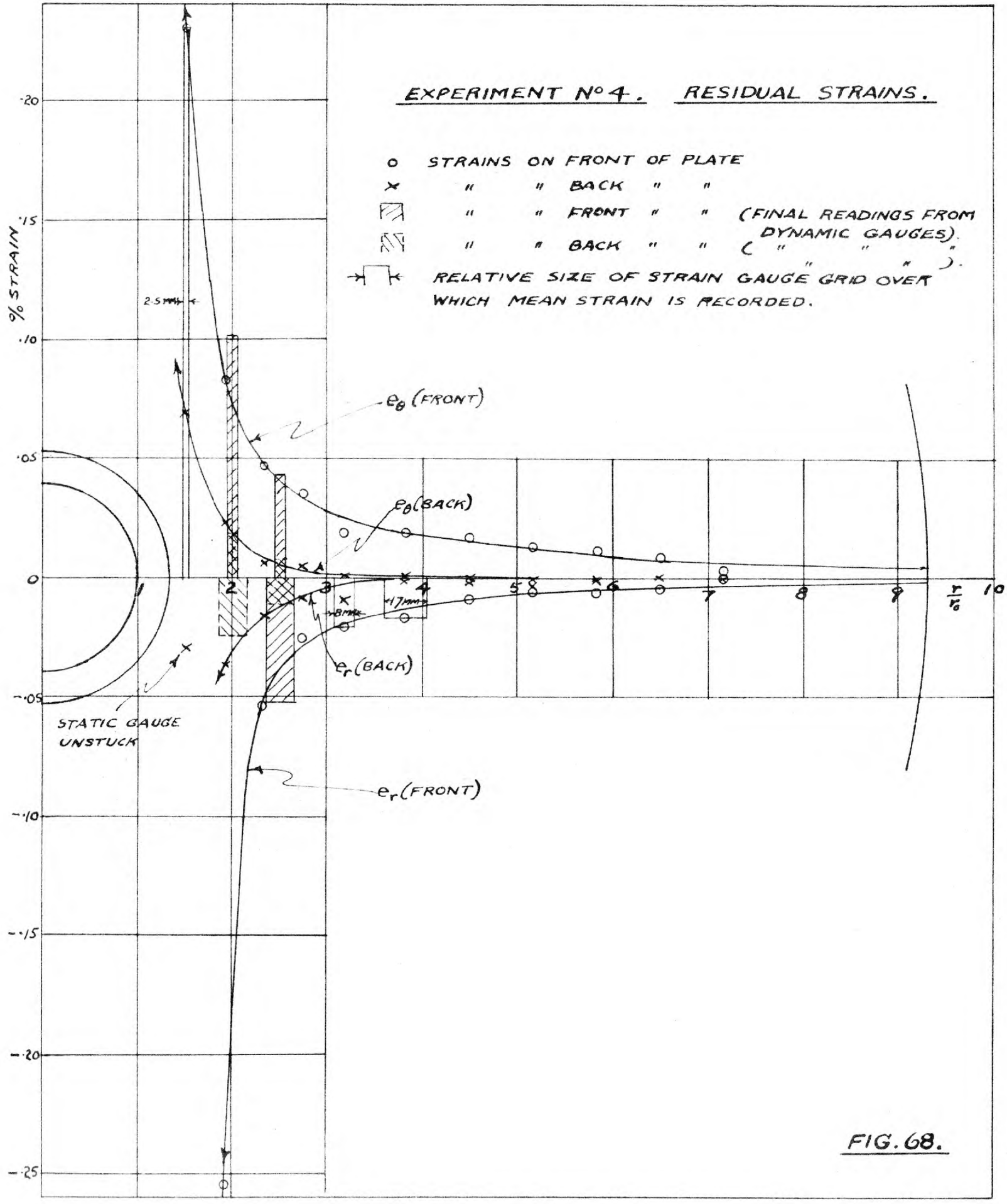
EXPERIMENT Nº 4. RESIDUAL STRAINS.
STRAINS ON FRONT OF PLATE
" " BACK " "
" " FRONT " " (FINAL READINGS FROM DYNAMIC GAUGES).
" " BACK " " (" " ").
RELATIVE SIZE OF STRAIN GAUGE GRID OVER WHICH MEAN STRAIN IS RECORDED.
% STRAIN
·20
·15
·10
·05
0
-·05
-·10
-·15
-·20
-·25
2·5mm
·8mm
1·7mm
e_θ (FRONT)
e_θ (BACK)
e_r (BACK)
e_r (FRONT)
STATIC GAUGE UNSTUCK
1
2
3
4
5
6
7
8
9
10
$\frac{r}{r_0}$

FIG. 68.

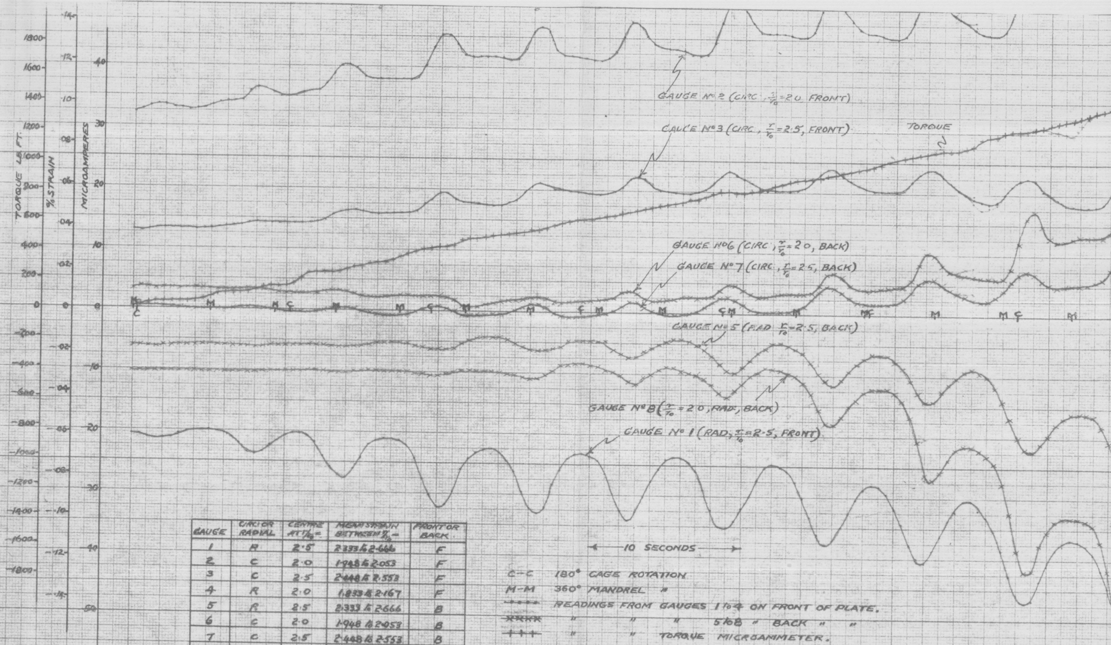

GAUGE	CIRC OR RADIAL	CENTRE AT r/r_0 =	MEAN STRAIN BETWEEN r/r_0 =	FRONT OR BACK
1	R	2·5	2·333 to 2·666	F
2	C	2·0	1·948 to 2·053	F
3	C	2·5	2·448 to 2·553	F
4	R	2·0	1·833 to 2·167	F
5	R	2·5	2·333 to 2·666	B
6	C	2·0	1·948 to 2·053	B
7	C	2·5	2·448 to 2·553	B
8	R	2·0	1·833 to 2·167	B

→ FOURTH EXPANDING OF SPECIMEN 4.

EXPERIMENT Nº 4a.

FIG. 69.

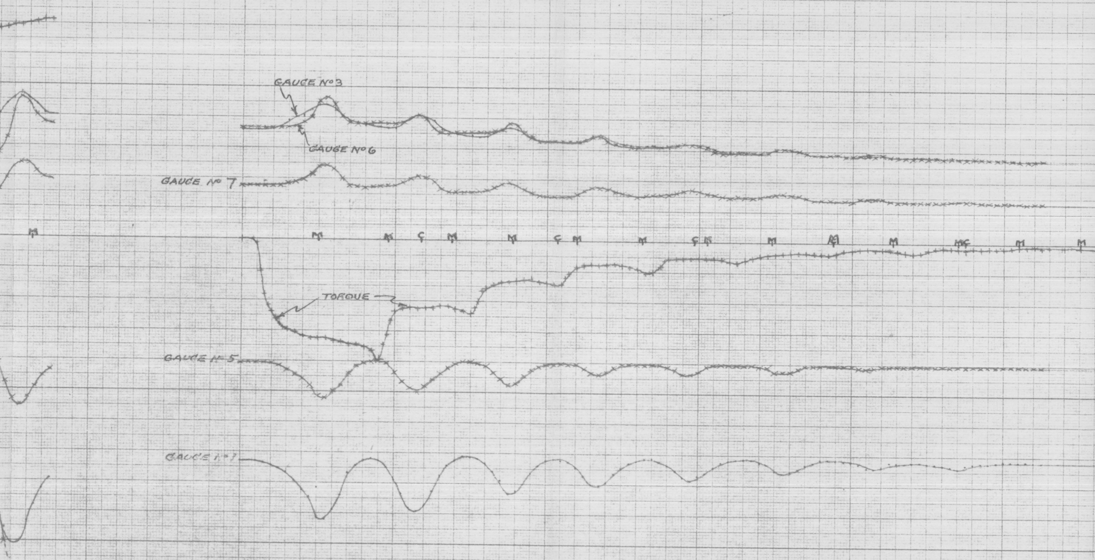

→ FOURTH REMOVAL OF EXPANDERS.

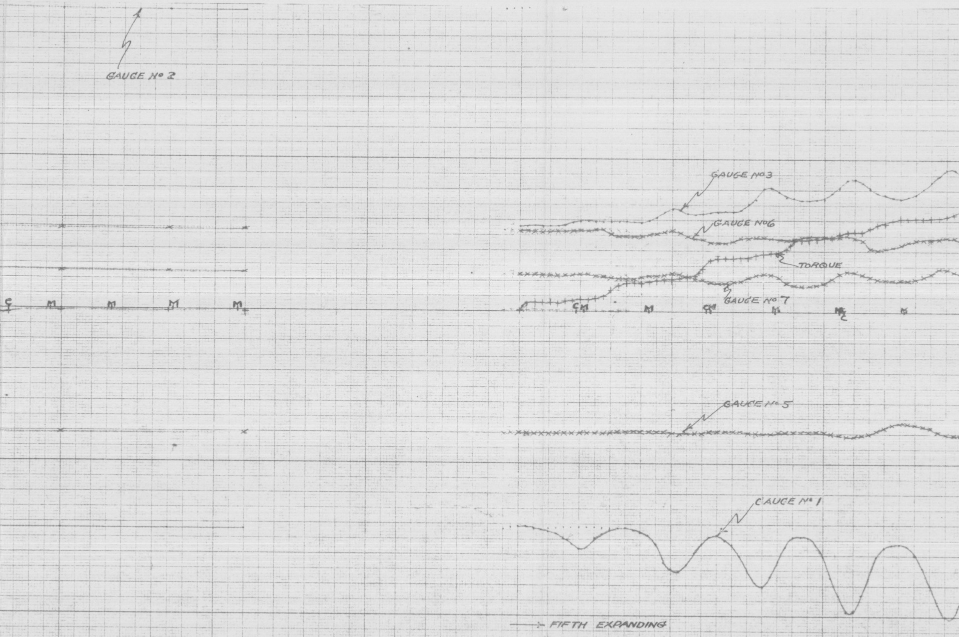

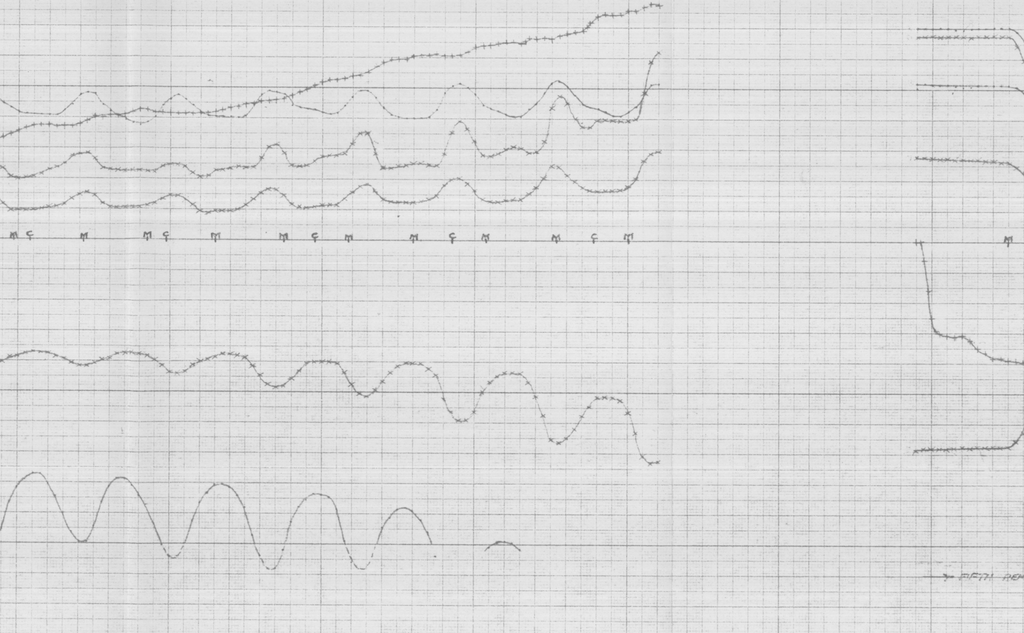

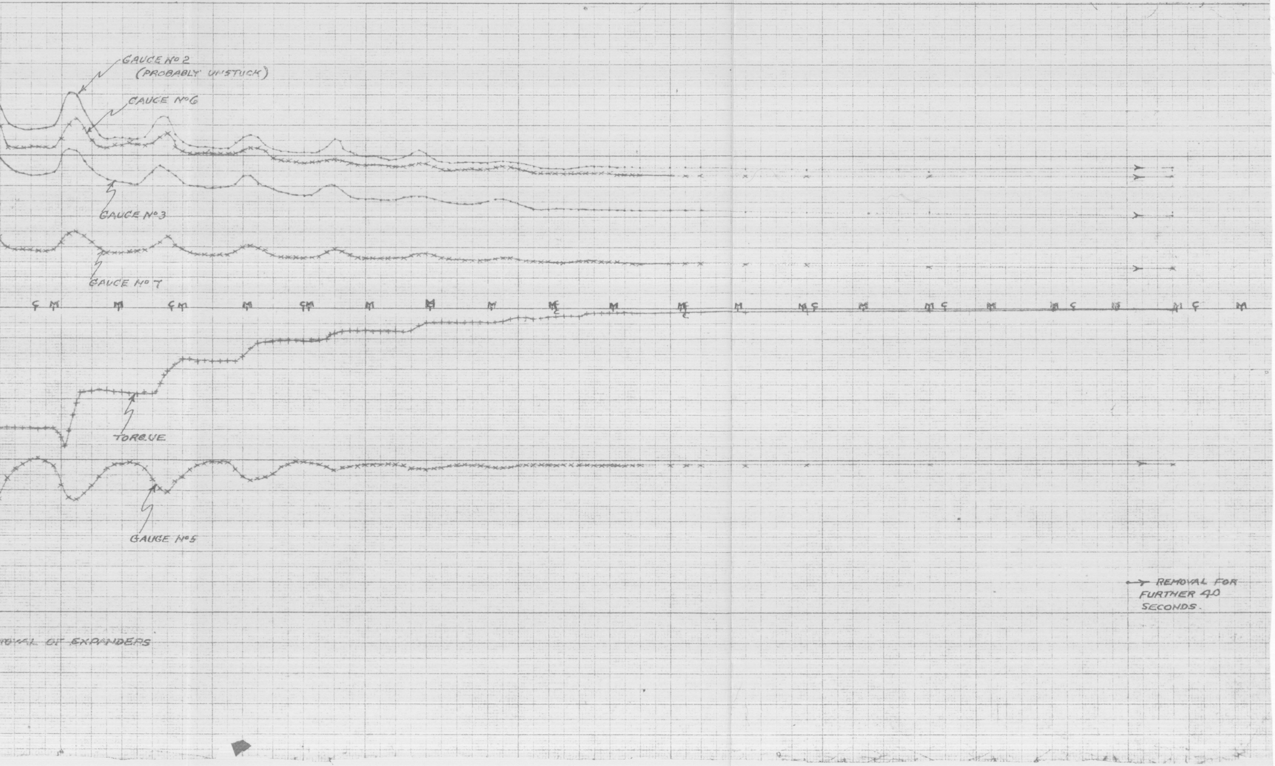

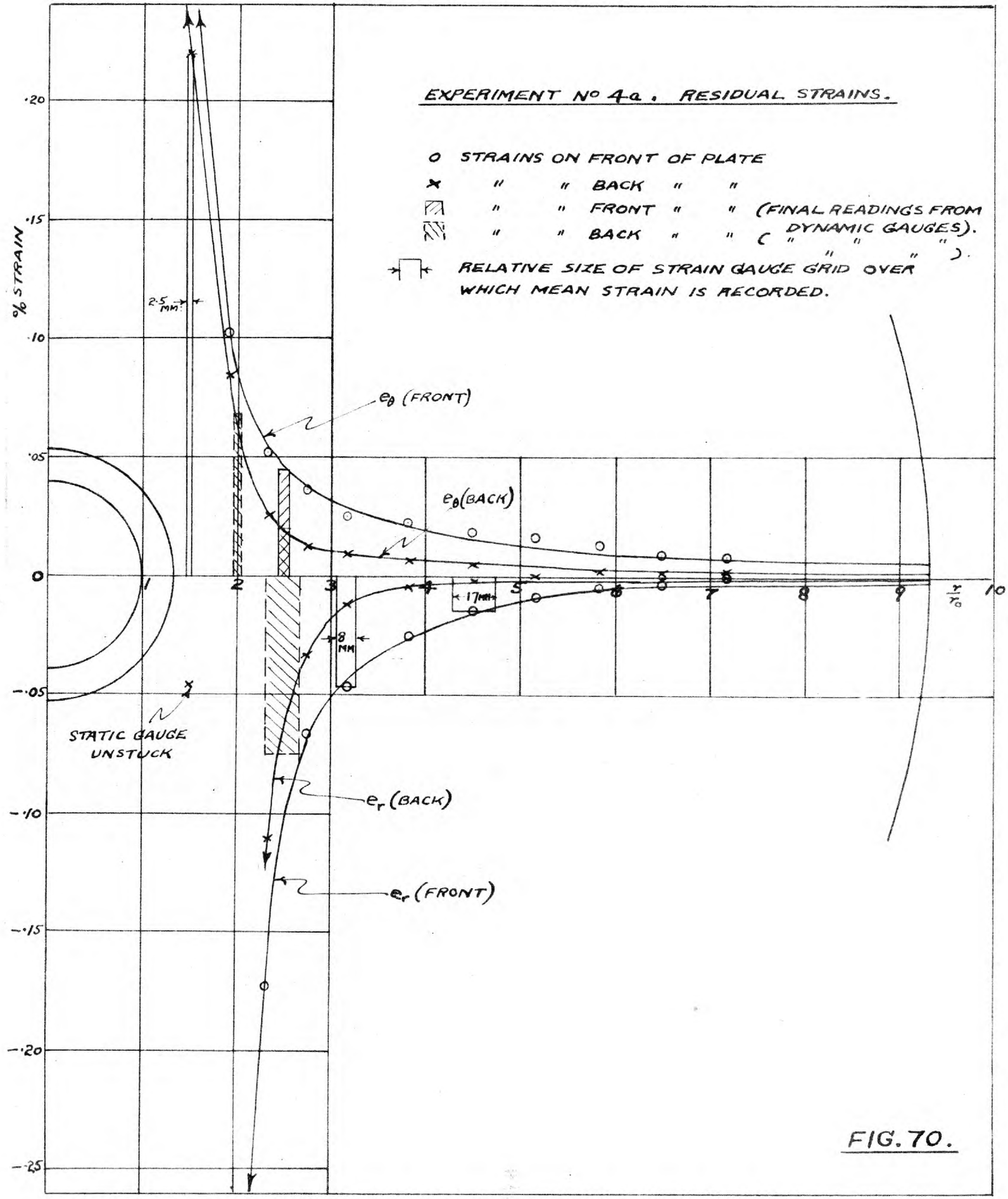
EXPERIMENT No 4a. RESIDUAL STRAINS.
O STRAINS ON FRONT OF PLATE
× " " BACK " "
" " FRONT " " (FINAL READINGS FROM DYNAMIC GAUGES).
" " BACK " " (" " " ").
RELATIVE SIZE OF STRAIN GAUGE GRID OVER WHICH MEAN STRAIN IS RECORDED.
% STRAIN
·20
·15
·10
·05
0
-·05
-·10
-·15
-·20
-·25
2·5 MM
17 MM
8 MM
e_θ (FRONT)
e_θ (BACK)
e_r (BACK)
e_r (FRONT)
STATIC GAUGE UNSTUCK
1
2
3
4
5
6
7
8
9
10
$\frac{r}{r_0}$

FIG. 70.

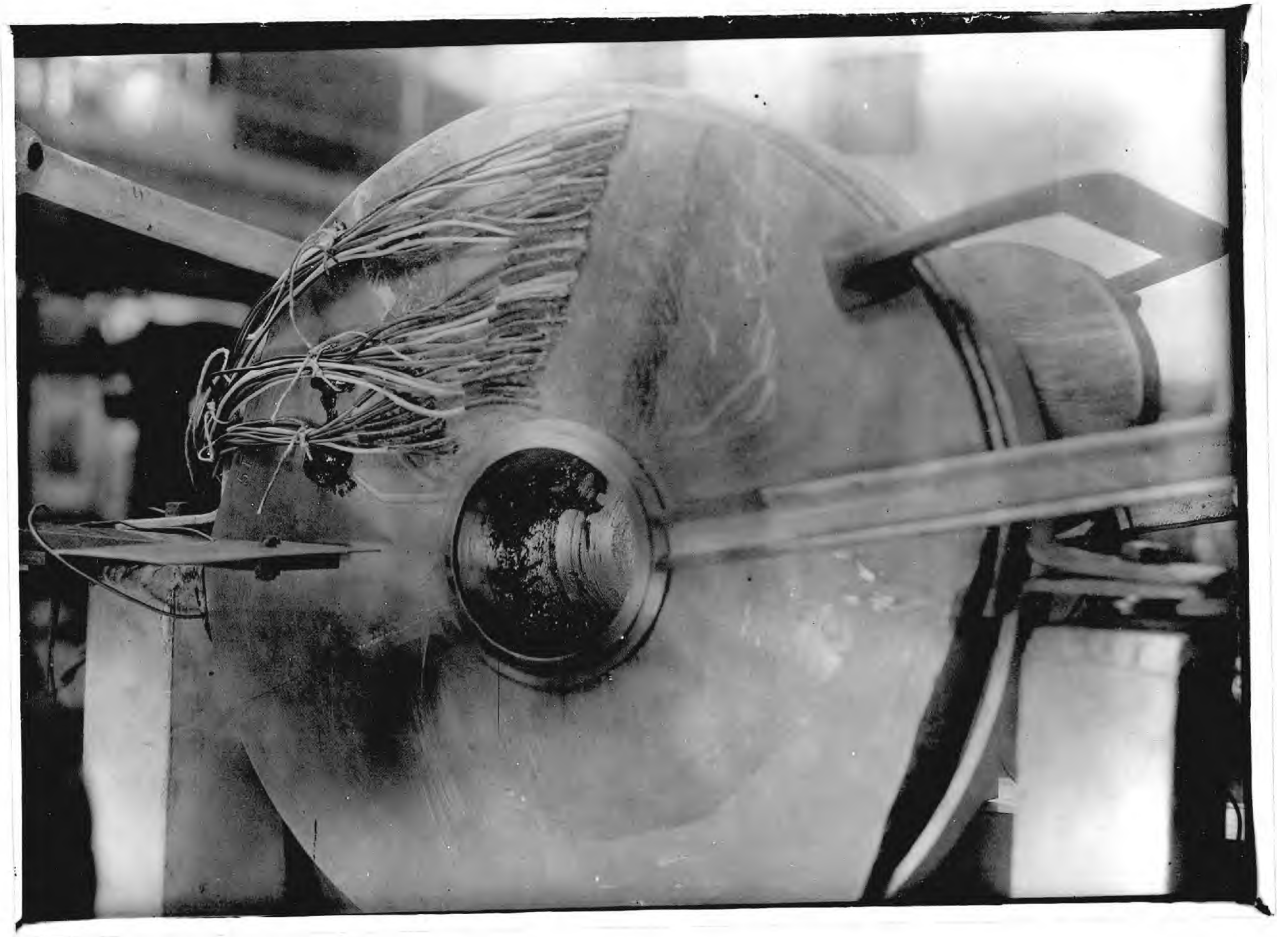

FIG. 71.

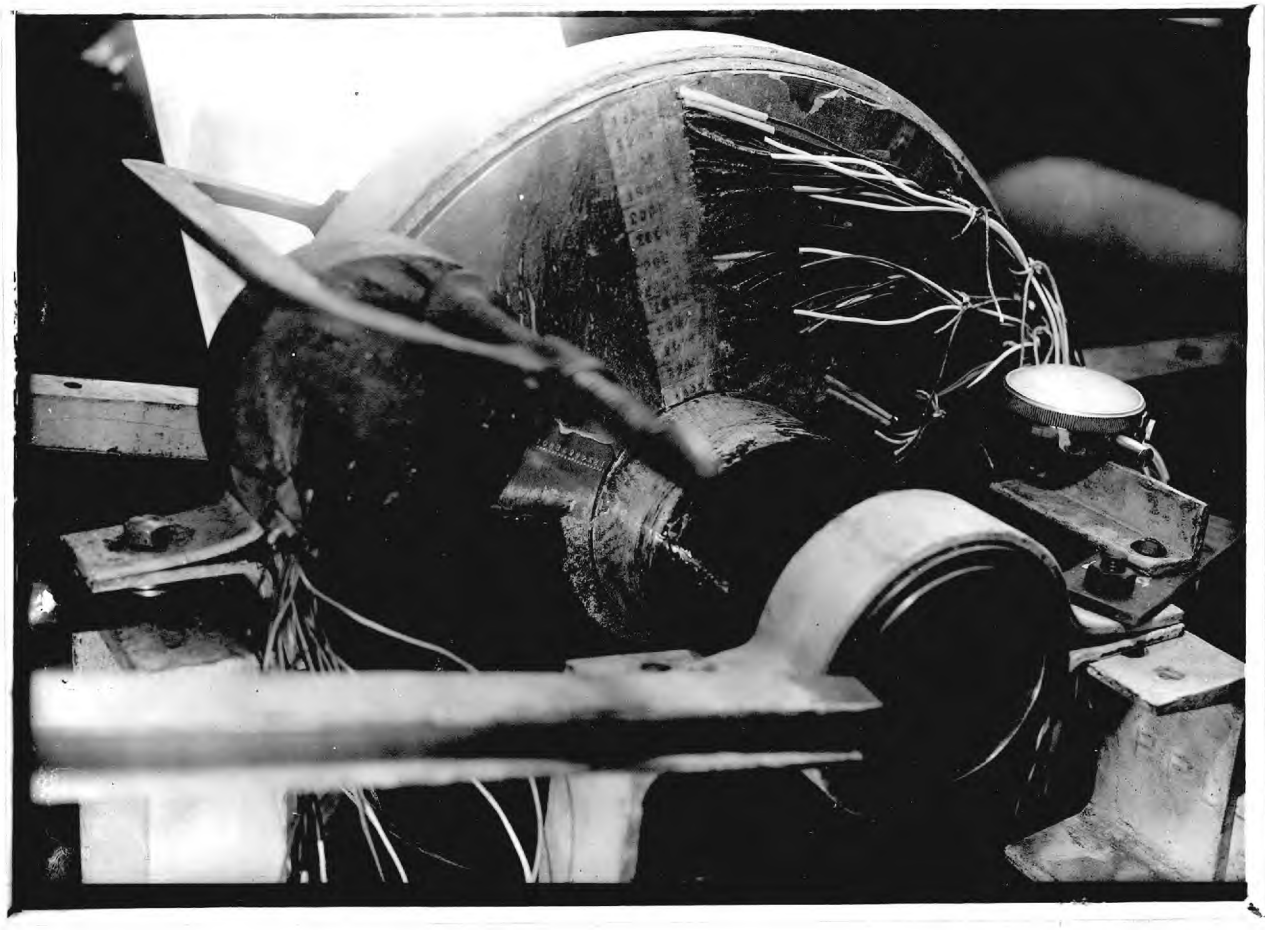

FIG. 72.

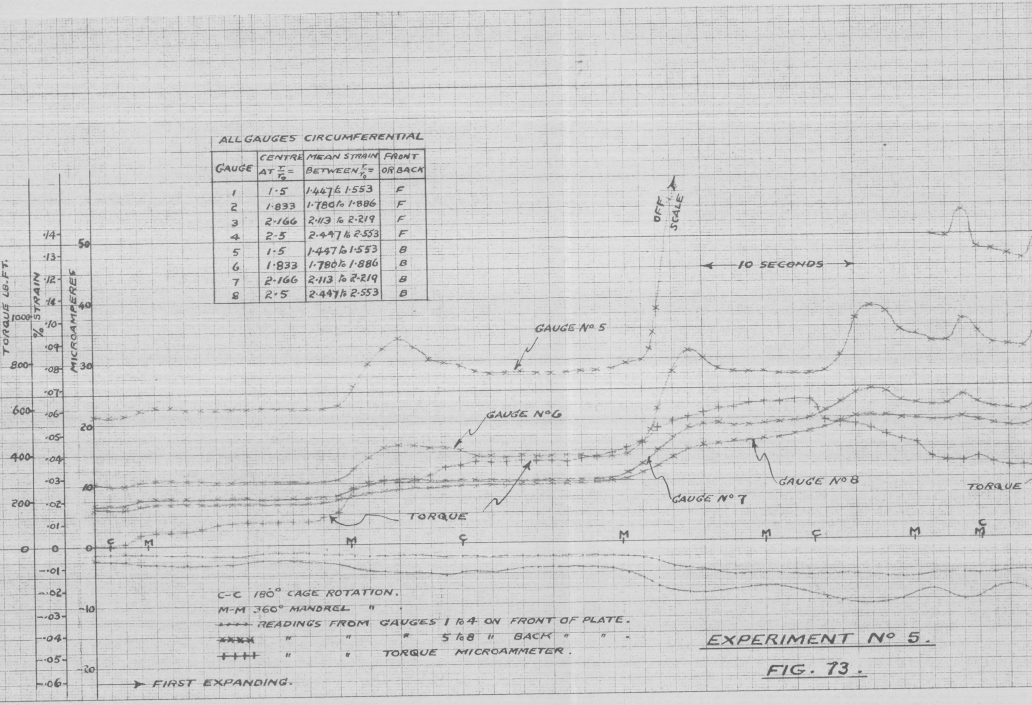

ALL GAUGES CIRCUMFERENTIAL

GAUGE	CENTRE AT $\frac{r}{r_0}=$	MEAN STRAIN BETWEEN $\frac{r}{r_0}=$	FRONT OR BACK
1	1·5	1·447 to 1·553	F
2	1·833	1·780 to 1·886	F
3	2·166	2·113 to 2·219	F
4	2·5	2·447 to 2·553	F
5	1·5	1·447 to 1·553	B
6	1·833	1·780 to 1·886	B
7	2·166	2·113 to 2·219	B
8	2·5	2·447 to 2·553	B

EXPERIMENT No 5.

FIG. 73.

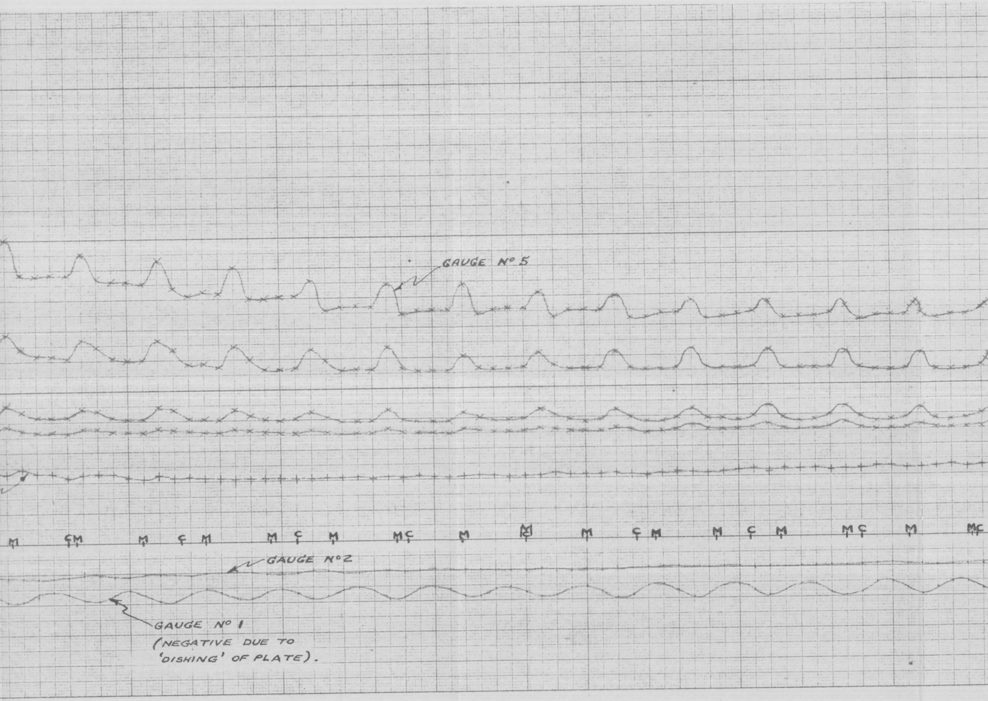

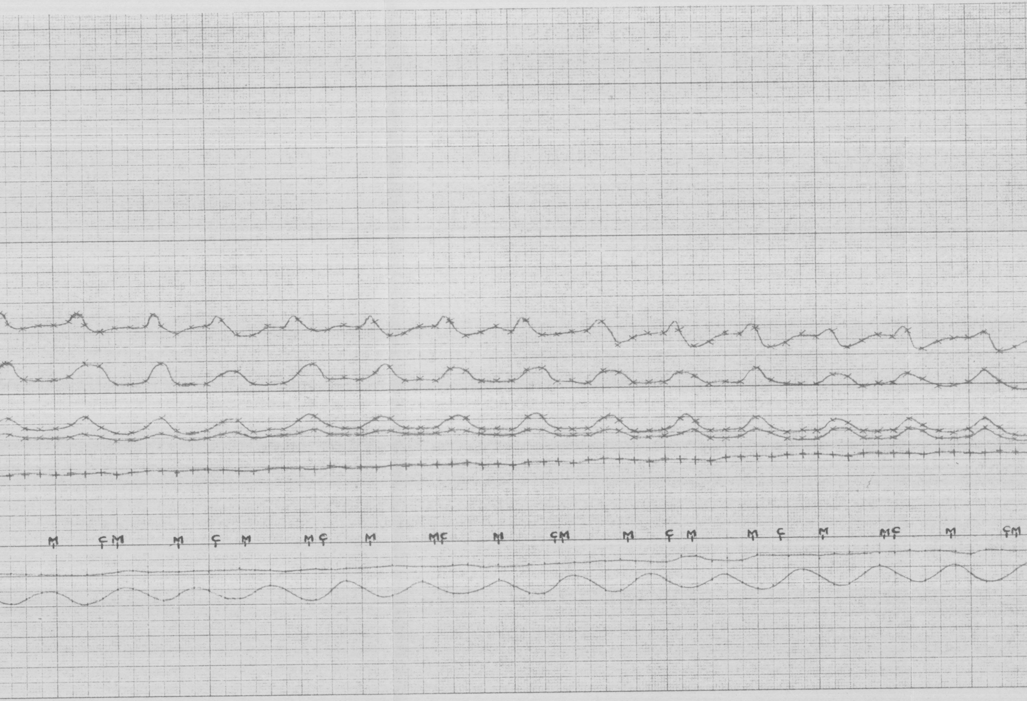

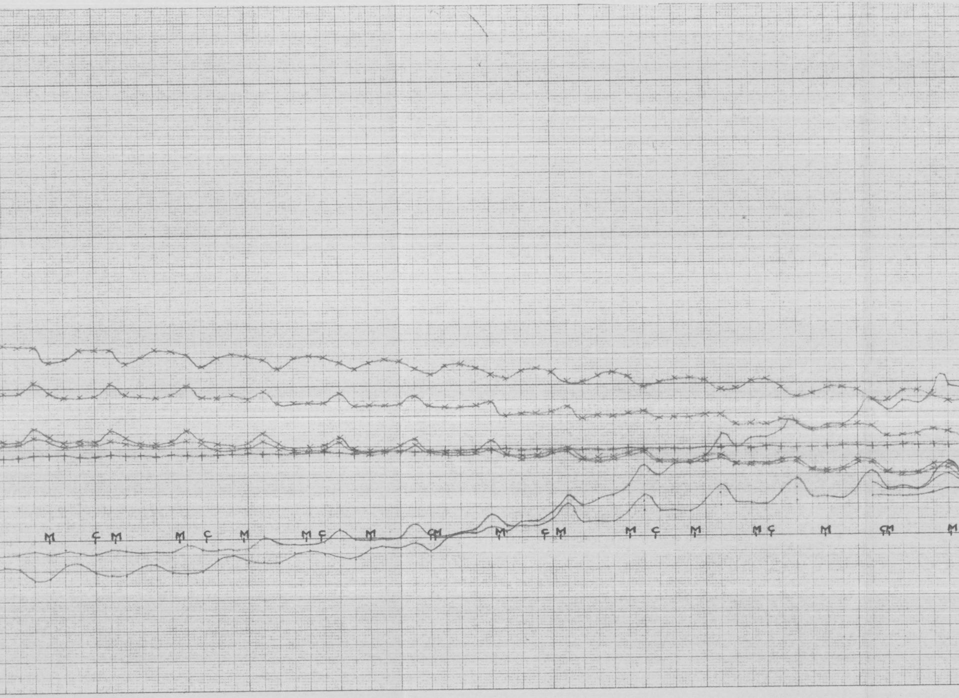

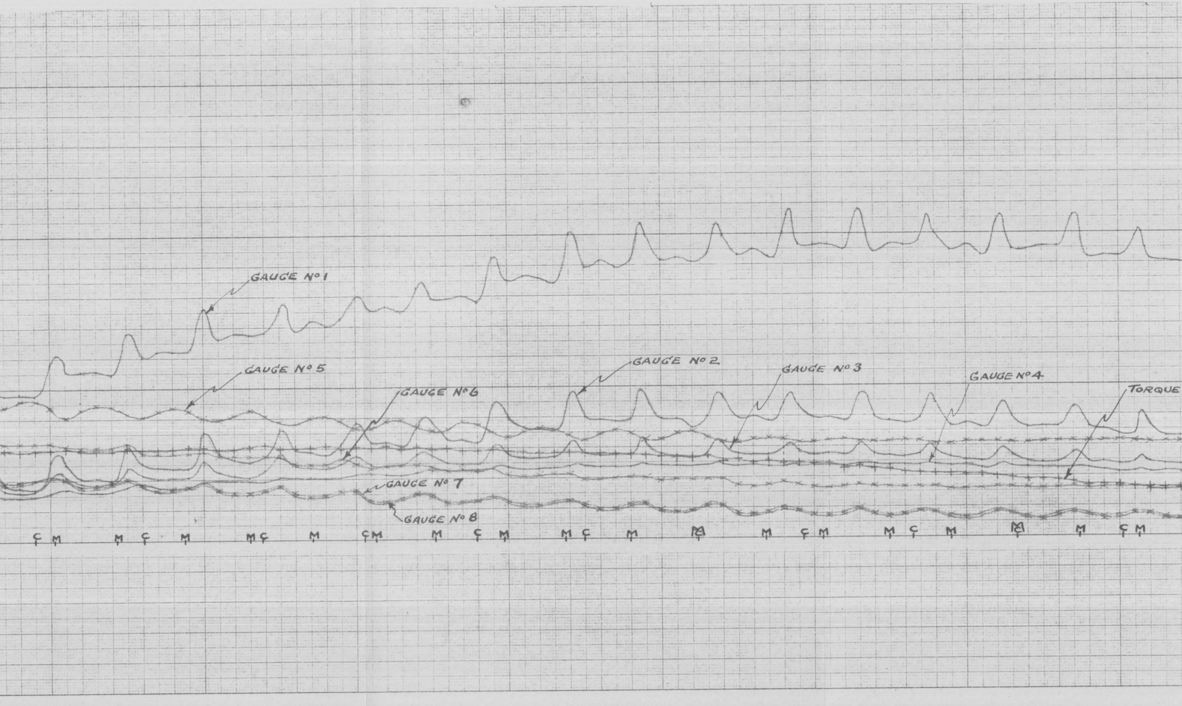

END OF FIRST PASS
(RETRACTIVE EXPANDERS).

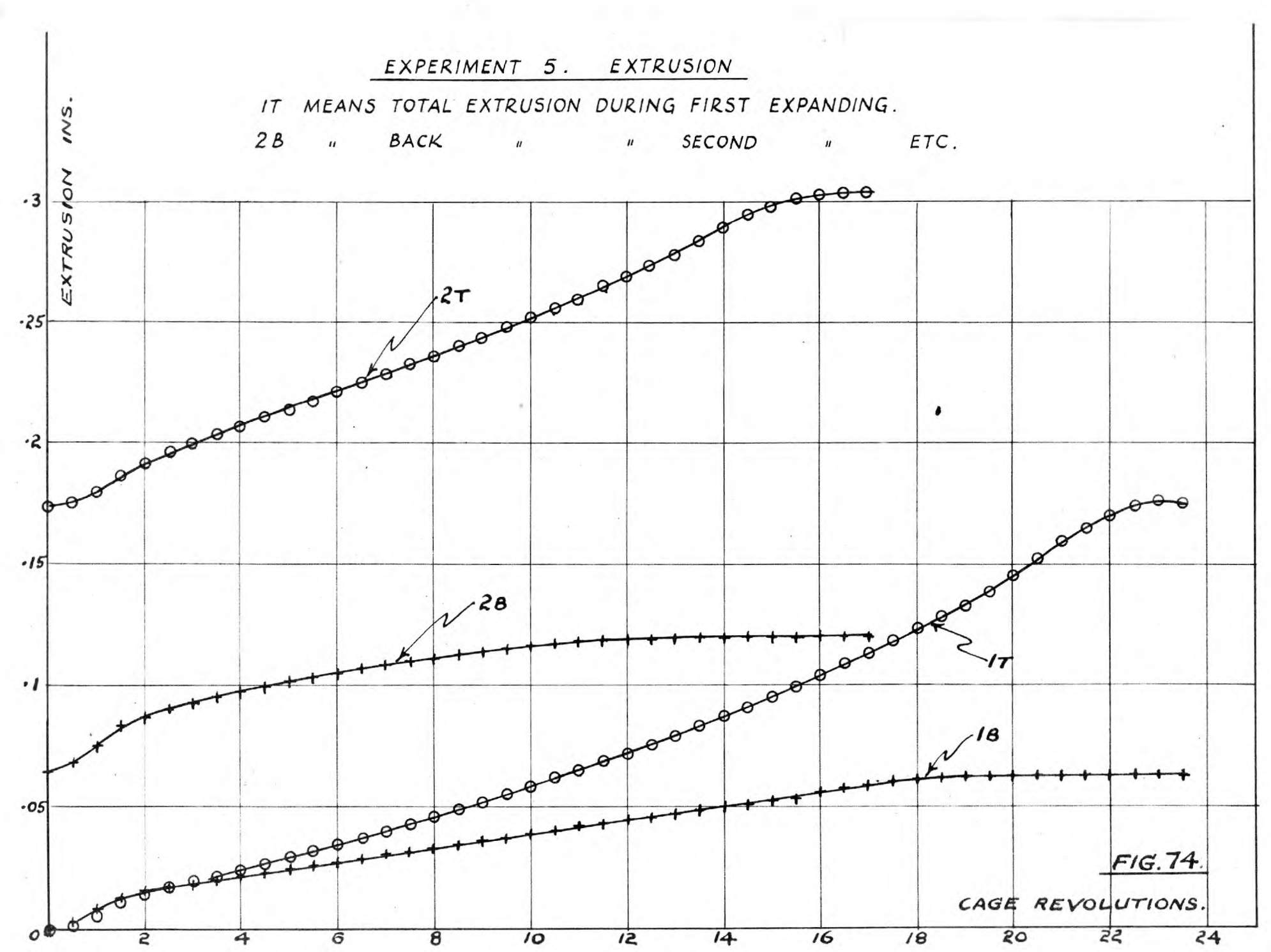
EXPERIMENT 5. EXTRUSION
IT MEANS TOTAL EXTRUSION DURING FIRST EXPANDING.
2B " BACK " " SECOND " ETC.
EXTRUSION INS.
·3
·25
·2
·15
·1
·05
0
2T
2B
1T
1B
2
4
6
8
10
12
14
16
18
20
22
24
CAGE REVOLUTIONS.

FIG. 74.

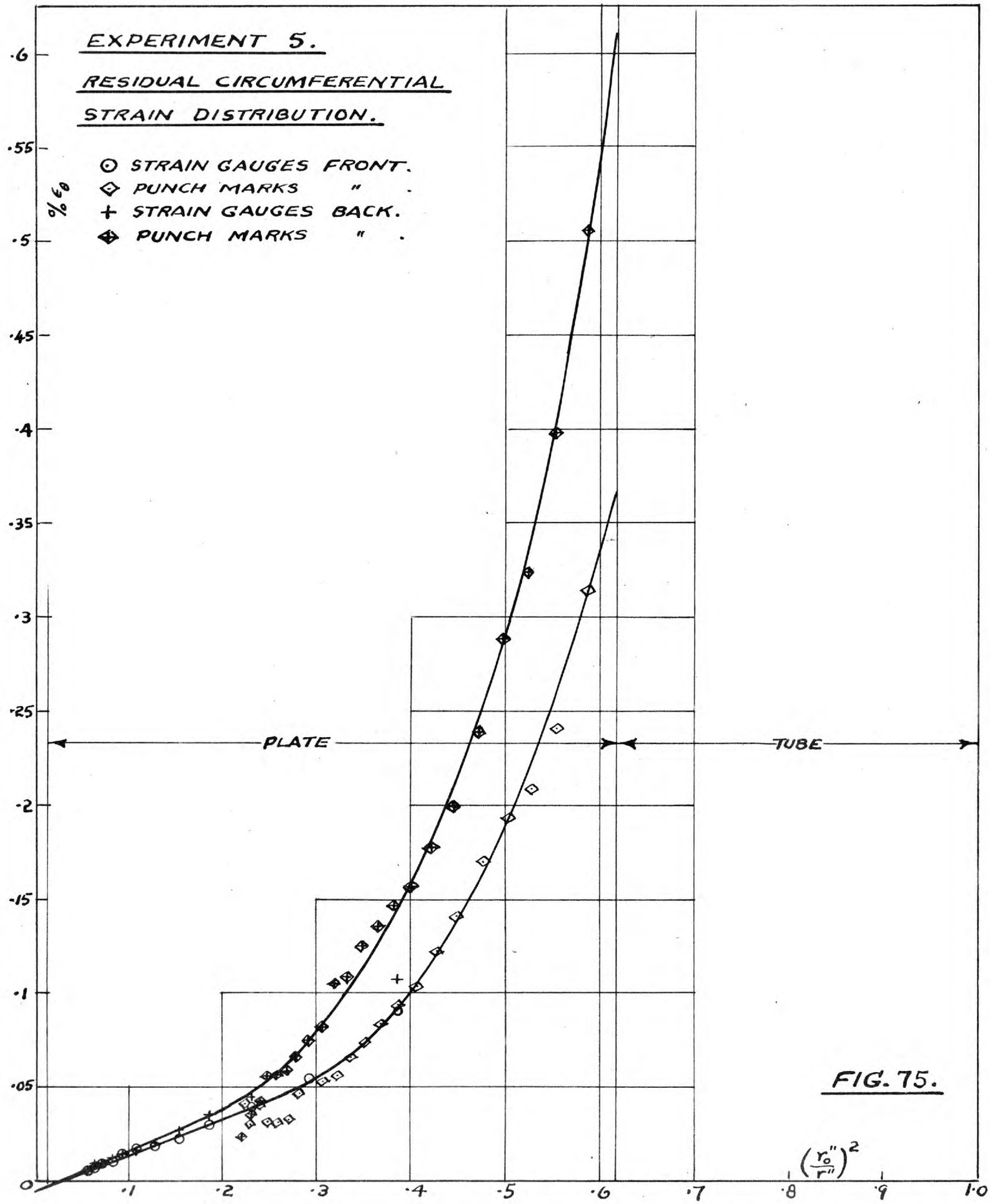
EXPERIMENT 5.
RESIDUAL CIRCUMFERENTIAL STRAIN DISTRIBUTION.
⊙ STRAIN GAUGES FRONT.
◇ PUNCH MARKS " .
+ STRAIN GAUGES BACK.
◈ PUNCH MARKS " .
% ϵ_θ
·6
·55
·5
·45
·4
·35
·3
·25
·2
·15
·1
·05
0
PLATE
TUBE
·1
·2
·3
·4
·5
·6
·7
·8
·9
1·0
$\left(\frac{r_o''}{r''}\right)^2$

FIG. 75.

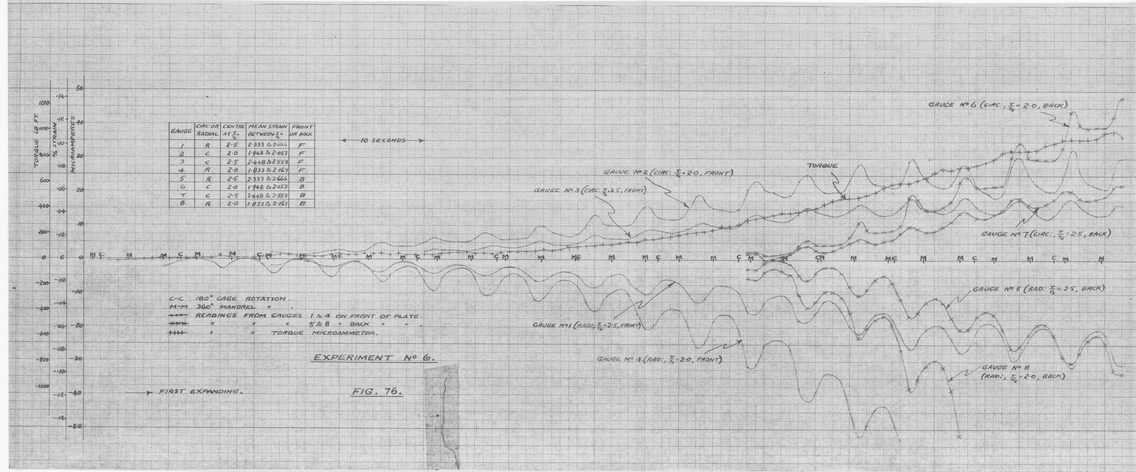

GAUGE	CIRC OR RADIAL	r/r0	CENTRE BETWEEN	MEAN STRAIN	FRONT OR BACK
1	R	2·5	2333 & 2466		F
2	C	2·0	1968 & 2403		F
3	C	2·5	2468 & 2533		F
4	R	2·0	1833 & 2467		F
5	R	2·5	2333 & 2466		B
6	C	2·0	1968 & 2403		B
7	C	2·5	2468 & 2533		B
8	R	2·0	1833 & 2467		B

EXPERIMENT Nº 6.

FIG. 76.

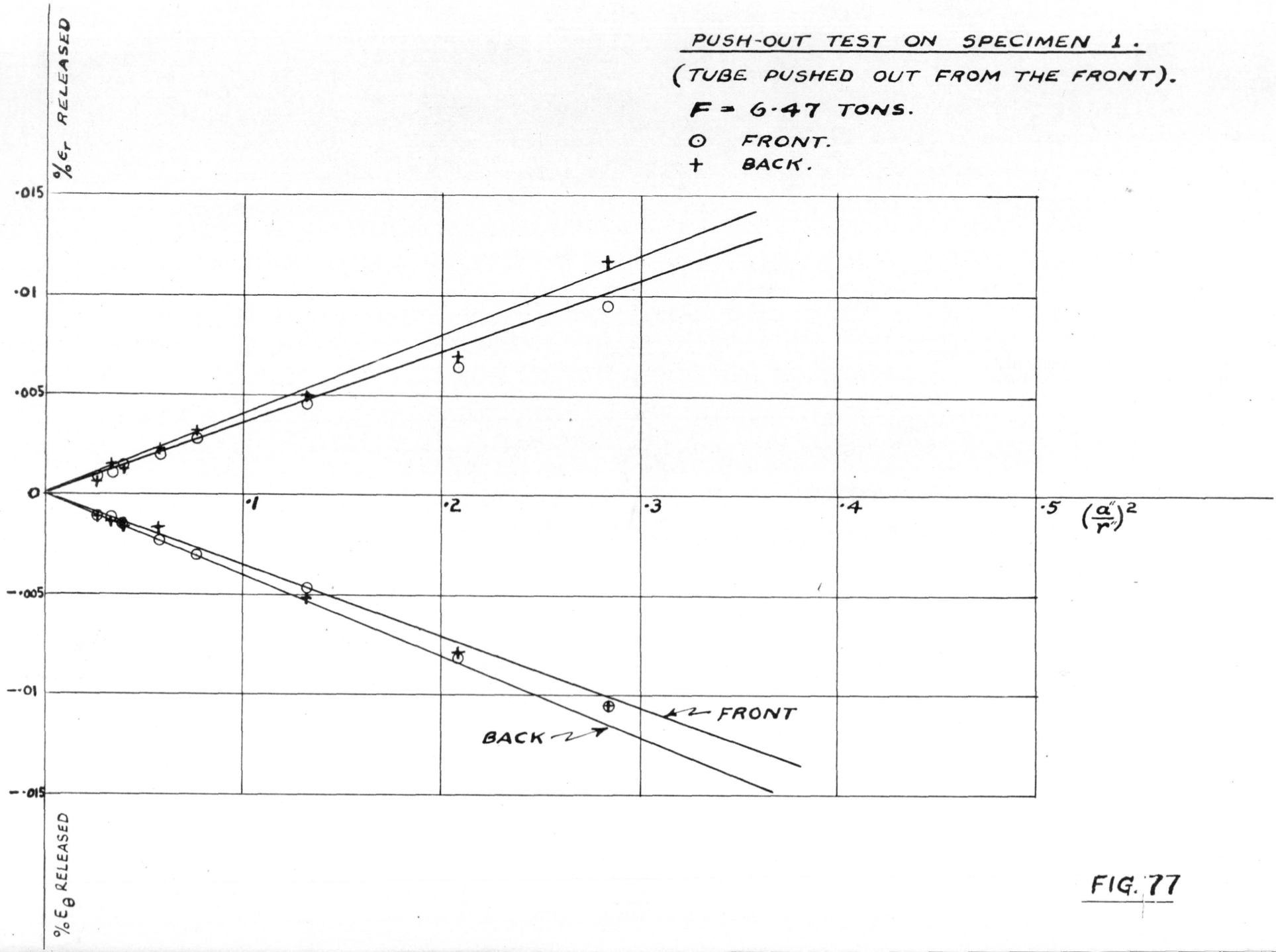
PUSH-OUT TEST ON SPECIMEN 1.
(TUBE PUSHED OUT FROM THE FRONT).
F = 6·47 TONS.
⊙ FRONT.
+ BACK.
% ϵ_r RELEASED
·015
·01
·005
0
·1
·2
·3
·4
·5
$(\frac{a''}{r''})^2$
-·005
-·01
-·015
FRONT
BACK
% ϵ_θ RELEASED

FIG. 77

PUSH-OUT TEST ON SPECIMEN 2.

(TUBE PUSHED OUT FROM THE BACK).

F = 3·97 TONS.

⊙ FRONT.

\+ BACK.

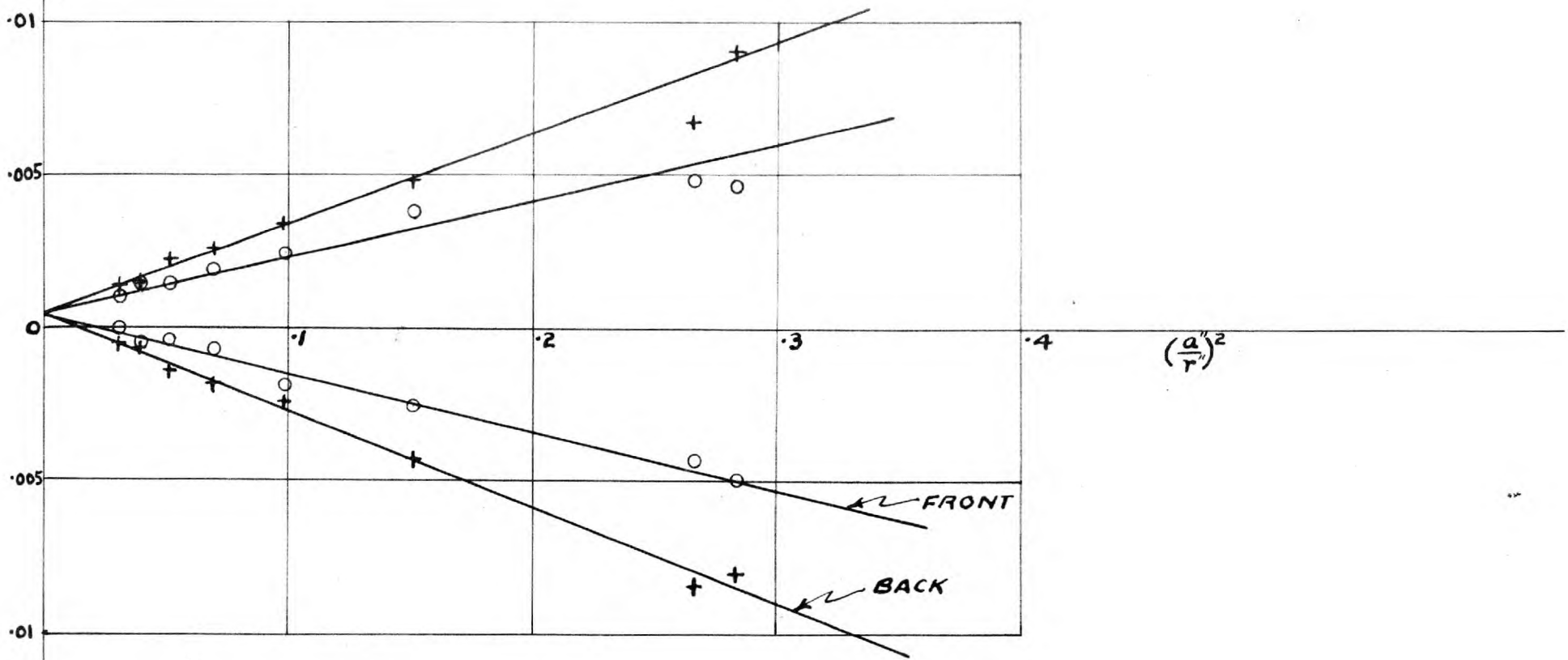

FIG. 78.

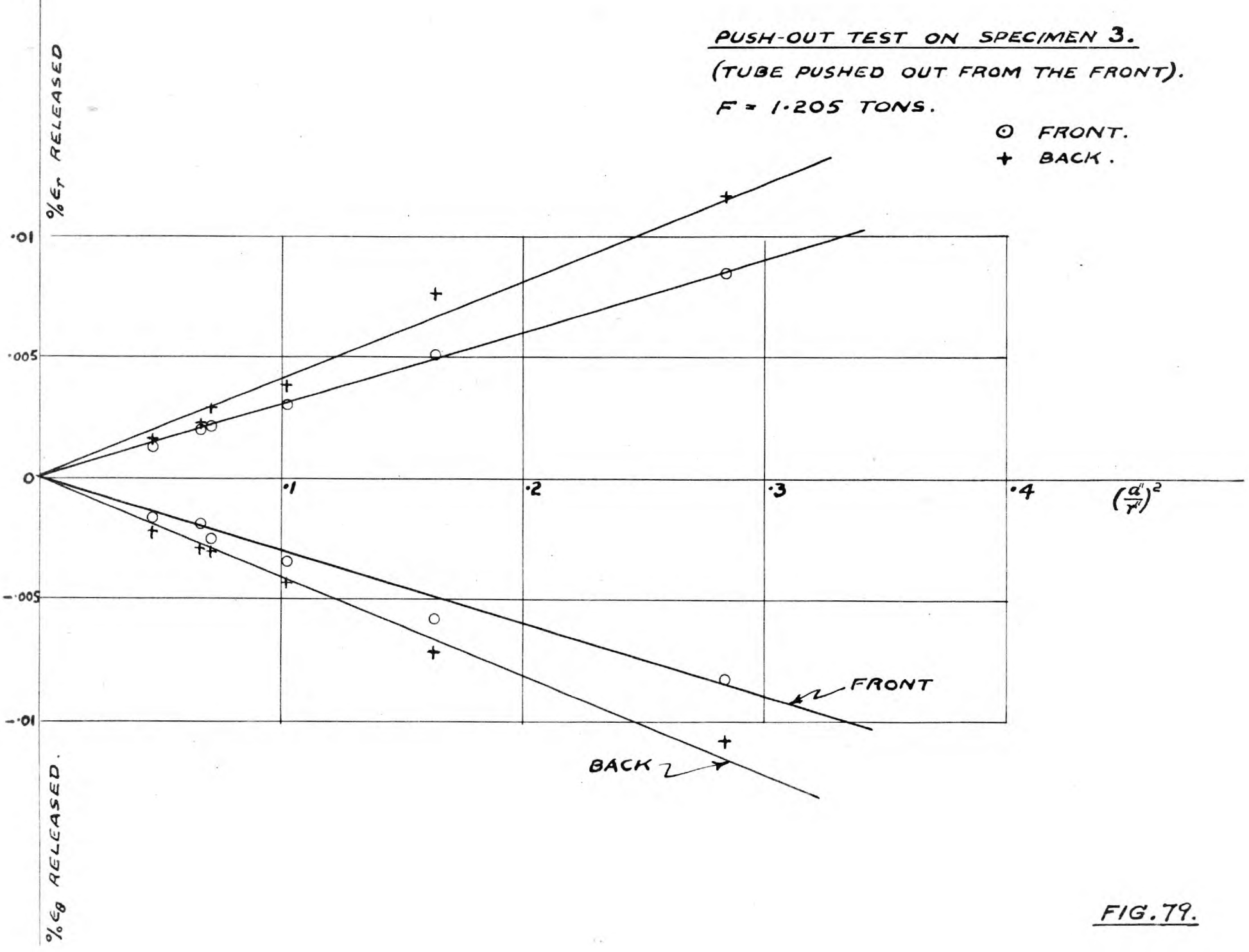
PUSH-OUT TEST ON SPECIMEN 3.
(TUBE PUSHED OUT FROM THE FRONT).
F = 1·205 TONS.
⊙ FRONT.
+ BACK.
%εr RELEASED
·01
·005
0
·1
·2
·3
·4
(a''/r'')²
-·005
-·01
FRONT
BACK
%εθ RELEASED.

FIG. 79.

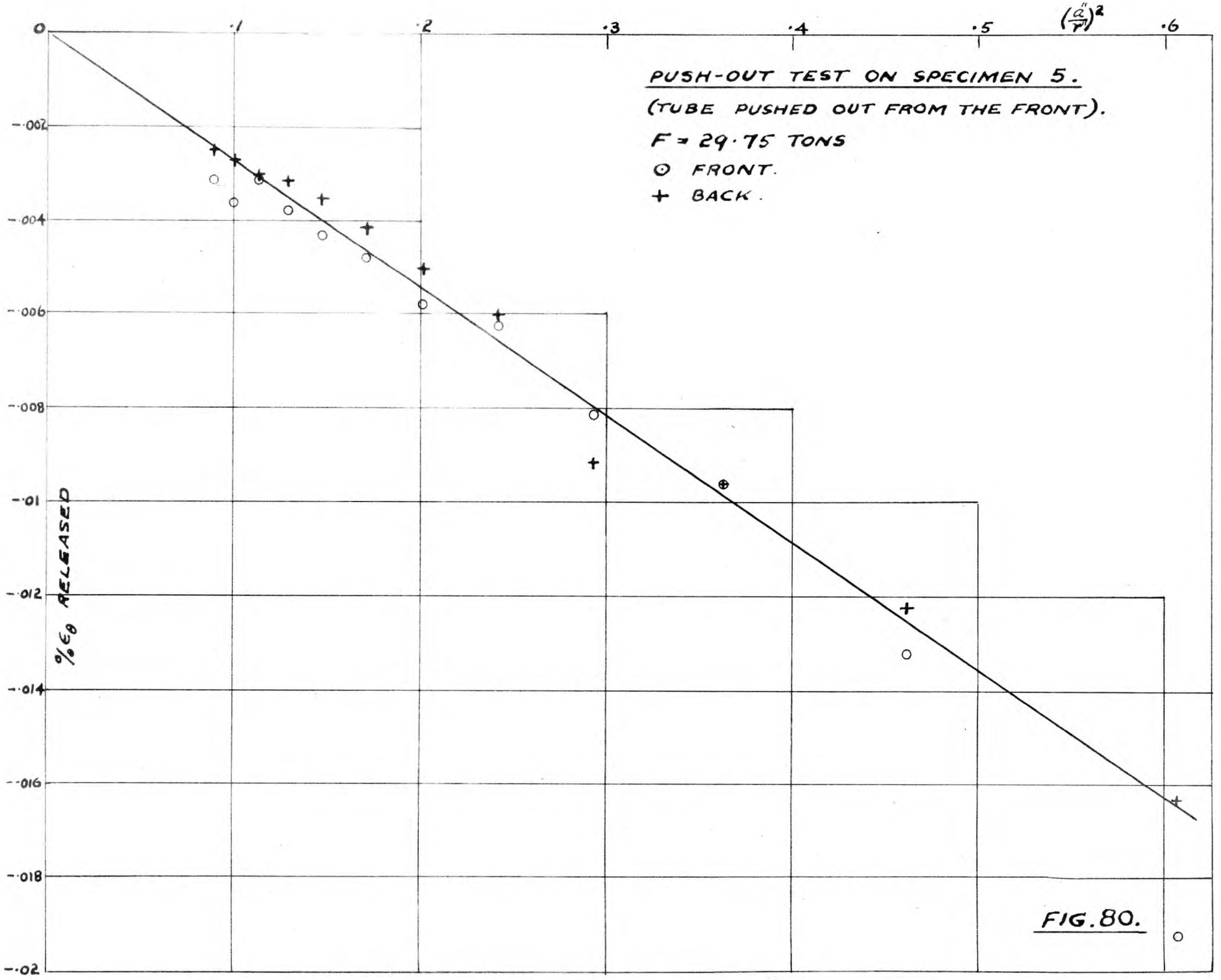
PUSH-OUT TEST ON SPECIMEN 5.
(TUBE PUSHED OUT FROM THE FRONT).
F = 29·75 TONS
⊙ FRONT.
+ BACK.
0
·1
·2
·3
·4
·5
·6
$(\frac{a''}{r'})^2$
-·002
-·004
-·006
-·008
-·01
-·012
-·014
-·016
-·018
-·02
% ϵ_θ RELEASED

FIG. 80.

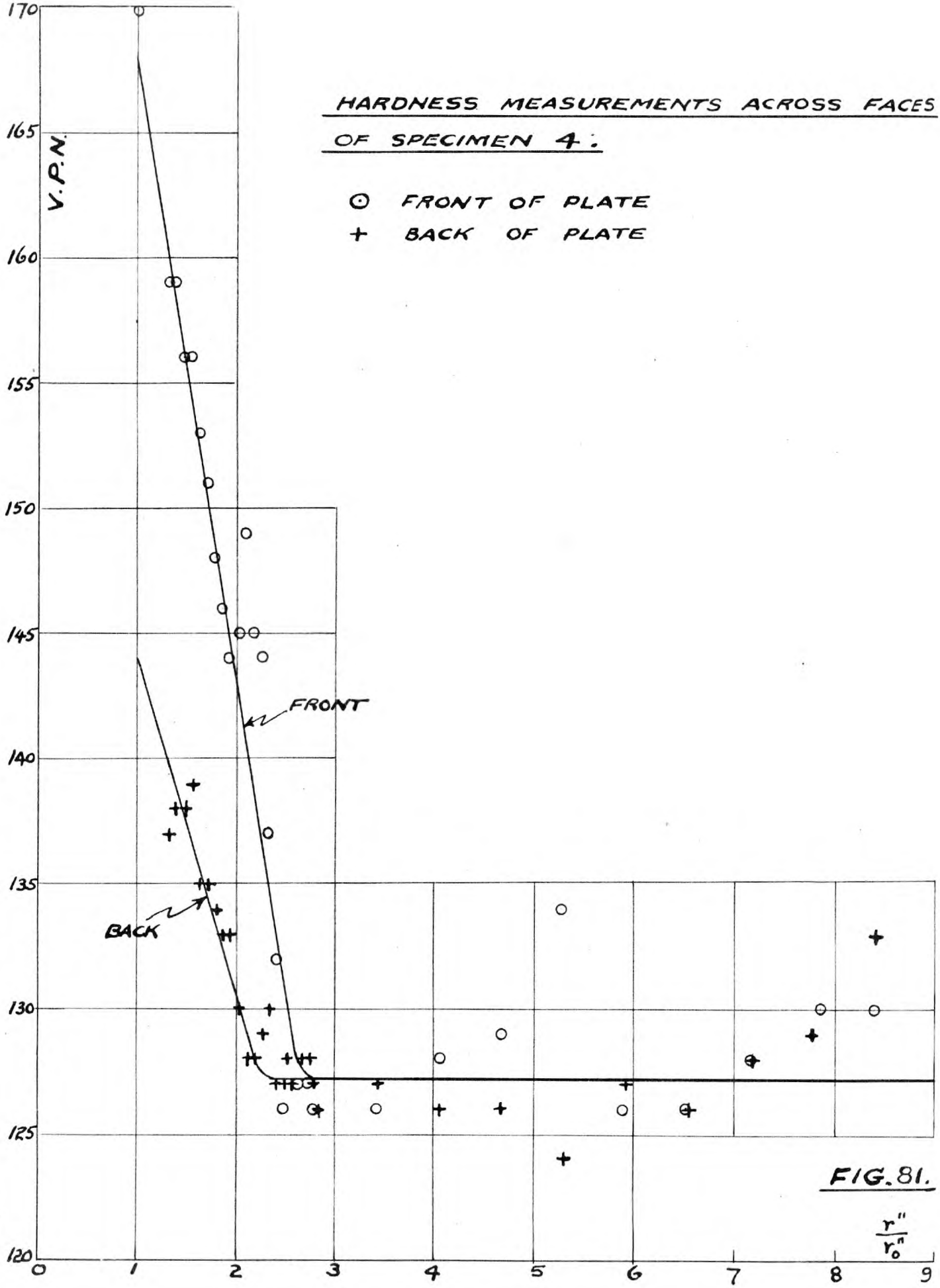
HARDNESS MEASUREMENTS ACROSS FACES OF SPECIMEN 4.
⊙ FRONT OF PLATE
+ BACK OF PLATE
V.P.N.
170
165
160
155
150
145
140
135
130
125
120
FRONT
BACK
0
1
2
3
4
5
6
7
8
9
r''/r₀''

FIG. 81.

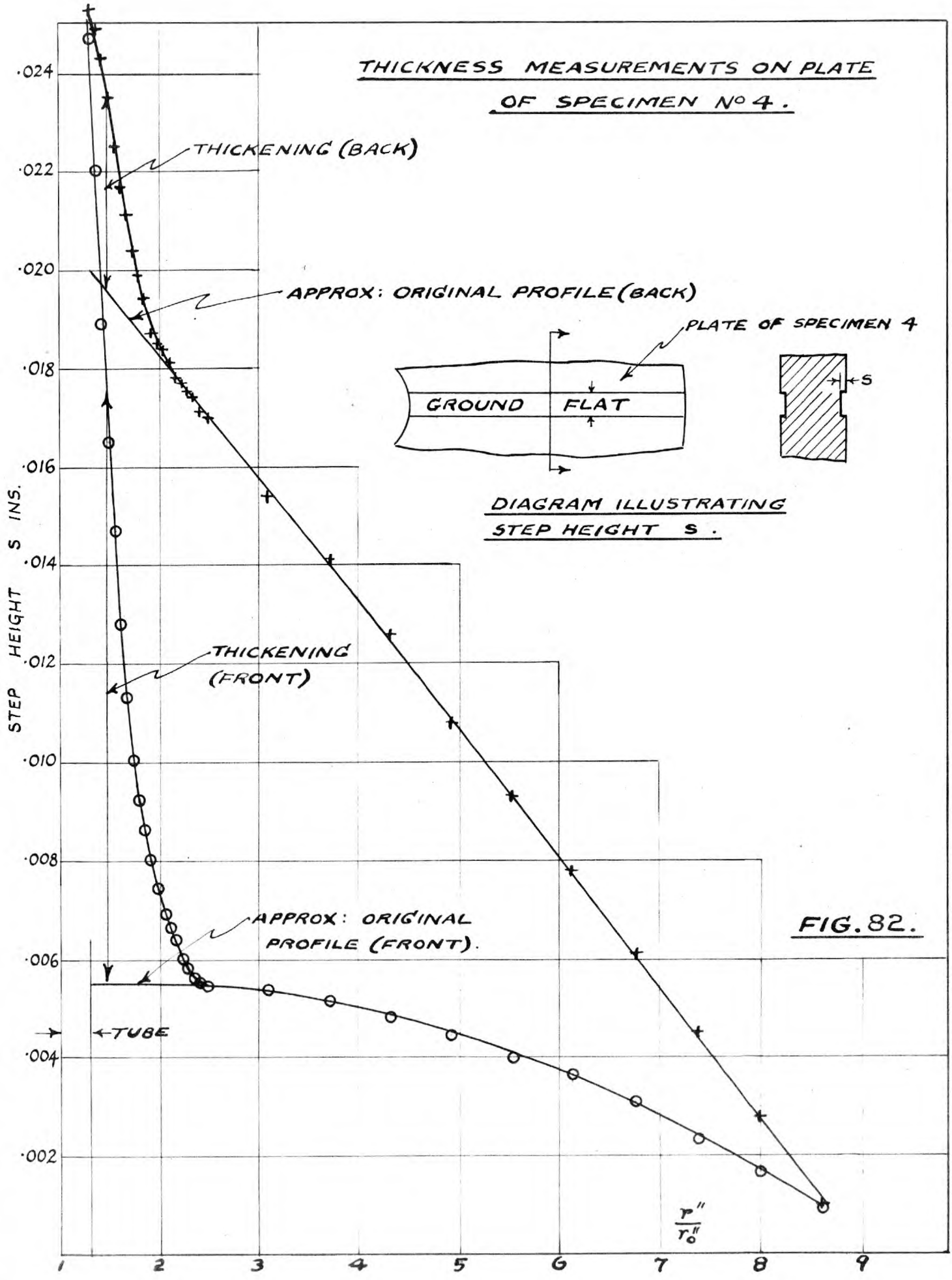
THICKNESS MEASUREMENTS ON PLATE
OF SPECIMEN No 4.
THICKENING (BACK)
APPROX: ORIGINAL PROFILE (BACK)
PLATE OF SPECIMEN 4
GROUND
FLAT
S
DIAGRAM ILLUSTRATING
STEP HEIGHT S.
THICKENING
(FRONT)
APPROX: ORIGINAL
PROFILE (FRONT).
TUBE
STEP HEIGHT S INS.
·024
·022
·020
·018
·016
·014
·012
·010
·008
·006
·004
·002
1
2
3
4
5
6
7
8
9
r''/r₀''

FIG. 82.

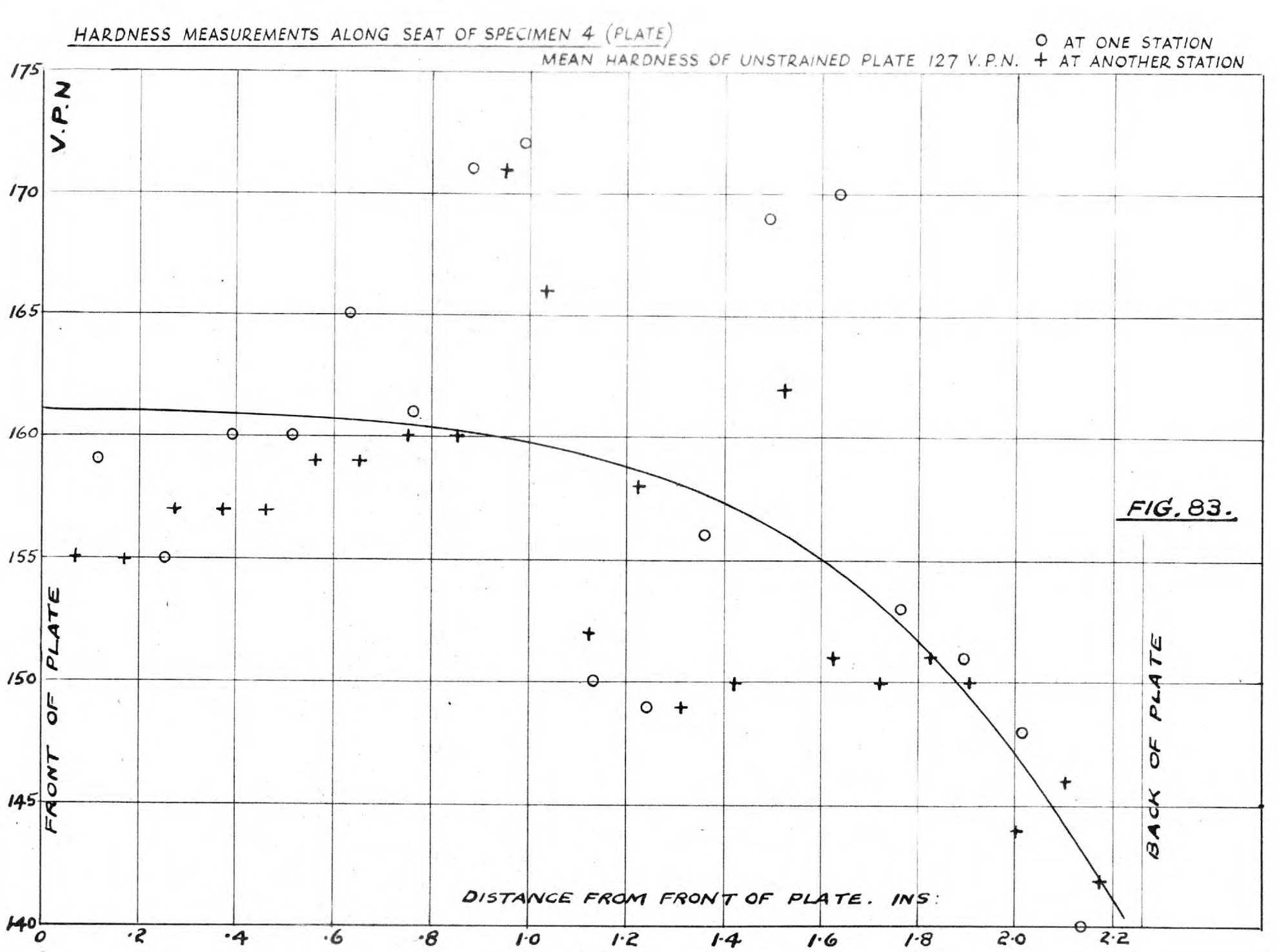
HARDNESS MEASUREMENTS ALONG SEAT OF SPECIMEN 4 (PLATE)
MEAN HARDNESS OF UNSTRAINED PLATE 127 V.P.N.
O AT ONE STATION
+ AT ANOTHER STATION
V.P.N
175
170
165
160
155
150
145
140
FRONT OF PLATE
BACK OF PLATE
DISTANCE FROM FRONT OF PLATE. INS:
0
·2
·4
·6
·8
1·0
1·2
1·4
1·6
1·8
2·0
2·2
FIG. 83.

HARDNESS ALONG OUTSIDE OF TUBE. (SEAT) (SPECIMEN 4)

MEAN HARDNESS OF UNSTRAINED TUBE 109 V.P.N.

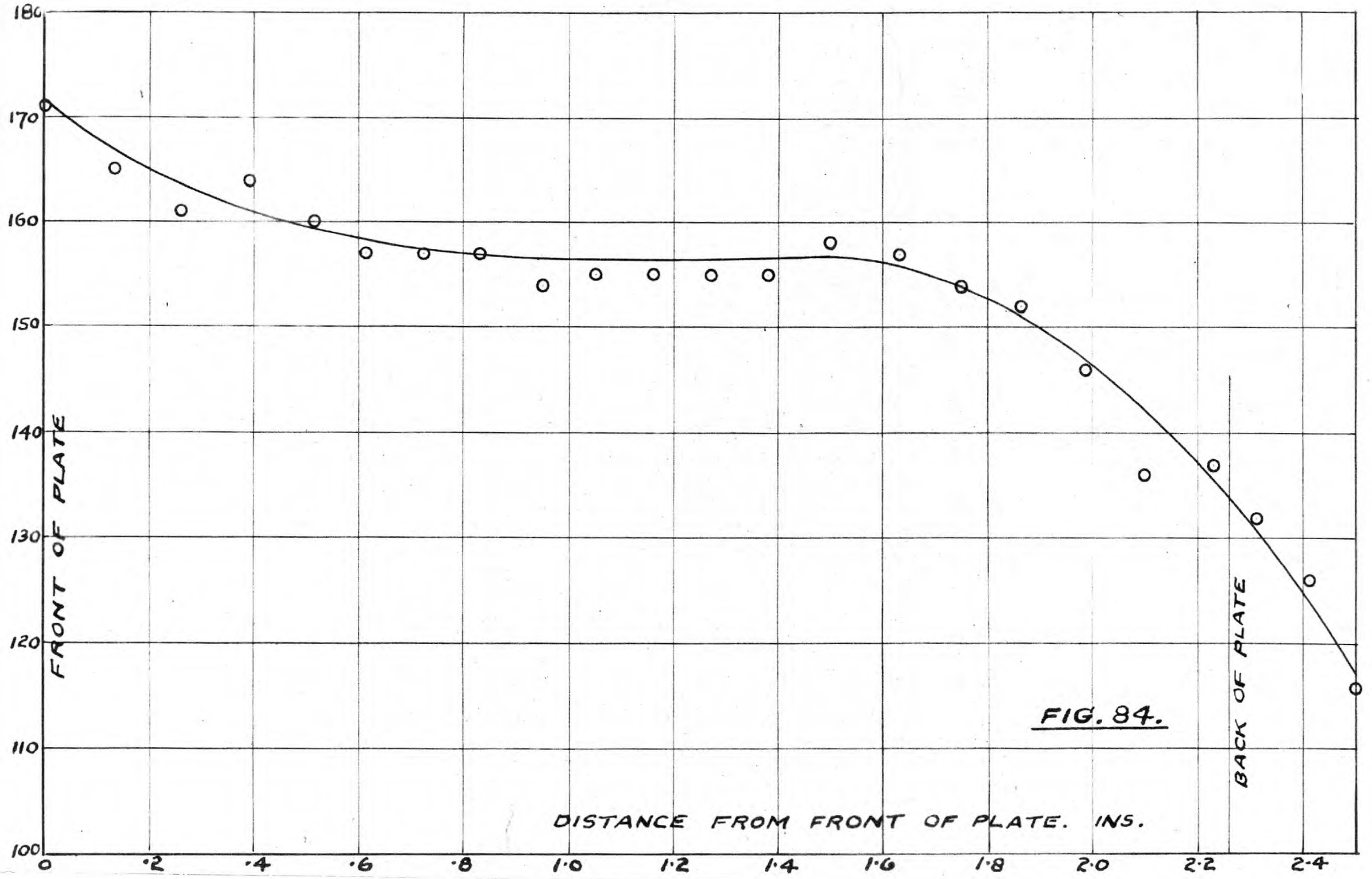

FIG. 84.

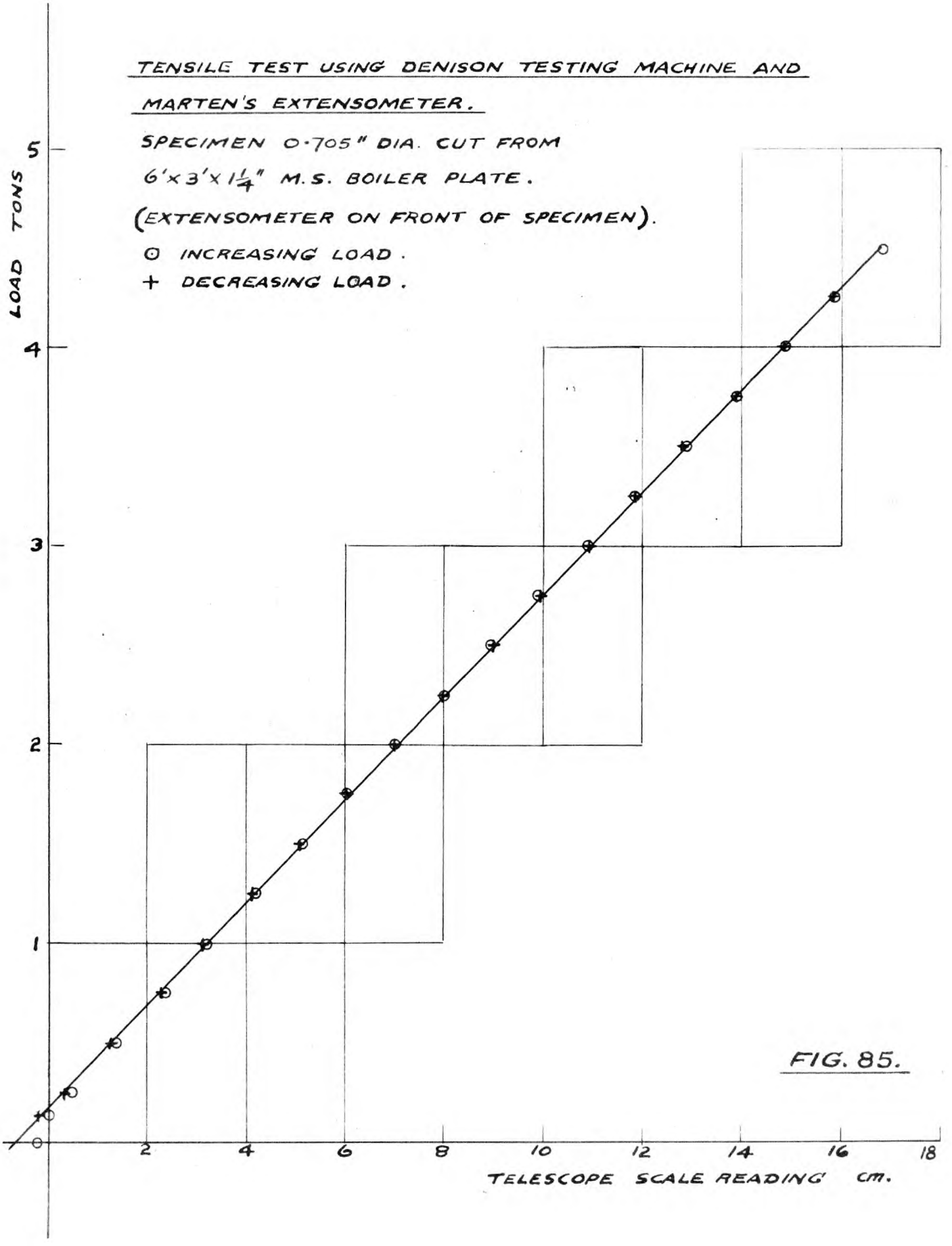
TENSILE TEST USING DENISON TESTING MACHINE AND
MARTEN'S EXTENSOMETER.
SPECIMEN 0·705" DIA. CUT FROM
6'x3'x1¼" M.S. BOILER PLATE.
(EXTENSOMETER ON FRONT OF SPECIMEN).
⊙ INCREASING LOAD.
+ DECREASING LOAD.
LOAD TONS
5
4
3
2
1
2
4
6
8
10
12
14
16
18
TELESCOPE SCALE READING cm.

FIG. 85.

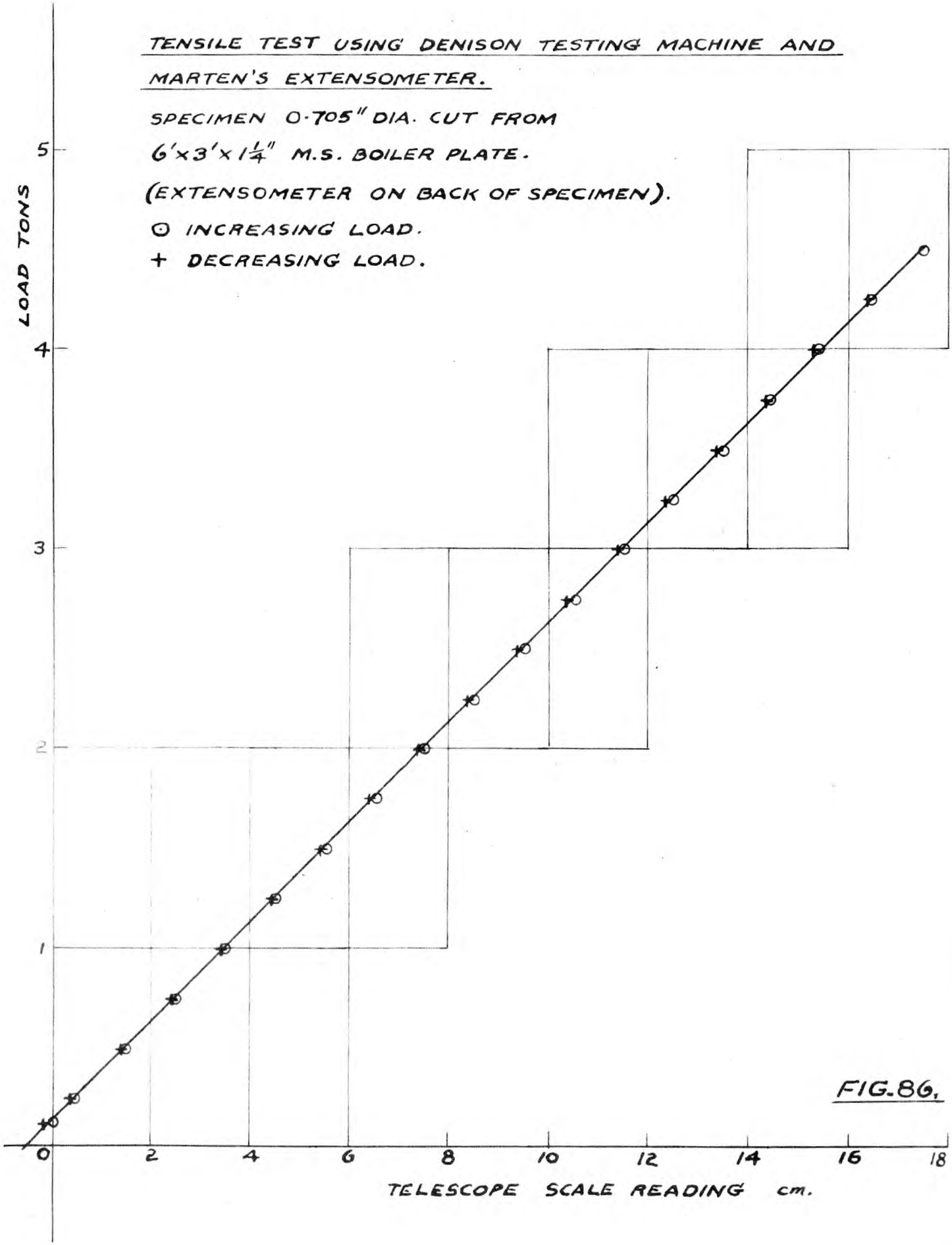
TENSILE TEST USING DENISON TESTING MACHINE AND MARTEN'S EXTENSOMETER.
SPECIMEN 0·705" DIA. CUT FROM 6'×3'×1¼" M.S. BOILER PLATE.
(EXTENSOMETER ON BACK OF SPECIMEN).
⊙ INCREASING LOAD.
+ DECREASING LOAD.
LOAD TONS
5
4
3
2
1
0
2
4
6
8
10
12
14
16
18
TELESCOPE SCALE READING cm.

FIG. 86.

TENSILE TEST USING DENISON TESTING MACHINE AND EWING 8" EXTENSOMETER.

SPECIMEN 0·693 IN DIA. CUT FROM 6'x3'x1¼" M.S. BOILER PLATE.

⊙ INCREASING LOAD.

\+ DECREASING LOAD.

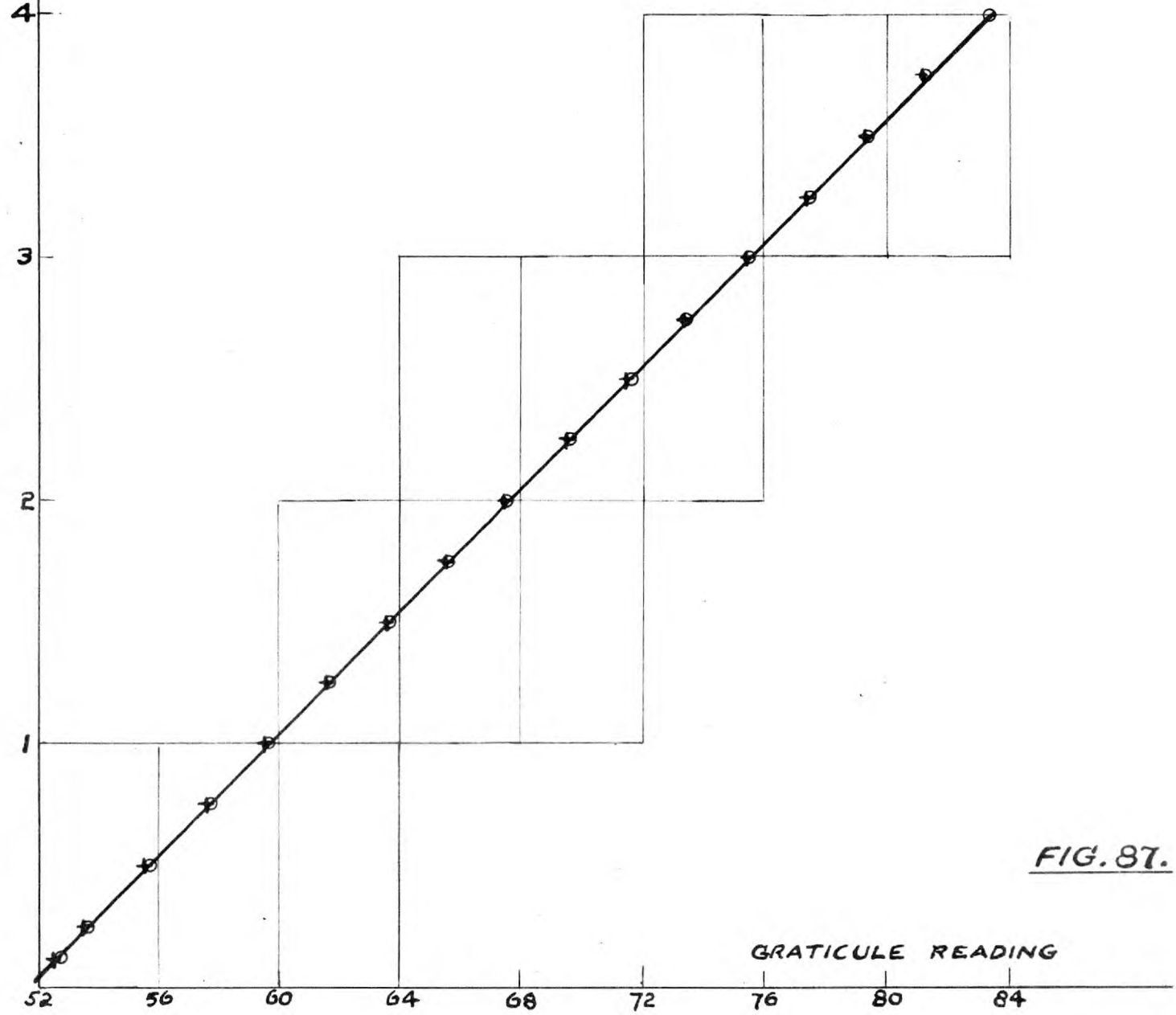

FIG. 87.

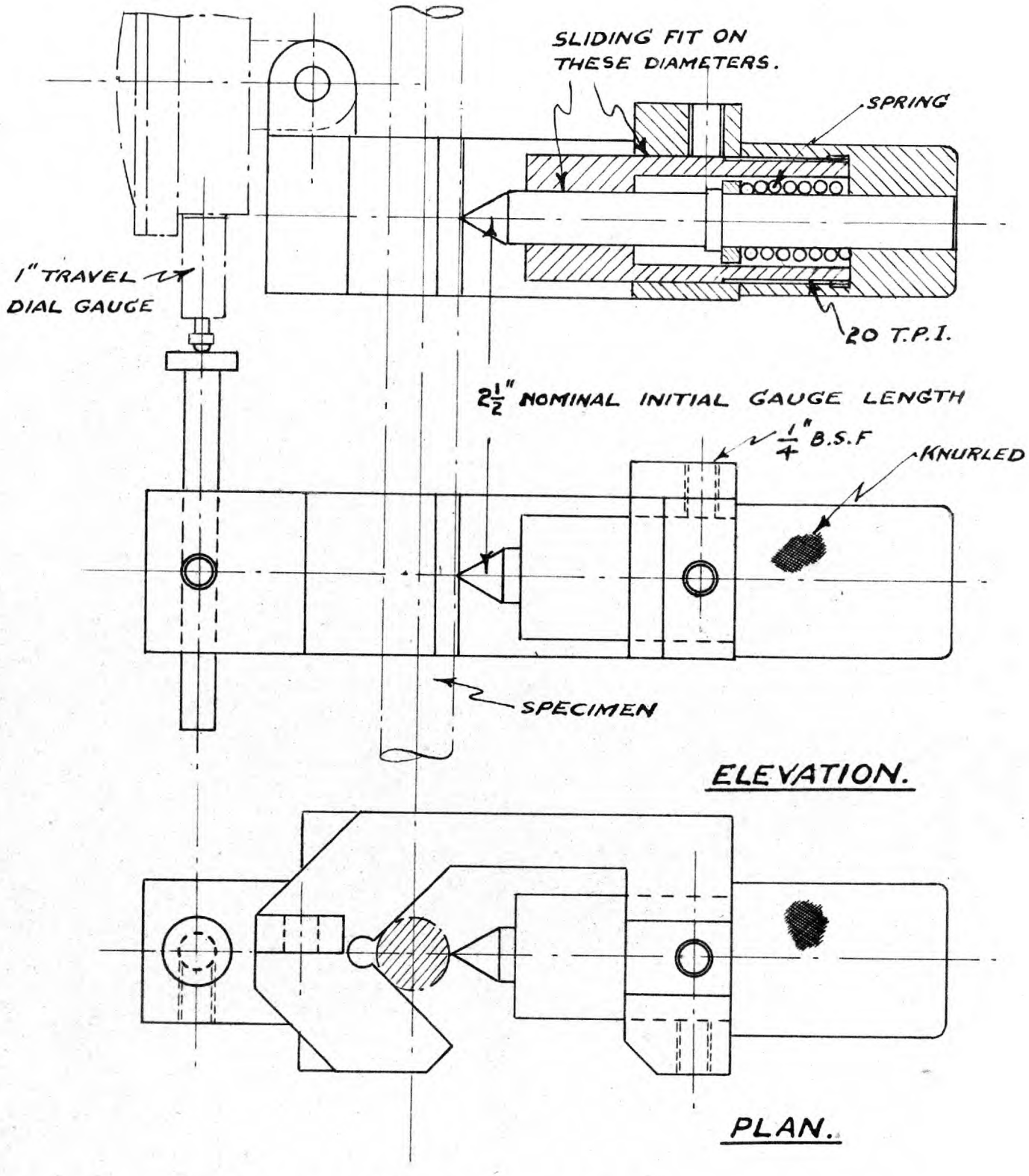

EXTENSOMETER FOR MEASURING LARGE STRAINS.

(FULL SCALE.)

FIG. 88.

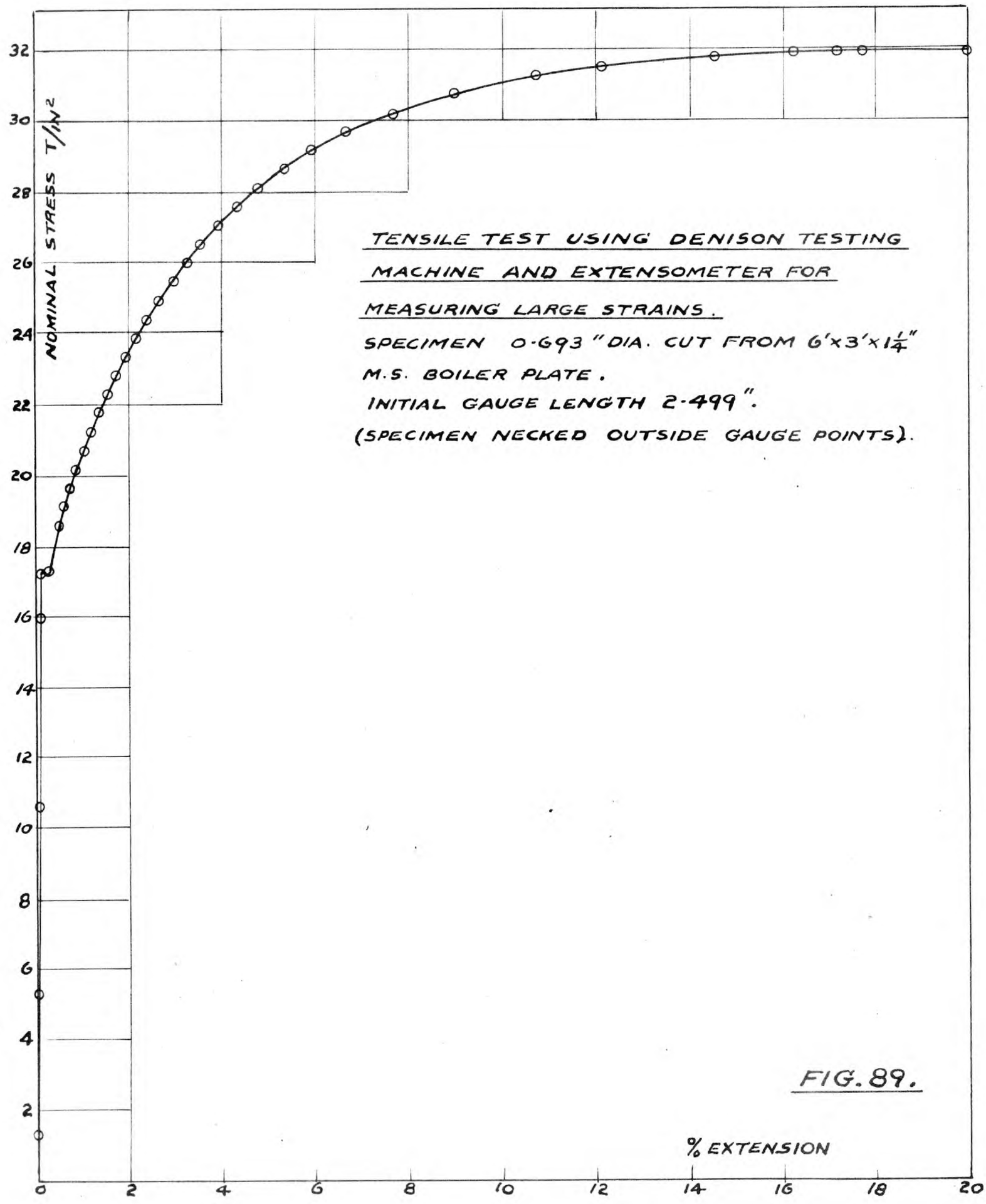

TENSILE TEST USING DENISON TESTING MACHINE AND EXTENSOMETER FOR MEASURING LARGE STRAINS.

SPECIMEN 0·693" DIA. CUT FROM 6'x3'x1¼" M.S. BOILER PLATE.

INITIAL GAUGE LENGTH 2·499".

(SPECIMEN NECKED OUTSIDE GAUGE POINTS).

FIG. 89.

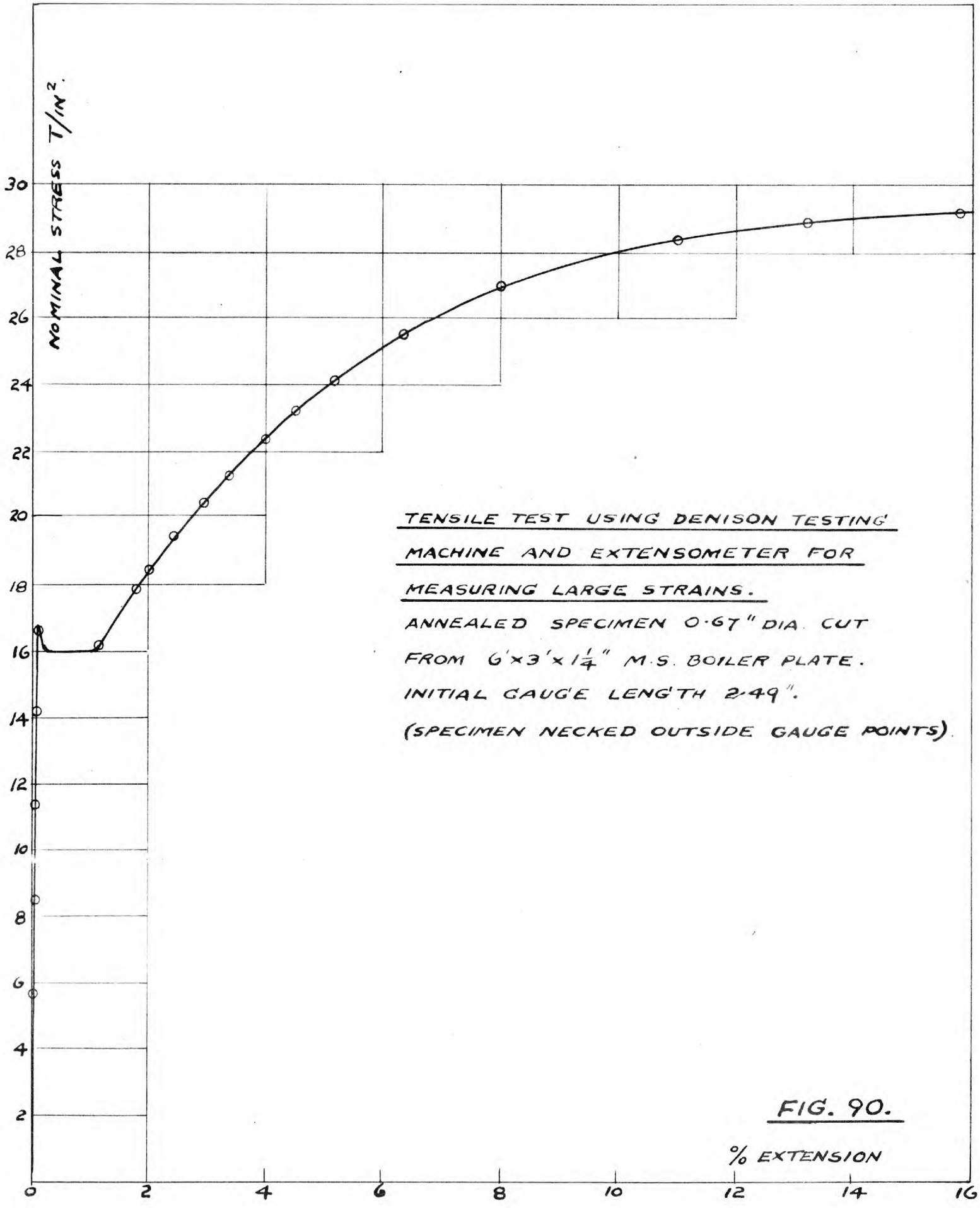

TENSILE TEST USING DENISON TESTING MACHINE AND EXTENSOMETER FOR MEASURING LARGE STRAINS.

ANNEALED SPECIMEN 0·67" DIA. CUT FROM 6'×3'×1¼" M.S. BOILER PLATE.

INITIAL GAUGE LENGTH 2·49".

(SPECIMEN NECKED OUTSIDE GAUGE POINTS).

FIG. 90.

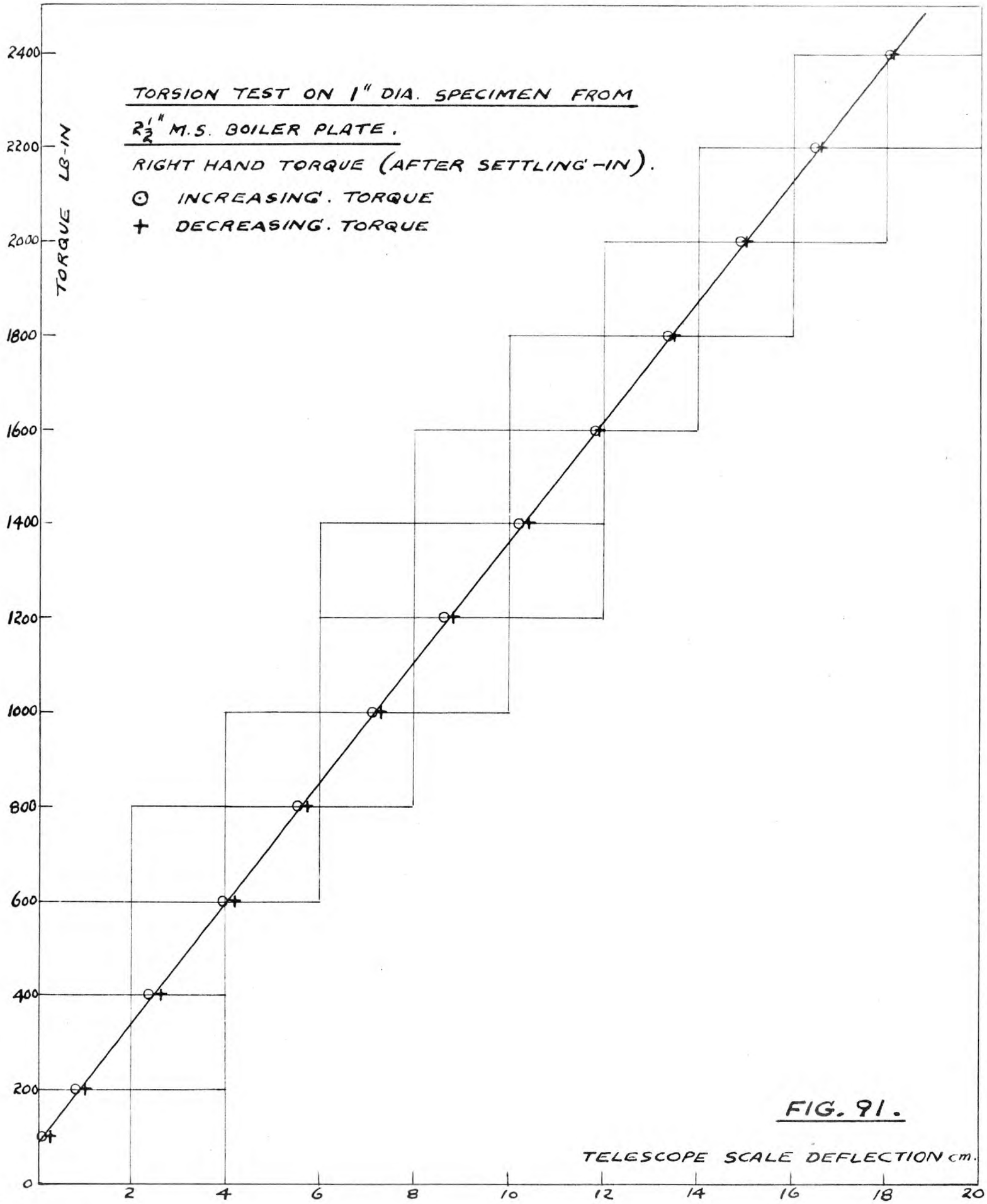
TORSION TEST ON 1" DIA. SPECIMEN FROM
2½" M.S. BOILER PLATE.
RIGHT HAND TORQUE (AFTER SETTLING-IN).
⊙ INCREASING. TORQUE
+ DECREASING. TORQUE
TORQUE LB-IN
2400
2200
2000
1800
1600
1400
1200
1000
800
600
400
200
0
2
4
6
8
10
12
14
16
18
20
TELESCOPE SCALE DEFLECTION cm.

FIG. 91.

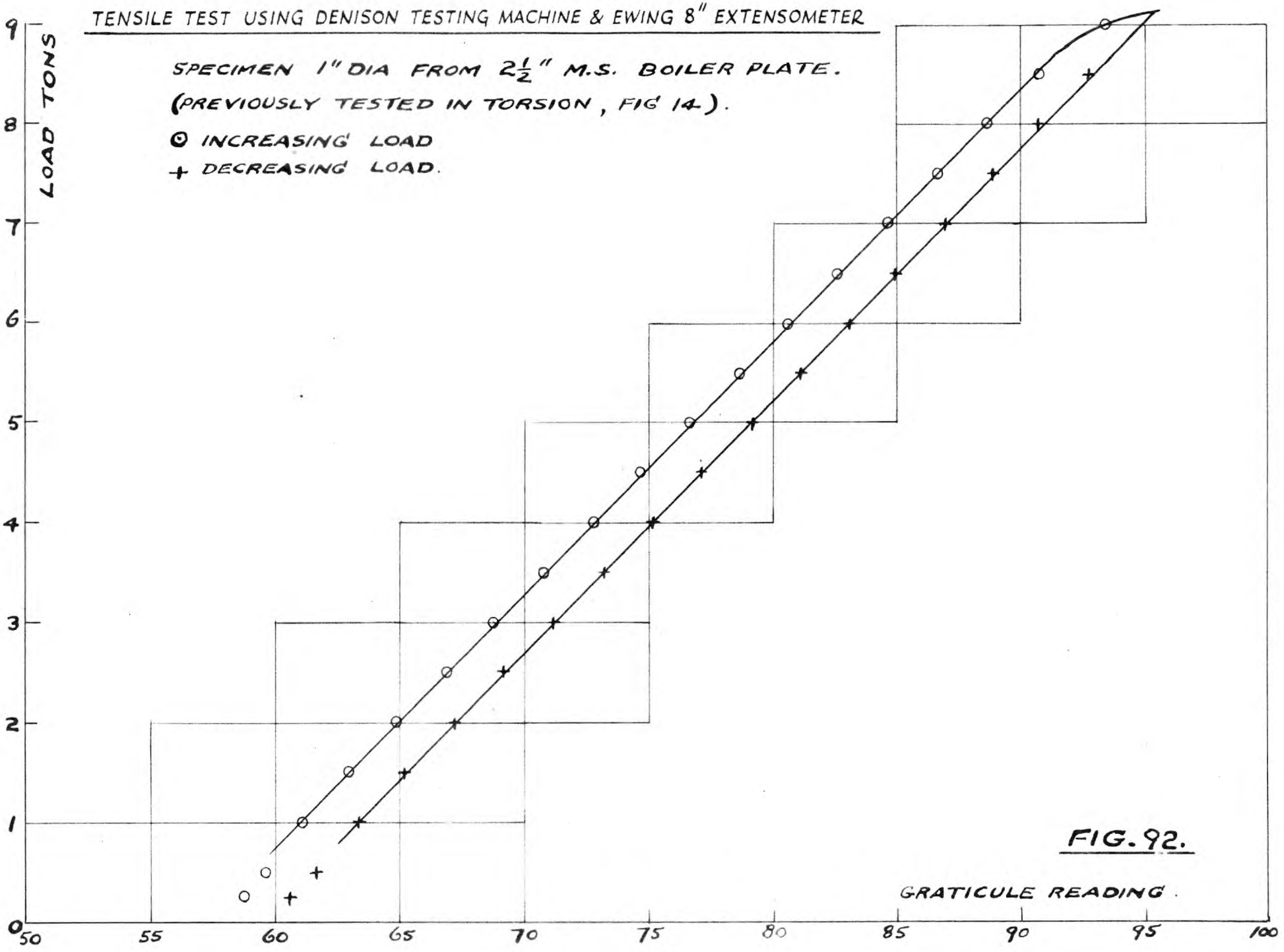
TENSILE TEST USING DENISON TESTING MACHINE & EWING 8" EXTENSOMETER
SPECIMEN 1" DIA FROM 2½" M.S. BOILER PLATE.
(PREVIOUSLY TESTED IN TORSION, FIG 14).
⊙ INCREASING LOAD
+ DECREASING LOAD.
LOAD TONS
0
1
2
3
4
5
6
7
8
9
50
55
60
65
70
75
80
85
90
95
100
GRATICULE READING.
FIG. 92.

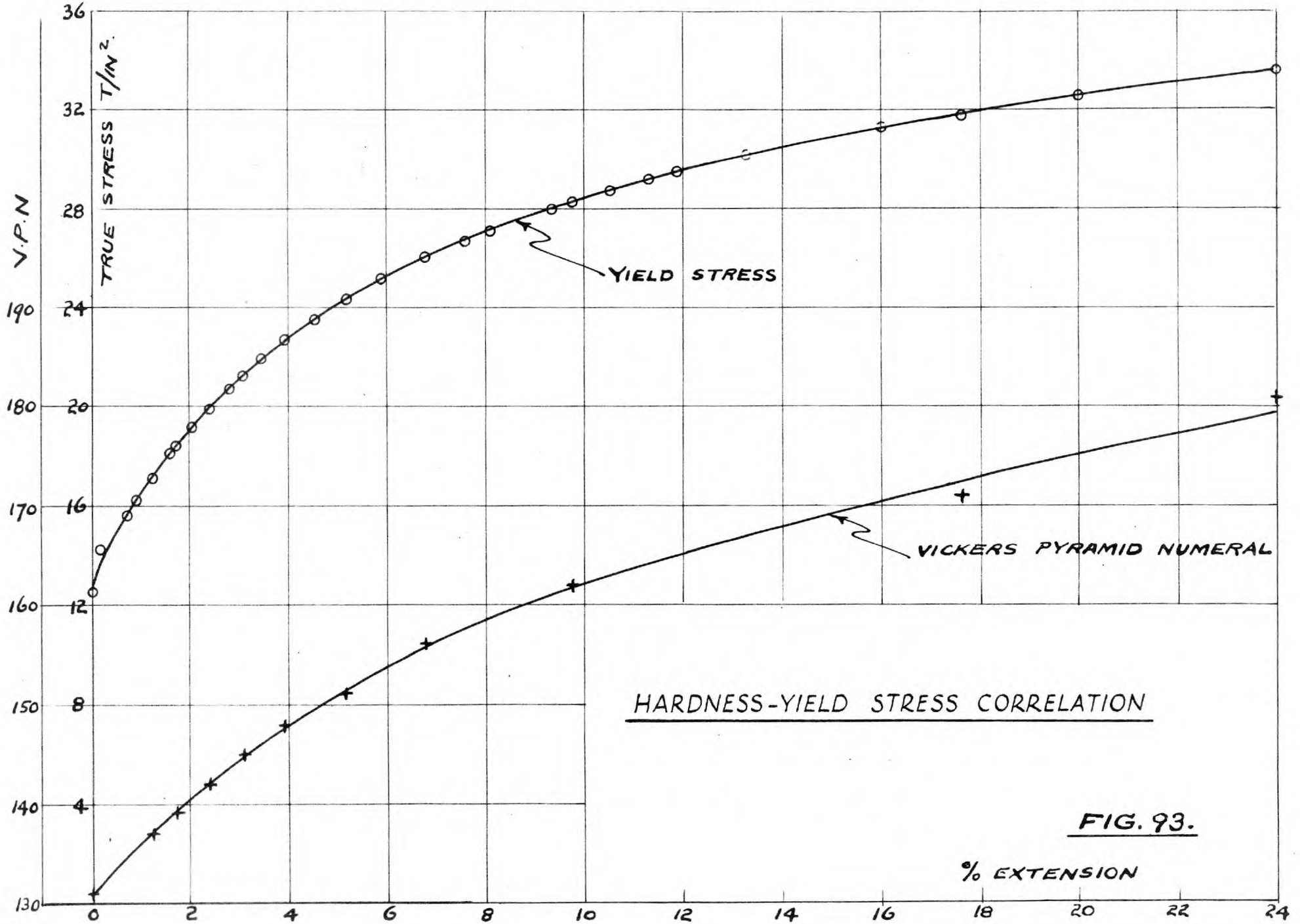

HARDNESS-YIELD STRESS CORRELATION

FIG. 93.

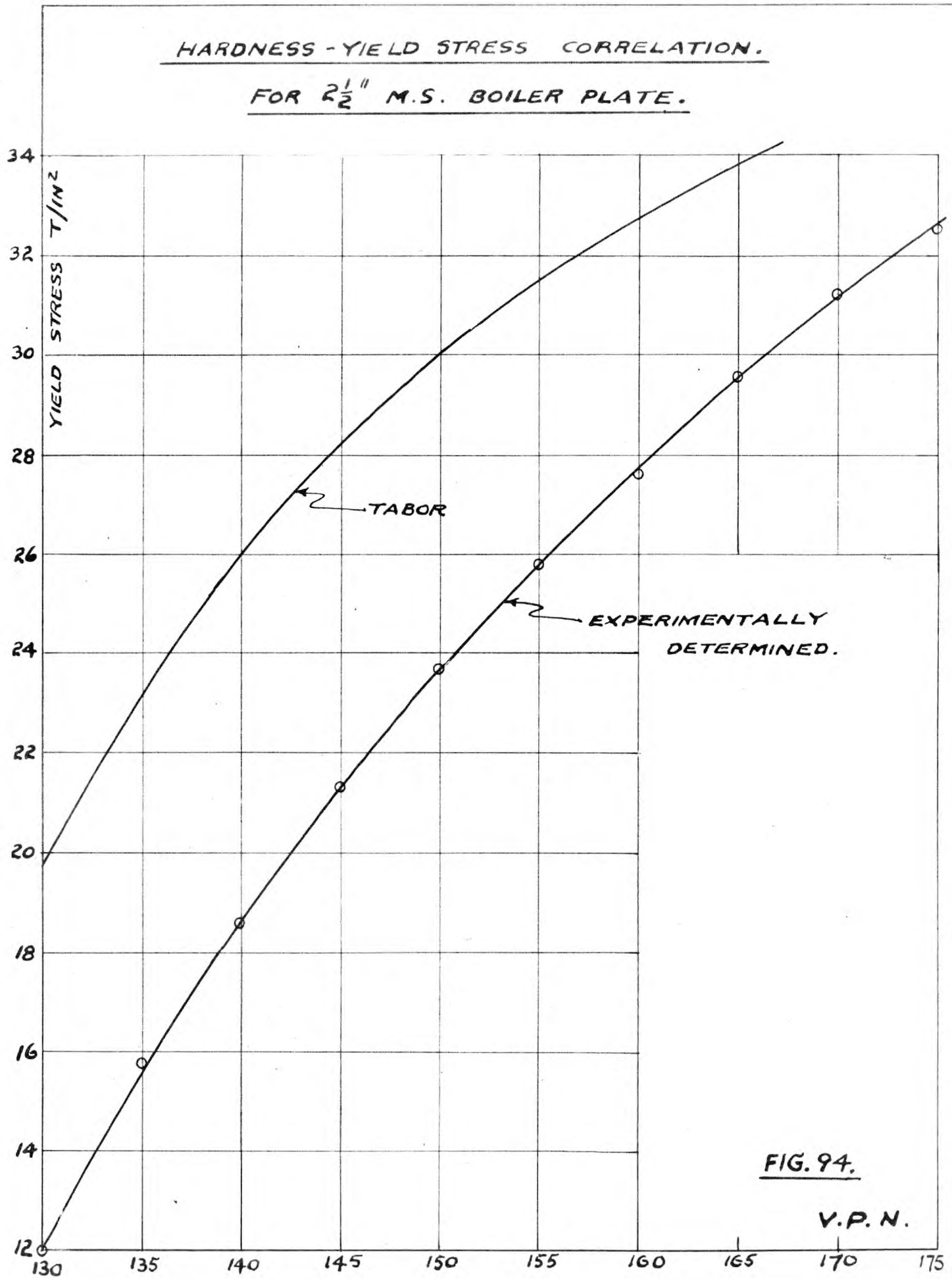
HARDNESS - YIELD STRESS CORRELATION.
FOR 2½" M.S. BOILER PLATE.
YIELD STRESS T/IN²
34
32
30
28
26
24
22
20
18
16
14
12
130
135
140
145
150
155
160
165
170
175
TABOR
EXPERIMENTALLY DETERMINED.
FIG. 94.
V.P.N.

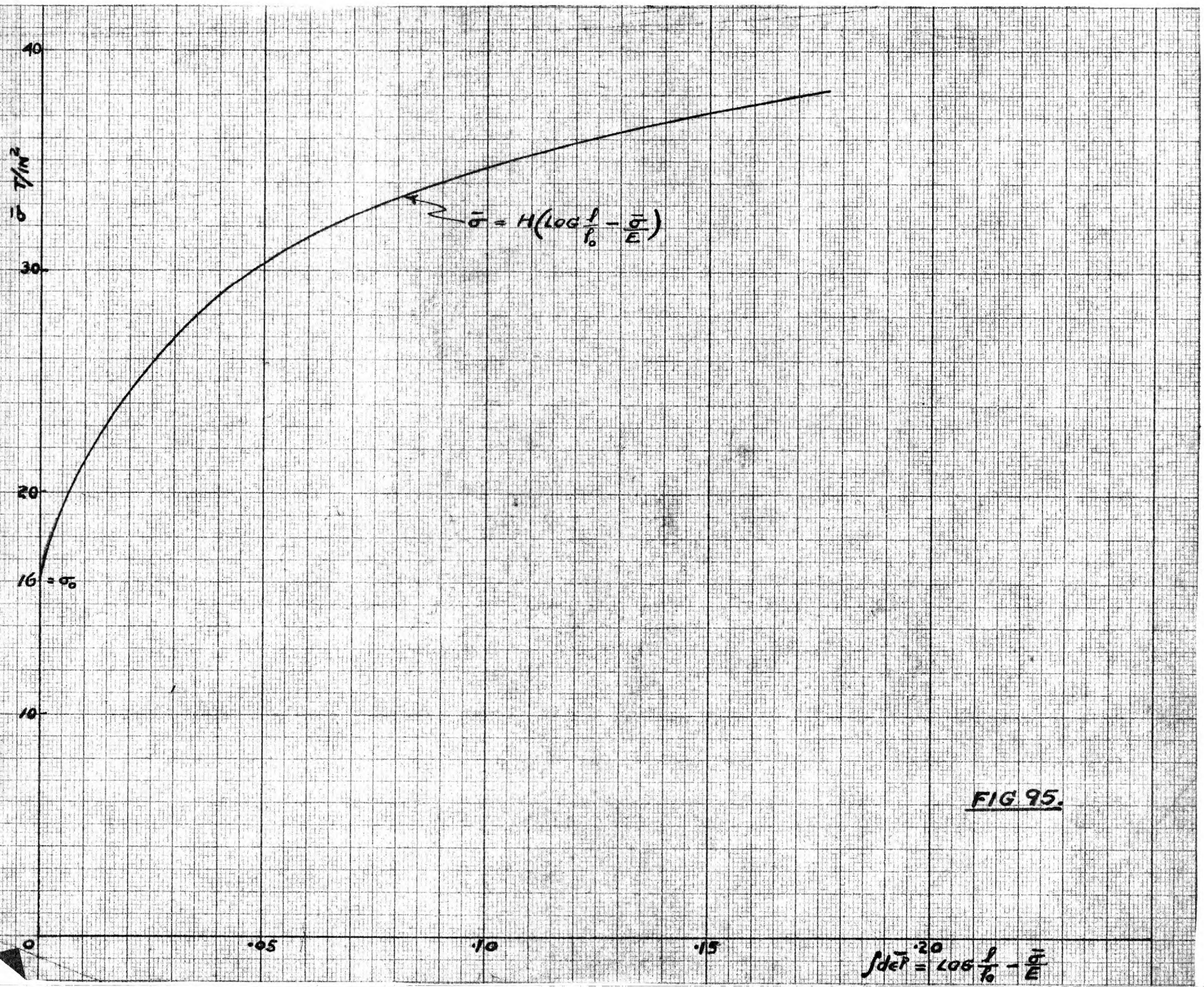
40
30
20
16 = σ₀
10
0
T/in²
·05
·10
·15
·20
$\bar{\sigma} = H\left(\log \frac{l}{l_0} - \frac{\bar{\sigma}}{E}\right)$
$\int d\bar{\epsilon}^p = \log \frac{l}{l_0} - \frac{\bar{\sigma}}{E}$

FIG 95.

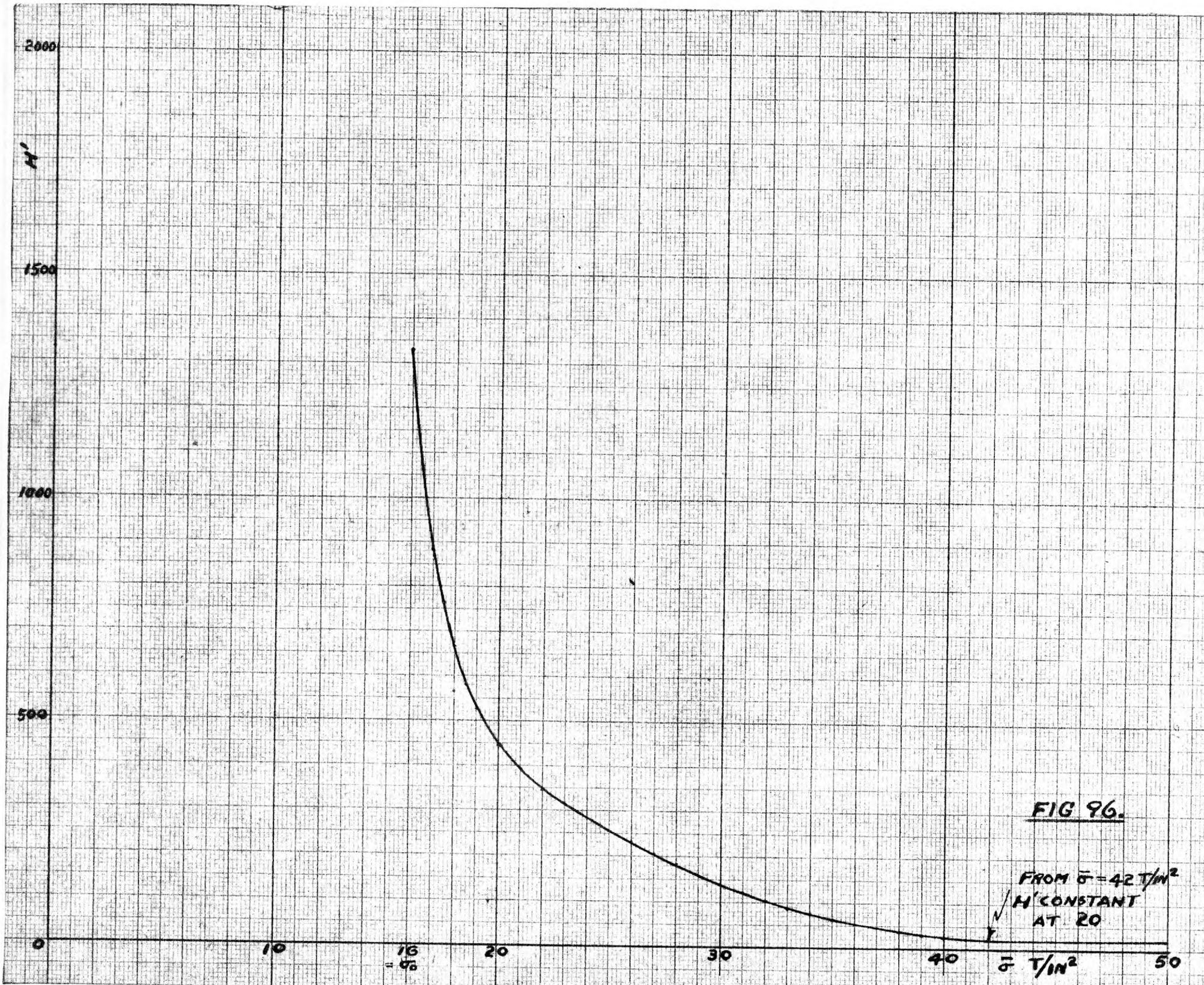
2000
H'
1500
1000
500
0
10
16
20
30
40
50
$\bar{\sigma}$ T/IN²
FROM $\bar{\sigma}$ = 42 T/IN²
H' CONSTANT
AT 20

FIG 96.

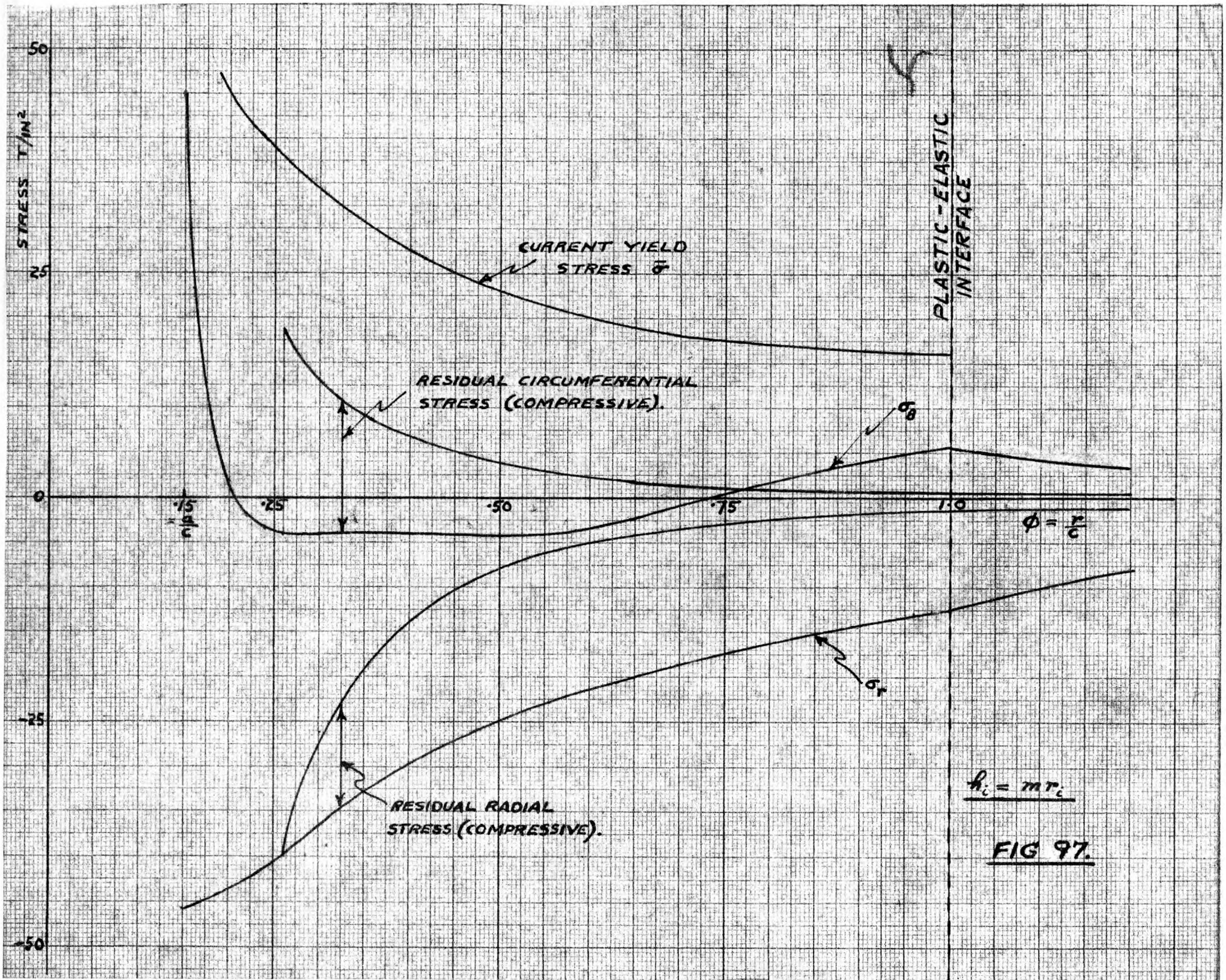
50
25
0
-25
-50
STRESS T/IN²
CURRENT YIELD STRESS σT
PLASTIC-ELASTIC INTERFACE
RESIDUAL CIRCUMFERENTIAL STRESS (COMPRESSIVE).
σθ
σr
RESIDUAL RADIAL STRESS (COMPRESSIVE).
·15
·25
·50
·75
1·0
Φ = r/c
hi = m ri

FIG 97.

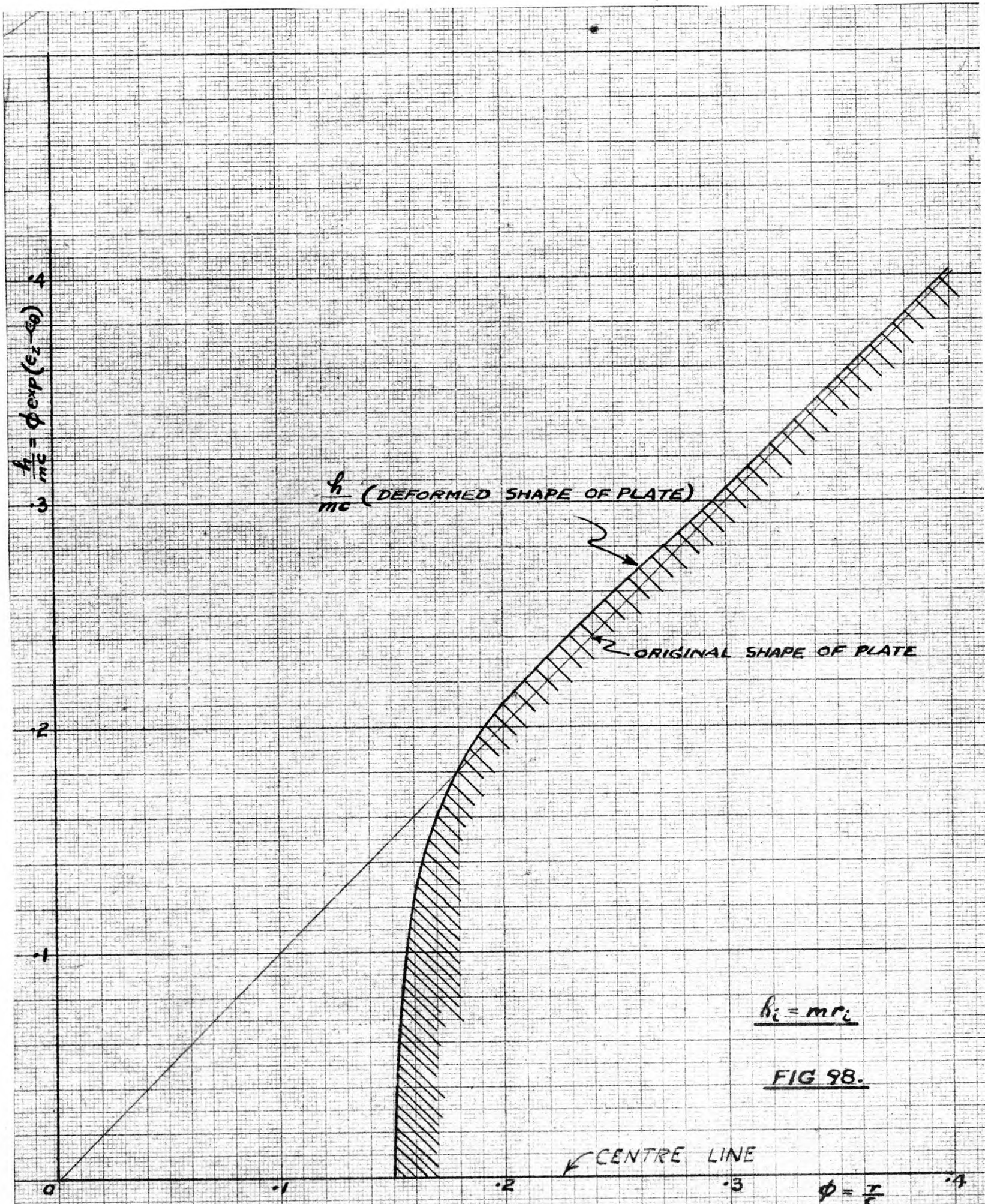
$\frac{h}{mc} = \phi \exp(\epsilon_z - \epsilon_\theta)$
.4
.3
.2
.1
0
$\frac{h}{mc}$ (DEFORMED SHAPE OF PLATE)
ORIGINAL SHAPE OF PLATE
$h_i = m r_i$
CENTRE LINE
.2
.3
.4
$\phi = \frac{r}{c}$

FIG 98.

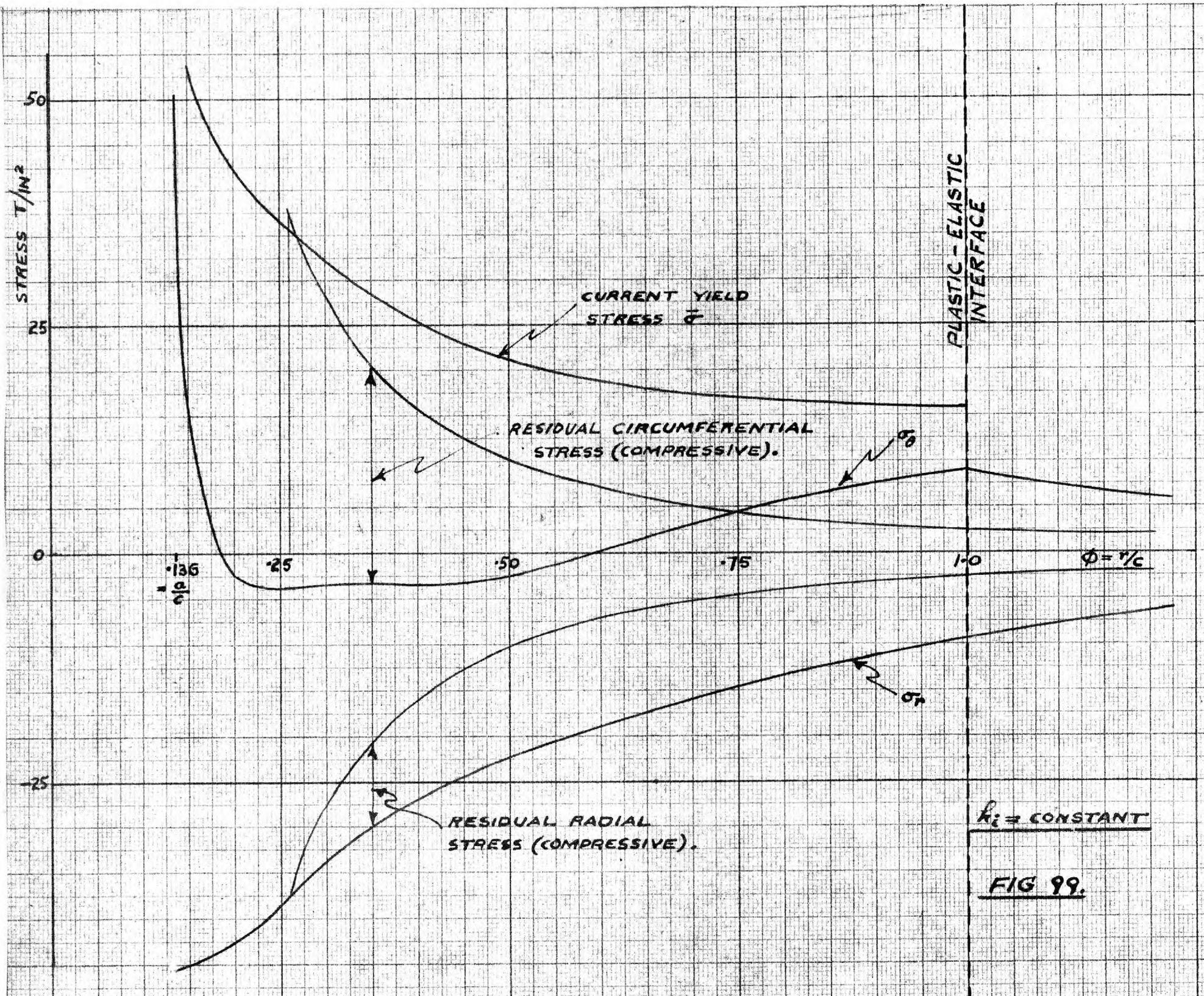
STRESS T/IN²
50
25
0
-25
CURRENT YIELD STRESS $\bar{\sigma}$
RESIDUAL CIRCUMFERENTIAL STRESS (COMPRESSIVE).
σ_θ
PLASTIC - ELASTIC INTERFACE
$\frac{1}{\cdot 136} = \frac{a}{c}$
·25
·50
·75
1·0
$\Phi = r/c$
σ_r
RESIDUAL RADIAL STRESS (COMPRESSIVE).
k_i = CONSTANT

FIG 99.

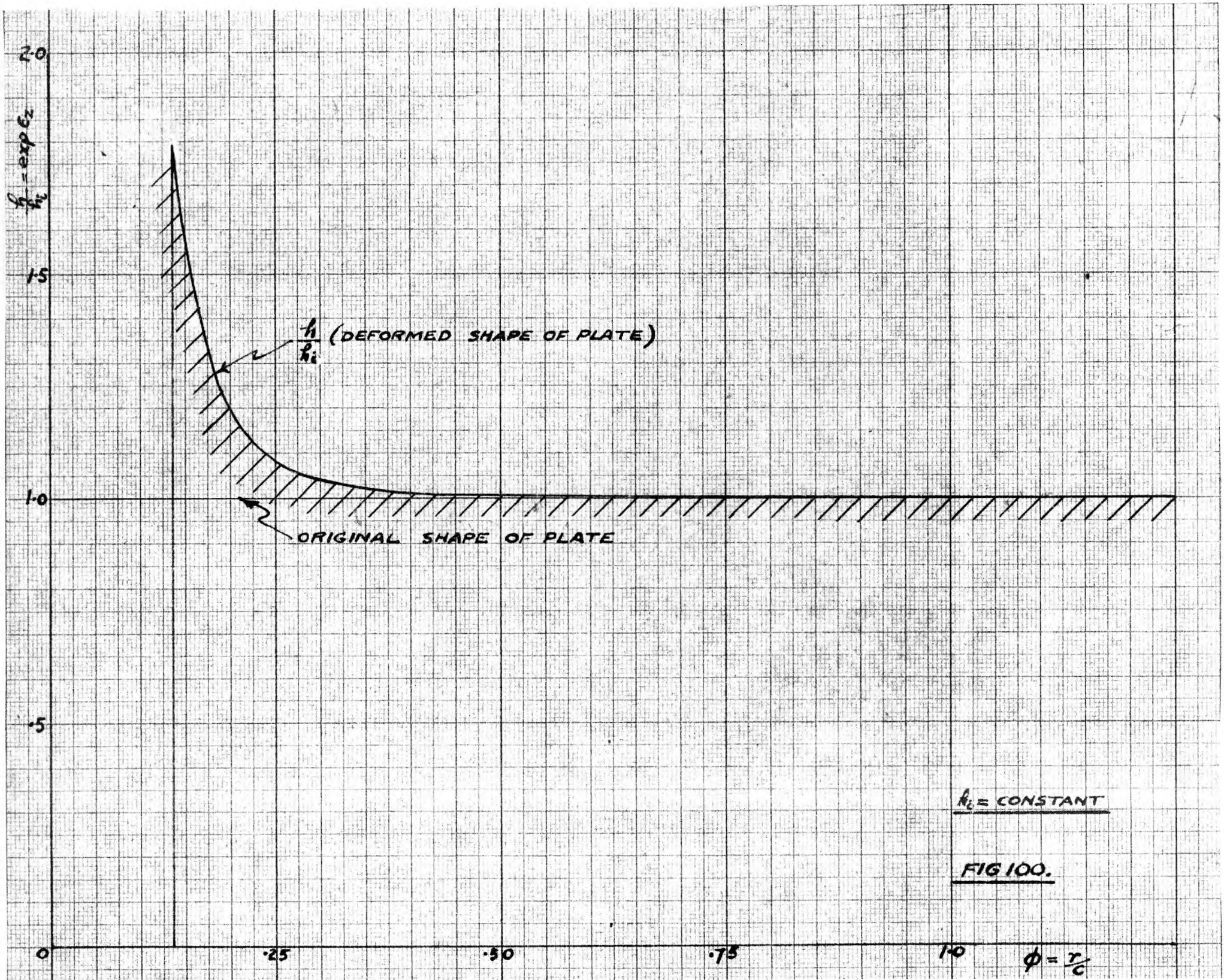
2·0
$\frac{h}{h_i} = \exp \varepsilon_z$
1·5
$\frac{h}{h_i}$ (DEFORMED SHAPE OF PLATE)
1·0
ORIGINAL SHAPE OF PLATE
·5
h_i = CONSTANT
0
·25
·50
·75
1·0
$\phi = \frac{r}{c}$

FIG 100.

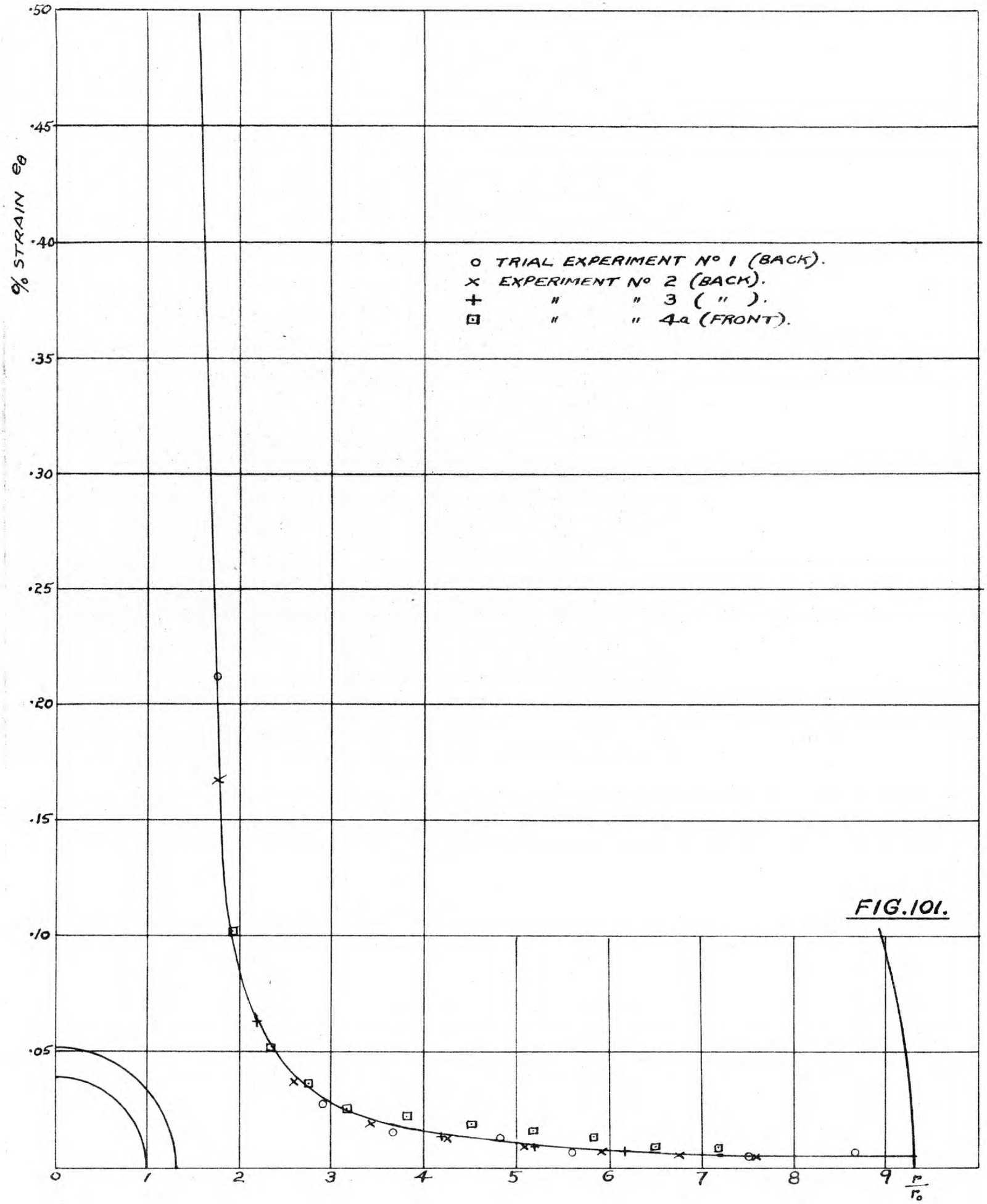
·50
·45
·40
·35
·30
·25
·20
·15
·10
·05
% STRAIN e_θ
o TRIAL EXPERIMENT Nº 1 (BACK).
× EXPERIMENT Nº 2 (BACK).
+ " " 3 (").
⊡ " " 4a (FRONT).
0
1
2
3
4
5
6
7
8
9
$\frac{r}{r_0}$

FIG.101.

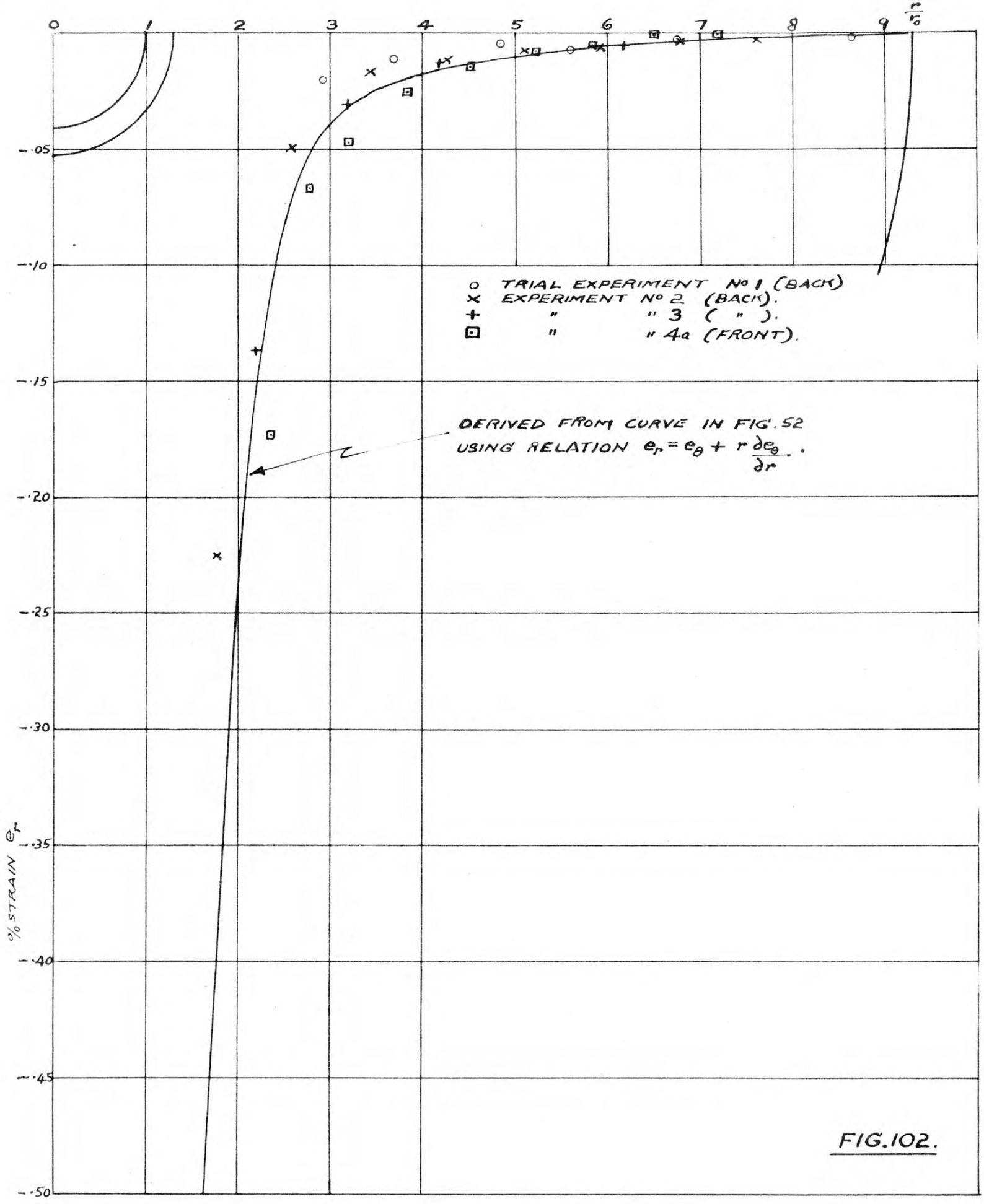
0
1
2
3
4
5
6
7
8
9
$\frac{r}{r_0}$
-·05
-·10
-·15
-·20
-·25
-·30
-·35
-·40
-·45
-·50
% STRAIN e_r
o TRIAL EXPERIMENT No 1 (BACK)
× EXPERIMENT No 2 (BACK).
+ " " 3 (").
⊡ " " 4a (FRONT).
DERIVED FROM CURVE IN FIG. 52
USING RELATION $e_r = e_\theta + r\frac{\partial e_\theta}{\partial r}$.

FIG.102.

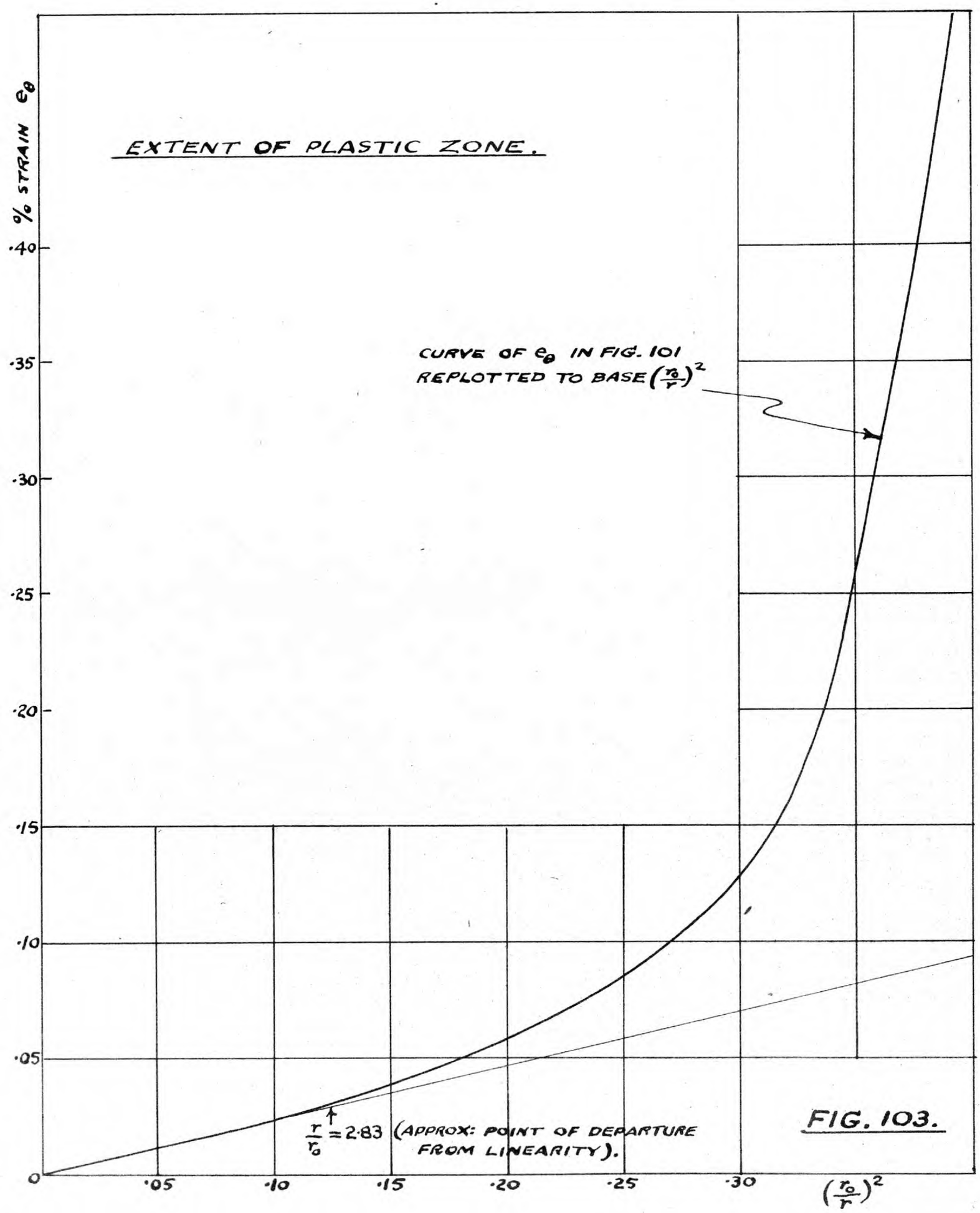
EXTENT OF PLASTIC ZONE.
% STRAIN e_θ
·40
·35
·30
·25
·20
·15
·10
·05
0
CURVE OF e_θ IN FIG. 101
REPLOTTED TO BASE $\left(\frac{r_0}{r}\right)^2$
$\frac{r}{r_0} = 2.83$ (APPROX: POINT OF DEPARTURE FROM LINEARITY).
·05
·10
·15
·20
·25
·30
$\left(\frac{r_0}{r}\right)^2$

FIG. 103.

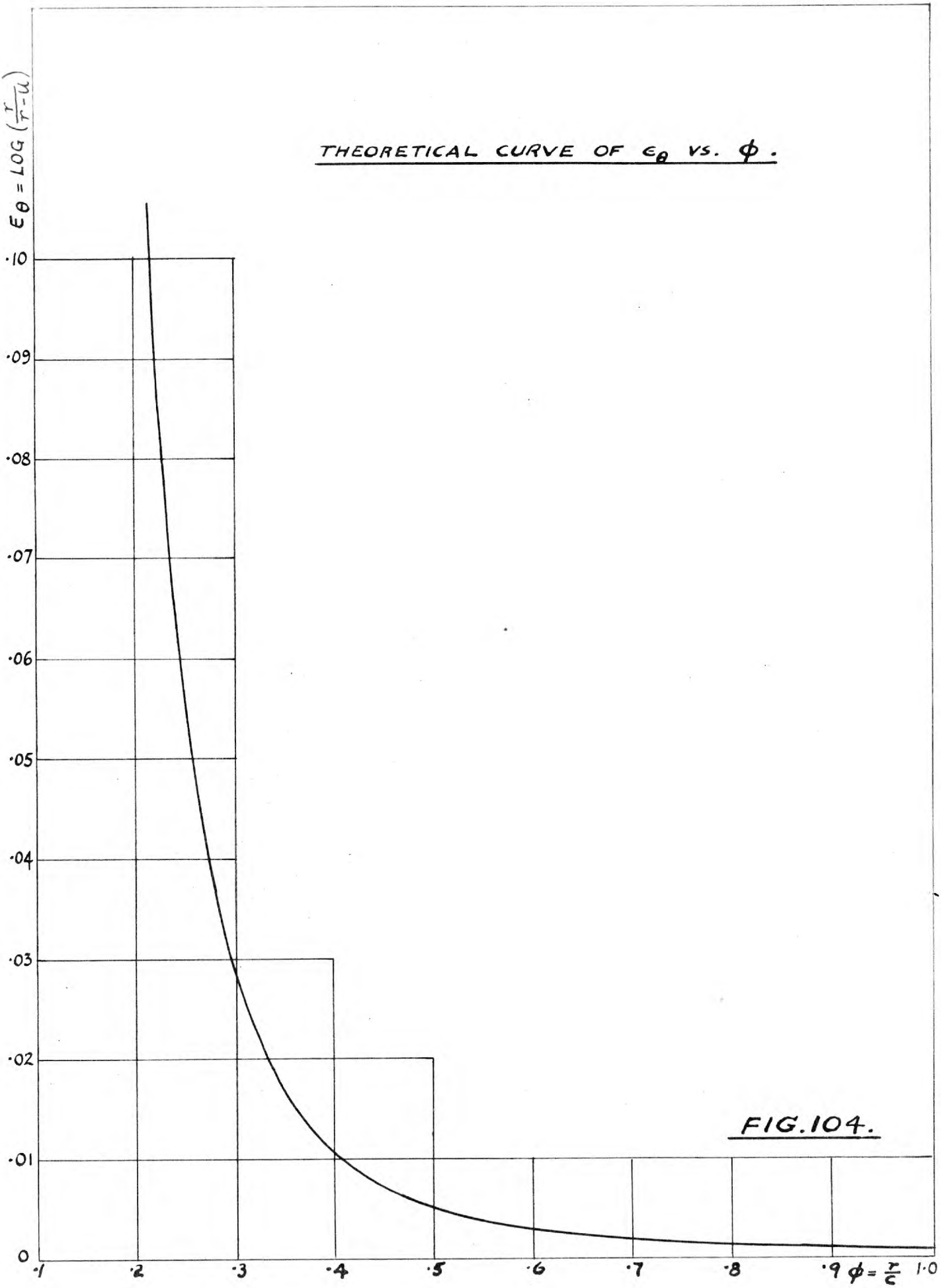
THEORETICAL CURVE OF ϵ_θ VS. ϕ.
$\epsilon_\theta = \text{LOG}\left(\frac{r}{r-u}\right)$
·10
·09
·08
·07
·06
·05
·04
·03
·02
·01
0
·1
·2
·3
·4
·5
·6
·7
·8
·9
$\phi = \frac{r}{c}$
1·0

FIG.104.

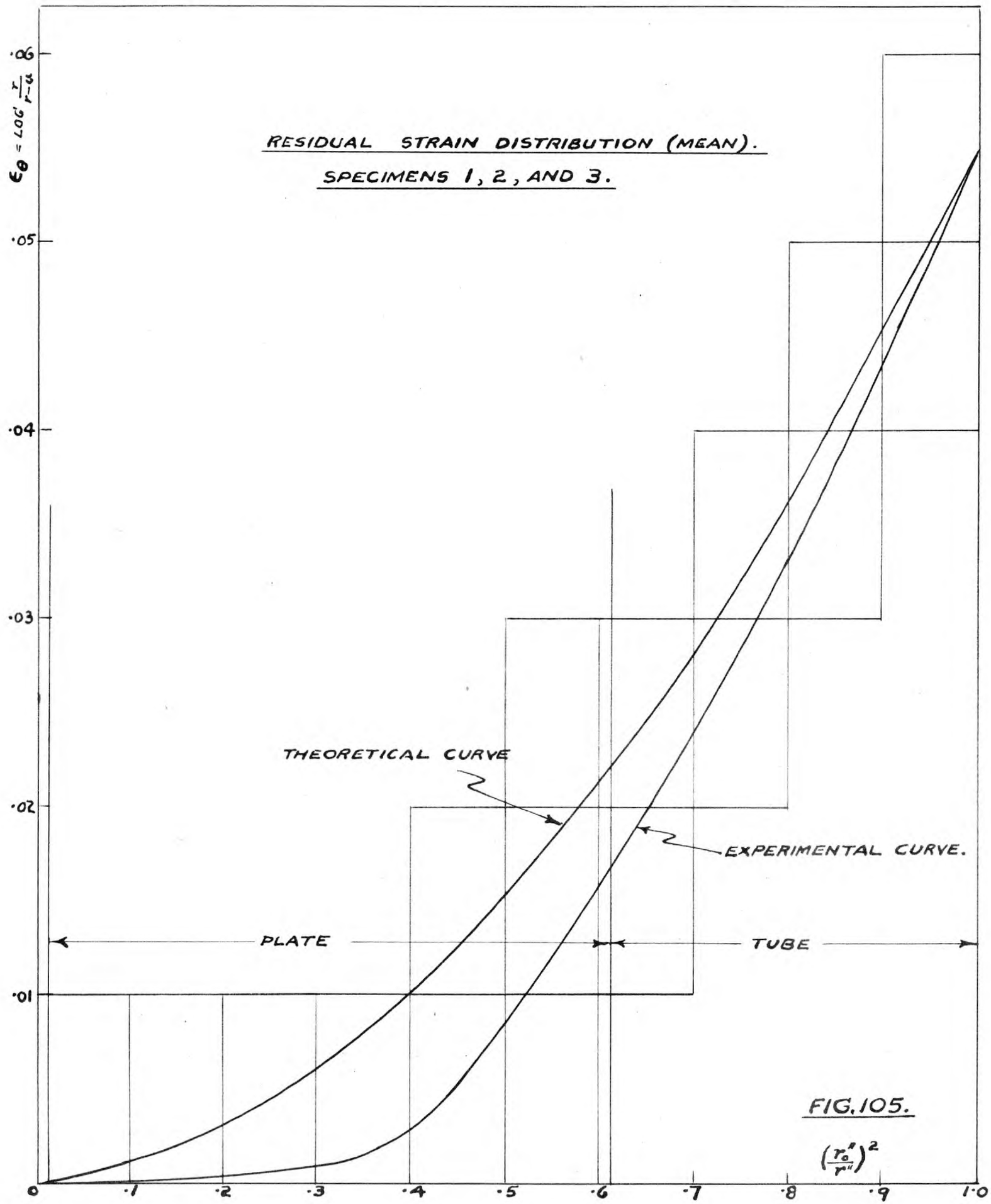
RESIDUAL STRAIN DISTRIBUTION (MEAN).
SPECIMENS 1, 2, AND 3.
$\epsilon_\theta = \log' \frac{r}{r-u}$
·06
·05
·04
·03
·02
·01
0
·1
·2
·3
·4
·5
·6
·7
·8
·9
1·0
$\left(\frac{r_0''}{r''}\right)^2$
THEORETICAL CURVE
EXPERIMENTAL CURVE.
PLATE
TUBE

FIG. 105.

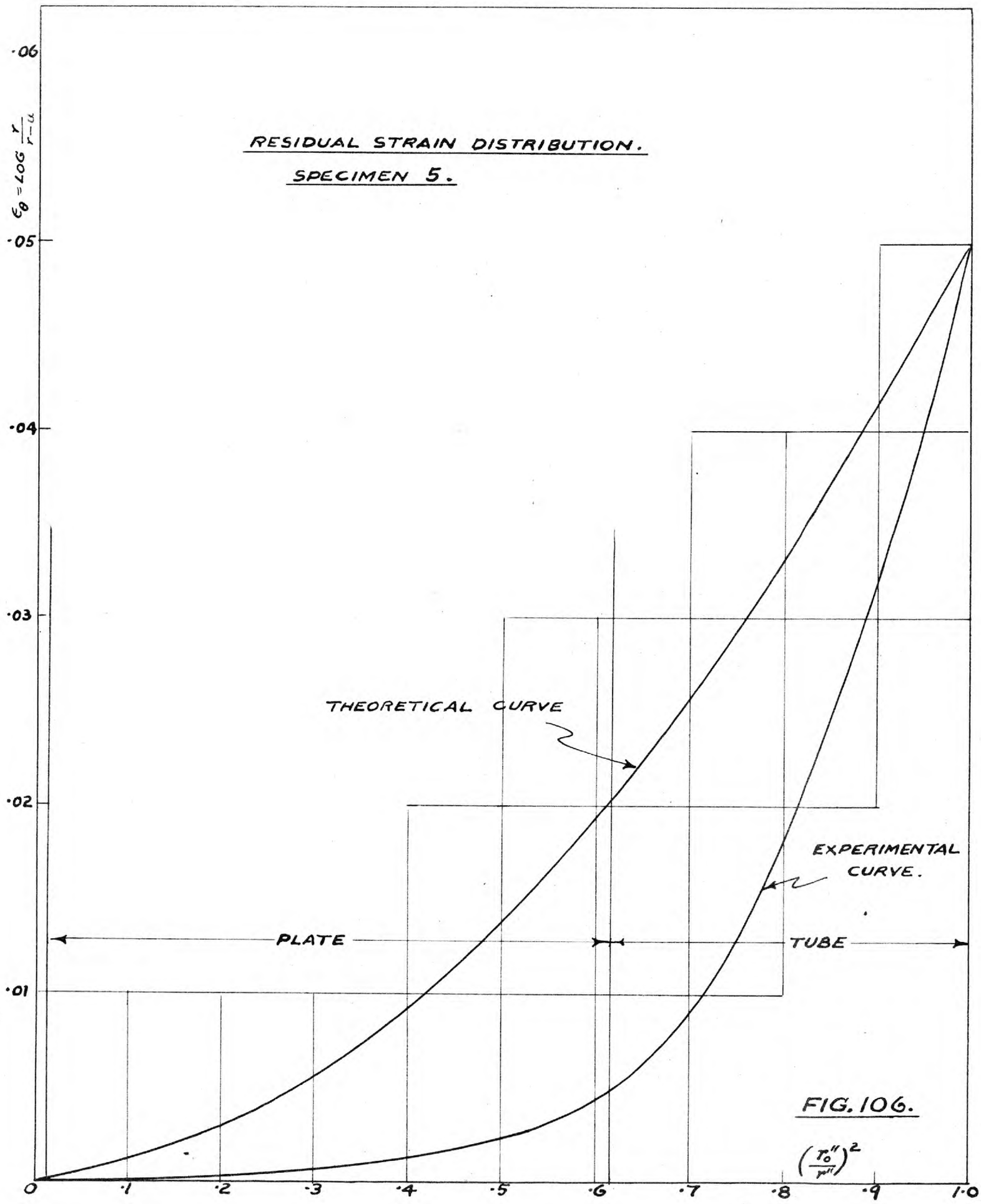
RESIDUAL STRAIN DISTRIBUTION.
SPECIMEN 5.
$\epsilon_\theta = LOG \frac{r}{r-u}$
·06
·05
·04
·03
·02
·01
THEORETICAL CURVE
EXPERIMENTAL CURVE.
PLATE
TUBE
0
·1
·2
·3
·4
·5
·6
·7
·8
·9
1·0
$\left(\frac{r_0''}{\mu''}\right)^2$

FIG. 106.

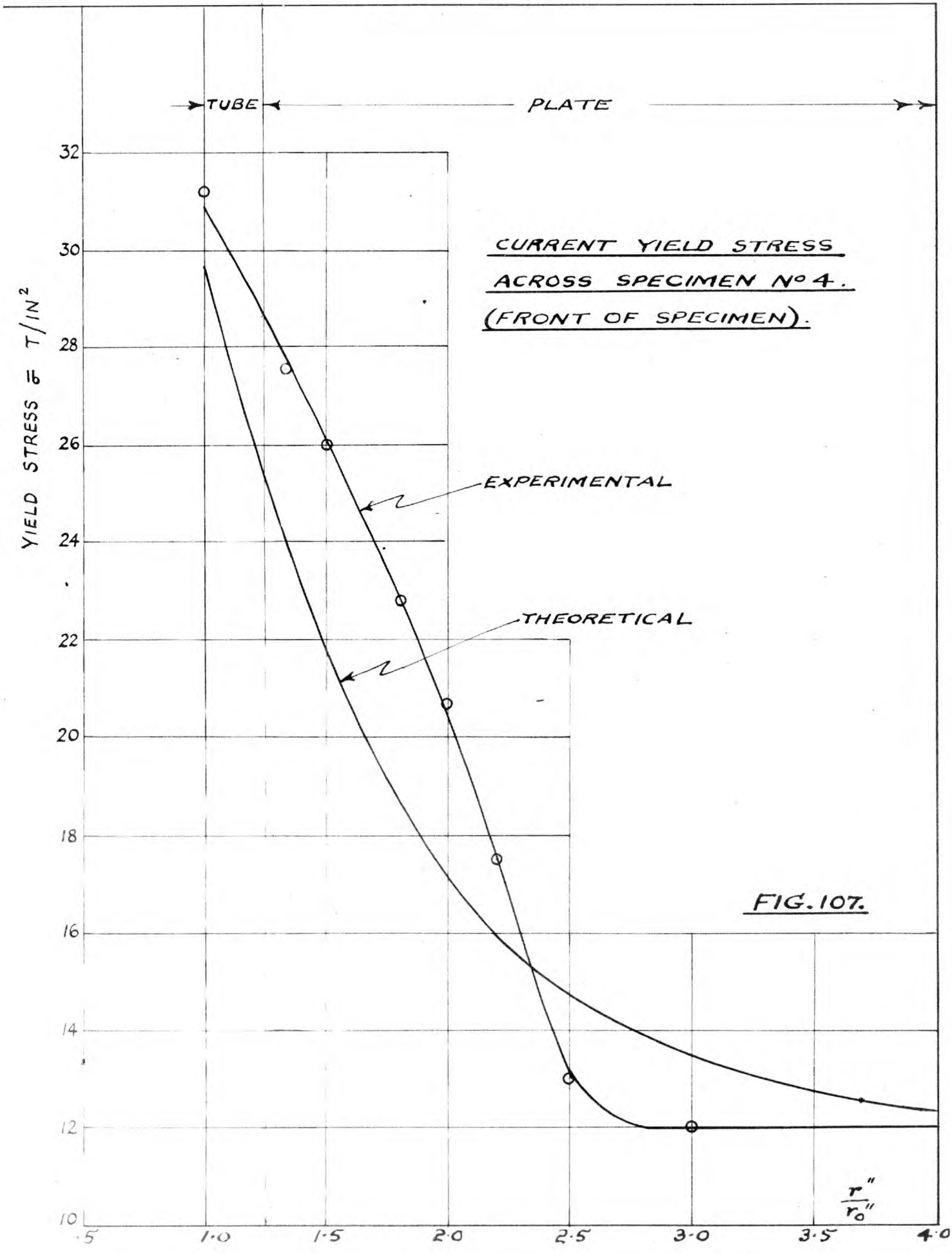
TUBE
PLATE
CURRENT YIELD STRESS ACROSS SPECIMEN Nº 4. (FRONT OF SPECIMEN).
EXPERIMENTAL
THEORETICAL
YIELD STRESS $\bar{\sigma}$ T/IN^2
32
30
28
26
24
22
20
18
16
14
12
10
·5
1·0
1·5
2·0
2·5
3·0
3·5
4·0
$\frac{r''}{r_0''}$

FIG. 107.

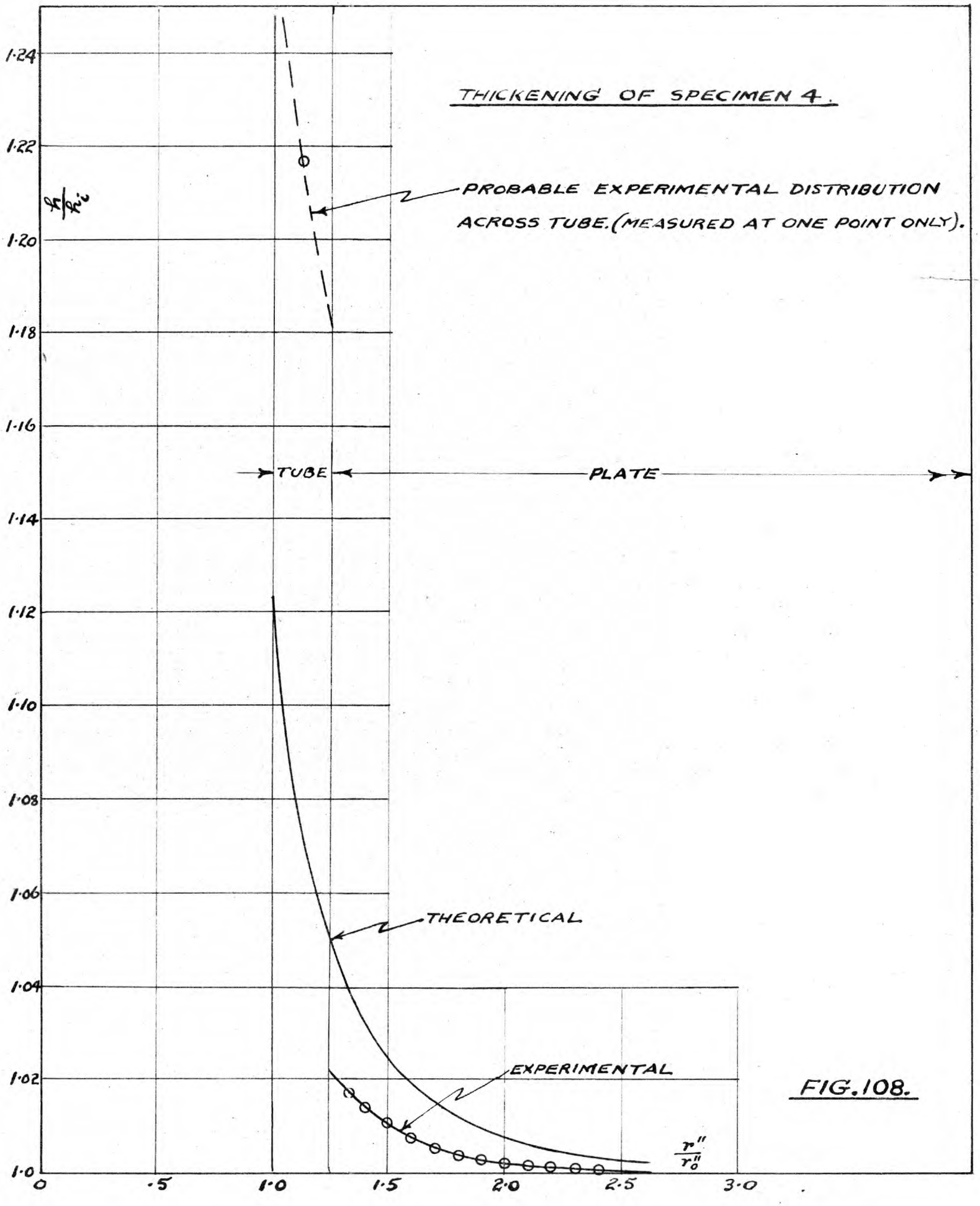
THICKENING OF SPECIMEN 4.
PROBABLE EXPERIMENTAL DISTRIBUTION ACROSS TUBE. (MEASURED AT ONE POINT ONLY).
h/hi
TUBE
PLATE
THEORETICAL
EXPERIMENTAL
r''/r''o
1·24
1·22
1·20
1·18
1·16
1·14
1·12
1·10
1·08
1·06
1·04
1·02
1·0
0
·5
1·0
1·5
2·0
2·5
3·0

FIG. 108.

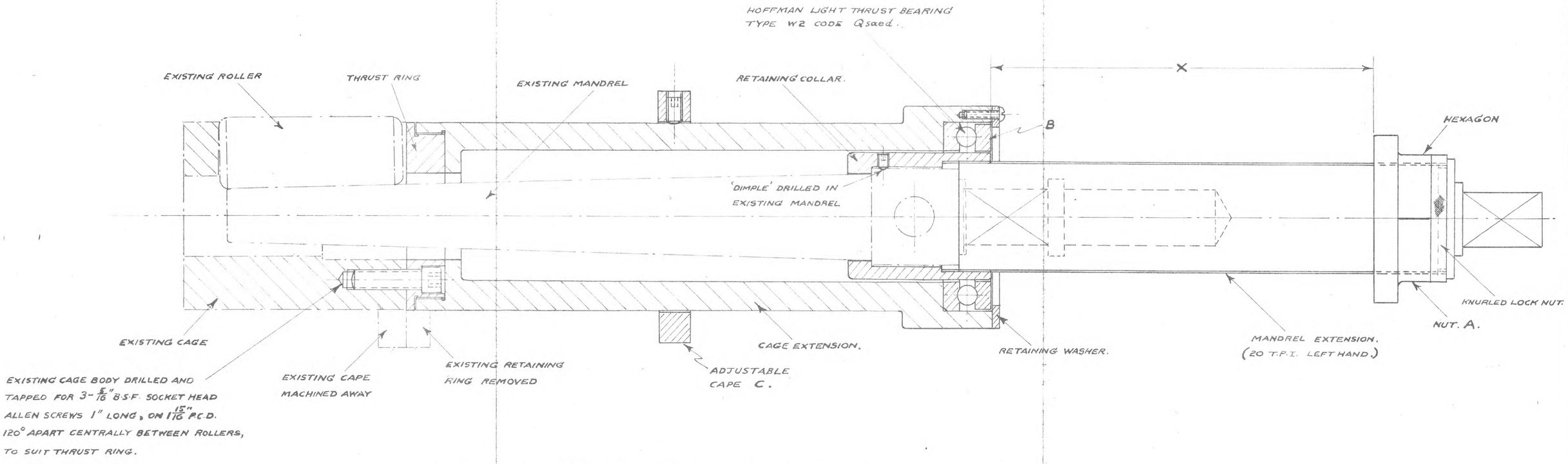

GENERAL ARRANGEMENT OF MODIFIED

PROPULSIVE TYPE EXPANDER. (FULL SCALE).

FIG.109.

DETAILS OF SPECIMENS 7 & 8.

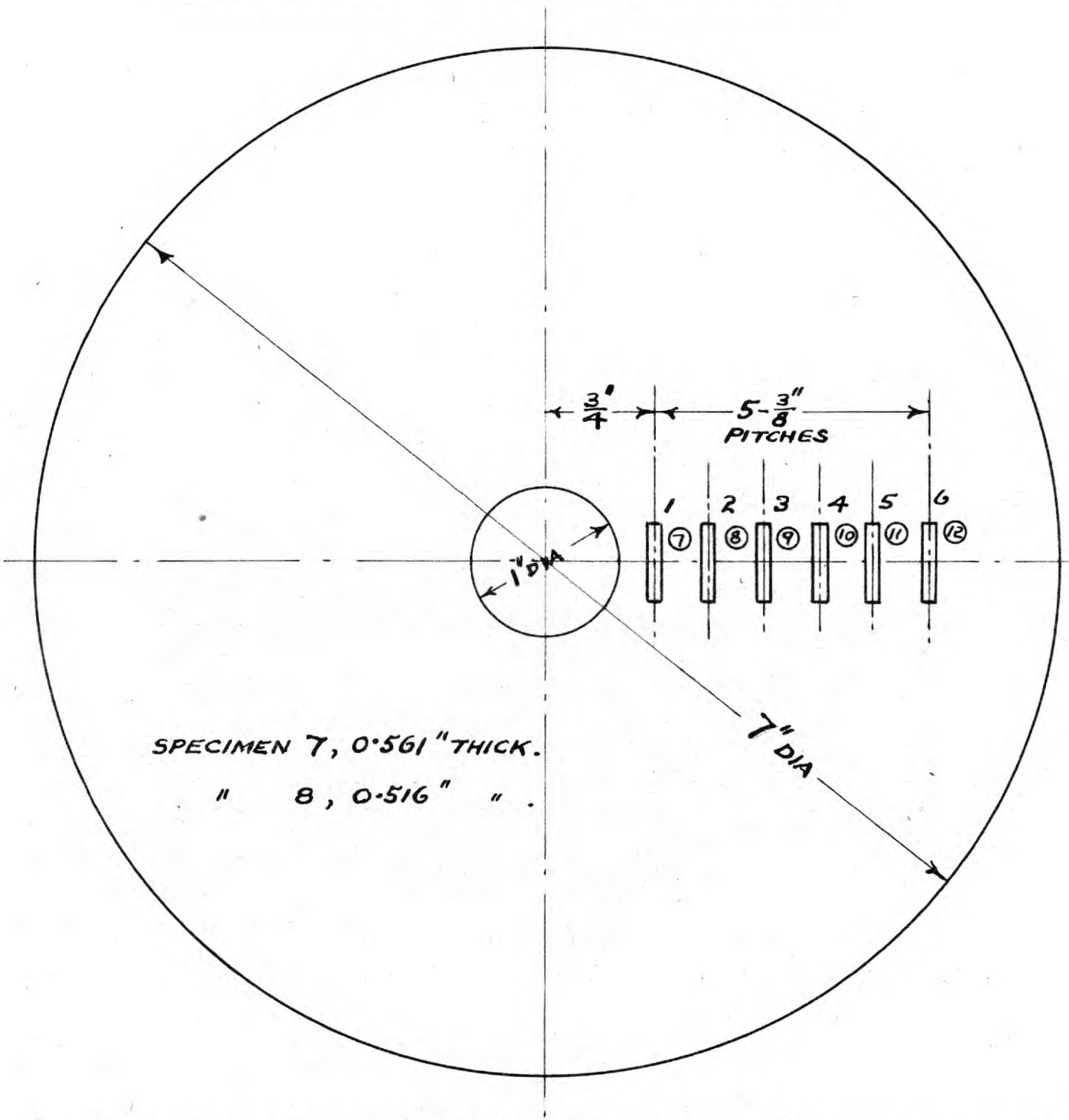

SPECIMEN 7, 0·561" THICK.

" 8, 0·516" " .

ALL GAUGES 17 × 2·5 mm. 100 Ω TINSLEY GAUGES (H.S. DUROFIX CEMENT).

FRONT OF SPECIMEN SHOWN, NUMBERS OF GAUGES ON BACK CIRCLED.

FIG. 110.

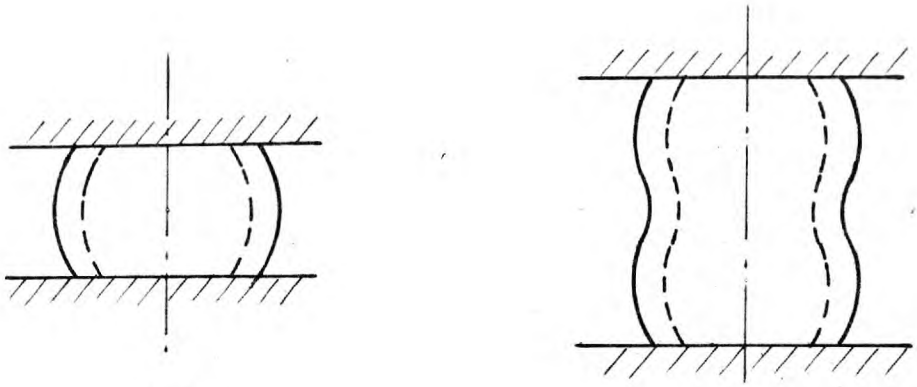

(a). (b).

EXAGGERATED MODES OF DEFORMATION OF 1 IN: OUTSIDE DIA: $\frac{1}{8}$ IN: THICK TUBES UNDER AXIAL COMPRESSION.

(a). ORIGINAL LENGTH 1 IN:
(b). " " 2 INS:

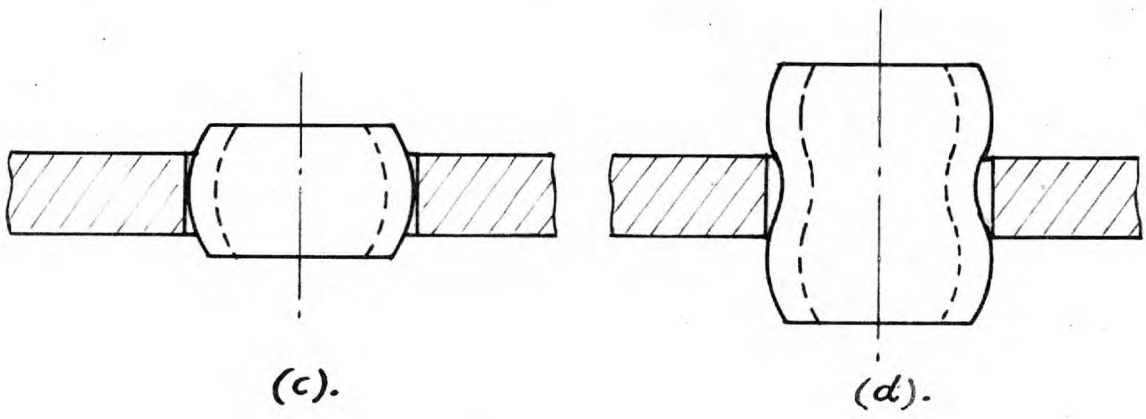

(c). (d).

RELATIVE POSITIONS OF SEAT PLATES DURING RIVETING EXPERIMENTS.

FIG. III.

SPECIMEN 7 PUSH-OUT TEST

1" LENGTH TUBE, RIVETING LOAD 25 TONS, PUSH-OUT LOAD 3·13 TONS

O FRONT $P_F = 7{\cdot}04$ T/IN²

\+ BACK $P_B = 5{\cdot}67$ "

$\bar{P} = 6{\cdot}35$ "

$\mu = {\cdot}267.$

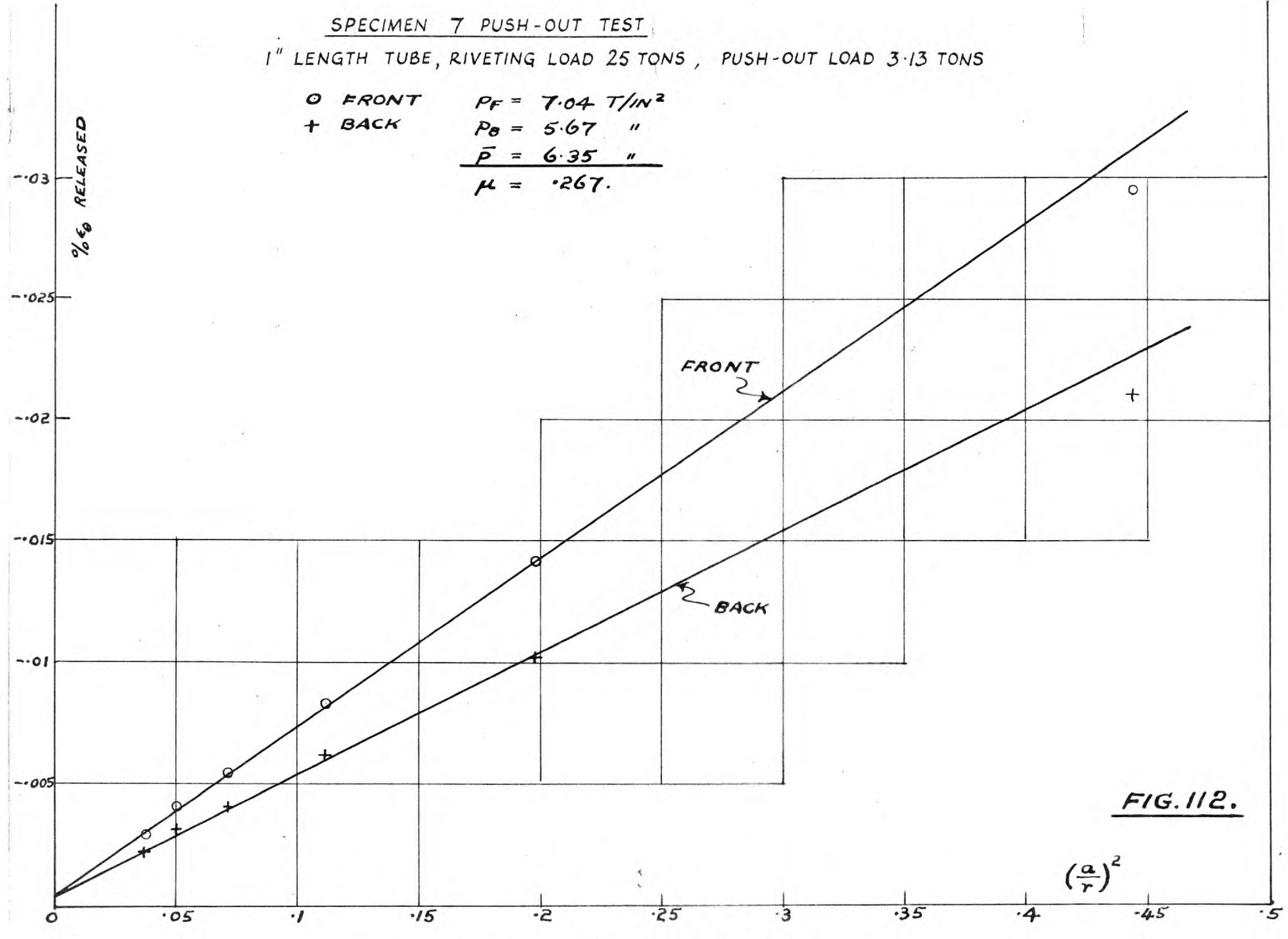

FIG. 112.

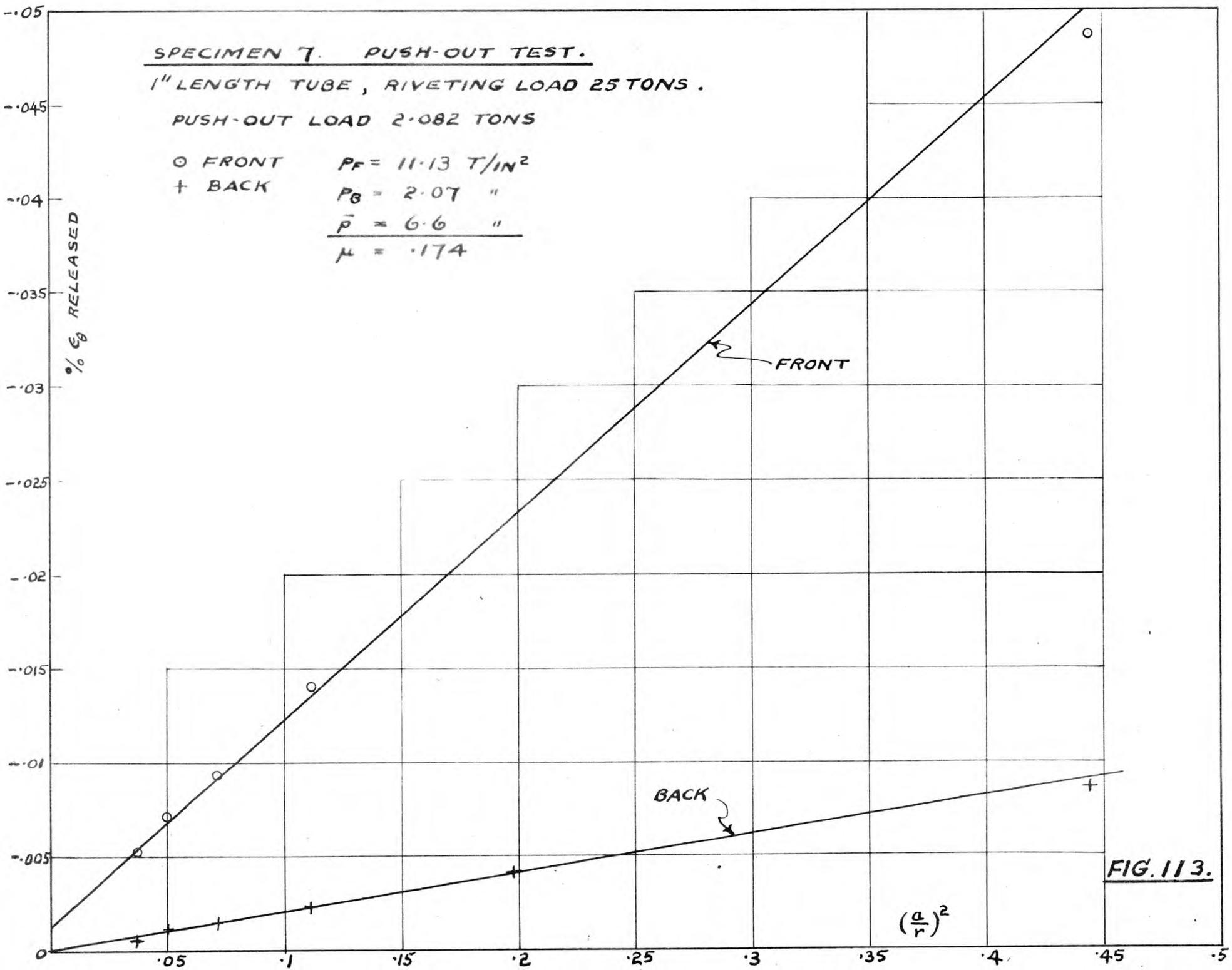
SPECIMEN 7. PUSH-OUT TEST.
1" LENGTH TUBE, RIVETING LOAD 25 TONS.
PUSH-OUT LOAD 2·082 TONS
⊙ FRONT
+ BACK
P_F = 11·13 T/IN²
P_B = 2·07 "
$\bar{P}$ = 6·6 "
μ = ·174
% ϵ_θ RELEASED
FRONT
BACK
$(\frac{a}{r})^2$
-·05
-·045
-·04
-·035
-·03
-·025
-·02
-·015
-·01
-·005
0
·05
·1
·15
·2
·25
·3
·35
·4
·45
·5

FIG. 113.

SPECIMEN 7. PUSH-OUT TEST

2" LENGTH TUBE, RIVETING LOAD 12·5 TONS

PUSH-OUT LOAD 1·56 TONS

⊙ FRONT

\+ BACK

P_F = 2·84 T/IN²

P_B = 2·32 "

$\bar{P}$ = 2·58 "

μ = ·324

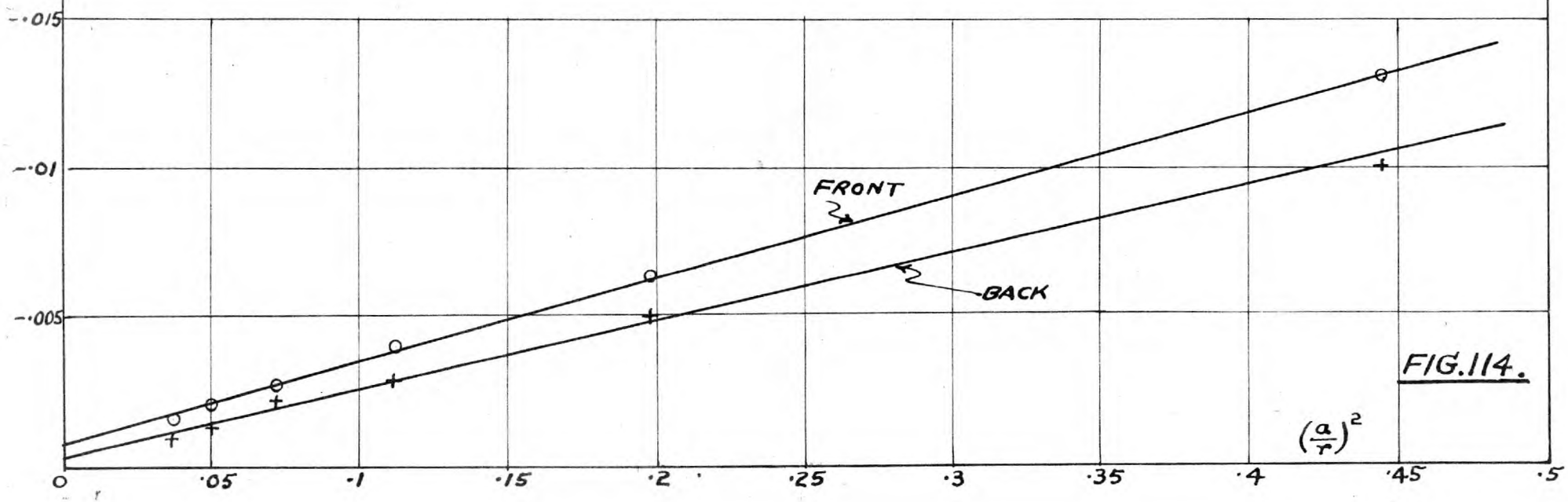

FIG.114.

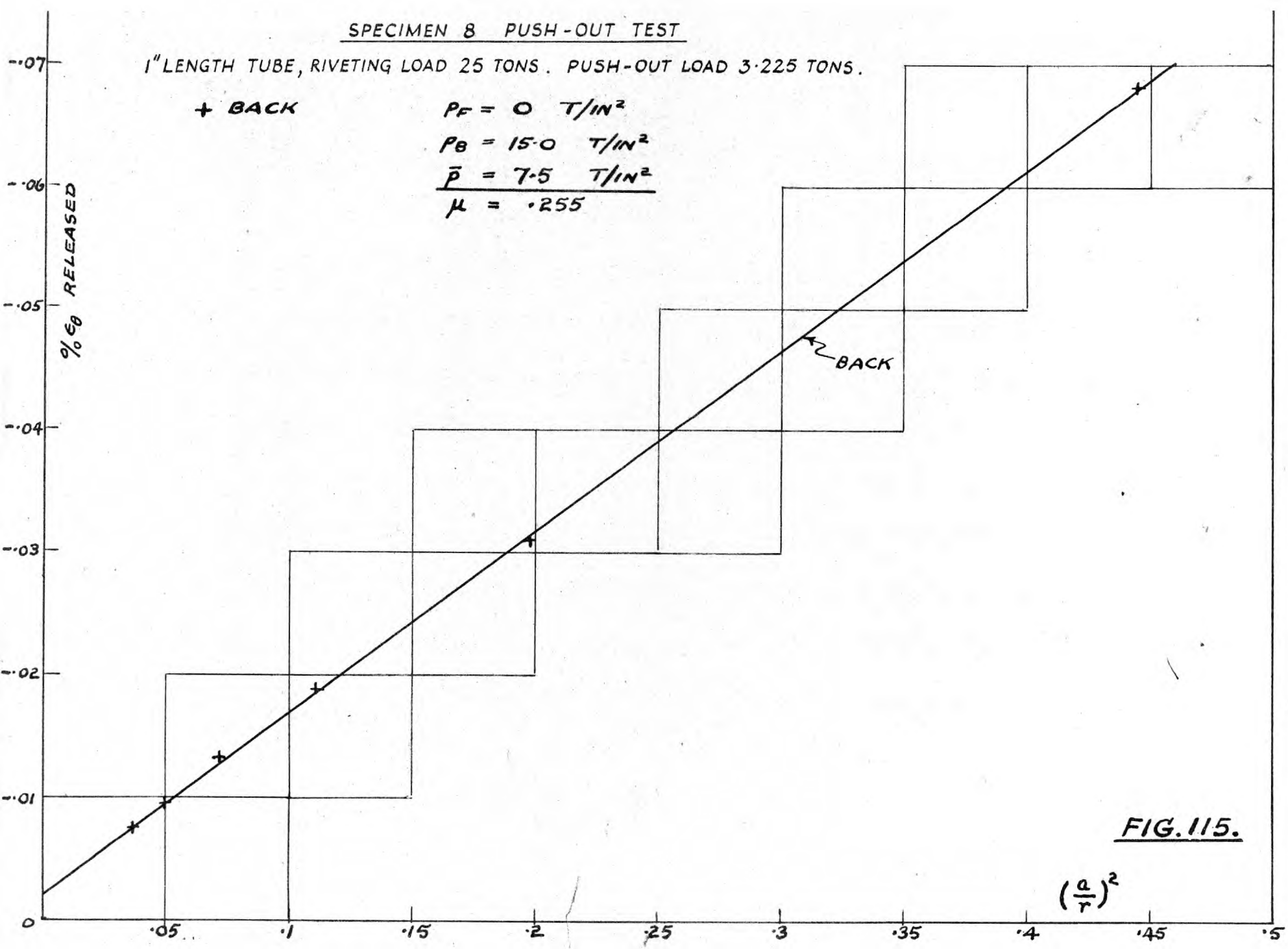
SPECIMEN 8 PUSH-OUT TEST
1" LENGTH TUBE, RIVETING LOAD 25 TONS. PUSH-OUT LOAD 3·225 TONS.
+ BACK
P_F = 0 T/IN²
P_B = 15·0 T/IN²
$\bar{p}$ = 7·5 T/IN²
μ = ·255
% ϵ_B RELEASED
·07
·06
·05
·04
·03
·02
·01
0
BACK
·05
·1
·15
·2
·25
·3
·35
·4
·45
·5
$(\frac{a}{r})^2$

FIG. 115.

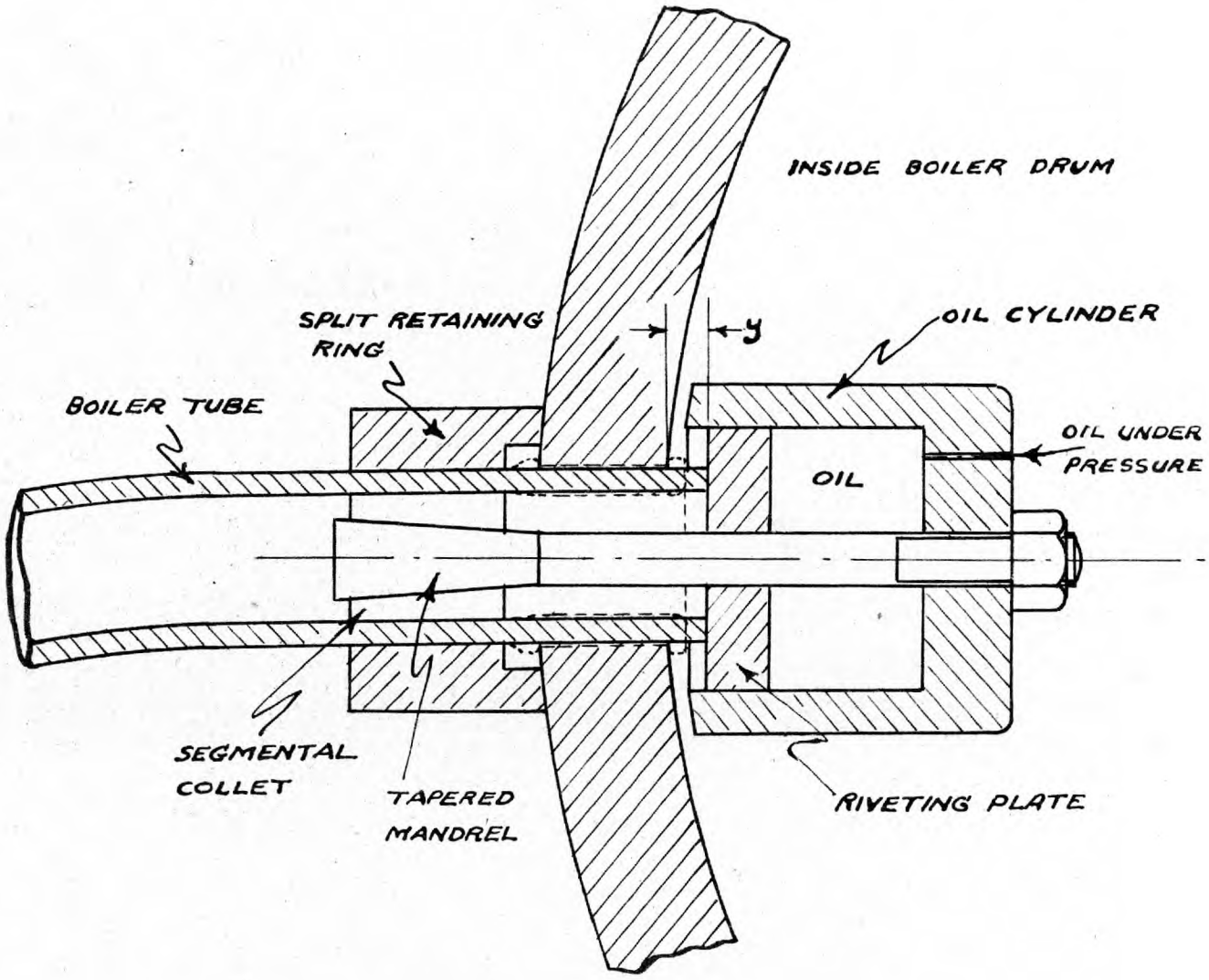

SUGGESTED DESIGN OF TUBE RIVETING MACHINE.

FIG. 116.

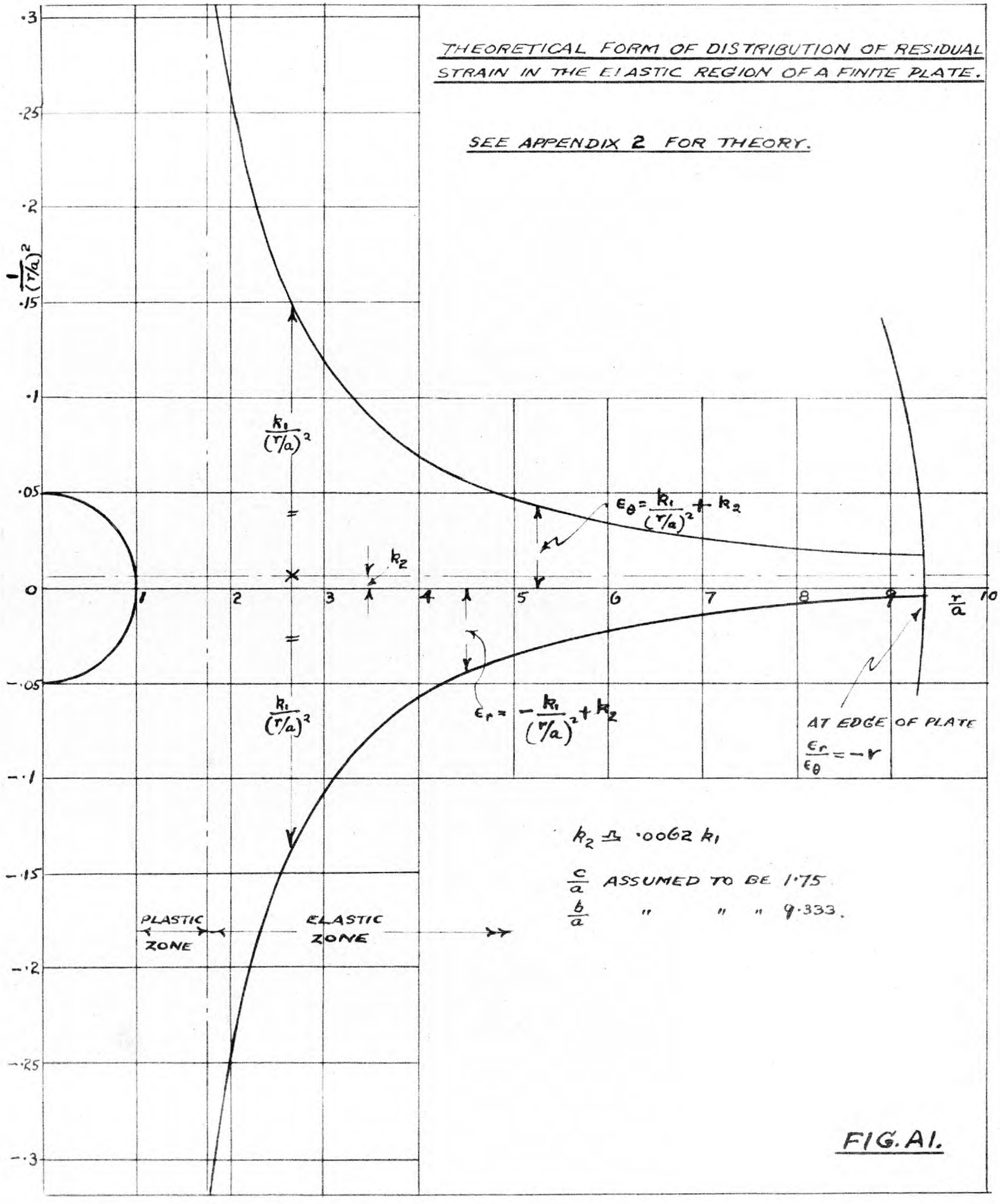
THEORETICAL FORM OF DISTRIBUTION OF RESIDUAL STRAIN IN THE ELASTIC REGION OF A FINITE PLATE.
SEE APPENDIX 2 FOR THEORY.
$\frac{1}{(r/a)^2}$
·3
·25
·2
·15
·1
·05
0
-·05
-·1
-·15
-·2
-·25
-·3
1
2
3
4
5
6
7
8
9
10
$\frac{r}{a}$
$\frac{k_1}{(r/a)^2}$
=
k_2
$\epsilon_\theta = \frac{k_1}{(r/a)^2} + k_2$
$\epsilon_r = -\frac{k_1}{(r/a)^2} + k_2$
AT EDGE OF PLATE
$\frac{\epsilon_r}{\epsilon_\theta} = -\nu$
PLASTIC ZONE
ELASTIC ZONE
$k_2 = \cdot 0062\, k_1$
$\frac{c}{a}$ ASSUMED TO BE 1·75
$\frac{b}{a}$ " " " 9·333.

FIG. A1.

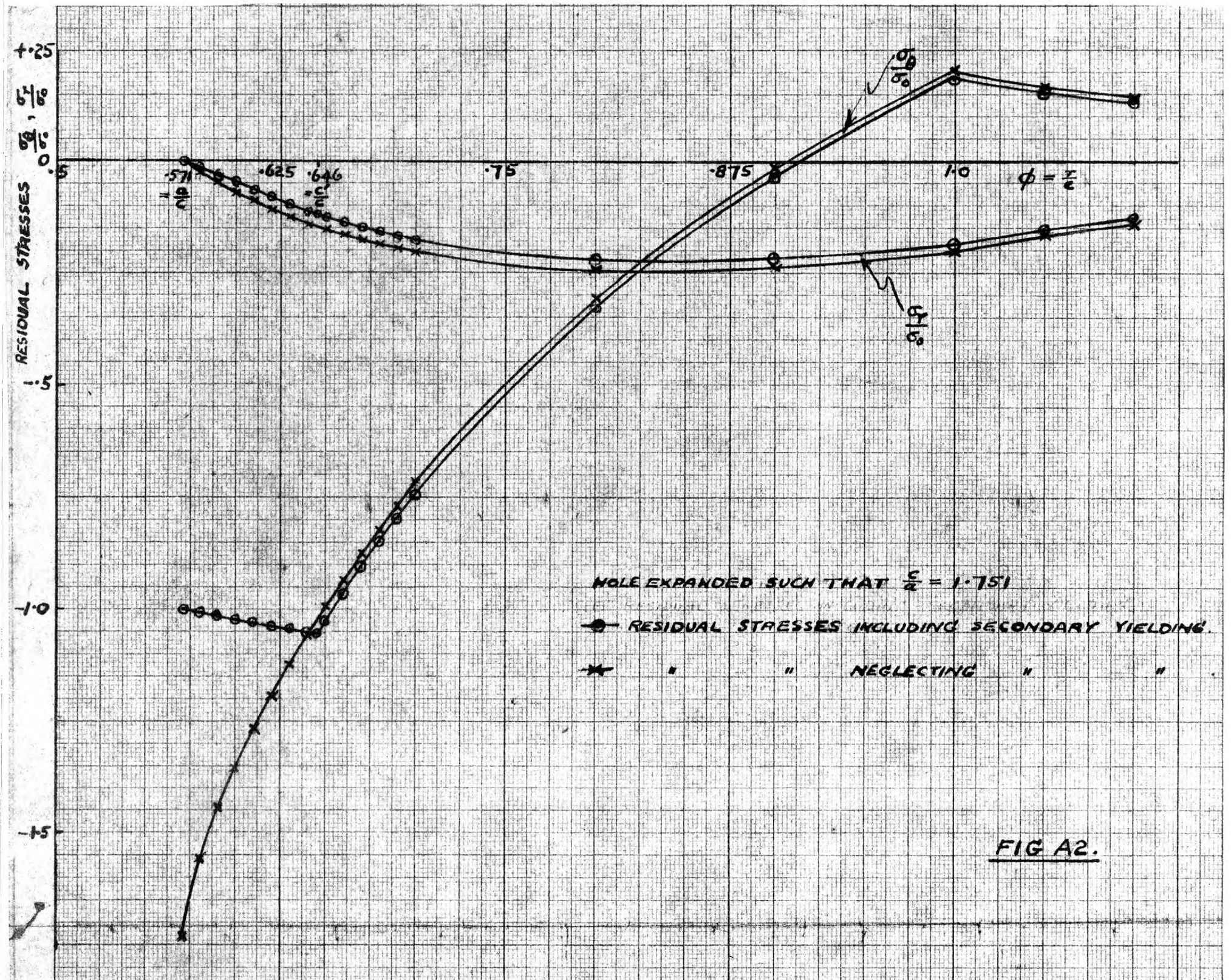
RESIDUAL STRESSES $\frac{\sigma_\theta}{\sigma_0}$, $\frac{\sigma_r}{\sigma_0}$
+·25
0
·5
1·0
1·5
·571 = $\frac{a}{c}$
·625
·646 = $\frac{c'}{c}$
·75
·875
1·0
$\phi = \frac{r}{c}$
$\frac{\sigma_\theta}{\sigma_0}$
$\frac{\sigma_r}{\sigma_0}$
MOLE EXPANDED SUCH THAT $\frac{c}{a}$ = 1·751
RESIDUAL STRESSES INCLUDING SECONDARY YIELDING.
" " NEGLECTING " "

FIG A2.